Generation of high expressing CHO cell lines for the production of recombinant antibodies using optimized signal peptides and a novel ER stress based selection system

Von der Fakultät für Lebenswissenschaften

der Technischen Universität Carolo-Wilhelmina

zu Braunschweig

zur Erlangung des Grades eines

Doktors der Naturwissenschaften

(Dr. rer. nat.)

genehmigte

D i s s e r t a t i o n

von Lars Kober

aus Riesa

1. Referent: apl. Professor Dr. Jürgen Bode

2. Referent: Professor Dr. Stefan Dübel

Eingereicht am: 02.02.2012

Mündliche Prüfung (Disputation) am: 15.06.2012

Druckjahr 2012

Vorveröffentlichungen der Dissertation

Teilergebnisse aus dieser Arbeit wurden mit Genehmigung der Fakultät für Lebenswissenschaften, vertreten durch den Mentor der Arbeit, in folgenden Beiträgen vorab veröffentlicht:

Publikationen

Kober L, Zehe C, Bode J. 2012. Development of a novel ER stress based selection system for the isolation of highly productive clones. (ahead of print)

Kober L, Zehe C, Bode J. 2012. Optimized signal peptides for the development of high expressing CHO cell lines. (in submission)

„The fact that an opinion has been widely held is no evidence whatever it is not utterly absurd"

Bertrand Russell (1872-1970)

Contents page

List of figures page

List of tables page

1. Zusammenfassung

Der Bedarf an biopharmazeutischen Produkten für neuartige medizinische Anwendungen und klinische Studien wächst permanent. Biotherapeutika sind häufig rekombinante Proteine, wie zum Beispiel monoklonale Antikörper, welche meist in Säugerzellkultur produziert werden, um möglichst menschenähnliche posttranslationale Modifizierungen zu erhalten. Chinese hamster ovary (CHO) Zellen sind sehr gebräuchliche Wirtszelllinien, da sie aus behördlicher Sicht weder infektiös noch pathogen sind. Allerdings ist die Gewinnung von Produktionszelllinien sehr zeit- und arbeitsaufwendig und damit teuer. Deshalb sind viele pharmazeutische Unternehmen daran interessiert, diese zu beschleunigen und Kosten zu sparen. In diesem Zusammenhang war es das Ziel der vorliegenden Arbeit, eine produktunabhängige Plattformtechnologie für die Entwicklung und Selektion von hochproduktiven Klonen zu verbessern.

Es wurde berichtet, dass einer der geschwindigkeitsbestimmenden Schritte bei der Produktion von sekretorischen Proteinen die Translokation in das Lumen des Endoplasmatischen Retikulums (ER) ist. Der erste Teil der Arbeit beschäftigt sich daher mit der Optimierung der Sekretionseffizienz. Dazu wurden verschiedene natürliche und künstliche Signalpeptide mit einem rekombinanten Antikörper fusioniert und in transienten Experimenten getestet. Die vielversprechendsten Kandidaten wurden, um ihre Leistungsfähigkeit weiter zu verbessern, gezielt mutiert. Interessanterweise konnte die Effizienz der Signalpeptide dadurch nicht erhöht werden. Die besten Ergebnisse wurden folglich mit den natürlichen Albumin- und Azurocidin-Signalpeptiden erzeugt. Diese Ergebnisse wurden in fed-batch-Experimenten mit stabil transfizierten Zellpools bestätigt, wobei durch die Verwendung des Albumin-Signalpeptides zellspezifische Produktivität von bis zu 90 pg/Zelle/Tag und Produktkonzentrationen von bis zu 4 g/L gemessen werden konnten. Der Fakt, dass diese Ergebnisse mit nicht optimierten fed-batch-Prozessen unter der Verwendung von Zellpools anstatt von klonalen Zelllinien erzeugt wurden, zeigt eindrucksvoll, welches Potenzial die identifizierten Signalpeptide haben.

Die Selektion von Klonen mit hoher Produktivität ist momentan einer der arbeits- und zeitaufwendigsten Schritte während der Entwicklung von Zelllinien zur Produktion von rekombinanten Proteinen. Daher war es im zweiten Teil der Arbeit das Ziel ein neuartiges Selektionssystem zu entwickeln, welches eine einfache und schnelle Identifikation und Isolation von hochproduktiven Klonen aus einem Zellpool erlaubt. Der Grundgedanke war dabei, dass die Überexpression von rekombinanten sekretorischen Proteinen ER Stress auslöst, welcher gemessen und zur Identifikation von hochproduktiven Klonen benutzt werden kann. Dazu wurden in einem Vorexperiment verschiedene Klone, welche unterschiedliche Mengen eines rekombinanten Antikörpers bilden, mittels Echtzeit RT-PCR untersucht. Dabei wurde eine

Korrelation zwischen der gebildeten Antikörpermenge und der Menge an mRNA für verschiedene ER Stress-Faktoren, wie zum Beispiel CALR, GRP78, GRP94 und XBP1 (gespleißt), beobachtet. Basierend auf diesen Ergebnissen wurden verschiedene ER Stress-Reporter-Konstrukte generiert. Diese bestanden aus GFP, welches entweder mit den natürlichen CALR, GRP78 und GRP94 Promotern oder einem SV40 Promoter, in Kombination mit verschiedenen ER Stress assoziierten Transkriptionsfaktor-Bindungsstellen (ERSE I, ERSE II, UPRE und AARE), zur Expression gebracht wurde. Zusätzlich wurde ein Reporter-Konstrukt bestehend aus einem modifizierten GFP und einen XBP1 Fragment inklusive eines Introns generiert. Um die Leistungsfähigkeit aller Reporter-Konstrukte zu testen, wurden diese in Antikörper bildende und in Kontrollzellen ohne Antikörperexpression eingebracht und ihre GFP Fluoreszenz gemessen. Die Vergleichbarkeit wurde dabei durch die gezielte Integration (Rekombinase-vermittelten Kassettenaustausch) der Reporter-Konstrukte in denselben Integrationslokus gewährleistet. Auf diese Weise konnte gezeigt werden, dass weder die ER Stress-Response-Elemente (ERSE I, ERSE II, UPRE und AARE) noch der CALR, der GRP94 Promoter oder das XBP1 Fragment signifikant durch die Antikörperbildung stimuliert wurden. Im Gegensatz dazu wurde eine starke Stimulation des GRP78 Promoters durch die Antikörperexpression beobachtet. Daraufhin wurde ein verkürzter GRP78 Promoter in einen GFP Reporter eingebracht und stabil in CHO DG44 Zellen integriert. Danach wurde in diese Zelllinien ein rekombinanter Antikörper eingebracht und eine standardisierte Zelllinienentwicklung durchgeführt. Die isolierten Klone zeigten erneut eine starke Korrelation zwischen der gebildeten Antikörpermenge und der gemessen GFP Fluoreszenz. Daher kann geschlussfolgert werden, dass der GRP78 Reporter in einem ER Stress basierten Selektionssystem für die Identifizierung und Isolierung von hochproduktiven Klonen eingesetzt werden kann.

2. Abstract

The demand for biopharmaceutical drugs for novel medical applications and clinical trials increases permanently. Common biotherapeutics are recombinant proteins such as monoclonal antibodies which are mostly produced in mammalian cell cultures in order to obtain human-like post-translational modifications. Chinese hamster ovary (CHO) cells are widely used as host cell line because they are accepted by regulatory bodies as safe regarding infectious and pathogenic agents. However, the generation of production cell lines is very time-consuming, labour-intensive and expensive and pharmaceutical companies are interested in speeding up and reducing costs for this process. In this context, it was the aim of the present thesis to improve a product-independent platform technology for the development and selection of highly productive clones.

In a first approach, the optimization of secretion efficiency was addressed, because it has been reported that the translocation into the lumen of the endoplasmatic reticulum (ER) is one of the rate limiting steps during the production of secretory proteins. Therefore, a variety of natural and artificial signal peptides were fused to a recombinant antibody and analysed by transient expression experiments. The most promising candidates were modified by introducing specific mutations to further improve their performance. Interestingly, it was not possible to achieve higher efficiencies in this way. Therefore, the best data were obtained with the natural signal peptides derived from human albumin and human azurocidin. These results were confirmed by fed-batch experiments with stably transfected cell pools, in which cell specific productivities up to 90 pg/cell/day and product concentrations of 4 g/L were measured using the albumin signal peptide. The fact that these data were generated in a non-optimized fed-batch process with cell pools instead of clonal cell lines demonstrates the potency of the identified signal peptides even more impressively.

The selection of high-producing clones is currently one of the most laborious and time-consuming steps during the development of cell lines expressing recombinant proteins. Thus, the second part of the present thesis was aimed at the establishment of a novel selection system for the rapid and easy identification and isolation of rare high producers out of cell pools. The basic idea of the selection system was that the overexpression of secretory recombinant proteins triggers ER stress, which could be measured and used to detect high-producing clones. In a preliminary experiment, several clones producing different amounts of a recombinant antibody were analysed by real time RT-PCR and a correlation between antibody expression and the mRNA level of the ER stress factors CALR, GRP78, GRP94 and spliced XBP1 was observed. Based on these results, several ER stress reporter constructs were

generated. They consisted of GFP driven either by the natural promoters of CALR, GRP78 and GRP94 or by a SV40 promoter in combination with ER stress-related transcription factor binding sites (ERSE I, ERSE II, UPRE and AARE). Additionally, a construct with a modified GFP version comprising an intron-containing XBP1 fragment was created. In order to evaluate their performance, all reporter constructs were once introduced in an antibody expressing producer cell line and once in a non-expressing control cell line and GFP fluorescences were determined. Comparability was ensured by using a targeted integration (recombinase mediated cassette exchange) approach, which allowed the integration of all constructs at the same genomic locus. In this way it was demonstrated that neither the ER stress response elements (ERSE I, ERSE II, UPRE, AARE) nor the CALR, the GRP94 promoter or the XBP1 fragment were significantly stimulated by antibody expression. In contrast, a strong stimulation was observed for the GRP78 promoter upon antibody expression. Based on these data, a truncated version of the GRP78 promoter was used to create a modified GFP reporter construct, which was stably integrated into CHO DG44 cells. Subsequently, the obtained cell line was applied to a standard cell line development procedure employing an antibody expression construct. The isolated clones showed a strong correlation between the amount of secreted antibody and the measured GFP fluorescence. Therefore, it was concluded, that the GRP78 reporter construct can be used as ER stress based selection system, which should be suitable for the identification and isolation of high producers.

3. Introduction

3.1. High-level production of recombinant proteins in CHO cells

The demand for biotherapeutics increases permanently, because many biopharmaceutical drugs are reaching later stage clinical trials. Most biotherapeutic drugs are recombinant monoclonal antibodies which are widely produced in mammalian cell lines (Birch 2006; Dübel 2007; Winder 2005), because of the need for post-translational modifications (e.g. glycosylation) that should be identical or at least similar to those obtained in humans. The chinese hamster ovary cell line CHO DG44 is a very suitable expression system for this purpose (Walsh 2006; Schmidt 2004) that is accepted by regulatory bodies as safe regarding infectious and pathogenic agents (Wagner 2009; Hesse 2000). CHO DG44 cells have a number of intrinsic disadvantages causing their cultivation to be complicated, time–consuming and expensive. Especially the generation of monoclonal high-producer cell lines has been referred to be a main bottleneck in getting the first material required for clinical tests or in getting access to the manufacturing environment (Borth et al. 2000; Carroll 2004; Birch 2006). Hence, pharmaceutical companies are interested in speeding up and reducing costs for their upstream development. One approach is to establish a product-independent platform technology for the development of large-scale production processes for therapeutic proteins. Such a platform includes an adequate expression and selection system, which allows the generation of stable high expression cell lines, corresponding basal and feed media and a process scalable in larger bioreactors (Birch 2006).

One of the most efficient expression and selection systems is based on the enzyme dihydrofolate reductase (dhfr), which catalyses the reduction of folic acid (FA) into 7,8-dihydrofolate (7,8-DHF) and 5,6,7,8-tetrahydrofolate (5,6,7,8-THF) (Bailey 2009). 5,6,7,8-THF is required for the de novo biosynthesis of purines, thymidylate, and glycine. Therefore, when dhfr-deficient CHO DG44 cells are transfected with a vector composed of a GOI and the dhfr-gene as a marker, cells expressing the GOI can be selected by cultivating in medium without hypoxanthine, thymidine and glycine. Additionally, cells can be treated with MTX, a competitive inhibitor of dhfr, which causes an amplification process leading to increased gene copy numbers and thereby to increased productivity (Ludwig 2006; Kaufman 1982). However, it has been reported that the productivity of a cell line does not always correlate with its gene copy number (Bode 2003; Barnes 2003; Barnes 2004), because the level of transcription depends also on the genomic site of integration. Several strategies are used to overcome this so-called position effect (Kwaks 2006; Barnes 2006, Birch 2006). For example insulator elements (Recillas-Targa 2002; Pikaart 1998) and Ubiquitous Chromatin Opening Elements (UCOEs) were

successfully applied in order to protect against unwanted transcriptional silencing mediated by the chromosomal environment (Harland 2002; Antoniou 2003; Williams 2005; Benton 2002). Moreover, Scaffold/Matrix Attachment Regions (S/MARs) (Bode 1992; Heng 2004; Boulikas 1993; Hancock 2000; Zahn-Zabal 2001; Kim 2004) and stabilizing and antirepressor elements (STAR elements) were implemented in order to block chromatin associated transcriptional silencing (Kwaks 2003; Kwaks 2005) or repeat induced silencing (Garrick 1998).

Other ways to increase protein expression levels are the choice of alternative promoters (Addison 1997; Young 2008) or the optimization of the mRNA structure. Especially the removal of cryptic splice sites, cryptic poly-A signals and undesired structures such as stem-loops as well as the optimization of codon usage and GC content can result in increased productivity (Kalwy 2006; Young 2008; Stemmer 1993; Knappskog 2007). Furthermore, it has been reported that the rate-limiting step in the expression of proteins might not be the mRNA level, but rather inefficiencies in translocation, posttranslational modifications, folding or secretion of recombinant proteins (Shuster 1991; Barnes 2004; Birch 2006; Schweickhard 2002 (AU 2002/338947 B2)). For this purpose, cell engineering tools were used to enhance the capacity of mammalian cell lines, e.g. by over-expressing chaperones like protein disulfide isomerase (PID) (Borth 2005) or factors related to the secretory pathway like ceramide transfer protein (CERT) (Florin 2009; Schlatter 2010 Sep; Schlatter 2010 Oct).

3.2. Protein secretion and signal peptides

A huge variety of strategies are used to improve the production of recombinant proteins in mammalian cell lines. Many approaches are aimed at enhancing transcription of the GOI, but it has been reported that the expression of recombinant proteins does not always correlate with their mRNA levels (Barnes 2004). On the other hand, one limiting step within the classical secretory pathway is the translocation of secretory proteins into the lumen of the endoplasmic reticulum (ER) and it has been demonstrated that alternative signal peptides (signal sequences) can lead to an increased protein secretion (Knappskog 2007; Rance 2010; Young 2008 (WO 2008/148519 A2), Zhang 2005).

Most secretory proteins contain N-terminal signal peptides (von Heijne 1983) that emerge during their translation on the ribosomal exit tunnel. Hence, the signal recognition particle (SRP) recognizes and binds the signal peptide and the translation slows down (Keenan 1998). This process is called “translation arrest” and enables the complex consisting of SRP, nascent polypeptide chain and ribosome to bind to the SRP receptor, which is located within the ER membrane (Walter 1981; Walter 1994). Subsequently, the complex interacts with the translocon (Sec61p complex) as well as with the TRAM protein and the SRP is released. Hence, translation is re-initiated and the nascent protein is pushed through the translocon whereas the signal peptide remains within the translocon or moves laterally into the membrane of the ER (Gorlich 1992; Kalies 1994; Jungnickel 1995; Mothes 1998; Martoglio 1995; Voigt 1996; Mothes 1997). Signal peptidase cleaves the signal peptide from the mature protein upon appearance of the cleavage site in the lumen of the ER (Blobel 1975).The cleaved signal peptide can be degraded by the signal peptide peptidase (Lemberg 2001; Lyko 1995; Martoglio 1997). This process was postulated to be required in order to clear the ER membrane (Martoglio 2003) and it might be favourable for host cells, which secrete large amounts of recombinant proteins. Following translocation and cleavage of their signal peptides, proteins are transported through the ER and the Golgi apparatus and subjected to folding and assembly reactions as well as to post-translational modifications during this passage. Finally, processed proteins are packaged into secretory vesicles and externalized upon fusion of these vesicles with the plasma membrane.

Signal peptides consist of a polar N-terminal region (n-region), a hydrophobic core (h-region) and a C-terminal region (c-region). Very often the n-region contains positively or negatively charged residues (von Heijne 1985; Zheng 1996), whereas the h-region consists of 6 to 15 hydrophobic amino acids, which are able to form an alpha-helix (Bruch 1989). In the c-region, small uncharged residues like alanine, glycine, and serine are required at positions -3 and -1 for efficient cleavage by the signal peptidase (Folz 1988; Nielsen 1997), whereas aromatic or

hydrophobic residues are often found at position -2, and a proline at position -5. Hydrophobic residues like leucine or isoleucine are tolerated at position -4 (von Heijne 1983). However, signal peptides do not have a defined consensus sequence and are highly variable regarding their length and amino acid composition. The size of mammalian signal peptides mostly ranges between 15 and 30 amino acids residues in length (Johnson 1999; Martoglio 1998). The frequency of occurrence of important amino acids within the h- and c-region, which was determined based on a large number of different eukaryotic signal peptides, is shown in Tab. 1.

Tab. 1: Frequency of occurrence of amino acids within eukaryotic signal peptides. About 118 eukaryotic signal peptides, all with known cleavage site were evaluated (von Heijne 1985)

position of residues	-10	-9	-8	-7	-6	-5	-4	-3	-2	-1	+1
Leu	58	52	34	43	29	6	19	5	17	1	6
Val	11	11	9	11	17	2	8	21	2	0	7
Phe	8	6	7	13	13	2	4	2	10	0	4
Ala	11	18	15	13	13	15	15	34	4	53	12
Gly	2	2	8	3	2	15	27	2	4	35	7
Pro	2	0	2	2	6	20	10	1	0	0	1
highest probability	L	L	L	L	L	P	G	A	L	A	A

Taking into account the observed variability, the optimization of signal peptides by changing their amino acid pattern is very difficult. Nevertheless, there are some clues how signal peptides should be constructed in order to enhance protein secretion. For example, it has been demonstrated that an increase of positive charges within the n-region leads to improved protein secretion (Tsuchiya 2003, Tsuchiya 2004). It is still unclear how many charged residues are required. Whereas Zhang et al. report that two arginines are optimal (Zhang 2005) and Tsuchiya et al. prefer three (Tsuchyia 2003, Tsuchya 2004). Surprisingly, signal peptides with negatively charged n-regions translocate as well (von Heijne 1986).

The hydrophobic core of a signal peptide is of high importance, because the SRP binds this region and mediates a translation arrest, which is necessary to prevent that synthesized proteins are released into the cytosol (Belin 1996). Moreover, the hydrophobic core unlocks the translocon and is required to position the signal peptide within the ER membrane for the cleavage (von Heijne 1998; Nilsson 2002). Therefore, length and hydrophobicity of a signal peptide can be optimized. For example, it has been shown that the substitution of a single amino acid within the h-region can enhance translocation efficiency dramatically by increasing hydrophobicity (Rapoport 1986). The natural h-region can also be replaced by a single stretch of 10 leucines in order to improve translocation (Tsuchiya 2003, Tsuchiya 2004 and Zhang 2005). Additionally, the cleavage efficiency of a signal peptide depends on the length of its h-region (Nilsson 2002). The presence of small uncharged residues at position -3 and -1 and

the absence of proline at position -2 are essential for signal peptide cleavage (von Heijne 1983; Ping 1993; Nothwehr 1989). Additionally, the cleavage efficiency depends on the length of the h-region (Nilsson 2002). Interestingly, also mutations within the protein immediately downstream of the signal peptide can influence secretion efficiency by affecting signal peptide cleavage and protein translocation (Folz 1986; Andrews 1988; Wiren 1988). Finally, the c-region of a signal peptide is often separated from its hydrophobic core by a strong helix breaker like proline or glycine, the optimal distance between cleavage site and helix breaker being 4 to 6 residues (Nothwehr 1989; Yamamoto 1989; Chou 1978).

It has been demonstrated that signal peptides are extremely heterogeneous and that many prokaryotic and eukaryotic signal peptides are functionally interchangeable even between different species (von Heijne 1985; Gierasch 1989; Tan 2002). Based on these observations, signal peptides from other species can be used to express a gene of interest in a defined host cell system. Moreover, it has been demonstrated in CHO cells that a native signal peptide is not necessarily the most effective one (Hesketh 2005 (WO 2005/001099 A2)) and that signal peptides from other species can mediate an increased antibody secretion (Young 2008 (WO 2008/148519 A2)). All the above mentioned observations might be exploited to select or design potent signal peptides that can be fused to recombinant proteins, in order to improve their secretion efficiency.

3.3. Mammalian ER stress

Most secretory and membrane proteins are synthesized on the ER surface and co-translationally translocated into the ER lumen, where they undergo folding, oligomerization and posttranslational modifications before they leave the ER and are transported to the Golgi apparatus. Proper protein folding and modifications depend on the availability of molecular chaperones and enzymes located in the ER such as protein disulfide isomerase (PDI), calnexin (CANX), calreticulin (CALR), glucose-regulated protein 78 kDa (GRP78), glucose-regulated protein 94 kDa (GRP94). Conditions that exceed the protein folding capacity of the ER provoke ER stress and trigger the unfolded protein response (UPR), the ER overload response (EOR) or ER associated degradation (ERAD) (Rao 2004; Kaufman 1999; Kozutsumi 1988; El-Hadi 2005). The key UPR sensors are three transmembrane proteins called Inositol requiring enzyme 1 (IRE1), pancreatic ER kinase (PKR)-like ER kinase (PERK) and activating transcription factor 6 (ATF6), which are localized in the ER membrane. Under normal physiological conditions, the luminal domains of all three proteins are associated with GRP78. When unfolded proteins accumulate within the ER, GRP78 is released (Step 1 in Fig. 1) to support protein folding thereby activating UPR. Interestingly, the binding of GRP78 to UPR sensors can be also influenced by the expression of membrane proteins. For example, it has been reported that

GRP78 is involved in the folding and assembly of several viral membrane proteins (Cho 2003 and Earl 1991). In the following, the underlying molecular mechanisms of the UPR are described in more detail:

Upon dissociation of GRP78, IRE1 dimerizes and is autophosphorylated (Step 2 in Fig. 1) the IRE1 dimer causes a nonconventional splicing of X-box binding protein (XBP1) mRNA, which enables translation of the corresponding transcription factor XBP1 due to a frame shift (Sidrauski 1997; Yoshida 2001; Calfon 2002). In a similar way, dimerization and autophosphorylation (Step 3 in Fig. 1) of PERK occurs after GRP78 is released, resulting in the phosphorylation of eukaryotic translation initiation factor 2 (eIF2) by the PERK dimer. On the one hand, this modification downregulates global protein synthesis by reducing cap-dependent translation initiation, which antagonizes overloading of the protein folding capacity in the ER. On the other hand, provokes the phosphorylation of eIF2 selective translation and expression of the transcription factor ATF4 (Harding 1999; Harding 2000; Vattem 2004). In case of ATF6, the release of GRP78 from the full-length protein ATF6 (p90) mediates its translocation to the Golgi apparatus (Step 4 in Fig. 1), where it is cleaved by Site-1 and Site-2 protease. This liberates ATF6 (p50), the cytosolic domain of the protein, which acts as a transcription factor (Chen 2002; Haze 1999; Shen 2005; Ye 2000).

The transcription factors XBP1, ATF4 and ATF6 translocate to the nucleus (Step 5 in Fig. 1) and bind to unfolded protein response elements (UPRE), ER stress elements (ERSE) and amino acid response elements (AARE). These are located in promoters such as GRP78, GRP94, CALR and CHOP, which are responsible for the transcription of genes involved in different posttranslational modifications, protein folding, protein synthesis and degradation as well as amino acid transport or other ER functions. Upon transcription factor binding, expression of the corresponding genes is upregulated and cells are able to expand and adjust the capacity of the ER on demand (Shaffer 2004; Pollard 2007). This is very important to prevent the accumulation of malfolded proteins and aggregates which are potentially toxic (Lai 2007).

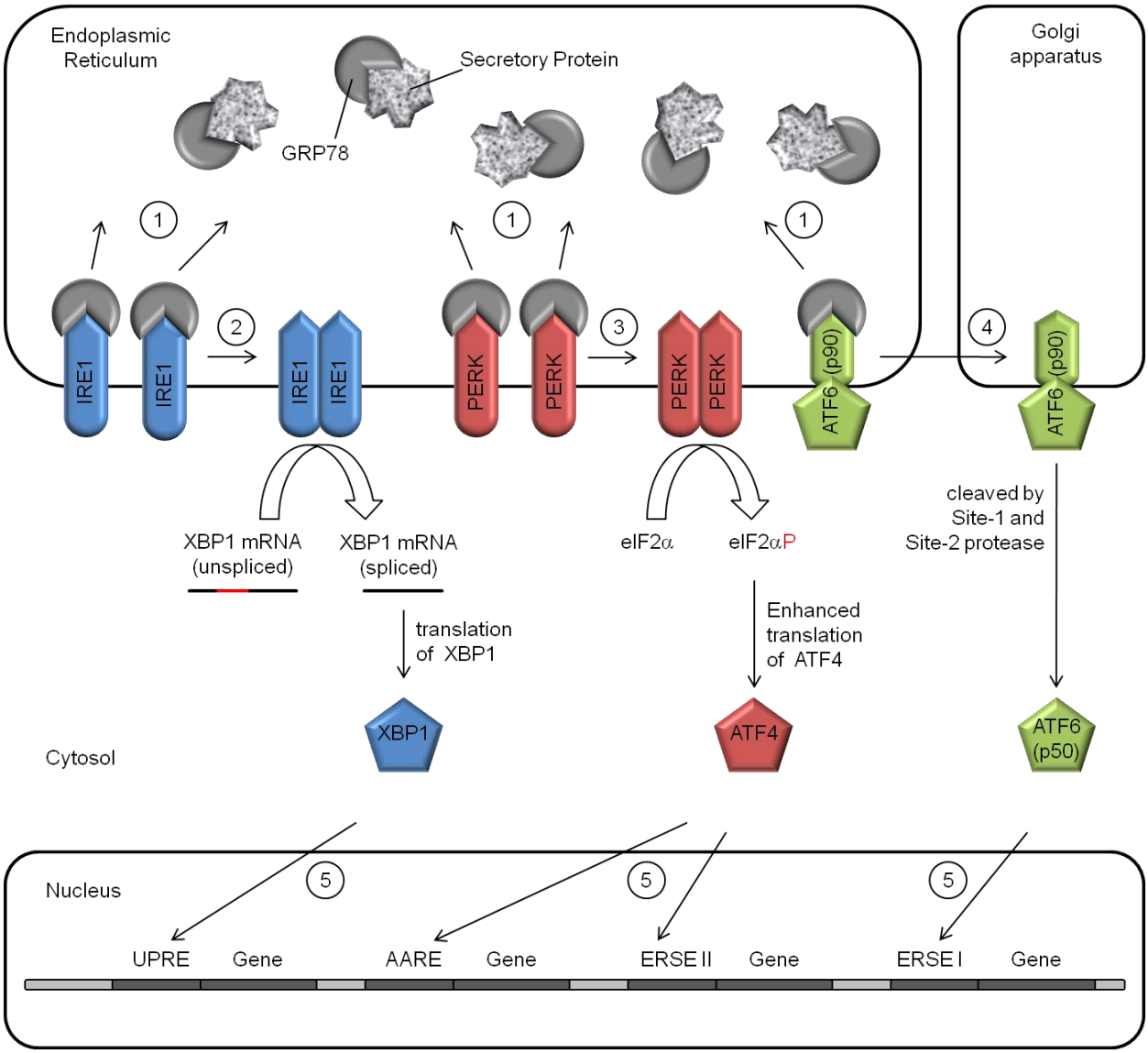

Fig. 1: Schematic representation of ER stress pathways

The ER overload response (EOR), another signal pathway triggered by ER stress, is activated by the accumulation of membrane proteins, e.g. due to protein over-expression (Meyer 1992; Pahl 1995 Mar; Pahl 1996; Pahl 1999; Liu 1995). Moreover, the EOR might be important for antiviral defence (Pahl 1995 Jun; Pahl 1997). Although parts of the EOR pathway remain to be elucidated, it is known that ER stress induces the phosphorylation and degradation of IκB resulting in the release of NF-κB from a NF-κB/IκB heterodimer located in the cytoplasm. Subsequently, the transcription factor NF-κB translocates to the nucleus and genes involved in immune response and inflammation such as interferones and cytokines are upregulated (Pahl 1995 Jun; Kaufman 1999).

ER-associated degradation (ERAD) is another way to prevent the accumulation of toxic malfolded proteins in the ER. In this case, malfolded proteins are posttranslationally

retranslocated through the Sec61 pore complex and degraded by the ubiquitin-proteasome system (Meusser 2005; Tsai et al., 2002). Failed degradation can result in the inclusion of aggregated proteins within the ER, which are referred to as Russell bodies (Russell 1890; Martin-Noya 1999). Moreover, unresolved stress can activate the transcription factor C/EBP homologous protein (CHOP) or the c-Jun N-terminal kinase (JNK), which mediates a caspase activation thereby promoting apoptotic cell death (Szegezdi 2006). Both UPR and EOR can be also induced by drugs that perturb the normal ER function. An overview of these drugs, which are often used to stimulate ER stress in experimental systems, and their modes of action is given in Tab. 2. Brefeldin A (BFA), for example, disrupts the structure of the Golgi apparatus, by which the exit of proteins from the ER is blocked (Pollard 2007; Wang 2000). Tunicamycin and Castanospermine inhibit the formation of complex N-glycosylated proteins (Varki 1999; Saul 1985; Ahmed 1995), whereas Thapsigargin blocks calcium pumps, which disrupts the calcium homeostasis in the ER (LI 2000).

Tab. 2: Drugs that induce ER stress (Pahl 1999)

Drugs that induce the UPR	**Drugs that activate NFκB**
Drugs perturbing ER function	Drugs perturbing ER function
Tunicamycin	Tunicamycin
2-Deoxyglucose	2-Deoxyglucose
Brefeldin A	Monensin
Castanospermine	Brefeldin A
Glucosamine	Thapsigargin
Thapsigargin	Cyclopiazonic acid
AlF^{4-}	
Reducing agents	
2-Mercaptoethanol	
Dithiothreitol	
Heavy metals	
Cobalt	
Nickel	
Calcium ionophores	
A-23187	
Ionomycin	

4. Aim of the thesis

Platform technologies for the development of stable cell lines for the production of recombinant proteins are based on suitable expression and selection systems. Most approaches, which are performed to improve the expression of recombinant proteins focus on the optimization of the transcription and translation process. However, the translocation into the lumen of the ER has been reported as a limiting step during the production of secretory proteins. Considering these data, the aim of the first part of the present thesis is to enhance the productivity of expression cell lines by improving the ER translocation process. For this purpose, potent natural and artificial signal peptides are identified in a screening approach based on transient expression and promising candidates are optimized by introducing specific mutations. Finally, the performance of the best signal peptides in stably transfected cell lines is analyzed. The selection of high-producing clones is currently a very time-consuming and labour-intensive step during the development of cell lines expressing recombinant proteins. In this context, the aim of the second part of the present thesis is to establish a novel selection system based on ER stress, which allows the rapid identification and isolation of high-producers. The rationale of this approach is the assumption that the overexpression of secretory recombinant proteins triggers ER stress and that the extent of the stress response correlates with the expression level of the protein. In a first set of experiments, this hypothesis is verified by analyzing different production clones. Regulatory elements involved in ER stress pathways are identified, which could be suitable as sensors for ER stress. Several test cell lines are generated and the selected elements are used to create GFP-based reporter constructs for the detection of ER stress. Subsequently, the performance of the different constructs is analyzed by introducing them into the test cell lines using RMCE. Finally, the best construct is applied to the generation of a stable production cell line in order to evaluate its suitability as a selection system for high-expressing clones.

5. Materials and methods

5.1. Materials

5.1.1. Chemicals

1 kb DNA Ladder	New England Biolabs, Frankfurt
100 bp DNA Ladder	New England Biolabs, Frankfurt
Accudrop Beads	Becton, Dickinson, Franklin Lakes, USA
Agarose NEEO Ultra	Carl Roth, Karlsruhe
Ampicillin Ready Made Solution, 100 mg/mL	Sigma Aldrich Chemie, Steinheim
AquaGenomic Solution	MoBiTec, Göttingen
Brefeldin A (BFA)	Sigma Aldrich Chemie, Steinheim
BSA (Purified)	New England Biolabs, Frankfurt
Castanospermine (CSN)	Sigma Aldrich Chemie, Steinheim
Casy ton isotonic saline solution	Roche Diagnostic, Mannheim
dNTP Mix	Fermentas, Sankt Leon-Rot
Dulbecco's Phosphate Buffered Saline (PBS)	Sigma Aldrich Chemie, Steinheim
Ethanol, 99.8%, p.a	Carl Roth, Karlsruhe
Ethanol, 70.0%, p.a.	Carl Roth, Karlsruhe
Ethidium bromide solution, 1%	Carl Roth, Karlsruhe
FACS Clean	Becton Dickinson, Franklin Lakes, USA
Folinic acid calcium salt hydrate	Sigma Aldrich Chemie, Steinheim
Gel Loading Dye Blue, 6x	New England Biolabs, Frankfurt
Glycerol, 87%	AppliChem, Darmstadt
Glycine	Sigma Aldrich Chemie, Steinheim
D-Glucose	Sigma Aldrich Chemie, Steinheim
H_2SO_4 (2M)	Carl Roth, Karlsruhe
HCl (2M)	Merk, Darmstadt
Human Reference Serum	Bethyl Laboratories, USA
Kanamycin Solution, 50 mg/mL	Sigma Aldrich Chemie, Steinheim
NaCl	Merk, Darmstadt
NaH_2PO_4	Merk, Darmstadt
NaOH (2M)	Merk, Darmstadt
TMB Supersensitive One Component HRP Mircowell substrate	BioTX Laboratories, OwingsMills, USA
Tris Buffer, pH 8.0 (1M)	AppliChem, Darmstadt
Tris Buffered Saline, with BSA, pH 8.0	Sigma Aldrich Chemie, Steinheim

Tris Buffered Saline, with Tween 20, pH 8.0	Sigma Aldrich Chemie, Steinheim
Turbofect in vitro Transfection Reagent	Fermentas, Sankt Leon-Rot
Tween 20, 10%	Bethyl Laboratories, USA
L-Glutamine	Sigma Aldrich Chemie, Steinheim
LB-Agar	Carl Roth, Karlsruhe
LB-Broth	Carl Roth, Karlsruhe
Methotrexate hydrate (MTX)	Sigma Aldrich Chemie, Steinheim
PEG 4000, 50% (w/v)	Fermentas, Sankt Leon-Rot
Rotiphorese 10X TBE Buffer	Carl Roth, Karlsruhe
2-Propanol, 99.8%, p.a	Carl Roth, Karlsruhe
S.O.C. Medium	New England Biolabs, Frankfurt
Terrific-Broth modified	Carl Roth, Karlsruhe
Wasser für die Molekularbiologie	Carl Roth, Karlsruhe
Water for injection (WFI)	Rentschler Biotechnologie, Laupheim

5.1.2. Buffers, media and supplements for cell culture

CD CHO Medium	Invitrogen, Karlsruhe
CD DG44 Medium	Invitrogen, Karlsruhe
CD Hybridoma Medium	Invitrogen, Karlsruhe
Cholesterol Lipide Concentrate, 250x	Invitrogen, Karlsruhe
FB Serum	Hyclone, Logan, USA
G-418 Sulphate Solution, 50 mg/mL	PAA Laboratories, Pasching, Austria
HT Supplement, 50x	Invitrogen, Karlsruhe
Hygromycin B Solution, 50 mg/mL	PAA Laboratories, Pasching, Austria
Modified CD CHO Medium	Invitrogen, Karlsruhe
Medium C1	Described in capter 5.3.5
Medium C2	Described in capter 5.3.5
Medium D1	Described in capter 5.3.1
Medium D2	Described in capter 5.3.2
Medium D3	Described in capter 5.3.2
Medium D4	Described in capter 5.3.2
Medium D5	Described in capter 5.3.2
Medium D6	Described in capter 5.3.2
Medium K1	Described in capter 5.3.1
Medium K2	Described in capter 5.3.2
Medium S1	Described in capter 5.3.1
Medium S2	Described in capter 5.3.1
PID1-MD-SMD10	Cellca, Laupheim
PID1-MD-SMD13	Cellca, Laupheim
PID1-MD-PM55	Cellca, Laupheim
PID1-MD-FMA70	Cellca, Laupheim
PID1-MD-FMB16	Cellca, Laupheim
Pluronic F-68 Solution, 10%	Invitrogen, Karlsruhe
Production Medium	Described in capter 5.3.6

5.1.3. Enzymes and reaction buffers

Antarctic Phosphatase	New England Biolabs, Frankfurt
Baseline-Zero DNase	Epicentre, Madison, USA
Baseline-Zero DNase Reaction Buffer, 10x	Epicentre, Madison, USA
Baseline-Zero DNase Stop Solution, 10x	Epicentre, Madison, USA
Buffer for T4 DNA Ligase, 10X	New England Biolabs, Frankfurt
M-MuIV Reverse Transcriptase	Fermentas, Sankt Leon-Rot
Mung Bean Nuclease	New England Biolabs, Frankfurt
NEBuffer 1	New England Biolabs, Frankfurt
NEBuffer 2	New England Biolabs, Frankfurt
NEBuffer 3	New England Biolabs, Frankfurt
NEBuffer 4	New England Biolabs, Frankfurt
NEBuffer for Antartic Phosphatase	New England Biolabs, Frankfurt
NEBuffer for EcoRI	New England Biolabs, Frankfurt
NEBuffer for Mung Bean Nuclease	New England Biolabs, Frankfurt
Oligo (dT)18 Primer	Fermentas, Sankt Leon-Rot
Phusion DNA Polymerase	Finnzymes, Espoo, Finland
Phusion GC Reaction Buffer, 5x	Finnzymes, Espoo, Finland
Phusion HF Reaction Buffer, 5x	Finnzymes, Espoo, Finland
Reaction Buffer for M-MuLV RT, 5x	Fermentas, Sankt Leon-Rot
Restriction enzymes (diverse)	New England Biolabs, Frankfurt
ScriptGuard RNase	Epicentre, Madison, USA
T4 DNA Ligase	New England Biolabs, Frankfurt
T4 DNA Ligase Reaction Buffer, 10X	New England Biolabs, Frankfurt
T4 DNA Polymerase	New England Biolabs, Frankfurt

5.1.4. Molecular biological and biochemical kits

Clone JET PCR Cloning Kit	Fermentas, Sankt Leon-Rot
Dual-Glo Luciferase Reporter Assay System	Promega, Madison, USA
DyNamo Flash SYBR Green qPCR Kit	Finnzymes, Espoo, Finland
E.Z.N.A. Gel Extration Kit	Omega Bio-Tek, Norcross, USA
E.Z.N.A. Plasmid Mini Kit I	Omega Bio-Tek, Norcross, USA
Human IgG ELISA Quantitation Kit	Bethyl Laboratories, USA
Nucleofector Kit V for CHO	Lonza Cologne, Köln
Phusion High Fidelity PCR-Kit	New England Biolabs, Frankfurt
PureLink HiPure plasmid Filter Maxiprep Kit	Invitrogen, Karlsruhe

QIAshredder (50)	Qiagen, Hilden
QuikChange II Site-Directed Mutagenesis Kit	Stratagene, La Jolla, USA
RNeasy Plus Mini Kit (50)	Qiagen, Hilden

5.1.5. Bacterial strains

JM110 Stratagene Competent cells	Stratagene, La Jolla, USA
NEB 5-alpha Competent *E. coli*	New England Biolabs, Frankfurt
NEB 10-beta Competent *E. coli*	New England Biolabs, Frankfurt

5.1.6. Mammalian cells

CHO K1 cells (ATCC no.: CCL-61)	DSMZ, Braunschweig
CHO DG44 cells	L. Chasin, Columbia University, New York

5.1.7. Consumables

Casy cups	Roche Diagnostic, Mannheim
CryoPure Tube, 1.8 mL white	Sarstedt, Nümbrecht
Shake Flask 125 mL (Erlenmeyer)	Corning, NY, USA
Shake Flask 250 mL (Erlenmeyer)	Corning, NY, USA
Shake Flask 500 mL (Erlenmeyer)	Corning, NY, USA
LightCycler 480 Multiwell Plate 96, white	Roche Diagnostic, Mannheim
MultiDish 6 Wells	Nunc, Roskilde, Denmark
SafeSeal Tubes 1.5 mL	Sarstedt, Nümbrecht
SafeSeal Tubes 2.0 mL	Sarstedt, Nümbrecht
Surgical blades	Swann Morton, Sheffield, UK
TC Microwell 96U	Nunc, Roskilde, Denmark
TC Microwell 96F	Nunc, Roskilde, Denmark
TC Plate 24-Well Flat Susp Cell	Sarstedt, Nümbrecht
TC-Plate 12 Well	greiner bio-one, Frickenhausen
Tube 13 mL	Sarstedt, Nümbrecht
Tube 15 mL	Sarstedt, Nümbrecht
Tube 50 mL	Sarstedt, Nümbrecht
Polystyrene Round-Bottom Tube with Cell Strainer Cap 5 mL	Becton Dickinson, Franklin Lakes, USA
Polystyrene Round-Bottom Tube 5 mL	Becton Dickinson, Franklin Lakes, USA
Ziploc bags	Melitta Haushaltsprodukte, Minden

5.1.8. Technical devices

ABL800 FLEX	Radiometer, Willich
Appliskan microplate reader	Thermo Scientific, Karlsruhe
Biofuge fresco	Heraeus, Hanau
Biofuge pico	Heraeus, Hanau
Biofuge stratos	Heraeus, Hanau
Bio Photometer	Eppendorf, Hamburg
Bühler Shaker, KS-15	Edmund Bühler, Hechingen
Certomat IS incubation shaker	Sartorius, Göttingen
Cell Counter Analyser System (CASY), Model TTC	Roche Diagnostic, Mannheim
E.A.S.Y. 440K Win32 Gel Documentation System	Herolab Laborgeräte, Wiesloch
Electrophoresis chamber Sub-Cell GT WIDE MINI	Bio-Rad Laboratories, München
FACSAria	Becton Dickinson Bioscience, Heidelberg
Galaxy Mini Star centrifuge	VWR International, Darmstadt
HERA cell 240 incubator	Thermo Scientific, Karlsruhe
HERA safe laminar flow	Heraeus, Hanau
HPLC, Finnigan Surveyor Plus	ThermoFinnigan, San Jose, USA
Incu-line incubation shaker	VWR International, Darmstadt
LA 230P-OCE balance	Sartorius, Göttingen
Leica DM IL microscope	Leica Microsystems, Wetzlar
Light Cycler 480	Roche Diagnostic, Mannheim
Multifuge 3s-r	Heraeus, Hanau
MyCycler termal cycler	Bio-Rad Laboratories, München
Nucleofector II	Lonza Cologne, Köln
Pipetboy acu	Integra Biosciences, Fernwald
Pipet Research 2.5 µL	Eppendorf, Hamburg
Pipet Research 10 µL	Eppendorf, Hamburg
Pipet Research 100 µL	Eppendorf, Hamburg
Pipet Research 200 µL	Eppendorf, Hamburg
Pipet Research 1000 µL	Eppendorf, Hamburg
Power Pac 200 gel electrophoresis system	Bio-Rad Laboratories, München
Protein A column, Poros, 20 µm	Applied Biosystems, Foster City, USA
Thermomixer compact	Eppendorf, Hamburg
UV Detector, Surveyor PDA Plus Detector	Thermo Electron, San Jose, USA
Vortex-Genie2	Scientific Industries, Bohemia, USA

Water bath W22	Preiss-Daimler, Medingen, Dresden
Wellwash 4 Mk 2 microplate washer	Thermo Scientific, Karlsruhe

5.1.9. Software

Chrom Quest Software	ThermoFinnigan, Waltham, USA
Light Cycler 480 Software, LCS480 1.5.0.39	Roche Diagnostic, Mannheim
Universal ProbeLibrary	Roche Diagnostic, Mannheim
AUG_hairpin	Kochetov, A.V. et al. 2007
BD FACSDiva software	Becton Dickinson Bioscience, Heidelberg
QuikChange Primer Design	Stratagene, La Jolla, USA
Vector NTI software	Invitrogen, Karlsruhe

5.1.10. Plasmids

Tab. 3: Overview of first generation expression vectors (Signal peptide constructs)

Vector number	Containing signal peptide	Provider
446	A2	created during this study
447	B	created during this study
448	C	created during this study
449	D	created during this study
450	E	created during this study
451	F	created during this study
452	G	created during this study
453	H	created during this study
455	J	created during this study
456	K	created during this study
457	L	created during this study
458	M	created during this study
459	N	created during this study
460	O	created during this study
461	P	created during this study
462	Q	created during this study
463	R	created during this study
464	S	created during this study
465	T	created during this study

Tab. 4: Overview of second generation expression vectors (Signal peptide constructs)

Vector number	Containing signal peptide	Provider
601	A2	created during this study
602	B	created during this study
603	E	created during this study
604	M	created during this study
661	B1	created during this study
662	E1	created during this study
663	E2	created during this study
664	E3	created during this study
665	E4	created during this study
666	E5	created during this study
841	E6	created during this study
842	E7	created during this study
843	E8	created during this study

Tab. 5: Overview of third generation expression vectors (Signal peptide constructs)

Vector number	Containing signal peptide	Provider
1171	A2	created during this study
1157	B	created during this study
1158	E	created during this study
1159	E3	created during this study

Tab. 6: Overview of ER stress RMCE donor constructs

Vector number	Containing ER stress reporter	Provider
1188	SV40-eGFP control	created during this study
1192	3 x ERSE I	created during this study
1193	3 x ERSE II	created during this study
1194	3 x UPRE	created during this study
1995	3 x AARE	created during this study
917	SV40-d2eGFP control	created during this study
1023	Intron	created during this study
1101	CALR	created during this study
1103	GRP78	created during this study
1104	GRP94	created during this study

Tab. 7: Overview of additional vectors

Vector number	Containing construct	Provider
314	LC HC dhfr	Cellca, Laupheim
527	trunc GRP78 Reporter	created during this study
673	FLPO	created during this study
726	HC LC dhfr	Cellca, Laupheim
957	DsRed RMCE Acceptor	Cellca, Laupheim
1071	GTN RMCE Donor	Cellca, Laupheim
1096	dhfr	created during this study

Tab. 8: Overview of vectors from external providers

Vector number	Containing construct	Vector name of provider	Provider (Reference)
719	GTN	pF3ESGTNWF	kindly provided by Prof. Bode (Baer 2002)
721	FLPO	pFlpo-Puro (flpo-IRES-pac)	kindly provided by Prof. Bode (Raymond 2007)
722	DsRed HygTK	pF3HygTKF	kindly provided by Prof. Bode (Schlake 1994)
944	DsRed	pDsRed-Express-N1	Clontech
N/A	Cloning site	pJET1.2/blunt vector	Fermentas

Tab. 9: Overview of cloning vectors

Vector number	Type of cloning vector	Provider
377	basic	Cellca, Laupheim
386	basic	Cellca, Laupheim
526B	basic	Cellca, Laupheim
556	basic	Cellca, Laupheim
560	basic	Cellca, Laupheim
881	basic	Cellca, Laupheim
949	basic	Cellca, Laupheim
951	basic	Cellca, Laupheim
1152	basic	Cellca, Laupheim
377B	intermediate	created during this study
412	intermediate	created during this study
556B	intermediate	created during this study
560B	intermediate	created during this study
701	intermediate	created during this study
952	intermediate	created during this study
954	intermediate	created during this study
955	intermediate	created during this study

5.2. Molecular biological methods

5.2.1. Cloning of DNA constructs

Molecular cloning means the creation of a DNA construct by the assembly of a DNA fragment and a plasmid, which enables the propagation of the construct in *E. coli*. For this purpose, the plasmid of choice (also referred to as vector or plasmid) was cleaved with appropriate restriction enzymes and enzymatically dephosphorylated. The desired DNA fragment (also referred to as insert) was excised with corresponding restriction enzymes. Both digestion reactions were subjected to gel electrophoresis and the fragments of interest were extracted and purified. Subsequently, vector and insert were ligated, introduced into *E. coli* by transformation and the cells were spread and cultivated on LB agar plates. Grown single colonies were cultivated in LB medium, plasmid DNA was isolated by mini preparation and correct clones were identified by restriction analysis.

5.2.2. Cloning of signal peptide constructs

During the first part of the present study, three types of vectors, each coding for the same recombinant model antibody were used. They differ only with regard to the composition (promoters, poly-A signals) and the arrangement of the individual expression cassettes on the plasmid. Moreover, different marker genes were placed on these constructs. The plasmids are designated as first, second and third generation expression vectors, respectively. The features of these vectors are summarized in Tab. 10

Tab. 10: Features of used signal peptide constructs

Expression vector	HC and LC expression was under control of	marker genes	Position of HC on vector	Position of LC on vector	Position of marker gene on vector
first generation	SV40 Promoter	hRluc	second	first	third
second generation	CMV Promoter	hRluc	first	third	second
third generation	SV40E Promoter	dhfr	first	second	third

Various signal peptides were inserted in front of the heavy and the light antibody chain of these vectors as described in Fig. 4, Fig. 5 and Fig. 6. In order to simplify the schematic representations, parts of vectors are shown as dashed line. Nevertheless, they are generally based on the pGL3 plasmid backbone comprising an origin of replication and the beta-lactamase gene who mediates an ampicillin resistance in *E. coli*.

In case of first and second generation expression vectors, an EcoRV restriction site was introduced within the first two codons of the immunoglobulin heavy and light chain in order to allow the insertion of different signal peptides. All necessary mutations were done by site-directed mutagenesis (see chapter 5.2.6), and the resulting changes in the nucleotide and the amino acid sequence are shown in Fig. 2.

```
      E   V
5'   gag gtg      wild-type

      D   I
5'   gat atc      mutation
```

Fig. 2: Nucleotide sequence of the first two codons of the immunoglobulin heavy chain

The first two amino acids of the mature immunoglobulin heavy chain are indicated with capital letters and the created EcoRV restriction site is underlined.

```
      D   I
5'   gac atc      wild-type

      D   I
5'   gat atc      mutation
```

Fig. 3: Nucleotide sequence of the first two codons of the immunoglobulin light chain

The first two amino acids of the mature immunoglobulin light chain are indicated with capital letters and the created EcoRV restriction site is underlined.

The cloning procedure for the insertion of signal peptides into first generation expression vectors is described in Fig. 4.

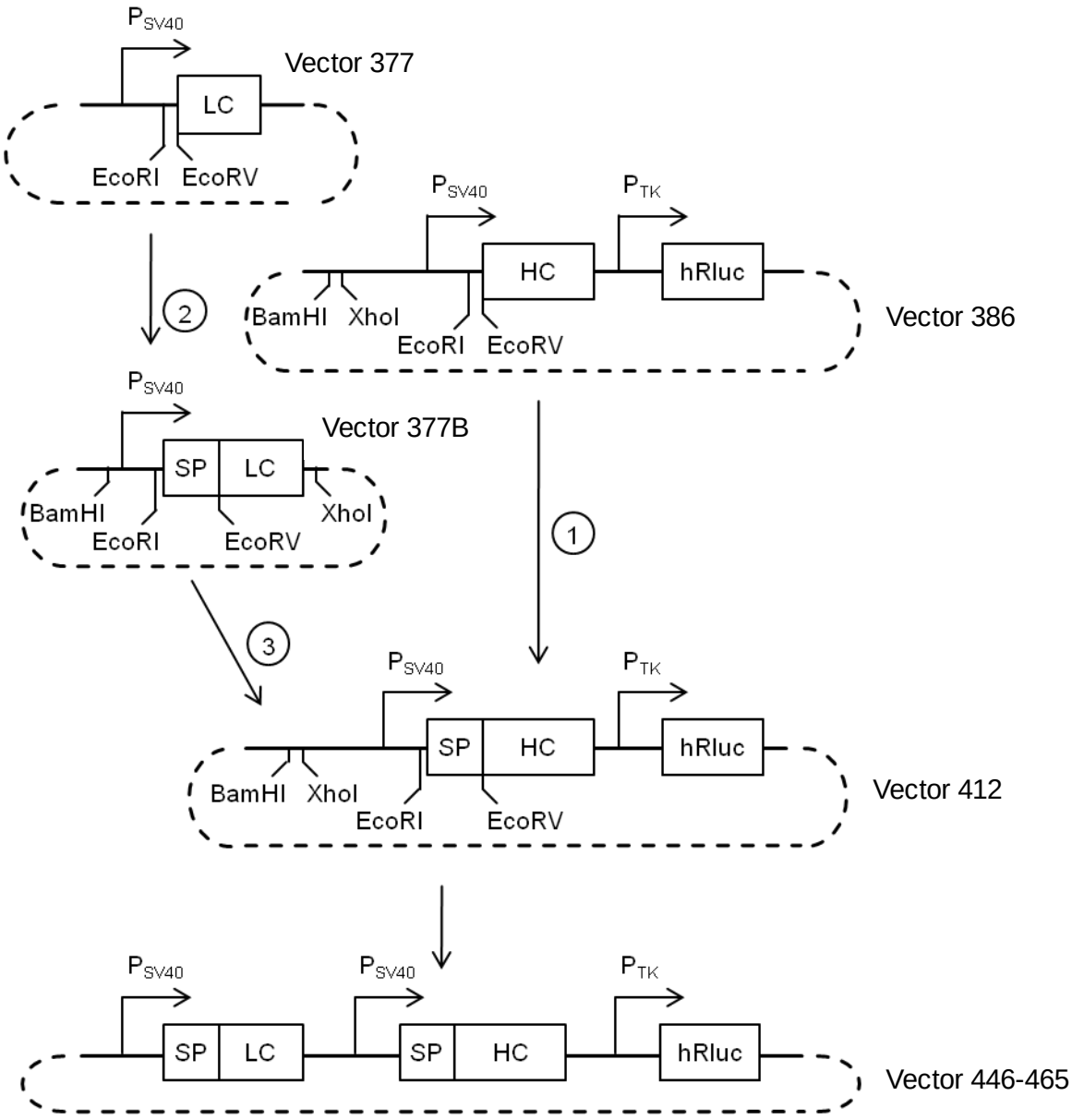

Fig. 4: Schematic representation of the cloning procedure for first generation expression vectors

For each signal peptide (listed in Tab. 34), oligonucleotides containing a Kozak consensus sequence and the respective sequence coding for the signal peptide were synthesized (Eurogentec) and annealed in order to create a dsDNA with a 5' aatt extension compatible with EcoRI as well as a blunt end. Step 1 and step 2: Vector 377 and vector 386 were digested with the restriction endonucleases EcoRI and EcoRV and the annealed oligonucleotides were cloned into these vectors. Step 3: A BamHI/XhoI DNA fragment was transferred from vector 377B into vector 412, resulting in the final expression vector.

The cloning procedure for the insertion of signal peptides into second generation expression vectors is described in Fig. 5.

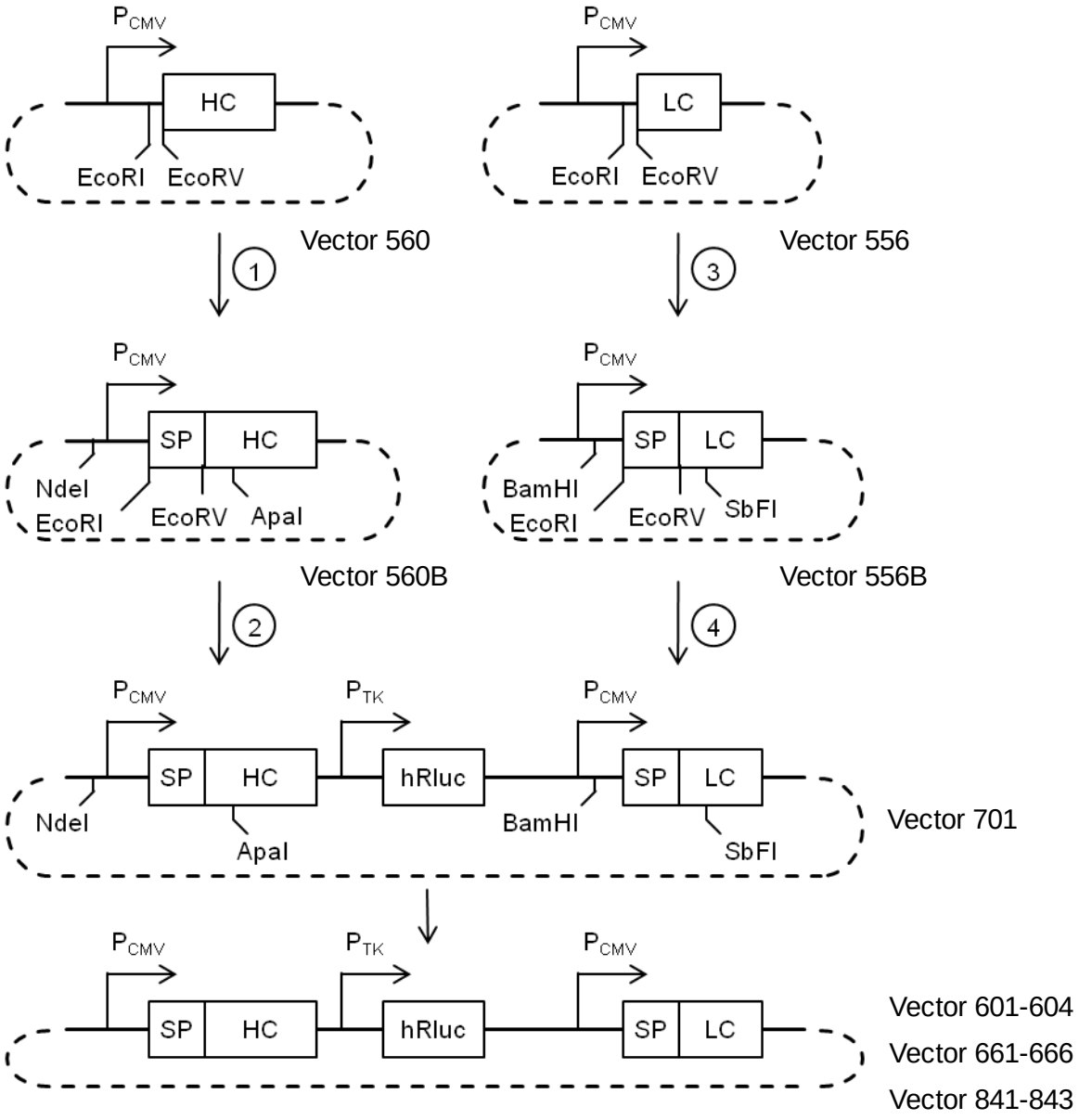

Fig. 5: Schematic representation of the cloning procedure for second generation expression vectors

For each signal peptide (listed in Tab. 35), oligonucleotides containing a Kozak consensus sequence and the respective sequence coding for the signal peptide were synthesized (Eurogentec) and annealed in order to create a dsDNA with a 5' aatt extension compatible with EcoRI as well as a blunt end. Step 1 and step 3: Vector 560 and vector 556 were digested with the restriction endonucleases EcoRI and EcoRV and the annealed oligonucleotides were cloned into these vectors. Step 2: A NdeI/ApaI DNA fragment was transferred from vector 560B to vector 701. Step 4: Following the insertion of the NdeI/ApaI fragment (Step 2), a BamHI/SbfI fragment was transferred from vector 556B to vector 701 resulting in the final expression vector.

The cloning procedure for the insertion of signal peptides into third generation expression vectors is described in Fig. 6. In this case, signal peptides were introduced via BbsI and BsmBI sites (see Fig. 7 and Fig. 8), thereby avoiding changes in the antibody amino acid sequence of the heavy and light chain.

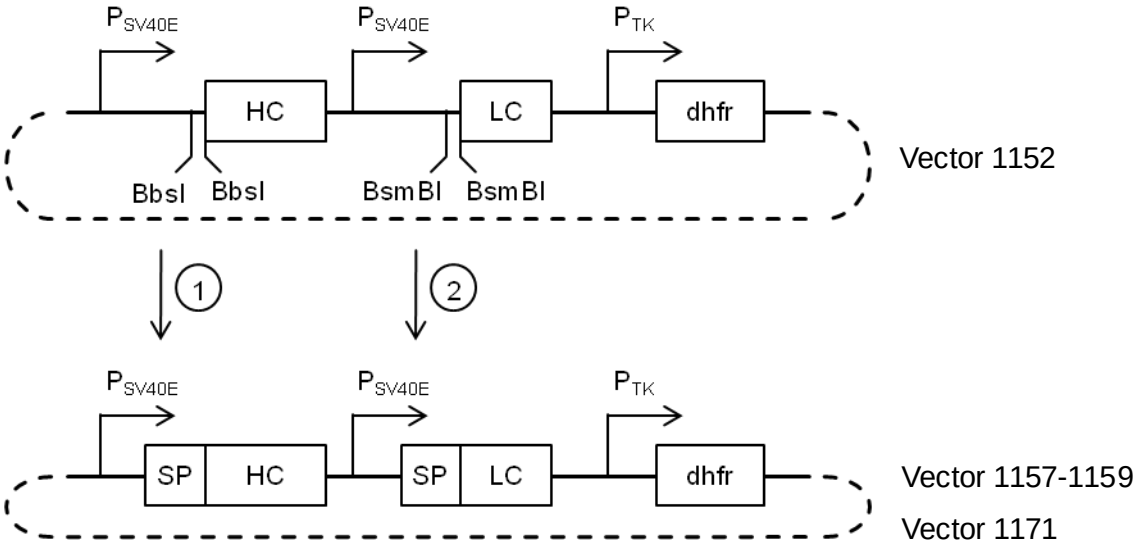

Fig. 6: Schematic representation of the cloning procedure for third generation expression vectors

For each signal peptide (listed in Tab. 35), oligonucleotides containing a Kozak consensus sequence and the respective sequence coding for the signal peptide were synthesized (Eurogentec) and annealed in order to create a dsDNA with a 5' aatt (sense strand) and a 5' tcgg (antisense strand) extension compatible with extensions created with restriction endonuclease BsbI and BsmBI (see Fig. 7 and Fig. 8). Step 1: Vector 1152 was digested with the restriction endonuclease BbsI and the annealed oligonucleotides were cloned into this vector. Step 2: Following the insertion of the annealed oligonucleotides via BbsI (Step 1), the vector was digested with the restriction endonuclease BsmBI and the annealed oligonucleotides were cloned in, resulting in the final expression vectors.

```
                                                        E  V
5'   gaattcggtc ttcatgaccg atatcttggg acagaagacc tccgaggtg
3'   cttaagccag aagtactggc tatagaaccc tgtcttctgg aggctccac
```

Fig. 7: Nucleotide sequence of the BbsI/BbsI cloning site in front of the immunoglobulin heavy chain

The BsbI restriction sites are underlined and the DNA extensions generated upon cleavage are boxed. The first two amino acids of the mature immunoglobulin heavy chain are indicated with capital letters

```
                                                    D  I
5'   gaattcgaga cgatgaccga tatcttggga cacgtctctc cgacatc
3'   cttaagctct gctactggct atagaaccct gtgcagagag gctgtag
```

Fig. 8: Nucleotide sequence of the BsmBI/BsmBI cloning site in front of the immunoglobulin light chain

The BsmBI restriction sites are underlined and DNA extensions generated upon cleavage are boxed. The first two amino acids of the mature immunoglobulin light chain are indicated with capital letters

5.2.3. Cloning of ER stress constructs

During the second part of the present thesis, a variety of vectors (also termed as RMCE donor constructs) were used. The cloning procedure of these constructs is described in the following. In order to create reporter constructs containing different ER stress response elements, vector 1188 comprising heterospecific FRT-sites (FRTwt and FRT3), a promoterless neomycin resistance gene, a AsiSI/BglII cloning site and an SV40 promoter followed by eGFP was used (see Fig. 9).

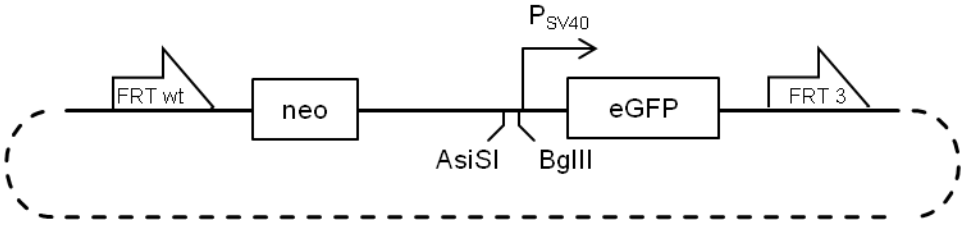

Fig. 9: Schematic representation of vector 1188 (SV40-eGFP control)

DNA fragments containing the transcription factor binding sites ERSE I, ERSE II, UPRE and AARE were synthesized (Gene art) and the elements were inserted into vector 1188 via AsiSI/BglII resulting in vector 1192, 1193, 1194 and 1195, respectively. The corresponding sequences of the promoter region upstream of eGFP are depicted for all generated constructs as well as for the SV40-eGFP control vector 1188 (Fig. 10).

```
-333                                tta attaatatcg gaccggctat cgtacgttct

-300   agacgttggc gatcgcttgc ttcgaagcat ggcgcgccag atctgcgatc tgcatctcaa

-240   ttagtcagca accatagtcc cgcccctaac tccgcccatc ccgcccctaa ctccgcccag

-180   ttccgcccat tctccgcccc atcgctgact aatttttttt atttatgcag aggccgaggc

-120   cgcctcggcc tctgagctat tccagaagta gtgaggaggc ttttttggag gcccaggctt

-60    ttgcaaaatc gattctatcc tagggtcagg gccggccgct agggatccga attcgccacc

+1     atggtgagca agggcgagga gctgttcacc ggggtggtgc ccatcctggt cgagctggac
```

Fig. 10: Nucleotide sequence upstream of the eGFP reporter gene of vector 1188 (SV40-eGFP control)

The AsiSI and the BglII restriction sites are underlined. The SV40 promoter region is located at -54 and -256, and the translation start site at +1.

```
-432                                                          tt aattaatatc
                                                                    ERSE I
-420   ggaccggcta tcgtacgttc tagacgttgg cgatcgcttg cttcgaactg ccaatcggcg
                                                  ERSE I
-360   gcctccacgc catcaagata tccaagggcc caatcggcgg cctccacgag ctgatttcga
                        ERSE I
-300   acggcgtccc aatcggcggc ctccacgcca ggcgcgccag atctgcgatc tgcatctcaa

-240   ttagtcagca accatagtcc cgcccctaac tccgcccatc ccgcccctaa ctccgcccag

-180   ttccgcccat tctccgcccc atcgctgact aatttttttt atttatgcag aggccgaggc

-120   cgcctcggcc tctgagctat tccagaagta gtgaggaggc ttttttggag gcccaggctt

-60    ttgcaaaatc gattctatcc tagggtcagg gccggccgct agggatccga attcgccacc

+1     atggtgagca agggcgagga gctgttcacc ggggtggtgc ccatcctggt cgagctggac
```

Fig. 11: Nucleotide sequence upstream of the eGFP reporter gene of vector 1192 (3 x ERSE I reporter)

The ERSE I consensus sequences are boxed and the AsiSI and the BglII restriction sites are underlined. The SV40 promoter region is located from -54 to -256, and the translation start site is located at +1.

```
-408                ttaattaa tatcggaccg gctatcgtac gttctagacg ttggcgatcg
                         ERSE II                              ERSE II
-360   cttgcttcga actgattggg ccacgccatc aagatatcca agggcattgg gccacgagct
                          ERSE II
-300   gatttcgaac ggcgtcattg ggccacgcca ggcgcgccag atctgcgatc tgcatctcaa

-240   ttagtcagca accatagtcc cgcccctaac tccgcccatc ccgcccctaa ctccgcccag

-180   ttccgcccat tctccgcccc atcgctgact aatttttttt atttatgcag aggccgaggc

-120   cgcctcggcc tctgagctat tccagaagta gtgaggaggc ttttttggag gcccaggctt

-60    ttgcaaaatc gattctatcc tagggtcagg gccggccgct agggatccga attcgccacc

+1     atggtgagca agggcgagga gctgttcacc ggggtggtgc ccatcctggt cgagctggac
```

Fig. 12: Nucleotide sequence upstream of the eGFP reporter gene of vector 1193 (3 x ERSE II reporter)

The ERSE II consensus sequences are boxed and the AsiSI and the BglII restriction sites are underlined. The SV40 promoter region is located from -54 to -256, and the translational start is located at +1.

```
-399                          ttaattaat atcggaccgg ctatcgtacg ttctagacgt
                                   UPRE                           UPRE
-360   tggcgatcgc ttgcttcgaa ctgtgacgtg gccatcaaga tatccaaggg ctgacgtgga
                                UPRE
-300   gctgatttcg aacggcgtct gacgtggcca ggcgcgccag atctgcgatc tgcatctcaa

-240   ttagtcagca accatagtcc cgcccctaac tccgcccatc ccgcccctaa ctccgcccag

-180   ttccgcccat tctccgcccc atcgctgact aatttttttt atttatgcag aggccgaggc

-120   cgcctcggcc tctgagctat tccagaagta gtgaggaggc ttttttggag gcccaggctt

-60    ttgcaaaatc gattctatcc tagggtcagg gccggccgct agggatccga attcgccacc

+1     atggtgagca agggcgagga gctgttcacc ggggtggtgc ccatcctggt cgagctggac
```

Fig. 13: Nucleotide sequence upstream of the eGFP reporter gene of vector 1194 (3 x UPRE reporter)

The UPRE consensus sequences are boxed and the AsiSI and the BglII restriction sites are underlined. The SV40 promoter region is located from -54 to -256, and the translation start site is located at +1.

```
-402                        tt aattaatatc ggaccggcta tcgtacgttc tagacgttgg
                               AARE                              AARE
-360   cgatcgcttg cttcgaactg gttgcatcac catcaagata tccaagggcg ttgcatcaag
                              AARE
-300   ctgatttcga acggcgtcgt tgcatcacca ggcgcgccag atctgcgatc tgcatctcaa

-240   ttagtcagca accatagtcc cgcccctaac tccgcccatc ccgcccctaa ctccgcccag

-180   ttccgcccat tctccgcccc atcgctgact aatttttttt atttatgcag aggccgaggc

-120   cgcctcggcc tctgagctat tccagaagta gtgaggaggc ttttttggag gcccaggctt

-60    ttgcaaaatc gattctatcc tagggtcagg gccggccgct agggatccga attcgccacc

+1     atggtgagca agggcgagga gctgttcacc ggggtggtgc ccatcctggt cgagctggac
```

Fig. 14: Nucleotide sequence upstream of the eGFP reporter gene of vector 1195 (3 x AARE reporter)

The AARE consensus sequences are boxed and the AsiSI and the BglII restriction sites are underlined. The SV40 promoter region is located from -54 to -256, and the translation start site is located at +1.

Additional reporter constructs (also termed RMCE donor constructs) were generated by the insertion of natural ER stress promoters into vector 917 comprising heterospecific FRT-sites (FRTwt and FRT3), a promoterless neomycin resistance gene, a BglII/EcoRI cloning site and an SV40 promoter followed by d2eGFP (see Fig. 15).

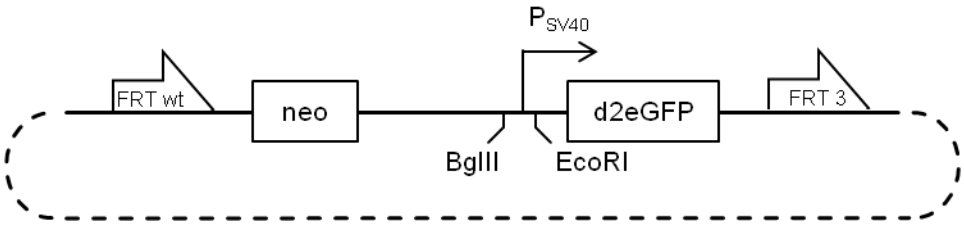

Fig. 15: Schematic representation of vector 917 (SV40-d2eGFP control)

By preparative PCR, the promoter regions of GRP78 and GRP94 were isolated using genomic DNA derived from CHO DG44 cells and the promoter region of CALR was isolated using genomic DNA derived from human blood. The obtained PCR products were cloned into the pJET1.2/blunt vector (Fermentas) and for each promoter, a 1500 bp fragment including the 5' UTR (except the Kozak sequence) was amplified by PCR. Thereby, BbsI restriction sites that upon cleavage result in DNA extensions compatible with BglII and EcoRI were introduced at the 5' and the 3' end, respectively. Subsequently, the SV40 promoter present in vector 917 was replaced by the individual ER stress promoters via BglII/EcoRI, resulting in vector 1101, 1103 and 1104. The corresponding DNA sequences upstream of d2eGFP are depicted for generated constructs as well as for the SV40-d2eGFP control vector 917.

```
-331                                  t taattaatat cggaccggct atcgtacgtt
-300   ctagacgttg gcgatcgctt gcttcgaagc atggcgcgcc agatctgcga tctgcatctc
-240   aattagtcag caaccatagt cccgccccta actccgccca tcccgcccct aactccgccc
-180   agttccgccc attctccgcc ccatcgctga ctaatttttt ttatttatgc agaggccgag
-120   gccgcctcgg cctctgagct attccagaag tagtgaggag gctttttttgg aggcccaggc
-60    ttttgcaaaa tcgattctat cctagggtca gggccggccg ctagggatcc gaattccacc
+1     atggtgagca agggcgagga gctgttcacc ggggtggtgc ccatcctggt cgagctggac
```

Fig. 16: Nucleotide sequence upstream of the d2eGFP reporter gene of vector 917 (SV40-d2eGFP control)

The BglII and the EcoRI restriction sites are underlined. The SV40 promoter region is located from -51 to -260, and the translation start site is located at +1.

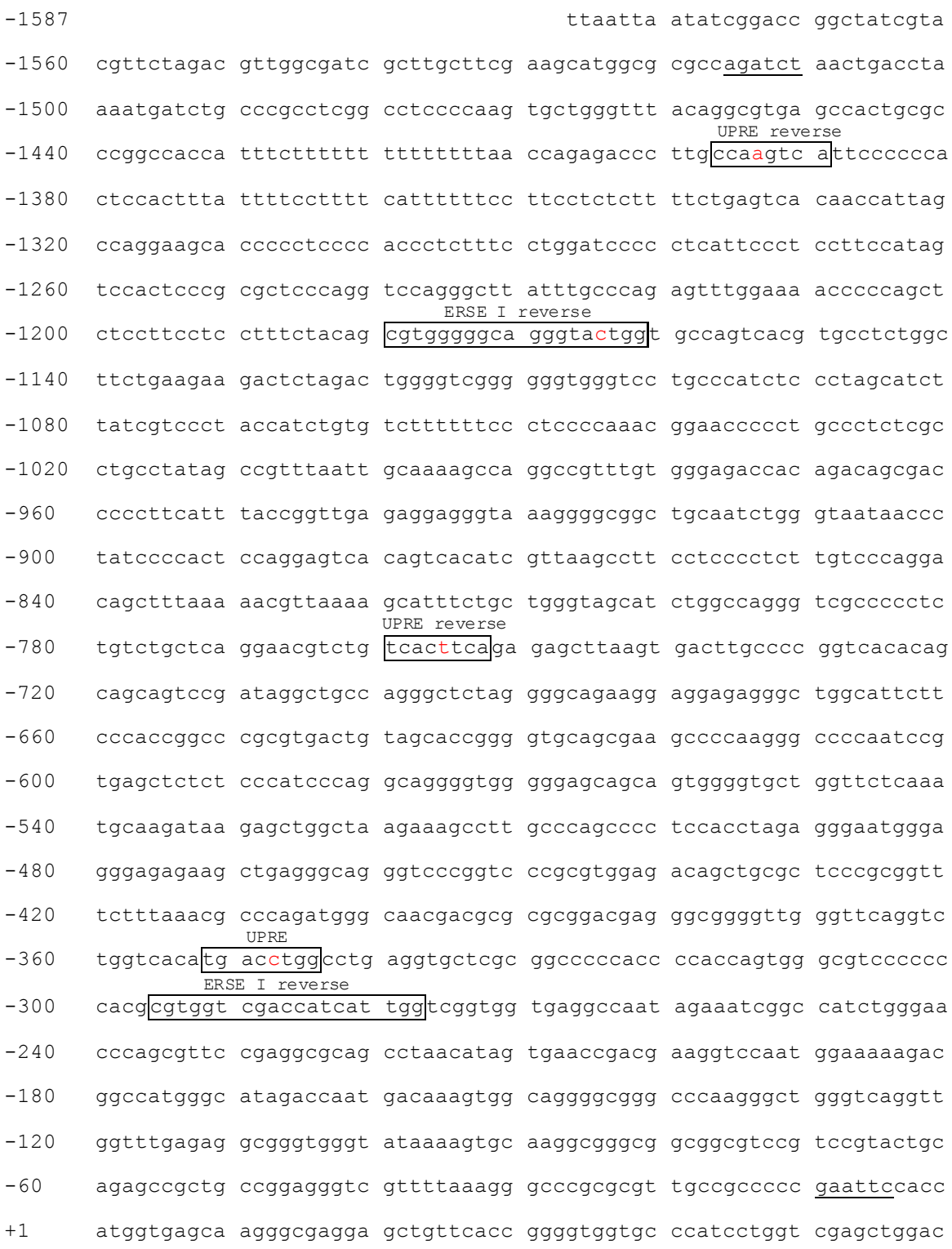

Fig. 17: Nucleotide sequence upstream of the d2eGFP reporter gene of vector 1101 (CALR reporter)

Different cis-acting elements are boxed and the BglII and the EcoRI restriction sites are underlined. Deviations from the consensus sequence of the cis-acting elements are indicated in red. The CALR promoter region including the 5' UTR is located from -11 to -1510, and the translation start site is located at +1.

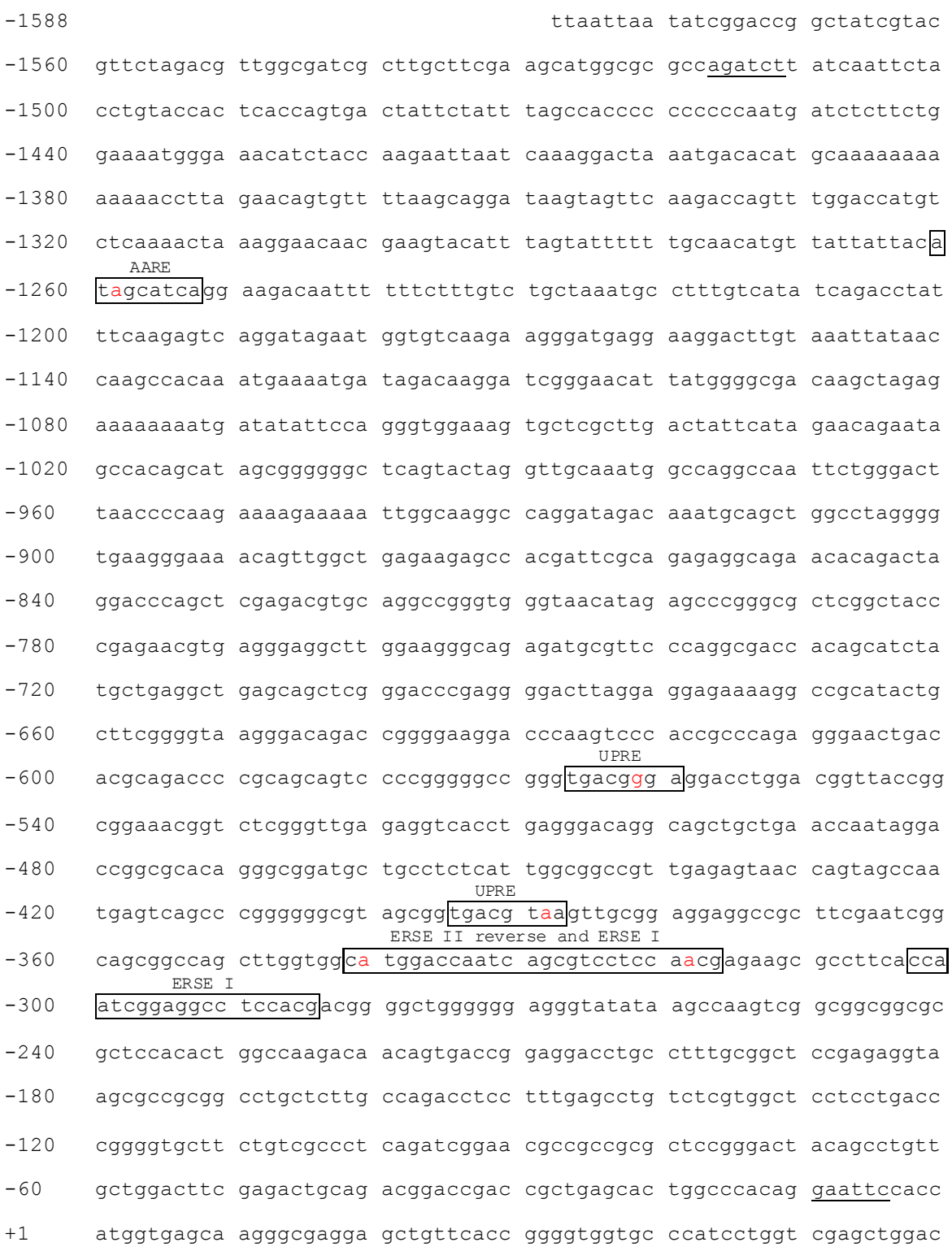

Fig. 18: Nucleotide sequence upstream of the d2eGFP reporter gene of vector 1103 (GRP78 reporter)

Different cis-acting elements are boxed and the BglII and the EcoRI restriction sites are underlined. Deviations from the consensus sequence of the cis-acting elements are indicated in red. The GRP78 promoter region including the 5' UTR is located from -11 to -1511, and the translation start site is located at +1.

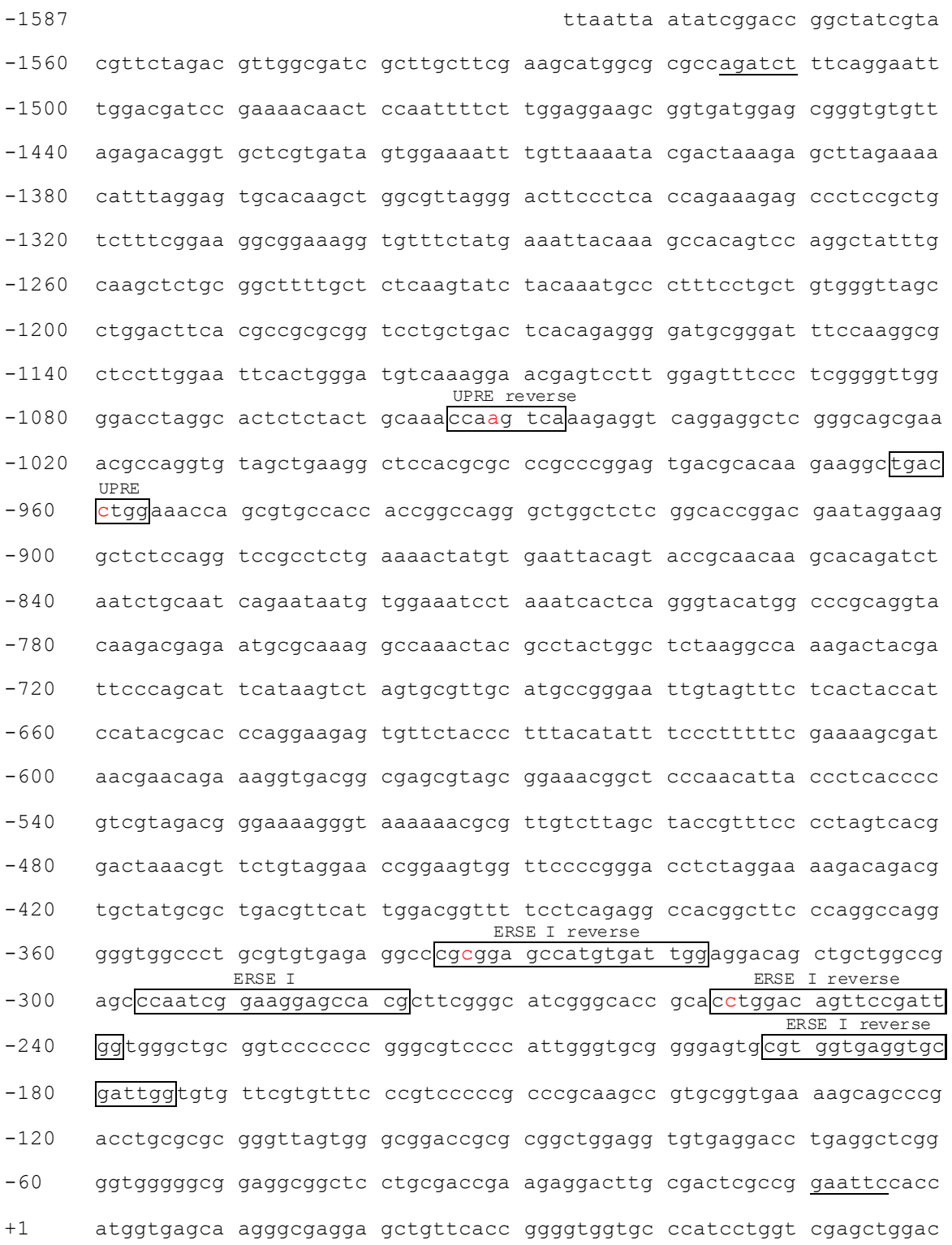

Fig. 19: Nucleotide sequence upstream of the d2eGFP reporter gene of vector 1104 (GRP94 reporter)

Different cis-acting elements are boxed and the BglII and the EcoRI restriction sites are underlined. Deviations from the consensus sequence of the cis-acting elements are indicated in red. The GRP94 promoter region including the 5' UTR is located from -11 to -1510, and the translation start site is located at +1.

In order to create a reporter construct responsive to XBP1-mediated ER stress, an intron sequence derived from XBP1 was inserted in the d2eGFP coding region of vector 917. Therefore, a NotI/SacII cloning site followed by an artificial translation stop codon (tag) were introduced between the coding sequence of eGFP and the adjacent PEST signal by site-directed mutagenesis. Subsequently, a XBP1 fragment was isolated from genomic DNA derived from CHO DG44 cells by preparative PCR, thereby introducing a NotI and a SacII site at the 5' and the 3' end, respectively. This fragment was inserted into the mutated vector 917 via NotI/SacII, resulting in vector 1023. The corresponding DNA sequence of the modified eGFP is depicted in Fig. 20.

```
+1     atggtgagca agggcgagga gctgttcacc ggggtggtgc ccatcctggt cgagctggac
+61    ggcgacgtaa acggccacaa gttcagcgtg tccggcgagg gcgagggcga tgccacctac
+121   ggcaagctga ccctgaagtt catctgcacc accggcaagc tgcccgtgcc ctggcccacc
+181   ctcgtgacca ccctgaccta cggcgtgcag tgcttcagcc gctaccccga ccacatgaag
+241   cagcacgact tcttcaagtc cgccatgccc gaaggctacg tccaggagcg caccatcttc
+301   ttcaaggacg acggcaacta caagacccgc gccgaggtga agttcgaggg cgacaccctg
+361   gtgaaccgca tcgagctgaa gggcatcgac ttcaaggagg acggcaacat cctggggcac
+421   aagctggagt acaactacaa cagccacaac gtctatatca tggccgacaa gcagaagaac
+481   ggcatcaagg tgaacttcaa gatccgccac aacatcgagg acggcagcgt gcagctcgcc
+541   gaccactacc agcagaacac ccccatcggc gacggccccg tgctgctgcc cgacaaccac
+601   tacctgagca cccagtccgc cctgagcaaa gaccccaacg agaagcgcga tcacatggtc
+661   ctgctggagt tcgtgaccgc cgccgggatc actctcggca tggacgagct gtacaaggcg
+721   gccgctgatc ctgacgaggt tccagagacg gagtccaagg gaaatggagt aaggccggtg
                                        intron
+781   gccgggtctg ctgagtccgc agcactcaga ctacgtgcac ctctgcagca ggtgcaggcc
+841   cagttgtcac ctccccagaa catcttcccg cggagtagcc atggcttccc gccggaggtg
+901   gaggagcagg atgatggcac gctgcccatg tcttgtgccc aggagagcgg gatggaccgt
+961   caccctgcag cctgtgcttc tgctaggatc aatgtgtag
```

Fig. 20: Nucleotide sequence of the XBP1 intron reporter gene of vector 1023 (Intron Reporter)

The NotI and SacII restriction sites are underlined, the introduced stop codon (TAG) and a 26 bp intron is boxed. The coding region of eGFP is located from +1 to +717, and the XBP1 fragment from +726 to +867. The coding region of the PEST sequence from murine ornithine decarboxylase (MODC) is located from +877 to +999.

A truncated GRP78 promoter was cloned into vector 526B using the SpeI restriction site. The obtained construct comprised a TK promoter followed by a neomycin resistance gene and the eGFP reporter gene driven by the truncated GRP78 promoter. The cloning procedure for the insertion of the truncated GRP78 promoter into vector 526B is described in Fig. 21.

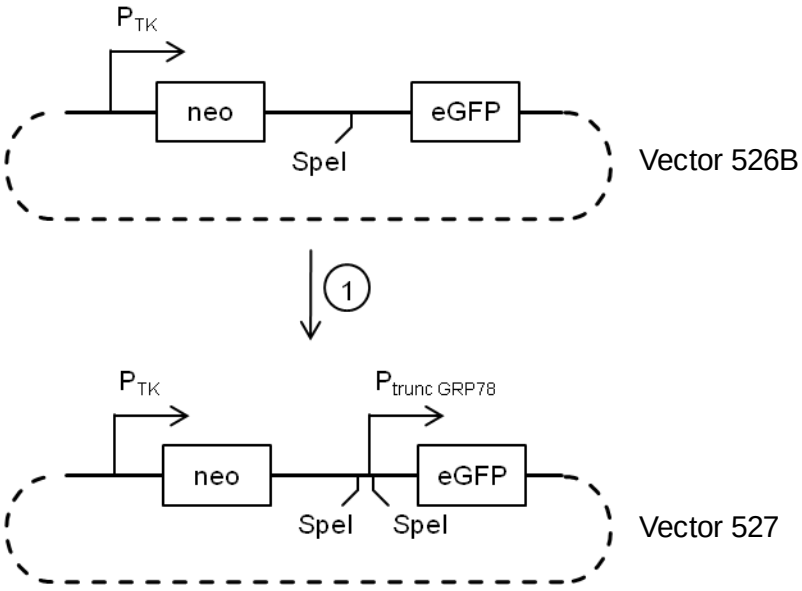

Fig. 21: Schematic representation of the cloning procedure of vector 527

By preparative PCR, a truncated GRP78 promoter region was isolated using genomic DNA derived from CHO DG44 cells. Thereby, a SpeI restriction site was introduced at the 5' and the 3' end. The obtained PCR product was digested with the restriction endonuclease SpeI and the GRP78 promoter (606 bp) was inserted in vector 526B via SpeI, resulting in vector 527. The corresponding DNA sequence upstream of the eGFP of the ER stress reporter constructs is shown in Fig. 22.

```
-691                                    t aaaatcgata agatccgtcg acaaaccaca
                                                                UPRE
-660   actagaatgc agtactagag gcgcccttgc tcaccatggt ggcgactagt gacgggagga

-600   cctggacggt taccggcgga aacggtctcg ggttgagagg tcacctgagg gacaggcagc

-540   tgctgaacca ataggaccgg cgcacagggc ggatgctgcc tctcattggc ggccgttgag
                                                          UPRE
-480   agtaaccagt agccaatgag tcagcccggg gggcgtagcg gtgacgtaag ttgcggagga
                                                ERSE II reverse and ERSE I
-420   ggccgcttcg aatcggcagc ggccagcttg gtggcatgga ccaatcagcg tcctccaacg
                                ERSE I
-360   agaagcgcct tcaccaatcg gaggcctcca cgacggggct ggggggaggg tatataagcc

-300   aagtcggcgg cggcgcgctc cacactggcc aagacaacag tgaccggagg acctgccttt

-240   gcggctccga gaggtaagcg ccgcggcctg ctcttgccag acctcctttg agcctgtctc

-180   gtggctcctc ctgacccggg gtgcttctgt cgccctcaga tcggaacgcc gccgcgctcc

-120   gggactacag cctgttgctg gacttcgaga ctgcagacgg accgaccgct gagcaactag

-60    tgaggggagg acctgaacgg tcagcccgcc tgcctgactg ctgagcgcct agtcgccacc

+1     atggtgagca agggcgagga gctgttcacc ggggtggtgc ccatcctggt cgagctggac
```

Fig. 22: Nucleotide sequence upstream of the eGFP reporter gene of vector 527

Different cis-acting elements are boxed, and the SpeI restriction sites are underlined. Deviations from the consensus sequence of the cis-acting elements are indicated in red. The truncated GRP78 promoter region is located from -66 to -671, and the translation start site is located at +1.

In order to achieve enhanced FLPO expression, vector 673 was created as described in Fig. 23.

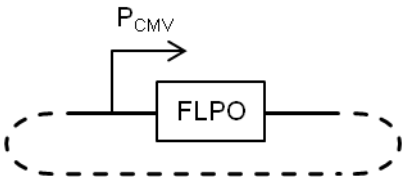

Fig. 23: Schematic representation of vector 673

Vector pFlpo-Puro (Raymond 2007) was kindly provided by Prof. Bode (HZI Braunschweig). The FLPO was isolated by a PCR and the obtained fragment was then cloned in a vector which enables to express the FLPO under the control of a CMV promoter.

Vector 957 was created in order to tag CHO DG44 cells with an exchangeable DsRed RMCE acceptor construct. The cloning procedure of vector 957, comprising a SV40E promoter, a DsRed fluorescence gene, an IRES element, a HygTK fusion protein and heterospecific FRT-sites (FRTwt and FRT3) is described in Fig. 24.

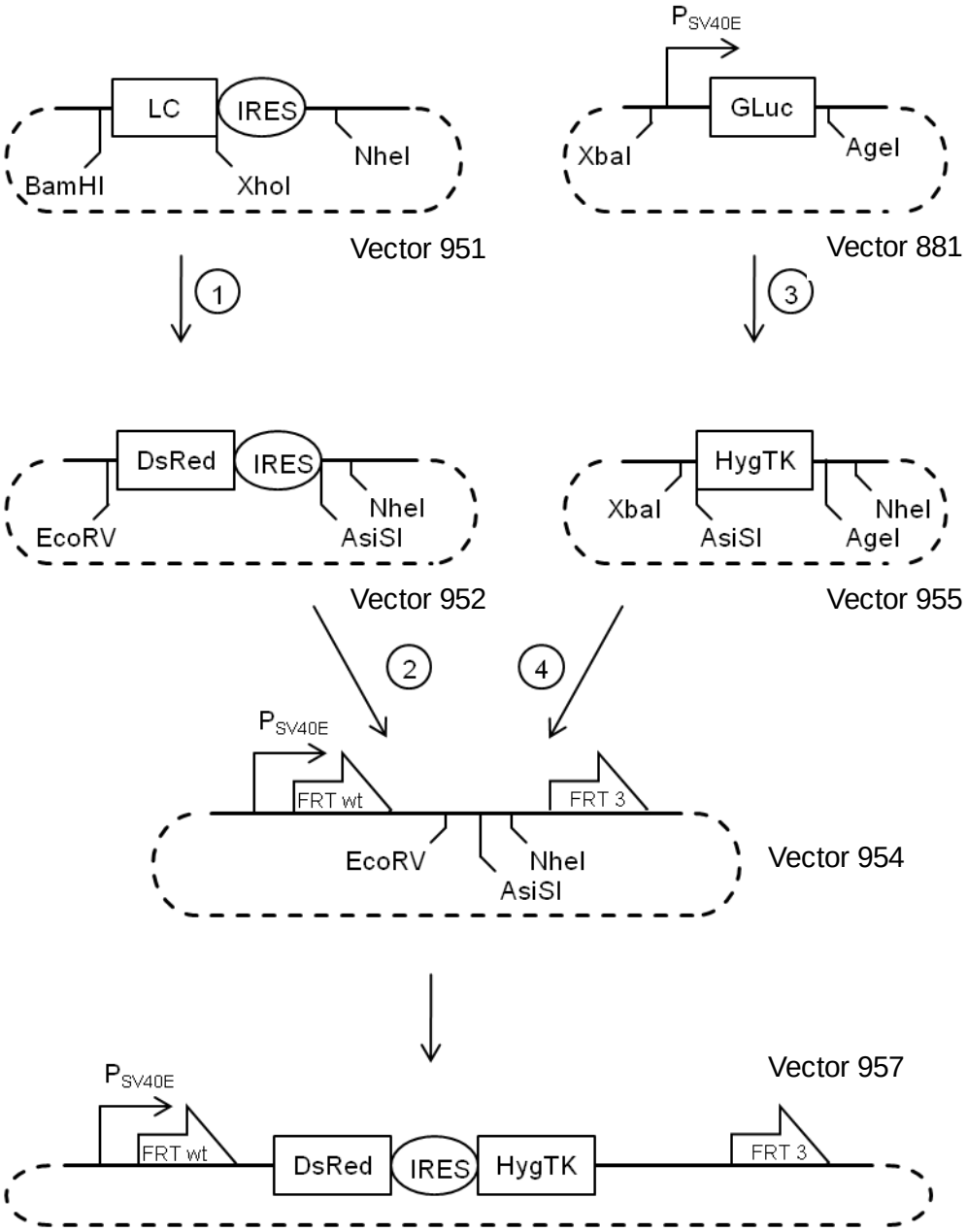

Fig. 24: Schematic representation of vector 957

Step 1: By preparative PCR, the coding region for DsRed was amplified using the pDsRed-Express-N1 vector (Clontech) as PCR template. Thereby, BglII and SalI restriction sites were introduced at the 5' and the 3' end, respectively. The obtained PCR product was cloned into the pJET1.2/blunt vector (Fermentas) and digested with the restriction endonucleases BglII and SalI. After that, vector 951 was digested with the restriction endonucleases BamHI and XhoI and the DsRed fragment was transferred into this vector, resulting in vector 952. (Comment: The cleavage with the restriction endonucleases BglII and BamHI as well as SalI and XhoI creates compatible DNA extensions). Step 2: The EcoRV/NheI DNA fragment was transferred from vector 952 to vector 954. Step 3: Vector pF3HygTKF (Schlake 1994) was used to isolate the HygTK sequence by preparative PCR. Thereby, the restriction sites XbaI/AsiSI and AgeI were introduced at the 5' and the 3' end, respectively. The obtained PCR product was cloned into the pJET1.2/blunt vector (Fermentas) and digested with the restriction endonucleases XbaI and AgeI. The obtained DNA fragment was cloned into vector 881, resulting in vector 955. Step 4: The AsiSI/NheI DNA fragment was transferred from vector 955 to vector 954 resulting in the final expression vector 957.

Vector 1071 is a RMCE donor construct coding for GTN, flanked by heterospecific FRT-sites. This vector was generated as described in Fig. 25.

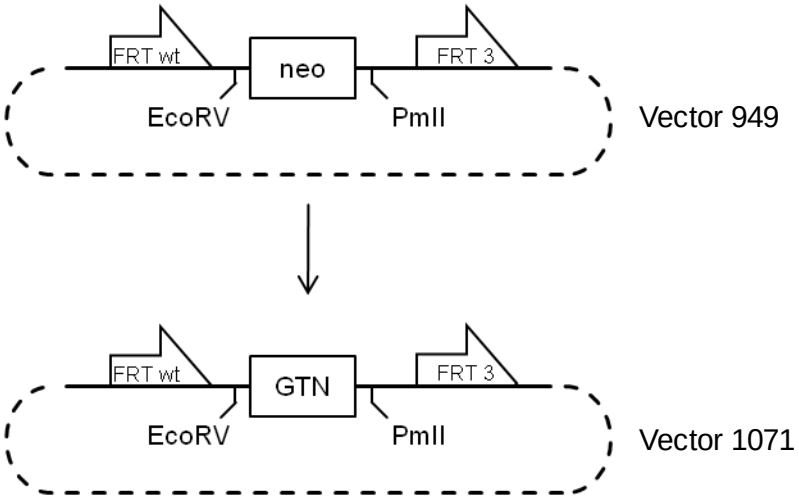

Fig. 25: Schematic representation of vector 1071

Vector pF3ESGTNWF (Baer 2002) was used by Cellca GmbH to isolate the GTN sequence by preparative PCR. Thereby, EcoRV and PmlI restriction sites were introduced at the 5' and the 3' end, respectively. The obtained PCR product was cloned into the pJET1.2/blunt vector (Fermentas). After that, the MluI, KpnI, BspEI and SpeI restriction sites within the coding sequence of GTN were destroyed by the silent mutations 742G>C, 1243C>T, 1136T>C and 1846T>C. All mutations were done with the aid of the QuikChange II Site-Directed Mutagenesis Kit (Stratagene). The obtained construct was digested with the restriction endonucleases EcoRV and PmlI and the optimized GTN fragment was cloned into vector 949, resulting in vector 1071.

Vector 726 has been used to develop antibody producing cell lines. As control construct a corresponding mock vector expressing only dhfr was developed. The cloning procedure is described in Fig. 26.

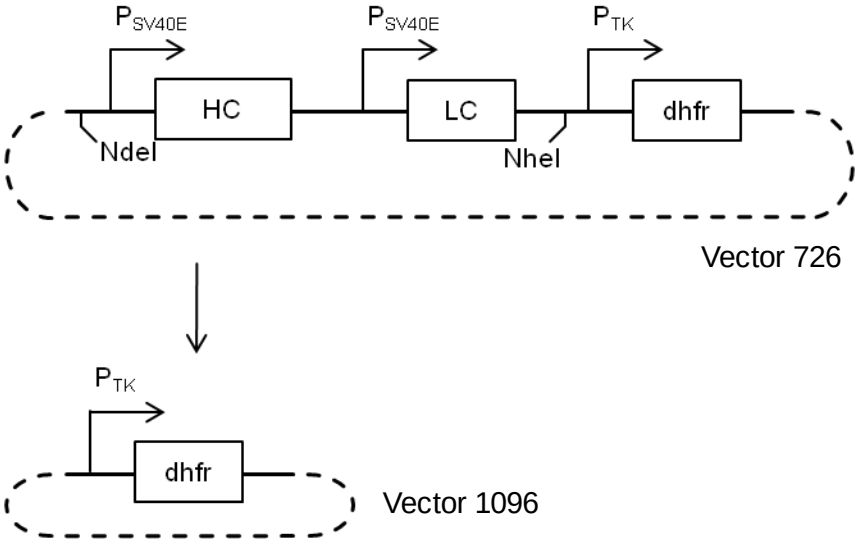

Fig. 26: Schematic representation of vector 1096

The coding region for the immunoglobulin heavy and light chains, as well as, their promoters were removed with the aid of the restriction endonucleases NdeI and NheI. After blunting with T4 polymerase and religation, the Mock vector was generated. This vector comprised the remaining TK promoter and the dhfr gene.

5.2.4. Preparative polymerase chain reaction on genomic DNA

In order to isolate specific DNA sequences from mammalian cells, genomic DNA was prepared (see chapter 5.2.21) and a PCR mixture was set up as shown in Tab. 11. The PCR was performed according to the cycling conditions listed in Tab. 12

Tab. 11: Reaction mixture for preparative PCR on genomic DNA

Volume	Component	Final concentration
9.85 µL	Water	
3.0 µL	HF buffer	1 x
0.2 µL	genomic DNA	2.0 ng/µL
0.75 µL	forward Primer	0.5 µM
0.75 µL	reverse Primer	0.5 µM
0.3 µL	dNTPs	200 µM
0.15 µL	Phusion DNA Polymerase	0.02 U/µL
---		
15 µL		

Tab. 12: PCR cycling conditions

Denaturation	98°C	for 30 s		
Amplification	98°C	for 15 s	Denaturation	35x
	X °C	for 15 s	Hybridization	
	72°C	for 90 s	Elongation	
Final Extension	72°C	for 10 min		
Cooling	4°C	hold endless		

All primers were self designed and synthesized by a commercial provider (Eurogentec). The sequences of the used primer pairs and the corresponding targets are shown in Tab. 13.

Tab. 13: Used PCR primers and their targets on genomic DNA

Target	Sequence of primer (5'-3')	Name of primer	Amplicon	T_M
CALR	agtggagatgggttttcacc	ON49-1D	1643 bp	60.0 °C
	acctccgtccaagaactgctc	ON49-2C		
GRP78	tcaatgttatgacagtattacaagc	ON49-5B	2463 bp	64.0 °C
	atcctccttcttgtcctcctc	ON49-6		
GRP94	catcatctgcagaaacttctacc	ON49-7	2012 bp	55.0 °C
	ggtcactcaccgaaggtcagc	ON49-8		
XBP1	gggaatgcggccgctgatcctgacgaggttccagag	ON48-1	168 bp	50.0 °C
	cagagtccgcgggaagatgttctgggg	ON48-2		

5.2.5. Analytical polymerase chain reaction on genomic DNA

To verify recombinase mediated cassette exchange (RMCE) of tagged clones, genomic DNA was prepared (see chapter 5.2.21) and PCR mixtures were set up as shown in Tab. 14. As described in Tab. 16, various primer combinations were used to differentiate between authentic exchange events (ON62-1C and ON62-3C), unexchanged acceptor cassettes (ON62-1C and ON62-4) and random integrations of the donor construct (ON62-2 and ON62-3C). All primers were self designed and synthesized by a commercial provider (Eurogentec). PCRs were performed according to the cycling conditions listed in Tab. 15.

Tab. 14: Standard analytical PCR reaction on genomic DNA

Volume	Component	Final concentration
9.3 µL	Water	
3.0 µL	Buffer	1 x
0.75 µL	genomic DNA	5.0 ng/µL
0.75 µL	forward Primer	0.5 µM
0.75 µL	reverse Primer	0.5 µM
0.3 µL	dNTPs	200 µM
0.15 µL	Phusion DNA Polymerase	0.02 U/µL
---		
15 µL		

Tab. 15: PCR cycling conditions

Denaturation	98°C	for 2 min		
Amplification	98°C	for 10 s	Denaturation	35x
	64°C	for 15 s	Hybridization	
	72°C	for 25 s	Elongation	
Final Extension	72°C	for 2 min		
Cooling	4°C	hold endless		

Tab. 16: Used PCR primers and their targets on genomic DNA

Target	Sequence of primer (5'-3')	Name of primer	Amplicon
SV40E on RMCE acceptor	tgaggcggaaagaaccag	ON62-1C	549 bp
neo on RMCE donor	atcagagcagccgattgtc	ON62-3C	
SV40E on RMCE acceptor	tgaggcggaaagaaccag	ON62-1C	749 bp
DsRed on RMCE acceptor	cgtcctcgaagttcatcac	ON62-4	
SR on RMCE donor	aaataggggttccgcgcac	ON62-2	293 bp
neo on RMCE donor	atcagagcagccgattgtc	ON62-3C	

5.2.6. Site-directed mutagenesis

Point mutations on plasmids were introduced with the QuikChange II Site-Directed Mutagenesis Kit (Stratagene) as described in the manufacturer's manual. The used primers had a length of 25 bp to 45 bp and annealed to the same sequence on opposite strands of the plasmid. They were designed with the web-based program QuikChange Primer Design (Stratagene) and synthesized by a commercial provider (Eurogentec).

5.2.7. Oligonucleotide annealing

In order to generate short dsDNA linkers (20-60 bp), two complementary oligonucleotides were annealed. Therefore, a solution containing 1x Buffer for T4 DNA Ligase (NEB), 25 µM of the forward and 25 µM of the reverse oligonucleotide was prepared, mixed and transferred to a thermocycler. Following an incubation period of 10 min at 95°C, the temperature was stepwise decreased every 27 s by 0.7°C. After 100 steps a temperature of 25°C was reached and the mixture was directly used or stored at -20°C.

5.2.8. Restriction digests, blunting, and dephosphorylation

Plasmid DNA or linear DNA, which was generated by PCR, was digested by restriction endonucleases (NEB), using the recommended buffer and 1x BSA solution as described by the manufacturer. 2 U enzym per 1 µg DNA were added and the reaction mixture was incubated for at least 1 h at the appropriate temperature (mostly at 37°C). Single-stranded 5' DNA extensions were filled up by using the 5' to 3' DNA synthesis activity of T4 DNA Polymerase (NEB). For this purpose, standard digestion reaction mixtures containing Buffer 1, 2, 3, or 4 (NEB) were supplemented with 100 µM dNTPs and 1 U T4 DNA Polymerase per 1 µg DNA followed by an incubation period of 15 min at 12°C. Alternatively, single-stranded 5' or 3' DNA extensions were removed by the endonuclease activity of Mung Bean Nuclease (NEB). For this purpose, standard digestion reaction mixtures containing Buffer 1, 2, or 4 (NEB) were supplemented with 1 U Mung Bean Nuclease per 1 µg DNA and incubated for 30 min at 30°C. To avoid religations of linearized vectors during ligation reactions, 5' phosphate groups were removed with Antarctic Phosphatase (NEB). Therefore, digestion reaction mixtures were supplemented with Antarctic Phosphatase Buffer (NEB) and 0.2 to 1 U Antarctic Phosphatase per 1 µg DNA. The reaction mixture was incubated at 37°C for 15 min in case of 5' extensions or blunt ends and for 60 min in case of 3' extensions.

5.2.9. Agarose gel electrophoresis

Agarose gel electrophoresis was used, in order to separate DNA fragments according to fragment size. For the preparation of agarose gels, between 0.8-3% agarose were dissolved in 100 mL 1x TBE buffer by heating in a microwave. Then, ethidium bromide was added in a final concentration of 0.5 µg/mL and the mixture was filled in a gel tray placed in a casting chamber. A plastic comb was inserted to form slots for the DNA samples. After the gel was cooled down, the comb was removed and the gel was transferred to an electrophoresis chamber (Bio-Rad) filled with 1x TBE buffer or stored at 4°C.

DNA samples supplemented with 5x Loading Dye (NEB) and DNA size standards (Tab. 17) were filled into the slots and a constant voltage of 140 V was applied for 30 to 60 min by a Power Pac 200 gel electrophoresis system (Bio-Rad). Subsequently, the separated DNA fragments were visualized and documented with a gel documentation system (E.A.S.Y. 400K Win32 Gel Documentation System; Herolab). If necessary, desired DNA fragments were excised with surgical blades (Swann Morton) and the DNA was extracted and purified as described in chapter 5.2.10.

Tab. 17: DNA size standards

Component	Specification
100 bp DNA Ladder (NEB)	100, 200, 300, 400, 500, 600, 700, 800, 900, 1000, 1200, 1517 bp
1 kb DNA Ladder (NEB)	0.5, 1.0, 1.5, 2.0, 3.0, 4.0, 5.0, 6.0, 8.0, 10.0 kb

5.2.10. Gel extraction and purification of DNA

To remove disturbing buffers and enzymes from DNA samples or to isolate DNA fragments from agarose gels, the E.Z.N.A. Gel Extraction Kit (Omega) was used according to the manufacturer's manual. The purified DNA was eluted with 30 µL WFI.

5.2.11. Ligation of DNA fragments

To ligate two DNA fragments, vector and insert DNA were used in a molar ratio of 1 to 4. A standard ligation mixture of 10 µL contained 100 ng total DNA, 1x Buffer for T4 DNA Ligase (NEB), 2.5% PEG 4000 (Fermentas) and 0.5 µL T4 DNA Ligase (NEB) was prepared and incubated for 1 to 2 h at room temperature.

5.2.12. Preparation of agar plates

Agar plates were prepared to cultivate transformed bacteria. Therefore, 40 g/L LB-agar (Roth) was dissolved in WFI and autoclaved for 20 min at 121°C. After the medium cooled down to about 50°C the appropriate antibiotics (100 µg/mL Ampicillin (Sigma) or 50 µg/mL Kanamycin (Sigma)) were supplemented. Hence approximately around 25 mL media has been filled into 10 cm petri dishes and after 1 h all plates were stored at +4°C.

5.2.13. Transformation of bacteria

An aliquot of 25 µL transformation competent *E. coli* (see Tab. 18) was thawed at 4°C and transferred to a pre-chilled 1.5 mL tube (Sarstedt). 2.5 µL DNA solution (e.g. a ligation mixture) was added, the cells were mixed by tapping and incubated for 30 min at 4°C. Subsequently, the cells were heat pulsed for 30 s at 42°C and placed again at 4°C for 5 min. 250 µL S.O.C. medium (NEB) was added followed by an incubation period of 1 h at 37°C and 300 rpm in a thermomixer (Eppendorf). Finally, the transformed cells were spread on agar plates containing appropriate antibiotics and cultivated over night at 37°C.

Tab. 18: Overview of *E. coli* stains and their application

***E. coli* stains**	**Recommended application**
NEB 5-alpha	used for plasmids smaller than 10 kbp
NEB 10-beta	used for plasmids larger than 10 kbp
JM100	used in order to produce plasmids free of Dam and Dcm methylation

5.2.14. Linearization of plasmids for transfection

In order to generate linear DNA constructs for the transfection of mammalian cells, a reaction mixture was prepared as shown in Tab. 19 and incubated at 37°C for at least 3 h.

Tab. 19: Standard reaction mixture for plasmid linearization

Volume	**Component**	**Final concentration**
108.5 µL	Water	
15.0 µL	10x Buffer 4	1 x
19.0 µL	plasmid DNA	0.25 µg/µL
7.5 µL	BspHI	2.0 U/µg DNA
---		
150 µL		

The linearized DNA was purified and concentrated by isopropanol precipitation (see chapter 5.2.16), dissolved in 50 µL Tris Buffer (10 mM, pH 8.0, Applichem) and stored at -80°C.

5.2.15. Excision of plasmids for transfection

In order to generate linear DNA constructs for the transfection of mammalian cells, which are free of the bacterial vector backbone, a reaction mixture was prepared as shown in Tab. 20 and incubated at 37°C for at least 3 h. Subsequently, the DNA was separated by agarose gel electrophoresis and the desired DNA fragment was excised and subjected to gel extraction. The eluted DNA was purified and concentrated by isopropanol precipitation (see chapter 5.2.16), dissolved in 50 µL of Tris Buffer (10 mM, pH 8.0, Applichem) and stored at -80°C.

Tab. 20: Standard reaction mixture for plasmid excision

Volume	Component	Final concentration
101.0 µL	Water	
15.0 µL	10x Buffer 3	1 x
19.0 µL	plasmid DNA	0.25 µg/µL
7.5 µL	MluI	2.0 U/µg DNA
7.5 µL	SalI-HF	2.0 U/µg DNA
---		
150 µL		

5.2.16. Isopropanol precipitation

Isopropanol precipitation was performed in order to concentrate linearized plasmid DNA prior to transfection. A standard mixture was prepared in a sterile 1.5 mL tube as exemplified shown in Tab. 21 and gently mixed.

Tab. 21: Standard mixture for isopropanol precipitation

Composion of standard mixture	
1.0 mL	DNA Solution
0.7 mL	2-propanol (99.8 %)
0.1 mL	sodium acetate (3 M, pH 5.2)

The mixture, containing the formed precipitate was centrifuged with a Biofuge fresco (Heraeus) for 30 min at 13000 rpm and 4°C and the supernatant was discarded. Subsequently, the DNA pellet was washed twice as follows: 1 mL ethanol (70%) was added, the tube was centrifuged at 4°C for 5 min at 13000 rpm and the supernatant was decanted. The tube was placed in a laminar flow box and dried until the pellet appeared transparent. The pellet was resuspended in sterile Tris Buffer (10 mM, pH 8.0, Applichem), mixed and incubated for about 1 h at room temperature. The DNA concentration was adjusted to 2000 ng/µL by using sterile Tris Buffer (10 mM, pH 8.0, Applichem). Before storage, concentration and quality of the prepared DNA was checked by measuring OD230, OD260 and OD280 with a Photometer (Bio Photometer,

Eppendorf). Pure DNA should have an OD260/OD280 ratio between 1.80 and 2.00 and an OD260/OD230 ratio between 1.90 and 2.40.

5.2.17. Preparation of glycerol stock cultures

Glycerol stock cultures were prepared to store transformed bacteria for a longer time. Therefore, 1 mL of a bacterial culture, grown for around 16 h, was transferred to a 1.8 mL CryoPure tube (Sarstedt) and supplemented with glycerol (Applichem) to a final concentration of 17.5%. The suspension was thoroughly mixed and stored at -80°C.

5.2.18. Preparation of LB and TB medium

LB and TB medium were used during mini or maxi preparation of plasmid DNA from bacteria. In order to prepare the LB medium 25 g/L LB-Broth (Roth) was dissolved in WFI, autoclaved for 20 min at 121°C and stored at +4°C. TB medium was autoclaved and stored in the same way, but this time 47.6 g/L TB medium powder (Roth) and 4 mL/L glycerol (Applichem) were dissolved in WFI. The appropriate antibiotics were supplemented immediately before use.

5.2.19. Maxi preparation of plasmid DNA from bacteria

In order to prepare large amounts of plasmid DNA, 200 mL TB medium (Roth) supplemented with 100 µg/mL Ampicillin (Sigma) or 50 µg/mL Kanamycin (Sigma) were filled in a 500 mL shake flask (Corning) and inoculated with a single bacterial colony or from a glycerol stock culture. The medium was placed in an incubator (Certomat IS, Sartorius) and shaken at 240 rpm and 37°C for 16 h. Subsequently, the plasmid DNA was prepared with the PureLink HiPure plasmid Filter Maxiprep Kit (Invitrogen) as described in the manufacturer's manual. The obtained DNA was dissolved in 200 µL Tris Buffer (10 mM, pH 8.0, Applichem) and stored at +4°C. Before storage, concentration and quality of the prepared DNA was checked by measuring OD230, OD260 and OD280 with a Photometer (Bio Photometer, Eppendorf). Pure DNA should have an OD260/OD280 ratio between 1.80 and 2.00 and an OD260/OD230 ratio between 1.90 and 2.40.

5.2.20. Mini preparation of plasmid DNA from bacteria

A single bacterial colony was used to inoculate a 13 mL tube (Sarstedt) filled with 5 mL LB-medium (Roth) containing 100 µg/mL Ampicillin (Sigma) or 50 µg/mL Kanamycin (Sigma). The tube was placed in an incubator (Certomat IS, Sartorius) and shaken at 240 rpm and 37°C for 16 h. Subsequently, the plasmid DNA was prepared with the E.Z.N.A. Plasmid Mini Kit I (Omega) according to the manufacturer's manual and stored at +4°C.

5.2.21. Preparation of genomic DNA from mammalian cells and from blood

In order to isolate genomic DNA from mammalian cells or from human blood, 6 x 10^5 cells or 1 mL blood, respectively, were treated with the AquaGenomic Kit (MoBiTec) as described in the manufacturer's manual. The prepared genomic DNA was dissolved in 100 µL water (Roth) and stored at -20°C.

5.2.22. Preparation of total RNA from mammalian cells and cDNA synthesis

In order to prepare total RNA from mammalian cells, 6 x 10^5 cells were transferred to a 1.5 mL tube (Sarstedt) and centrifuged with a Biofuge pico (Heraeus) for 2 min at 2000 rpm. The supernatant was discarded and the RNA was prepared using QIAshredder columns (Qiagen) and the RNeasy Plus Mini Kit (Qiagen) according to the manufacturer's instructions. To remove remaining genomic DNA, 3 µL of the obtained RNA solution were treated with 1x Baseline-Zero DNase Reaction Buffer (Epicentre) and supplemented with 1 µg/µL Baseline-Zero DNase I (Epicentre). After 30 min at 37°C, the reaction was stopped by the addition of 1x Baseline-Zero DNase Stop-Solution (Epicentre) followed by an incubation period of 10 min at 65°C.

The DNase-treated RNA was directly used for cDNA synthesis. For this purpose, the reaction mixture shown in Tab. 22 was prepared and incubated for 80 min at 37°C followed by 10 min at 70°C. The obtained cDNA was stored at -70°C.

Tab. 22: Reaction mixture for cDNA synthesis

Volume	Component	Final concentration
33.25 µL	Water (RNAse-free)	
7.0 µL	poly(A) Template RNA	1-50 ng
3.5 µL	oligo(dT)18 Primer	25.0 ng/µL
14.0 µL	Reaction buffer	1 x
1.75 µL	ScriptGuard Rnase Inhibitor	1.0 U/µL
7.0 µL	dNTP mix	1.0 mM
3.5 µL	M-MuLV Reverse Transcriptase	1.0 U/µL
---		
70 µL		

5.3. Cell biological methods

5.3.1. Mammalian cells and media

CHO K1 cells (ATCC no.: CCL-61) and CHO DG44 cells were obtained from the German Collection of Microorganisms and Cell Cultures (DSMZ) and from Lawrence Chasin (Columbia University, New York), respectively. CHO DG44 is a dhfr-deficient cell line, which was created by gamma ray mutagenesis of CHO K1 cells (Urlaub 1983). Originally, both cell lines were adherent and were cultivated in two different serum containing media Medium S1 and Medium S2, see Tab. 23.

At Cellca, the cells were adapted to serum free suspension growth conditions by using Medium D1 (for CHO DG44 cells) or Medium K1 (for CHO K1 cells)), respectively (see

Tab. 24). The serum concentration within both culture media was reduced gradually. Cells adapted to serum free media were finally cultivated under standard conditions as described in chapter 5.3.2.

Tab. 23: Culture media for adherent cell cultures

Composition of the first cultivation medium (Medium S1)	
1 L	CD Hybriboma Medium
100 mL	FB Serum
30 mL	L-Glutamine (200 mM)
20 mL	HT Supplement

Composition of the second cultivation medium (Medium S2)	
1 L	Modified CD CHO Medium
100 mL	FB Serum
30 mL	L-Glutamine (200 mM)
20 mL	HT Supplement

Tab. 24: Culture media for cell line adaption

Composition of adaption medium for CHO DG44 cells (Medium D1)	
1 L	CD DG44 Medium
100 mL	FB Serum
30 mL	L-Glutamine (200 mM)
10 mL	Pluronic F-68 Solution
Composition of adaption medium for CHO K1 cells (Medium K1)	
1 L	CD Hybridoma Medium
100 mL	FB Serum
30 mL	L-Glutamine (200 mM)
20 mL	HT Supplement
4 mL	Cholesterol Lipid Concentrate

5.3.2. Maintenance of cell lines cultivated under standard conditions

CHO DG44 and CHO K1 cells as well as all stable transfected cell lines created during this thesis were cultivated in 6 well plates filled with 3-5 mL or in 125 mL shake flasks (Corning) filled with 25 mL of the appropriate culture medium (see Tab. 25). After a cultivation period of 3 to 4 days, viable cell densities and viabilities were determined with a CASY cell counter (Roche) and cells were split into fresh medium at a concentration of 1 to 3 x 10^5 cells/mL. Throughout this study, all cells were cultivated under linear shaking (110 rpm, Bühler shaker, E. Bühler) in a humid atmosphere at 36.8°C and 7.5% pCO_2 (HERAcell 240, Thermo), unless otherwise noted (standard conditions).

Tab. 25: Culture media for cultivation under standard conditions

Composition of medium for CHO K1 wt cells (Medium K2)	
1 L	CD Hybridoma Medium
30 mL	L-Glutamine (200 mM)
20 mL	HT Supplement
4 mL	Cholesterol Lipid Concentrate

Composition of medium for CHO DG44 wt cells (Medium D2)	
1 L	CD DG44 Medium
30 mL	L-Glutamine (200 mM)

Composition of medium for CHO DG44 cells transfected with dhfr (Medium D3)	
1 L	CD CHO Medium
30 mL	L-Glutamine (200 mM)
10 mL	Pluronic F-68 Solution

Composition of medium for CHO DG44 wt cells (Medium D4)	
1 L	PID1-MD-SMD13
20 mL	HT Supplement
1 mL	Folinic acid (97.2 g/L)
1 mL	Glycine (4 g/L)

Composition of medium for CHO DG44 cells transfected with dhfr (Medium D5)	
/	PID1-MD-SMD13

Composition of medium for CHO DG44 cells transfected with dhfr (Medium D6)	
/	PID1-MD-SMD10

5.3.3. Transfection and sub-cultivation of CHO DG44 and CHO K1 cells

One day before transfection, cells were split 1:3 into fresh culture medium (Medium D2 for CHO DG44 cells and Medium K2 for CHO K1 cells). On the day of transfection, 3 to 10 µg circular, linearized or excised plasmid DNA were transferred to a 1.5 mL tube (Sarstedt) and 1 x 10^6 cells were centrifuged at 190 g for 3 min (Biofuge stratus, Heraeus). The supernatant was discarded, and the cell pellet was resuspended in 100 µL Nucleofector solution V (Nucleofector Kit for CHO, Lonza), which had been mixed before with Supplement 1 as described by the manufacturer. The cell suspension was transferred to the 1.5 mL tube containing the plasmid DNA and all components were mixed with a pipette and placed in an electroporation cuvette (Lonza). Subsequently, cells were transfected with a Nucleofector II device (Lonza) using program U24, 600 µL pre-warmed Medium D2 (for CHO DG44 cells) or Medium K2 (for CHO K1 cells) were added and the cell suspension was transferred to a 6-well plate filled with 3.3 mL

of the same medium. Following an incubation period of 1 h at 36.8°C and 7.5% pCO_2 without shaking, transfected cells were cultivated under standard conditions (see chapter 5.3.2).

5.3.4. Generation and sub-cultivation of mini-pools

Mini-pools were generated to separate different clones as early as possible, thereby avoiding overgrowth of high-expressing cells by low-producers. For this reason, 2 to 4 transfections each with 10 µg linearized DNA were performed as described in chapter 5.3.3. One day after transfection, all transfected cells were pooled and the viable cell concentration was determined. Subsequently, cells were subdivided into two pools and centrifuged at 190 g for 3 min (Biofuge stratus, Heraeus). One cell pellet was resuspended in pre-warmed Medium D3 and the other in pre-warmed Medium D3 supplemented with different MTX concentrations and with or without Hygromycin B. The viable cell concentrations were adjusted to 6667 cells/mL by using appropriate media volumes. For each pool, two 96 well flat bottom plates were filled with 150 µL cell suspension per well (resulting in 1000 cells/well) and incubated for 1 h under standard conditions without shaking. Subsequently, the plates were put into a ¾ closed Ziploc bag (Melitta) and cultivated under the same conditions for at least two weeks.

All grown mini-pools that covered 25-50% of the 96 well bottom were transferred into 24 well plates containing 1.0 mL/well of the appropriate selective medium (Medium D3 supplemented with different MTX concentrations and with or without Hygromycin B) and cultivated under standard conditions without shaking. Around three-fourths of the supernatant was exchanged for fresh medium every 3 to 4 days until clear cell accumulations became visible. All grown mini-pools were transferred into 12 well plates filled with 2.0 mL/well of the appropriate selective medium (Medium D3 supplemented with different MTX concentrations and with or without Hygromycin B) and treated as described for 24 well plates. Finally, all grown mini-pools were transferred to 6 well plates containing 4 mL/well of the same medium and cultivated under standard conditions for 3 to 4 days. From now on, mini-pools were subcultivated in 6 well plates or shake flask as described in chapter 5.3.2.

5.3.5. Single cell cloning and clone expansion

To generate monoclonal cell lines, single cell cloning employing a FACSAria cell sorter (Becton) was performed. For this purpose, at least 1 x 10^6 cells were filtered into a cell strainer tube (Becton) and used for FACS analysis and cell sorting. Death cells or cell aggregates were excluded by FSC/SSC gating and viable cells were analyzed with regard to DsRed or GFP fluorescence or other parameters, respectively. Desired clones were sorted (1 cell/well) into 96 well round bottom plates (TC Microwell 96U, Nunc) filled with 150 µL pre-warmed Medium C1 or

Medium C2. Following an incubation period of 1 h under standard conditions without shaking, the plates were put into a ¾ closed Ziploc bag (Melitta) and cultivated under the same conditions for at least two weeks.

All grown colonies with a diameter of around 2-3 mm were transferred into 24 well plates containing 1.0 mL/well of the selective medium (supplemented with MTX, G418 or Hygromycin B) which had been used before single cell cloning. Subsequently, cells were cultivated under standard conditions without shaking until a clear cell pellet was visible (usually after 3 to 5 days). After this time three-fourths of their supernatant was discarded, all grown clones were transferred into 12 well plates filled with 2.0 mL/well of the appropriate selective medium and cultivated for 3 to 4 days under standard conditions without shaking. Finally, all grown clones were transferred into 6 well plates filled with 4.0 mL/well of the same medium as described for 12 well plates and cultivated for 2 to 3 days under standard conditions. From now on, clones were subcultivated in shake flasks as described in chapter 5.3.2.

Tab. 26: Culture media for single cell cloning

Composition of medium for single cell cloning (Medium C1)	
1 L	CD CHO Medium
40 mL	Cellca´s proprietary cloning supplement
10 mL	L-Glutamine (200 mM)
0.5 mL	Cellca´s proprietary cloning supplement

Composition of medium for single cell cloning (Medium C2)	
1 L	CD DG44 Medium
40 mL	Cellca´s proprietary cloning supplement
10 mL	L-Glutamine (200 mM)
10 mL	Pluronic F-68 Solution
0.5 mL	Cellca´s proprietary cloning supplement

5.3.6. Fed-batch experiments

In order to perform fed-batch experiments, shake flasks containing 25 mL Production°Medium (Tab. 27) were inoculated with a viable cell concentration of 3 x 10^5 cells/mL and cultivated under standard conditions. The cultures were fed with Feed Medium A (PID1-MD-FMA70) and Feed Medium B (PID1-MD-FMB16) as depicted in Tab. 28. Every day, 1 mL sample was taken and viable cell density as well as viability were determined with a CASY cell counter (Roche).

Additionally, product concentrations were measured by Protein A-HPLC and pH, lactate and glucose concentration were determined with a blood gas analyzer (ABL800 FLEX, Radiometer). Whereas it was not necessary to adjust the pH or the L-glutamine concentration during the whole process, the glucose concentration was adjusted to 2 - 6 g/L by adding appropriate volumes of a 250 mM D-glucose solution.

Tab. 27: Culture media for fed-batch experiments

Composition of production medium (Production°Medium)	
1 L	PID1-MD-PM55
30 mL	L-Glutamine (200 mM)

Tab. 28: Feed media for fed-batch experiments

Day	3	4	5	6	7	8	9 until end of process
Feed Medium A [mL]	0.7	0.7	1.0	1.0	1.3	1.3	1.0
Feed Medium B [mL]	0.1	0.1	0.1	0.1	0.1	0.1	0.1

5.3.7. Recombinase mediated cassette exchange (RMCE)

For RMCE experiments, a genomically anchored DsRed RMCE acceptor construct comprising heterospecific FRT-sites (FRTwt and FRT3) has been used (Schlake 1994). An absolute lack of cross-interaction between both FRT-sites has been shown (Bode 2000 Sep-Oct). This enables a site specific exchange of the genomically anchored DsRed RMCE acceptor construct against a RMCE donor construct without a cross-interaction between both FRT-sites and the loss of the vector cassette (Bode 2000; Baer 2001).

RMCE of cell lines tagged with the DsRed RMCE acceptor construct was performed as follows: Cells were split into Medium D2 supplemented with 200 mg/L Hygromycin B at a viable cell concentration of 1 x 10^5 cells/mL and cultivated under standard conditions for 3 days. 1 x 10^6 cells were centrifuged (190 g, 3 min, room temperature), resuspended in 4 mL pre-warmed Medium D2 and transferred into a 6 well plate. Additionally, 0.4 mL Medium D2 was placed in a 1.5 mL tube and 6 µg of the desired RMCE donor construct, 1 µg of the FLPO construct, and 10 µL Turbofect reagent (Fermentas) were added. All components were mixed and incubated at room temperature for 15 min. The mixture was added to the cells previously prepared in 6 well plate followed by an incubation period of two days under standard conditions. Subsequently, the transfected cells were centrifuged (190 g, 3 min, room temperature), resuspended in Medium D2 supplemented with 500 mg/L G418 and subcultivated as described in chapter 5.2.2.

5.3.8. Calculation of cell specific productivity

Cell specific productivities were calculated based on viable cell densities measured with a CASY cell counter (Roche) and product concentrations determined with ELISA or Protein A-HPLC by using the following equation:

$$Q_P = \frac{P_2 - P_1}{\frac{(x_2 - x_1)}{\ln (x_2 - x_1)} \ (t_2 - t_1)}$$

Q_P = cell specific productivity [pg/cell/day]
P_1 = initial product concentration
P_2 = final product concentration
x_1 = initial cell concentration
x_2 = final cell concentration
t_1 = start date of cultivation
t_2 = final date of cultivation

5.3.9. Calculation of renilla specific product concentration

Product concentrations and renilla luminescence were determined on day 3 or 4 after transfection. The renilla specific product concentration was calculated by using the following equation:

$$P_{RL} = \frac{P_2 - P_1}{RL_2}$$

P_{RL} = Renilla specific product concentration [g/mL/RLU]
P_1 = initial product concentration
P_2 = final product concentration
RL_2 = final renilla luminescence

5.4. Analytical and biochemical methods

5.4.1. Measurement of viable cell concentration and viability

The viable and total cell concentration as well as the viability of a cell suspension was measured as follows: The cell suspension was thoroughly mixed by pipetting or swirling and an aliquot of 50 µL was taken and diluted in 10 mL CASY-ton isotonic solution (Roche) and analyzed with a CASY cell counter (Roche) as described in the manufacturer's manual. Because the CASY cell counter does not accept suspensions with very high cell concentrations, such samples were pre-diluted in an adequate volume of CASY-ton isotonic solution. For all measurements, the evaluation cursor (discriminates between live and dead cells) was set to 11.72 µm and the normalization cursor (discriminates between cell aggregates and dead cells) was set to 6.1 µm.

5.4.2. Human IgG enzyme-linked immunosorbent assay (qELISA, nqELISA)

Monoclonal antibody concentrations were determined by quantitative ELISA (qELISA) using the Human IgG ELISA Quantitation Kit (Bethyl) according to the manufacturer's instructions. Briefly, 96 well plates (MultiDish 6 Well, Nunc) were coated by adding 100 µL Coating Buffer containing 1 µL Capture Antibody Solution to each well. After 60 min, all wells were washed 3 times with 200 µL Wash Solution and 200 µL Blocking Solution were added. Following an incubation period of 30 min, the plates were washed again with 200 µL Wash Solution per well and stored at 4°C or used directly.

To create a standard curve, a series of 1:2 dilutions ranging from 0.5 µg/mL to 0.0078125 µg/mL was prepared with Human Reference Serum and Sample Diluent. Based on their expected concentration, the samples were diluted with Sample Diluent in an adequate manner to be within the range of the standard curve. 100 µL of samples and standards were then transferred to coated 96 well plates and incubated for 60 min. Subsequently, all wells were washed 5 times with 200 µL Wash Solution and incubated with 100 µL of a 1:150000 dilution of HRP Conjugate in Sample Diluent for 60 min. Again, all wells were washed 5 times with 200 µL Wash Solution and 100 µL "TMB Supersensitive One Component HRP Mircowell substrate" solution (BioTX Laboratories) were transferred to each well. After 10 min, the reaction was stopped by adding 100 µL 2 M H_2SO_4 (Roth) per well and absorbance at a wavelength of 450 nm was measured with an Appliskan microplate reader (Thermo). The antibody concentration was calculated according to the generated standard curve.

Non-qualitative ELISA (nqELISA) was performed in the same way as qELISA, but by comparison, all samples were diluted 1:20 and no standard curve was implemented.

Tab. 29: Used ELISA components

Component	Specification
Coating Buffer	0.05 M Carbonate-Bicarbonate, pH 9.6
Wash Solution	50 mM Tris, 0.138 M NaCl, 0.0027 M KCl, 0.05% Tween 20, pH 8.0
Blocking Solution	50 mM Tris, 0.138 M NaCl, 0.0027 M KCl, 1% BSA, pH 8.0
Sample Diluent	50 mM Tris, 0.138 M NaCl, 0.0027 M KCl, 1% BSA, 0.05% Tween 20
Capture Antibody Solution	Goat anti-Human IgG-Fc affinity purified
HRP Conjugate	Goat x-Human IgG-Fc HRP conjugated
Human Reference Serum	Human Reference Serum

5.4.3. High pressure liquid chromatography (HPLC)

Antibody concentrations of fed-batch experiments were determined with a HPLC device (Finnigan Surveyor Plus, Thermo Electron) equipped with a protein A column (Poros, 20 micron, Applied Bio systems). Depending on the expected antibody concentration between 1 and 50 µL sample (1 to 20 µg antibody) as well as 1, 5, 10, 15 and 20 µg of an antibody standard were injected, eluted as depicted in Tab. 30 and detected with an UV Detector (Surveyor PDA Plus Detector, Thermo Electron) at 280 nm. All chromatograms were integrated and the antibody concentration was calculated based on the generated standard curve by using Chrom Quest software (Thermo Electron).

Tab. 30: Elution conditions and components of mobile phase A and B

Time [min]	Fluids	Flow [mL/min]
01:00	100 % Mobile Phase A	2
03:05	Gradient: from 80/20 % Mobile Phase A/B to 100 % Mobile Phase B	2
00:15	100 % Mobile Phase B	2
02:55	100 % Mobile Phase A	2

Component	Specification
Mobile Phase A	10 mM NaH_2PO_4, 150 mM NaCl, pH 7.5
Modile Phase B	10 mM HCl, 150 mM NaCl, pH 2.0

5.4.4. FACS analysis

DsRed and GFP fluorescence of the cells were determined, employing a FACSAria flow cytometer (Becton). Therefore, around 1 x 10^6 cells were filtered into a cell strainer tube and used for FACS analysis. By a selective FSC/SSC gating procedure, dead cells and cell aggregates were excluded and viable cells were measured with regard to DsRed and GFP fluorescence.

5.4.5. Dual luciferase assay

All buffers and substrates required to determine renilla luminescence are included in the Dual-Glo Luciferase Reporter Assay System (Promega) and were prepared according to the manufacturer's instructions. Cell lines transiently transfected with plasmids coding for an antibody and the renilla luciferase reporter gene (hRluc) were used for analysis. For lysis, 75 µL cell suspension was transferred into a white flat bottom 96 well plate, 75 µL Dual-Glo Luciferase Reagent was added and the plate was mixed for 10 s. After an incubation time of 10 min at room temperature, 75 µL Dual-Glo Stop & Glo Reagent was added and the 96 well plate was mixed for 10 s and incubated for 10 min at room temperature. Finally, renilla luminescence was measured for 5 s using an Appliskan microplate reader (Thermo).

5.4.6. Real time RT-PCR

In order to perform real time RT-PCR reactions, the DyNamo Flash SYBR Green qPCR Kit (Finnzymes) was used according to the manufacturer's manual to set up a reaction mixture containing 0.5 µM of each primer (see Tab. 33) and around 7 µg cDNA (prepared as described in chapter 5.2.22). 20 µL of this mixture was transferred to a white "LightCycler 480 Multiwell Plate 96" (Roche) and the PCR program depicted in Tab. 31 was run using a Light Cycler 480 (Roche). All samples were analyzed in triplicate.

Tab. 31: PCR cycling conditions

Hot Start Activation	95°C	for 5 min		
Amplification	95°C	for 10 s	Denaturation	45x
	63°C	for 10 s	Hybridization	
	72°C	for 10 s	Elongation	

The crossing points were determined by the Light Cycler software and relative mRNA levels (fold induction) were calculated based on the following equation using beta-actin or neomycin as reference genes.

$$\text{Relative mRNA level} = \frac{2^{\text{CpTc}-\text{CpTs}}}{2^{\text{CpRc}-\text{CpRs}}}$$

Cp = crossing point
Tc = target gene, calibrator
Ts = target gene, sample
Rc = reference gene, calibrator
Rs = reference gene, sample

In order to determine PCR efficiencies, a 1 : 5 dilution series (5 dilutions) of one sample was prepared, the obtained crossing points were plotted against the logarithmic cDNA dilutions and a standard curve was generated. The PCR efficiency was calculated based on the slope of the standard curve with the following equation.

$$\text{E} = 10^{\left(\frac{-1}{\text{slope}}\right)}$$

Slope = slope of the standard curved derived from a cDNA dilution plot
E = PCR efficiency

PCR efficiencies were determined for all primer pairs they were very similar and almost 2.0. Primers for intron spanning assays were designed employing the “Universal ProbeLibrary” (Roche) for Cricetulus griseus. If a sequence was not available for Cricetulus griseus, one primer pair was calculated for Mus musculus and one for Rattus norvegicus (see Tab. 32), and the Cricetulus griseus primers were self-designed based on an alignment of the sequences obtained for mouse and rat. All primers were synthesized by a commercial provider (Eurogentec). The sequences of all primer pairs used during this study and the corresponding target genes are shown in Tab. 33.

Tab. 32: Rat and mouse target genes for RT-PCR primer design

Target gene	Accession number	Organism
CALR	NM_007591	Mus musculus
	NM_022399	Rattus norvegicus
GRP78	NM_022310	Mus musculus
	BC062017	Rattus norvegicus
GRP94	NM_011631	Mus musculus
	NM_001012197	Rattus norvegicus
XBP1 unspliced	NM_013842	Mus musculus
	NM_001004210	Rattus norvegicus
XBP1 spliced	NM_013842	Mus musculus
	NM_001004210	Rattus norvegicus

Tab. 33: RT-PCR primers and their corresponding target genes

Target gene	Accession number	Organism	Sequence of primer (5'-3')	Name of primer
beta actin	U20114	Cricetulus griseus	ccaaggccaaccgtgaaaag	ON40-13
			accagaggcatacagggaca	ON40-14
CALR	N/A	Cricetulus griseus	aagaatgtgctgatcaacaagg	ON45-3
			tgttgtctggccgcacaatc	ON45-4
GRP78	N/A	Cricetulus griseus	gtaacaatcaaggtctatgaagg	ON40-5
			aaggtgacttcaatctggggta	ON40-6
GRP94	N/A	Cricetulus griseus	tacttcatggctgggtcaagc	ON47-1
			attcatccacaggctctgtgag	ON47-2
neo	V00618	Escherichia coli	gatgcctgcttgccgaatatc	ON46-1
			gccacagtcgatgaatccaga	ON46-2
XBP1 unspliced	N/A	Cricetulus griseus	ggttgagaaccaggagttaag	ON43-1
			tgcagaggtgcacatagtctg	ON40-2
XBP1 spliced	N/A	Cricetulus griseus	ggttgagaaccaggagttaag	ON43-3
			ttctggggaggtgacaactg	ON40-4

5.4.7. DNA sequencing

All plasmids created during this study were analyzed by the sequencing provider GATC (Konstanz) to verify the DNA sequence of the constructs. Sequencing results were evaluated by using Vector NTI software (Invitrogen).

6. Results

6.1. Increase of antibody secretion by signal peptide optimization

The signal peptide has a major impact on the synthesis and secretion of recombinant proteins expressed in mammalian cells (Stern 2007). On the other hand, it has been demonstrated, that signal peptides are extremely heterogeneous regarding to their sequence, translocation and secretion efficiency. It has also been demonstrated, that many prokaryotic as well as eukaryotic signal peptides are functionally interchangeable between species (von Heijne 1985; Young 2008 (WO 2008/148519 A2); Stern 2007; Hesketh 2005 (WO 2005/001099 A2); Gierasch 1989; Tan 2002). Based on these observations, 19 promising signal peptides were identified by an extensive literature search and their potential to increase the extracellular amount of a monoclonal antibody expressed in CHO cells was tested. The selection included natural signal peptides covering a broad spectrum of species (mammals, fish, scorpions, snails, fungi, plants, viruses and bacteria) as well as artificial signal peptides, which are listed in Tab. 34. Especially, the signal peptides of human albumin, human azurocidin, human cystatin and yeast Alfa-Galactosidase (mutant m3) have been described as very potent (Sleep 2004 (WO 2004/009819 A2); Olczak 2006; Barash 2002; Hofmann 1991).

The three artificial signal peptides were designed according to rules reported in different publications, which are discussed in the following: Folz 1988 and Perlman 1983 report, that the c-region of a signal peptide requires small uncharged residues at position -3 and -1 for efficient cleavage by the signal peptidase (cf. Tab. 1). An aromatic and more often a hydrophobic residue are found at position -2, proline is very often found at position -5 and a hydrophobic residue like leucine or isoleucine is tolerated at position -4. (von Heijne 1983). Therefore, PLALA or PIALA was chosen as c-region of the designed signal peptides.

The key component of a signal peptide is its h-region, a simple stretch of about ten hydrophobic residues that primes the SRP, unlocks the translocon and positions the peptide for cleavage (von Heijne 1998). Rapoport 1986 showed, that the introduction of non-hydrophobic residues in the h-region dramatically reduces the translocation efficiency. Interestingly, an increase of hydrophobicity very often enhances the amount of secreted protein and a single poly-L10 stretch can be better than a natural h-region (Tsuchiya 2003; Tsuchiya 2004; Zhang 2005). Taking into account, that the maximum length of the hydrophobic poly-L stretch, which allows efficient cleavage, is 16 residues (Nilsson 2002), one h-region containing a poly-L12 and one containing a poly-I12 stretch was designed.

Moreover, it has been reported, that an increase of positive charge within the n-region resulted in an improved secretion (Tsuchiya 2003; Tsuchiya 2004), however, it is still unclear how many charged residues are required. Zhang 2005 postulated, that two arginine residues are optimal, whereas Tsuchiya 2003, Tsuchiya 2004 preferred 3 residues. Some signal peptides even contain negatively charged residues in their n-region (von Heijne 1986). Additionally, the most crucial element for efficient translation initiation is a guanine directly after the AUG start codon (Kozak 1986 Jan). In order to fulfil all these requirements, MARR or MAKK were used as n-region of the artificial signal peptides.

Tab. 34: Overview of all tested signal peptides

Name of construct	Signal peptide sequence	Accession number	Protein	Organism
A2	MDMRAPAGIFGFLLVLFPGYRS	/	Ig kappa light chain precursor (mutant A2)	Mus musculus
B	MKWVTFISLLFLFSSAYS	NP_000468	serum albumin preproprotein	Homo sapiens
C	MDWTWRVFCLLAVTPGAHP	AAA52897	immunoglobulin heavy chain	Homo sapiens
D	MAWSPLFLTLITHCAGSWA	AAA59018	immunoglobulin light chain	Homo sapiens
E	MTRLTVLALLAGLLASSRA	NP_001691	azurocidin preproprotein	Homo sapiens
F	MARPLCTLLLLMATLAGALA	NP_001890	cystatin-S precursor	Homo sapiens
G	MRSLVFVLLIGAAFA	AAC32752	trypsinogen 2 precursor	Pseudo-pleuronectes americanus
H	MSRLFVFILIALFLSAIIDVMS	ABR14604	potassium channel blocker	Mesobuthus martensii
J	MGMRMMFIMFMLVVLATTVVS	AAS93426	alpha conotoxin Ip1.3	Conus leopardus
K	MRAFLFLTACISLPGVFG	/	Alfa-Galactosidase (mutant m3)	Saccharo-myces cerevisiae
L	MKFQSTLLLAAAAGSALA	CAA03658	Cellulase	Aspergillus niger
M	MASSLYSFLLALSIVYIFVAPTHS	Q766C3	Aspartic proteinase nepenthesin-1	Nepenthes gracilis
N	MKTHYSSAILPILTLFVFLSINPS HG	ABF74624	acid chitinase	Nepenthes rafflesiana
O	MESVSSLFNIFSTIMVNYKSLVLA LLSVSNLKYARG	2205370A	K28 prepro-toxin	M28 Virus
P	MKAAQILTASIVSLLPIYTSA	AAM54023	killer toxin zygocin precursor	Zygosaccharo-myces bailii
Q	MIKLKFGVFFTVLLSSAYA	BAA06291	cholera toxin	Vibrio cholerae O139
R	MARRLLLLLLLLLLLPLALA	/	artificial construct	/
S	MARRIIIIIIIIIIIIPIALA	/	artificial construct	/
T	MAKKIIIIIIIIIIIIPIALA	/	artificial construct	/

6.1.1. Evaluation of natural and artificial signal peptides by transient transfection

In order to test their impact on the secretion of recombinant antibodies, all chosen signal peptides shown in Tab. 34 were fused to the N-terminus of the heavy and the light chain of a model antibody and inserted into a first generation standard expression vector (see chapter 5.2.2). These constructs were screened for antibody expression in transient transfection experiments, in order to identify the most promising signal peptides. For this purpose, 1 x 10^6 CHO K1 cells were transfected with 10 µg of each vector and cultivated in Medium K2. After an incubation time of 4 days, viable cell concentrations and antibody concentrations were measured and cell specific productivities were calculated.

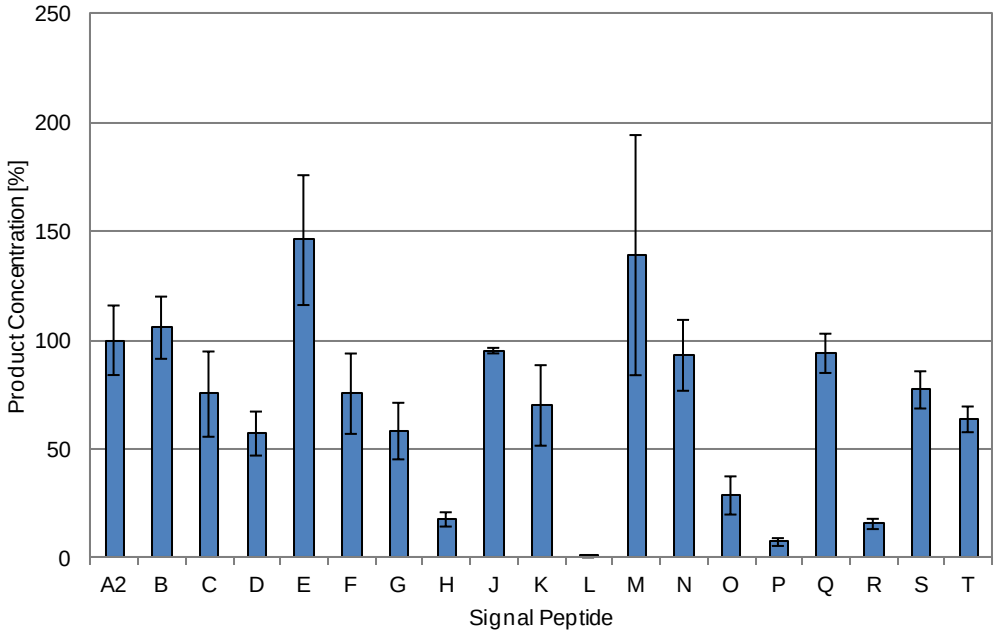

Fig. 27: Screening of different natural and artificial signal peptides in transiently transfected CHO K1 cells

CHO K1 cells were transiently transfected with different first generation expression vectors (see Fig. 4), comprising the heavy and the light chain of a model antibody fused to the indicated signal peptides (listed in Tab. 34). Four days after transfection, viable cell densities and product concentrations were determined and cell specific productivities were calculated. All values represent the average of three independent experiments and are normalized to signal peptide A2, which is set to 100%.

As depicted in Fig. 27, the determined cell specific productivity was strongly dependent on the used signal peptide. Interestingly, natural signal peptides from a human IgG heavy or light chain (Fig. 27 construct C and D) showed a 25% lower productivity than the control signal peptide (Fig. 27 construct A2). Most signal peptides derived from fungi or virus, showed a very low specific productivity (Fig. 27 construct L, O, and P) as well as signal peptide H and the artificial signal peptide R. Only signal peptides B, E and M resulted in increased productivity compared to the control.

To confirm these results, signal peptide B, E and M as well as the control signal peptide A2 were tested again by transient transfection as described above. In addition to cell specific productivities renilla specific product concentrations were calculated. The renilla luciferase reporter gene is localized on the expression vector and co-expressed as an internal control. In this way, different transfection efficiencies can be compensated by normalizing antibody concentrations to the activity of renilla luciferase.

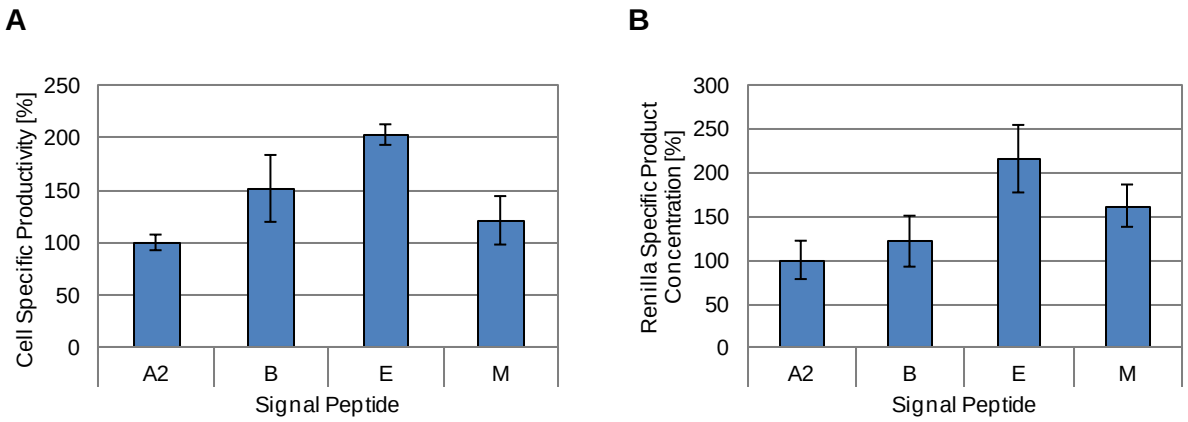

Fig. 28: Evaluation of selected signal peptides in transiently transfected CHO K1 cells

CHO K1 cells were transfected with selected first generation expression vectors (see Fig. 4) as described in Fig. 27. Four days after transfection, viable cell densities, product concentrations and the luminescence of co-expressed renilla luciferase were determined and cell specific productivities (A) as well as renilla specific productivities (B) were calculated. All values represent the average of three independent experiments and are normalized to signal peptide A2, which is set to 100%.

As shown in Fig. 28, signal peptides B, E and M mediated again higher cell specific productivities and the results were not distorted by varying transfection efficiencies.

6.1.2. Evaluation of mutated signal peptides by transient transfection

In chapter 6.1.1, the natural signal peptides B, E and M were identified as being more potent than the control signal peptide A2. In order to further improve productivities, specific mutations were inserted (see Tab. 35), that might optimize the performance of these signal peptides. The mutations were chosen based on observations from the literature as described in the following:

Tab. 35: Overview of all tested natural and mutated signal peptides

Signal peptides B and E are shown with their protein and nucleotide sequences. All mutations introduced into the wild-type signal peptides B and A are highlighted in red and noted according to the recommended system (den Dunnen 2001).

Name of construct	Signal peptide sequence	Nucleotide sequence	Mutation
A2	MDMRAPAGIFGFLLVLFPGYRS	ATGGATATGCGCGCGCCGGCCGGC ATTTTTGGCTTTCTGCTGGTACTG TTTCCGGGCTATCGCAGC	/
B	MKWVTFISLLFLFSSAYS	ATGAAGTGGGTGACCTTCATCTCC CTGCTGTTCCTGTTCTCCTCCGCC TACTCC	/
B1	MKWVTFISLLFLFSSA**R**S	ATGAAGTGGGTGACCTTCATCTCC CTGCTGTTCCTGTTCTCCTCCGCC AGGTCC	Y17R
E	MTRLTVLALLAGLLASSRA	ATGACCCGGCTGACCGTGCTGGCC CTGCTGGCCGGCCTGCTGGCCTCC TCCAGGGCC	/
E1	MTRLTVLALLAGLLASS**L**A	ATGACCCGGCTGACCGTGCTGGCC CTGCTGGCCGGCCTGCTGGCCTCC TCCCTGGCC	R18L
E2	M**A**RLTVLALLAGLLASSRA	ATGGCCCGGCTGACCGTGCTGGCC CTGCTGGCCGGCCTGCTGGCCTCC TCCAGGGCC	T2A
E3	M**A**TRLTVLALLAGLLASSRA	ATGGCCACCCGGCTGACCGTGCTG GCCCTGCTGGCCGGCCTGCTGGCC TCCTCCAGGGCC	M1_T2 insA
E4	MTRLTVLALLA**L**LLASSRA	ATGACCCGGCTGACCGTGCTGGCC CTGCTGGCCCTGCTGCTGGCCTCC TCCAGGGCC	G12L
E5	MTRL**L**VLALLAGLLASSRA	ATGACCCGGCTGCTGGTGCTGGCC CTGCTGGCCGGCCTGCTGGCCTCC TCCAGGGCC	T5L
E6	MTRLTVLAL-AGLLASSRA	ATGACCCGGCTGACCGTGCTGGCC CTGGCCGGCCTGCTGGCCTCCTCC AGGGCC	L10del
E7	MTRLTVLALL**L**AGLLASSRA	ATGACCCGGCTGACCGTGCTGGCC CTGCTGCTGGCCGGCCTGCTGGCC TCCTCCAGGGCC	L10_A11 insL
E8	MTRLTVLALLAGLLASSRA	ATGACCCGGCTGACCGTGCTGGCC CTGCTGGCCGGCCTGCTGGCCTCC TCC**C**G**C**GCC	52A>C; 54G>C
M	MASSLYSFLLALSIVYIFVAPTHS	ATGGCCTCCTCCCTGTACTCCTTC CTGCTGGCCCTGTCCATCGTGTAC ATCTTCGTGGCCCCCACCCACTCC	/

Signal peptide E contains an unusual arginine at position -2. In mutant E1, this arginine was substituted by a leucine, which is more common at this position (von Heijne 1983). On the other hand, one can speculate, that the high efficiency of signal peptide E could depend exactly on this arginine at position -2. Therefore, in signal peptide B1, the tyrosine residue at position -2 was replaced by an arginine in order to prove this assumption. Kozak (1986 Jan; 1987) reports, that a guanine directly after the AUG start codon is very important for translation initiation. Signal peptide E does not fulfil this requirement and might therefore suffer from a lowered translation rate. Codons with a guanine at the first position only exist for alanine, aspartatic acid, glutamic acid, glycine, and valine. Since aspartatic and glutamic residues are charged, valine is very hydrophobic, and glycine increases the protein flexibility, the alanine codon was used to introduce a guanine directly downstream of the AUG start codon of signal peptide E, resulting in mutant E3. In comparison in mutant E2 was the threonine at position -18 replaced by an alanine. The alanine and the glycine localized within the hydrophobic core of signal peptide E were substituted by a hydrophobic leucine, resulting in mutant E4 and E5, respectively. This was done, because it has been reported, that a hydrophobic core is required for a strong translation arrest, mediated by the signal recognition particle and that the translocation efficiency of a protein could be increased by this process (Belin 1996). Efficient cleavage was postulated to depend on the length of a signal peptide (Nilsson 2002). In order to test this issue, a shortened version of signal peptide E was generated by deleting (mutant E6) and an elongated version (mutant E7) by inserting a leucine within the hydrophobic core. It was shown that secondary mRNA structures close to the AUG start codon can influence translation initiation (Baim 1985; Kozak 1986 May; Kozak 1990). By mutating one codon (mutant E8), the secondary mRNA structure formed by signal peptide E was predicted to become less stable, resulting in a reduction of the calculated energy from -34.1 kcal/mol to -26.0 kcal/mol (see Fig. 29).

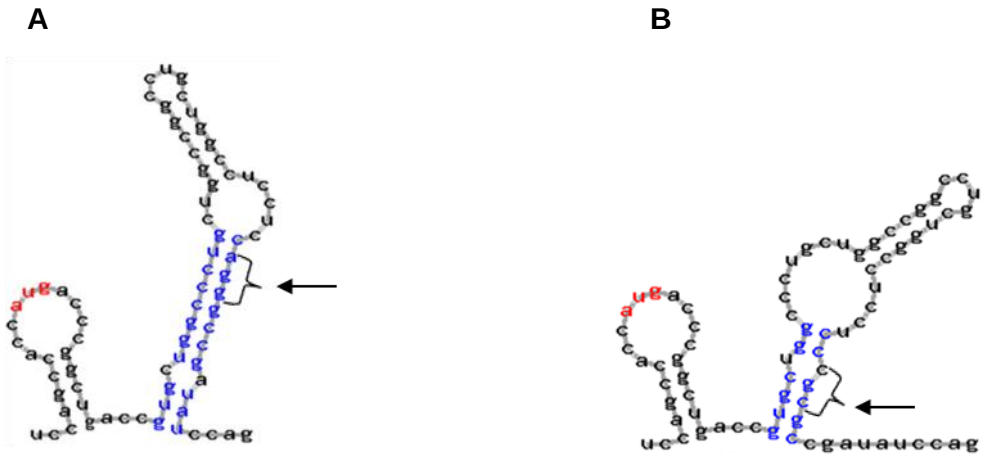

Fig. 29: Secondary mRNA structure of signal peptide E and E8

The secondary mRNA structure of signal peptide E (A) and E8 (B) was predicted with the "AUG_hairpin" software. The analyzed sequence includes 10 base pairs of the 5' UTR followed by the signal peptide and the first three codons of the mature antibody. Whereas the first three codons, of both chains (light and heavy chain) are similar. The methionine start codon is indicated in red and the main hairpin is indicated in blue. The arrow highlights the mutated codon.

Taken together, 8 mutants of signal peptide E, and one mutant of signal peptide B were generated. Those mutants as well as the wild-type signal peptides B, E, M and A2 (control) were fused to the model antibody and inserted into an optimized second generation expression vector containing a renilla luciferase gene as described in chapter 5.2.2. The performance of all signal peptides was analyzed by transient transfection using the respective constructs.

To this end, 1 x 10^6 CHO K1 cells were transfected with 10 µg of each vector and cultivated in Medium K2. After 3 days, viable cell concentration, antibody concentration and renilla fluorescence were measured and cell specific productivities as well as renilla specific product concentrations were calculated (Fig. 30). As expected, transfected cells showed much higher productivities when compared to Fig. 27 due to the improved expression vector.

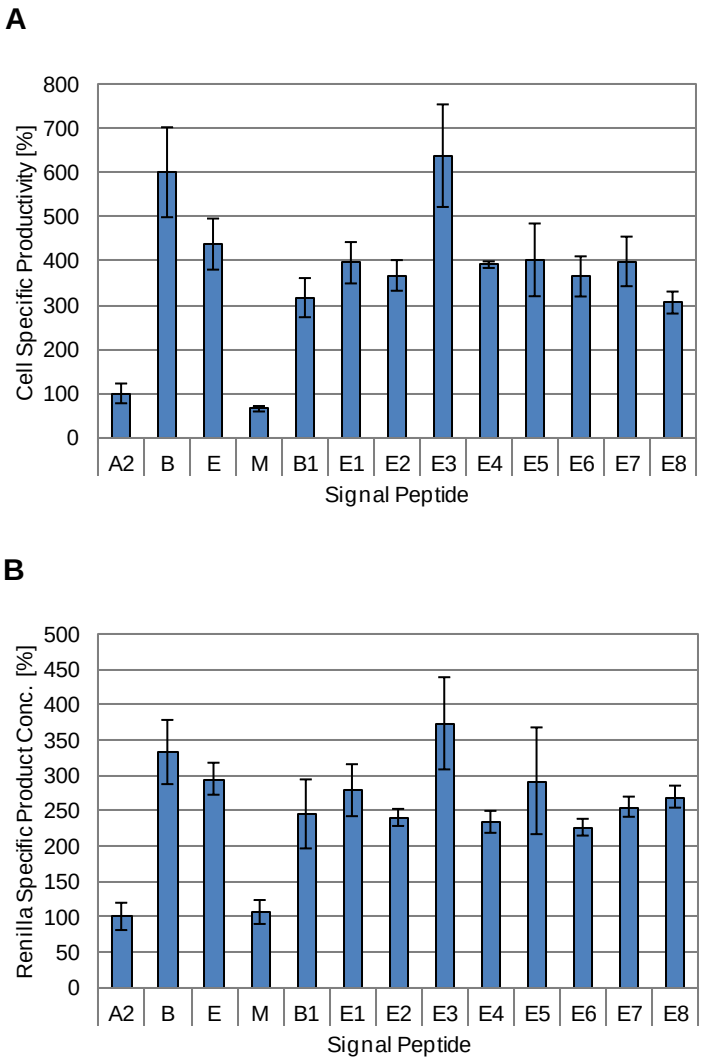

Fig. 30: Analysis of natural and mutated signal peptides in transiently transfected CHO K1 cells

CHO K1 cells were transiently transfected with different second generation expression vectors (see Fig. 5), comprising the heavy and the light chain of a model antibody fused to the indicated signal peptides (listed in Tab. 34). Three days after transfection, viable cell densities, product concentrations and the luminescence of co-expressed renilla luciferase were determined and cell specific productivities (A) as well as renilla specific productivities (B) were calculated. All values represent the average of three independent experiments and are normalized to signal peptide A2, which is set to 100%.

In accordance with the previous experiments, signal peptide B and E resulted in clearly increased cell specific productivities, whereas no improvement was observed for signal peptide M compared to the control (see Fig. 30). However, with the exception of E3, none of the mutated versions of signal peptide B or E showed substantially better productivities than the corresponding natural signal peptides, i.e. almost all mutations resulted in clearly decreased expression levels. Similar results were obtained when the antibody concentration was normalized to renilla luciferase to exclude influences of variable transfection efficiencies. In order to verify these observations, a selection of signal peptide constructs was transfected and analyzed again as described above.

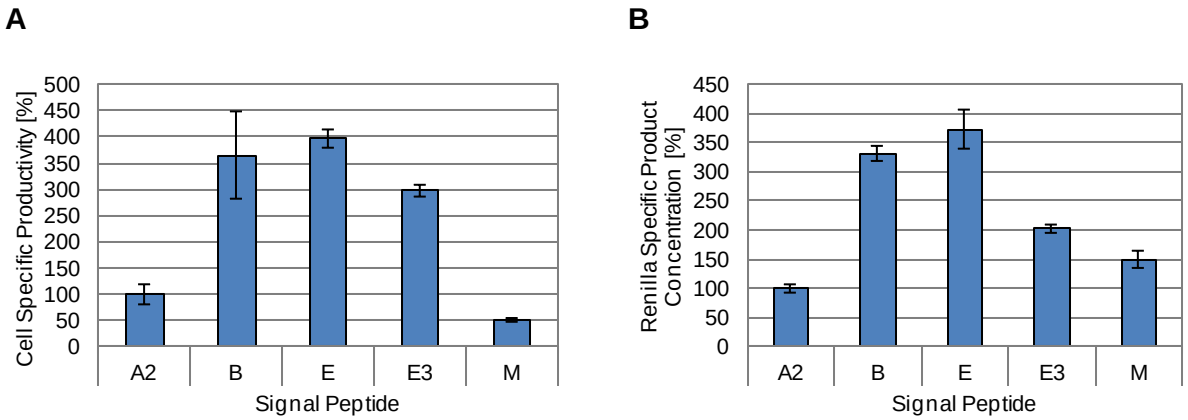

Fig 31: Evaluation of selected natural and mutated signal peptides in transiently transfected CHO K1 cells

CHO K1 cells were transfected with selected antibody expression constructs as described in Fig. 30. Three days after transfection, viable cell densities, product concentrations and the luminescence of co-expressed renilla luciferase were determined and cell specific productivities (A) as well as renilla specific productivities (B) were calculated. All values represent the average of three independent experiments and are normalized to signal peptide A2, which is set to 100%.

The overall results depicted in Fig 31 resembled thus derived from the previous experiment with the exception of signal peptide E3, which showed a slightly decreased performance. Taken together, based on all transient transfection experiments it can be concluded, that signal peptide B, E and E3 were the most potent ones in CHO K1 cells, because increased cell specific productivities were observed in case these signal peptides were fused to the heavy and the light chain of the used model antibody instead of the control signal peptide A2.

6.1.3. Evaluation of signal peptides in stably transfected cell lines (Mini-pools)

Although signal peptide B, E and E3 mediated improved cell specific productivities in transiently transfected cells, their performance in stable cell lines might differ (Rance 2010; Kalwy 2006). Hence, it had to be verified, whether these signal peptides were able to produce increased amounts of recombinant antibodies in stably transfected cells. Many clones had to be generated for this approach. For this purpose, heavy and light chain of the model antibody were fused to the selected signal peptides and to the control A2 followed by their insertion into third generation expression vectors as described in chapter 5.2.2. This vector contains a dhfr cassette and can be used for the development of stable cell lines in combination with dhfr-deficient CHO DG44 cells. Moreover, in order to achieve enhanced productivities, gene amplification processes can be induced by adding the competitive dhfr inhibitor methotrexate (MTX) to the culture medium (Ludwig 2006; Kaufman 1982).

Tab. 36: Third generation expression vectors used to create stable cell lines

Vector number	Containing signal peptide
1171	A2
1157	B
1158	E
1159	E3

The created expression vectors (see Tab. 36) were employed to develop stable cell lines according to the mini-pool method. Therefore, 1 x 10^6 CHO DG44 cells were transfected with 10 µg of each construct (linearized with BspHI), 384 mini-pools per signal peptide were generated and cultivated in Medium D3 supplemented with 10 nM MTX (see 5.3.4). Grown mini-pools were analyzed by nqELISA and for each signal peptide those 36 mini-pools showing the highest amount of expressed antibody were selected and transferred to 24 well plates. Every 3 to 4 days, about 75% of the supernatant was exchanged for Medium D3 containing 25 nM MTX until the cultures started to grow. Following this amplification procedure, all mini-pools were expanded up to 6 well level, where most of them had viabilities >90% and showed a good growth behaviour (see Tab. 37). At this time, antibody concentrations were determined by qELISA and 20 mini-pools with the best the cell specific productivities were selected for each signal peptide and used for further experiments.

Tab. 37: Overview of selected mini-pools

CHO DG44 cells were transfected with third generation antibody expression constructs comprising the indicated signal peptides and mini-pools were generated according to the standard procedure. For each signal peptide, 36 mini-pools were selected by nqELISA and inoculated with 2 x 10^5 cells/mL in 6-well plates. After 3 days, viable cell concentrations (VCD), viabilities and expressed antibody concentrations (Product c.) were measured and cell specific product concentrations (Q_P) were calculated. For each signal peptide 20 mini-pools showing the highest specific product concentrations (indicated in red) were tested for a performance test during fed-batch (fed-batch numbers are indicated).

Signal peptide A2				
VCD [10^5 c/mL]	Viability [%]	Product c. [mg/L]	Q_P [pg/cell/day]	Fed-batch no.
20.4	95	12	5	
25.4	94	30	11	1
23.0	95	23	9	2
16.8	93	13	6	
1.6	86	0	0	
16.6	96	11	5	
21.2	95	16	7	
18.4	94	12	5	
23.8	93	8	3	
22.4	92	29	11	3
17.8	92	8	4	
20.0	92	39	17	4
4.4	90	3	3	
17.6	93	29	13	5
11.6	93	14	9	6
12.6	94	20	11	7
15.8	92	19	10	8
25.6	91	19	7	
27.6	91	71	24	9
20.0	94	14	6	
20.0	94	24	10	10
17.4	93	25	12	11
17.8	94	18	8	
12.6	92	26	15	12
24.0	92	25	10	13
33.2	90	59	18	14
18.6	90	23	10	15
17.0	94	24	12	16
16.8	94	33	16	17
21.4	94	13	5	
19.2	93	24	10	18
19.2	92	23	10	19
15.2	94	23	12	20
15.4	96	16	8	
28.2	94	7	2	
26.4	93	18	6	

Signal peptide B				
VCD [10^5 c/mL]	Viability [%]	Product c. [mg/L]	Q_P [pg/cell/day]	Fed-batch no.
12.6	95	22	13	
11.8	94	37	22	21
8.0	85	120	92	22
18.0	92	45	20	23
21.2	92	51	21	24
22.8	94	45	18	
17.0	92	40	19	25
19.8	92	70	30	26
12.6	92	67	39	27
23.8	94	45	17	
14.4	93	51	27	28
26.6	92	33	11	
20.0	95	197	84	29
17.0	94	67	32	30
18.4	91	170	77	31
18.2	92	46	21	32
26.8	94	176	61	33
25.6	94	67	24	34
25.4	94	35	13	
2.4	84	2	3	
20.4	94	23	10	
20.2	96	28	12	
14.0	91	29	16	
15.8	92	26	13	
24.8	93	78	29	35
25.8	94	88	31	36
27.0	94	116	40	37
21.8	91	46	19	
17.2	93	28	13	
27.2	91	72	25	38
21.2	93	53	22	39
25.0	92	110	40	40
27.0	86	39	13	
26.0	91	43	15	
18.8	94	8	4	
25.0	94	32	12	

Signal peptide E				
VCD [10^5 c/mL]	Viability [%]	Product c. [mg/L]	Q_P [pg/cell/day]	Fed-batch no.
14.0	94	43	23	41
22.0	93	64	25	42
23.8	91	34	13	
25.0	92	62	23	43
20.4	93	48	20	44
19.6	94	14	6	
20.8	93	45	19	45
23.4	94	60	23	46
14.6	95	42	22	47
14.4	93	23	12	
20.4	94	30	13	
17.2	91	38	18	48
25.8	93	66	24	49
24.8	92	85	31	50
17.2	94	27	13	
6.0	92	14	13	
18.8	94	19	8	
15.6	93	31	16	
17.0	91	33	16	
16.2	93	18	9	
29.2	89	8	3	
28.8	91	51	17	
18.0	92	36	16	
31.2	93	42	13	
27.0	92	92	32	51
16.6	90	118	57	52
33.2	90	7	2	
14.8	93	60	31	53
15.4	95	83	42	54
16.0	92	42	21	55
23.8	91	59	22	56
15.8	92	87	43	57
18.6	94	59	27	58
20.4	93	64	27	59
15.6	94	37	19	60
12.6	93	24	14	

Signal peptide E3				
VCD [10^5 c/mL]	Viability [%]	Product c. [mg/L]	Q_P [pg/cell/day]	Fed-batch no.
20.4	93	54	23	61
19.0	94	13	6	
8.8	93	6	4	
22.2	93	61	24	62
20.0	93	27	12	
26.2	94	22	8	
31.0	91	79	25	63
26.6	92	18	6	
19.6	92	49	21	64
25.0	93	20	7	
23.2	90	71	27	65
22.8	92	47	18	66
17.2	91	35	16	67
38.8	90	88	24	68
28.8	92	13	4	
19.0	94	46	20	69
21.6	93	36	15	70
20.8	94	26	11	
20.0	92	26	11	
22.6	91	10	4	
21.2	93	20	8	
18.4	95	26	12	
18.8	95	27	12	
20.4	95	43	18	71
26.4	94	126	44	72
18.4	94	28	13	73
19.4	93	26	11	
18.6	94	31	14	74
14.6	93	39	20	75
28.4	93	42	14	76
39.2	91	45	12	77
8.2	92	7	5	
27.0	92	69	24	78
21.2	92	60	24	79
8.6	91	13	10	
29.6	91	97	32	80

In order to adapt the chosen mini-pools to fed-batch process conditions, they were cultivated for one passage on 6 well plates in Medium D5 containing 25 nM MTX, followed by two passages with 25 mL of the same medium in shake flasks. At this stage, all mini-pools grew very well and

had an average viability of 94%. Subsequently, fed-batch cultures were inoculated with all mini-pools and cell specific productivities were calculated at day 3.

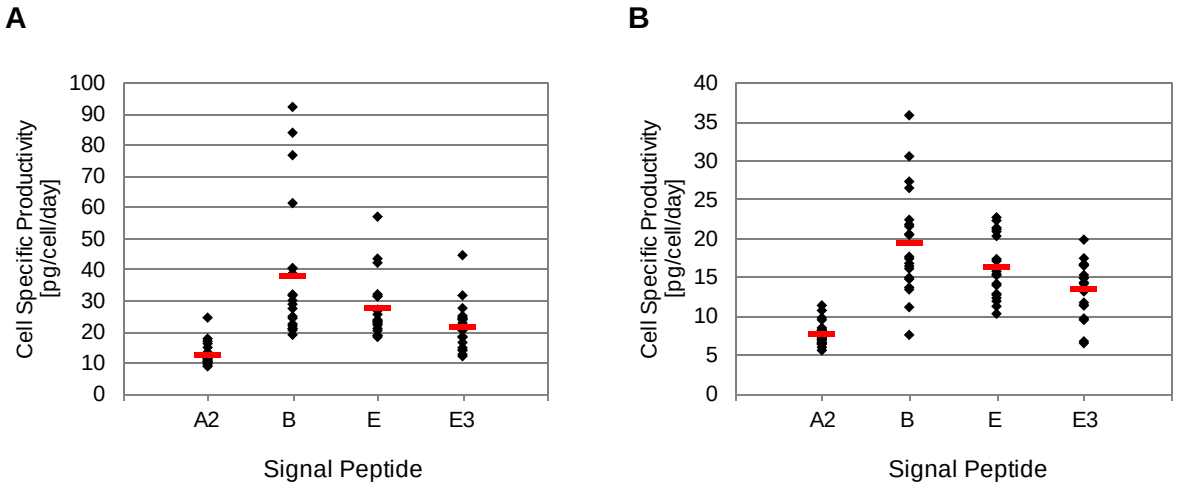

Fig. 32: Cell specific productivities of mini-pools used for fed-batch experiments

For each indicated signal peptide, 20 mini-pools selected for fed-batch experiments were cultivated in 6 well plates with Medium D3 (A) or in shake flasks with Production°Medium (B). After three days, viable cell densities and antibody concentrations were measured and cell specific productivities were calculated. Mean values are represented by red bars.

As shown in Fig. 32, the highest cell specific productivities were obtained for mini-pools generated based on signal peptide B followed by signal peptide E and A2, regardless of the cultivation level (6 well or shake flask). Surprising mini-pools generated based on signal peptide B showed a cell specific productivity up to 80 or 90 pg/cell/day. However, in 6 well plates and Medium D3 all mini-pools showed generally higher cell specific productivities than upon cultivation in shake flask and Production° Medium (see Tab. 27).

It is well known, that the cell specific productivity of a cell line does not always correlate with the product concentration observed during a fed-batch process (Birch 2006). Therefore, the performance of signal peptide B, E, E3 and A2 in a production process was analyzed by subjecting all selected mini-pools to fed-batch experiments.

A

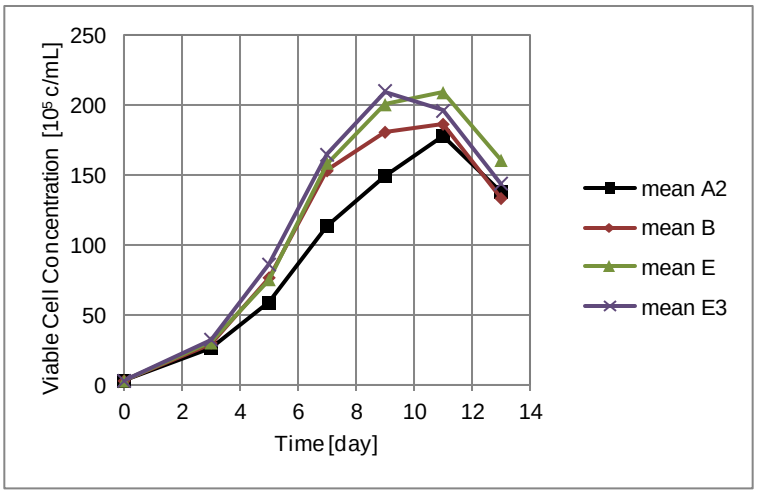

B

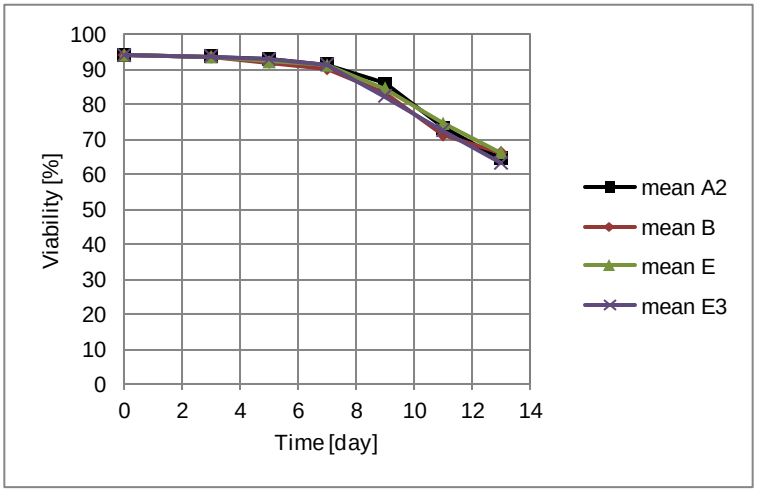

C

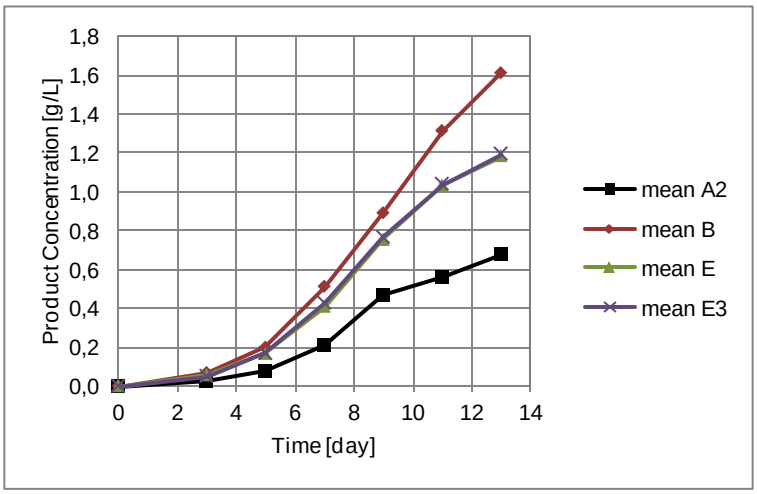

Fig. 33: Fed-batch experiments with selected mini-pools

For each indicated signal peptide, 20 mini-pools were subjected to fed-batch experiments. During the process all cultures were daily analyzed regarding their viable cell concentration (A), viability (B) and product concentration (C), and the respective mean values were calculated for every signal peptide.

During the fed-batch processes (Fig. 33 A and B), mini-pools grew very well independently of the used signal peptide and they showed similar viabilities. However, clear differences were observed regarding the measured product concentrations. Whereas an average final product concentration of 0.7 g/L was obtained for signal peptide A2, 1.2 g/L could be reached with signal peptide E and E3 and even 1.6 g/L with signal peptide B (see Fig. 33).

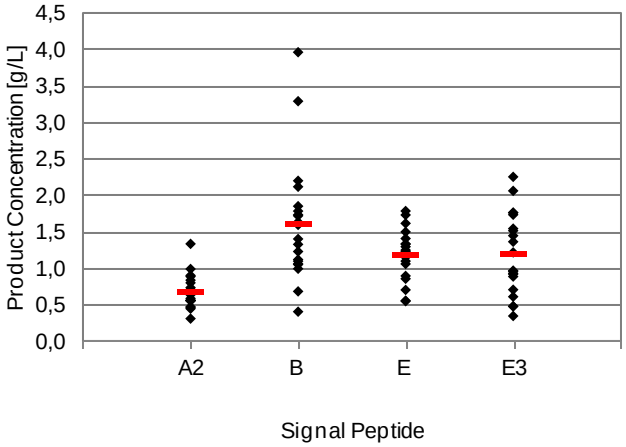

Fig. 34: Fed-batch experiments with selected mini-pools

For each indicated signal peptide, the final product concentration (day 13) of every individual mini-pool, which was obtained during the fed-batch process described in Fig. 33, is depicted. Mean values are represented by red bars.

Fig. 34 shows the individual product concentrations at day 13 for all tested mini-pools during the fed-batch as well as the mean values (red bars; correspond to the maximum values seen in Fig. 33 (C). Although the mean values are almost identical for signal peptide E and E3 and the individual mini-pools derived from E3 show an increased heterogeneity. The mini-pools with the most impressive product concentrations (3.3 g/L and 4.0 g/L antibody in 13 days) resulted from signal peptide B. In summary, it can be concluded, that regarding the development of stable antibody production cell lines, the control signal peptide A2 is clearly outperformed by all other tested signal peptides with signal peptide B being by far the most efficient one.

6.2. General outline: Development of an alternative selection system for high producing clones

The selection of rare high-expressing clones out of a pool predominantly consisting of low and medium producers is one of the most challenging problems during the development of mammalian cell lines for the production of recombinant antibodies or non-antibody proteins. Therefore, it was the aim of the second part of this thesis, to develop a novel selection system, which allows the fast and easy identification and isolation of clones producing high amounts of antibody. The chosen approach is based on the hypothesis that the overexpression of recombinant antibodies in CHO cells causes ER stress during the secretion process and that the extent of the triggered stress response is correlated to the level of antibody expression. The system is exemplified by Fig. 35.

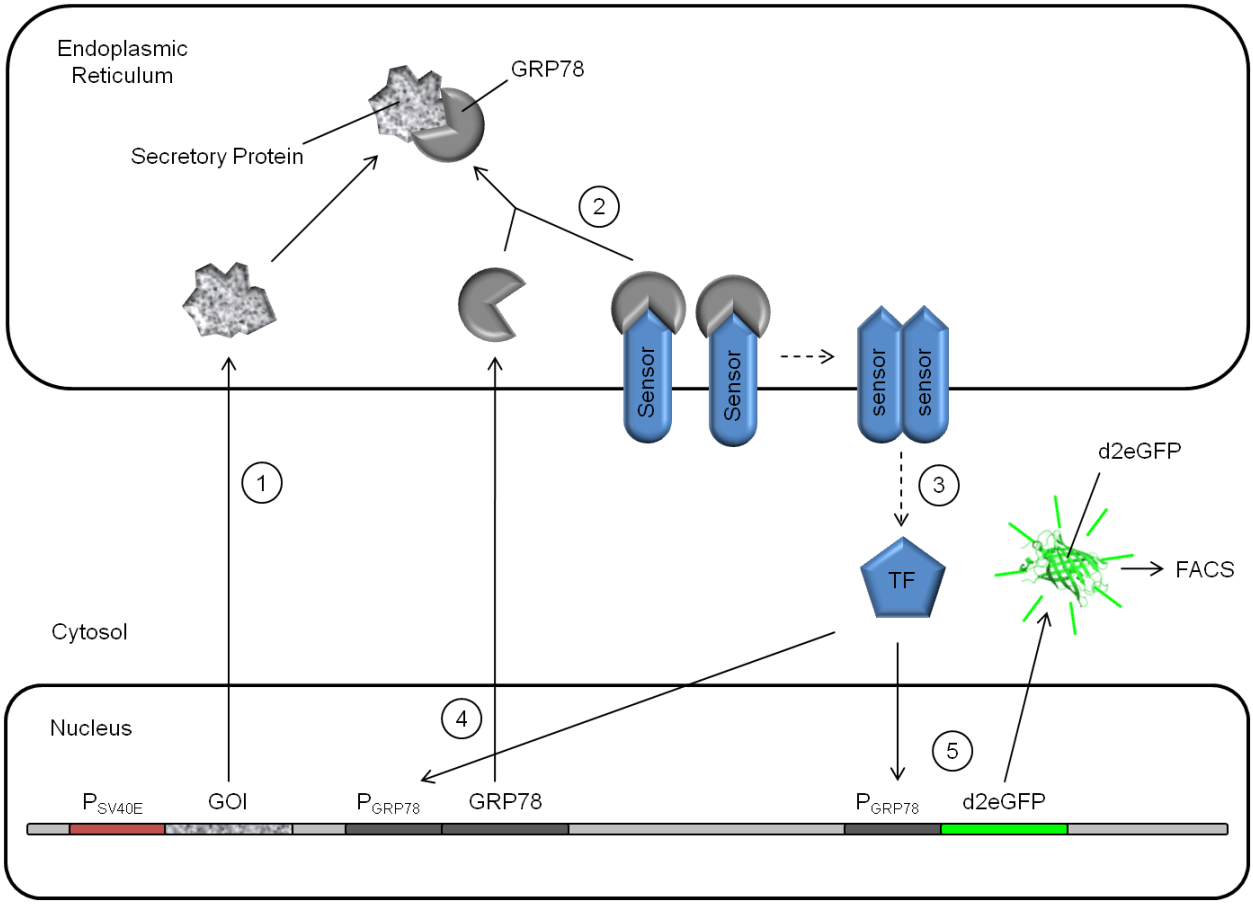

Fig. 35: Schematic representation of the novel selection system based on ER stress (exemplified shown with GRP78 promoter)

Step 1: Overexpression of secretory recombinant proteins causes dissociation of GRP78 from various ER stress sensors like IRE1, PERK or ATF6 (Step 2). Step 3: Transcription factors (TF) like XBP1, ATF4 or ATF6 are formed (Pathway is simplified shown). Step 4: Genes involved in many ER functions are upregulated upon transcription factor binding to UPRE, ERSE or AARE elements which are located in various promoters (e.g. GRP78). Step 5: If so, than reporter genes like d2eGFP are also stimulated by ER stress pathways and increased GFP fluorescence can be detected by FACS.

In a first set of experiments, this hypothesis was verified by analyzing the correspondence between antibody production and ER stress pathways. For this purpose, mRNA levels of several prominent factors involved in stress responses were determined in a variety of cell lines showing different antibody expression rates. At this way, promising ER stress promoters and regulatory elements that were stimulated by antibody production were identified. Later these promoters and regulatory elements were used to create several ER stress reporter constructs, which were intended to allow the detection of high producers based on their GFP fluorescence intensity. In a second set of experiments, the performance of different reporter constructs (identified as described in chapter 6.3) was assessed and compared by analyzing their response to antibody expression. For this purpose, several cell lines were generated as depicted in Fig. 36.

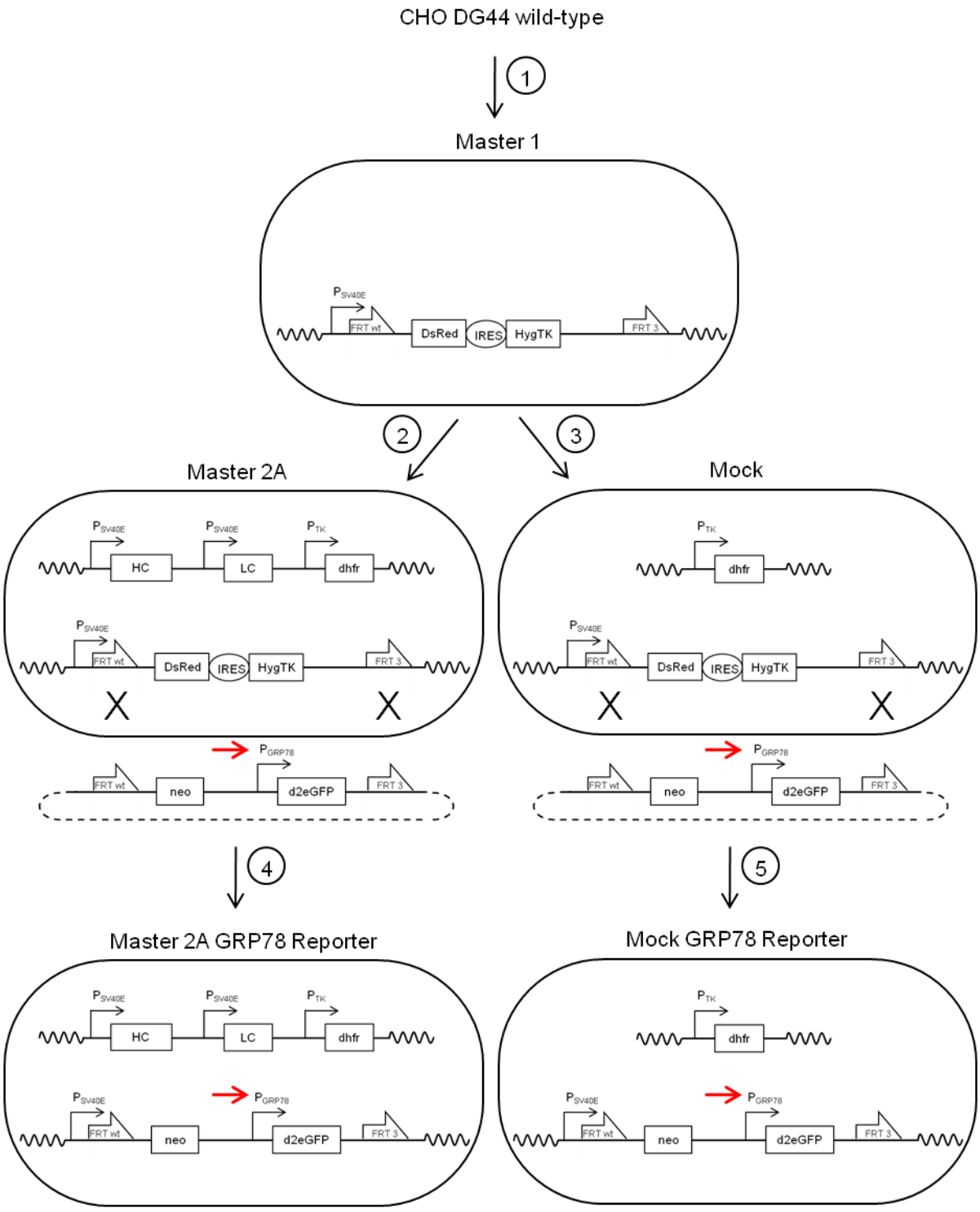

Fig. 36: General outline of the generation of Master 1 Master 2A and Mock cell lines and their conversion to ER stress reporter cell lines

Step 1: At first, the Master 1 cell line was created by tagging CHO DG44 cells with an exchangeable DsRed RMCE acceptor construct. Step 2: The Master 2 cell line was derived from Master 1 by introducing an antibody expression construct. Step 3: The Mock cell line was derived from Master 1 by introducing a dhfr expression construct. Step 4 and Step 5: The genomically anchored DsRed RMCE acceptor construct of three different Master cell lines (exemplified shown for Master 2A) and a Mock cell line was exchanged with an ER stress reporter construct (exemplified shown for the GRP78 Reporter construct) by targeted integration (RMCE). The ER stress reporter elements (GRP78 Promoter) are highlighted by red arrows.

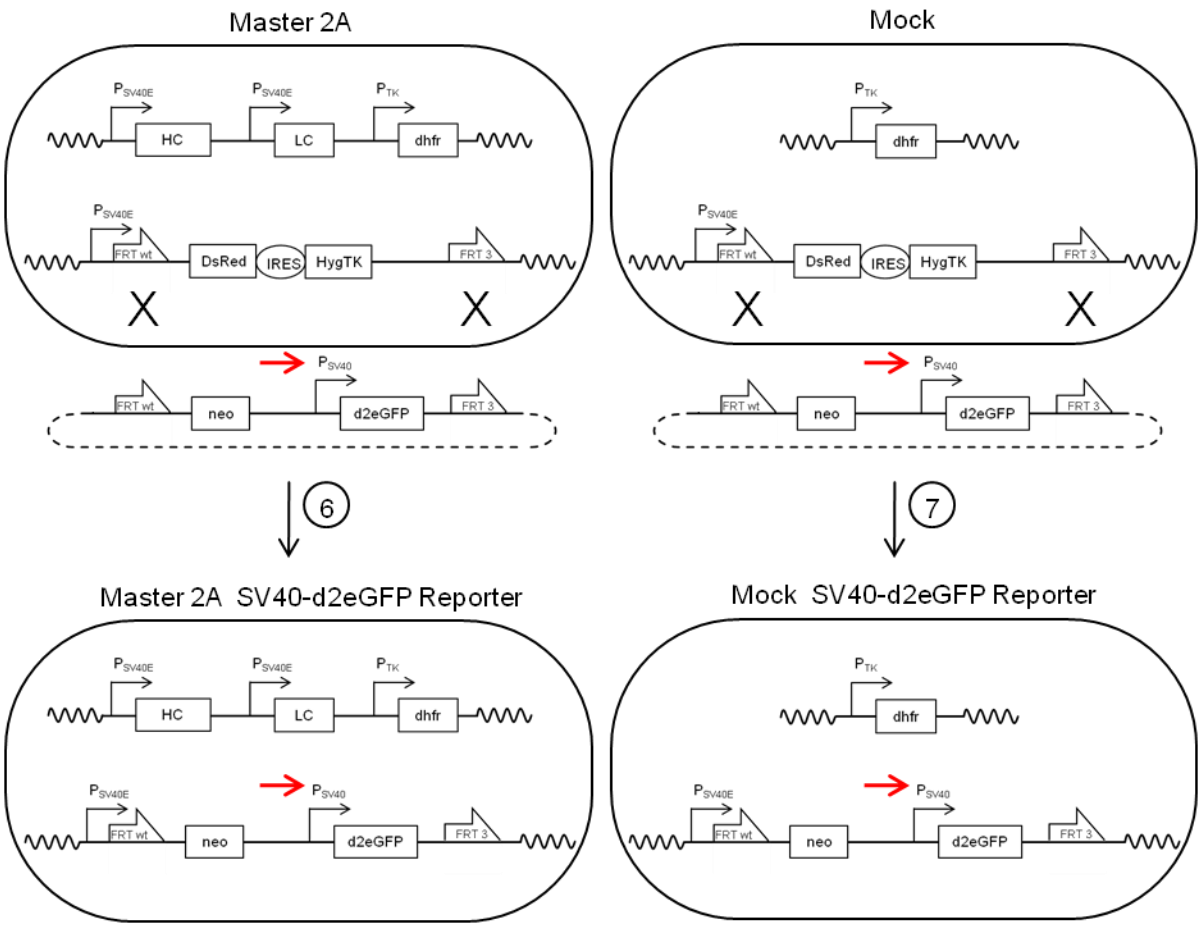

Fig. 37: General outline of the conversion of Master 2A and Mock cell lines in control cell lines

GRP78 Reporter constructs were introduced in Master 2A and Mock cell line by subjecting them to an RMCE procedure as shown in Fig. 36. All other ER stress reporter and control constructs were introduced in the same way as previously described. Exemplified shown is the integration of a control construct (SV40-d2eGFP control, highlighted by red arrow) by RMCE (Fig. 37 step 6 and 7).

As exemplified in Fig. 36 and Fig. 37, ER stress reporter cell lines and appropriate control cells were generated by using the Master 2 and the Mock cell line. This was achieved by recombinase mediated cassette exchange of the DsRed acceptor construct against the ER stress reporter constructs. At this way, it was possible to identify the construct, which mediated the most pronounced induction of GFP fluorescence upon antibody expression. Finally, a new reporter cell line was created with the best-performing construct and applied to the development of an antibody producing cell. Thus, it was evaluated whether the novel ER stress reporter system is suitable to identify and isolate high-expressing clones.

6.3. Analyzing the influence of antibody expression on ER stress

In order to investigate a potential correlation between antibody expression and ER stress, the expression of some prominent factors involved in ER stress responses was analyzed in a number of production clones. These cell lines were available at Cellca and cover a broad range of productivities from 1.1 to 3.8 g/L in fed-batch processes as shown in Tab. 38.

Tab. 38: Overview of fed-batch results for the selected clones used for real time RT-PCR analysis

Clone	1	2	3	4	5	6	7	8
Product concentration on day 11 [g/L]	1.9	3.8	1.7	2.2	1.1	3.4	1.3	1.5

All clones in stock culture were split into fresh Medium D5 containing 38 nM MTX with a concentration of 1 to 3 x 10^5 cells/mL and cultivated under standard conditions (see chapter 5.3.2). The corresponding wild-type cell CHO DG44 was cultivated in a comparable MTX free medium (Medium D4) and treated in the same way as previously described. On day 3, the total RNA was isolated from all clones as well as from the corresponding wild-type cell CHO DG44, and mRNA levels of CALR, GRP78, GRP94 and spliced XBP1 were determined by real time RT-PCR.

A CALR, $R^2 = 0.25$

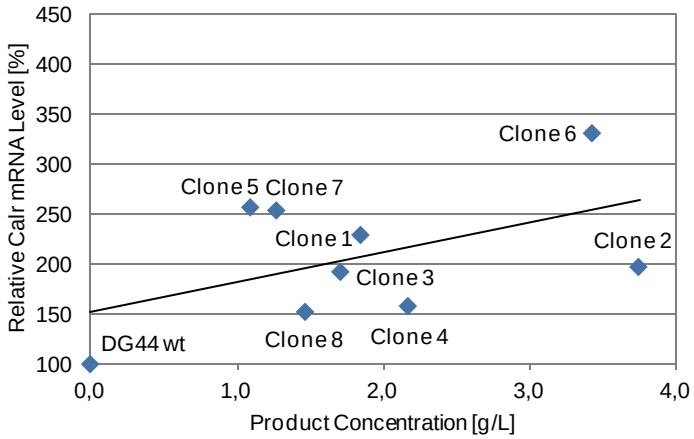

B GRP78, $R^2 = 0.78$

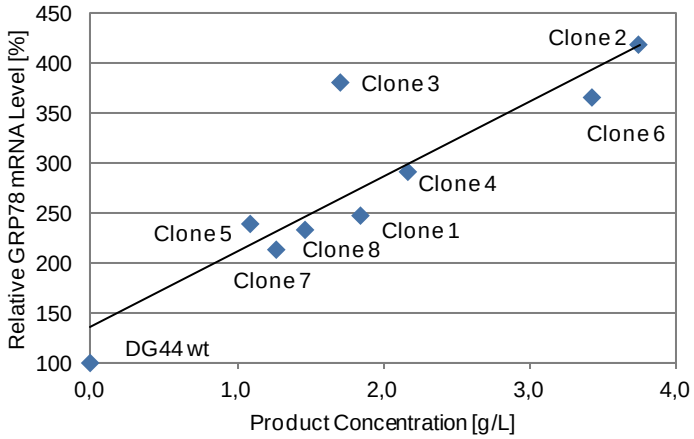

C GRP94, $R^2 = 0.75$

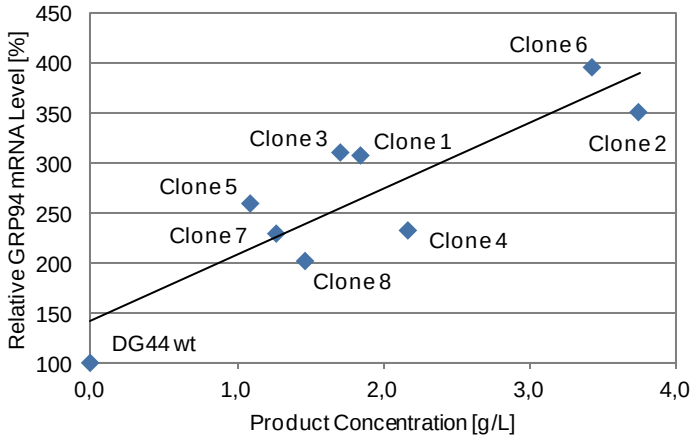

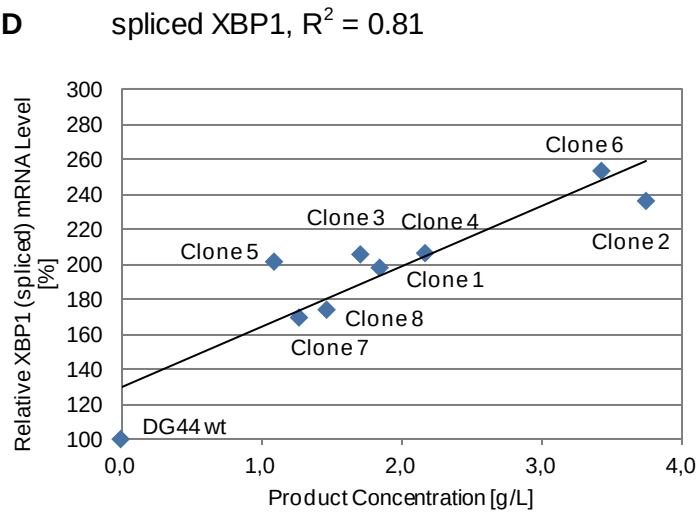

Fig. 38: Correlation between antibody productivity and mRNA levels of ER stress factors in selected production clones

8 production clones expressing a monoclonal model antibody were cultivated in fed-batch experiments and product concentrations were measured. The same clones as well as the CHO DG44 cell line were subjected to real time RT-PCR analysis in order to determine the mRNA levels of CALR, GRP78, GRP94 and spliced XBP1. All mRNA levels were normalized to beta-actin and to the results obtained for CHO DG44 cells, which were set to 100%. For each clone, the fed-batch product concentrations from day 11 were plotted against the relative mRNA levels of CALR (A), GRP78 (B), GRP94 (C) and spliced XPB1(D), respectively (The mRNA values represent the average of three independent experiments).

Fig. 38 shows for each individual clone the relative mRNA levels of CALR, GRP78, GRP94, and spliced XBP1 as well as the corresponding antibody concentration reached in a fed-batch process on day 11. For CALR, the relative mRNA level showed a weak correlation with antibody production (Fig. 38 A), whereas ((Fig. 38 B, C, and D) for GRP78, GRP94 and spliced XPB1 a stronger correlation was observed. From these results it can be concluded, that at least some ER stress response elements might be adequate detectors for antibody expression.

6.4. Generation and analysis of Master 1 cell lines containing an RMCE acceptor construct (RMCE target)

In order to evaluate the ability of the constructs generated in chapter 5.2.3 to function as reporter system for the expression of antibodies, several test cell lines were developed. In a first step, a so called Master 1 cell line was created by tagging wild-type cells with an exchangeable RMCE acceptor construct (Fig. 39).

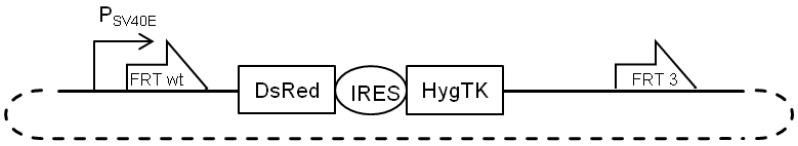

Fig. 39: Schematic representation of vector 957

For this purpose, 1 x 10^6 CHO DG44 cells were transfected with 3 µg of vector 957 excised with MluI and SalI. After two days, Medium D2 was replaced by Medium D2 containing 100 mg/L Hygromycin B. On day 8, the Hygromycin B concentration was increased to 200 mg/L. On day 18, clones showing a very high DsRed fluorescence (top 0.7%) were isolated as described in Fig. 40 and cultivated in Medium D2 for two weeks.

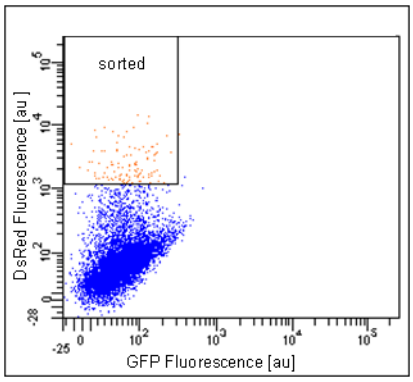

Fig. 40: Single cell sorting after transfection with vector 957

On day 18, following transfection of the CHO DG44 cells with a DsRed RMCE acceptor construct (vector 957) all cells were analyzed regarding DsRed and GFP fluorescence by flow cytometry. DsRed positive (top 0.7%) and GFP negative (low auto-fluorescence) single clones were isolated by sorting as indicated (gate "sorted").

All 19 grown clones were expanded up to the 24 well transferred into Medium D2 containing 200 mg/L Hygromycin B, and analyzed by FACS. Those 5 clones showing the highest DsRed fluorescence were selected (Fig. 41), and the exchangeability of the acceptor construct was analyzed by subjecting them to an RMCE procedure as shown in Fig. 42.

A **B** **C**

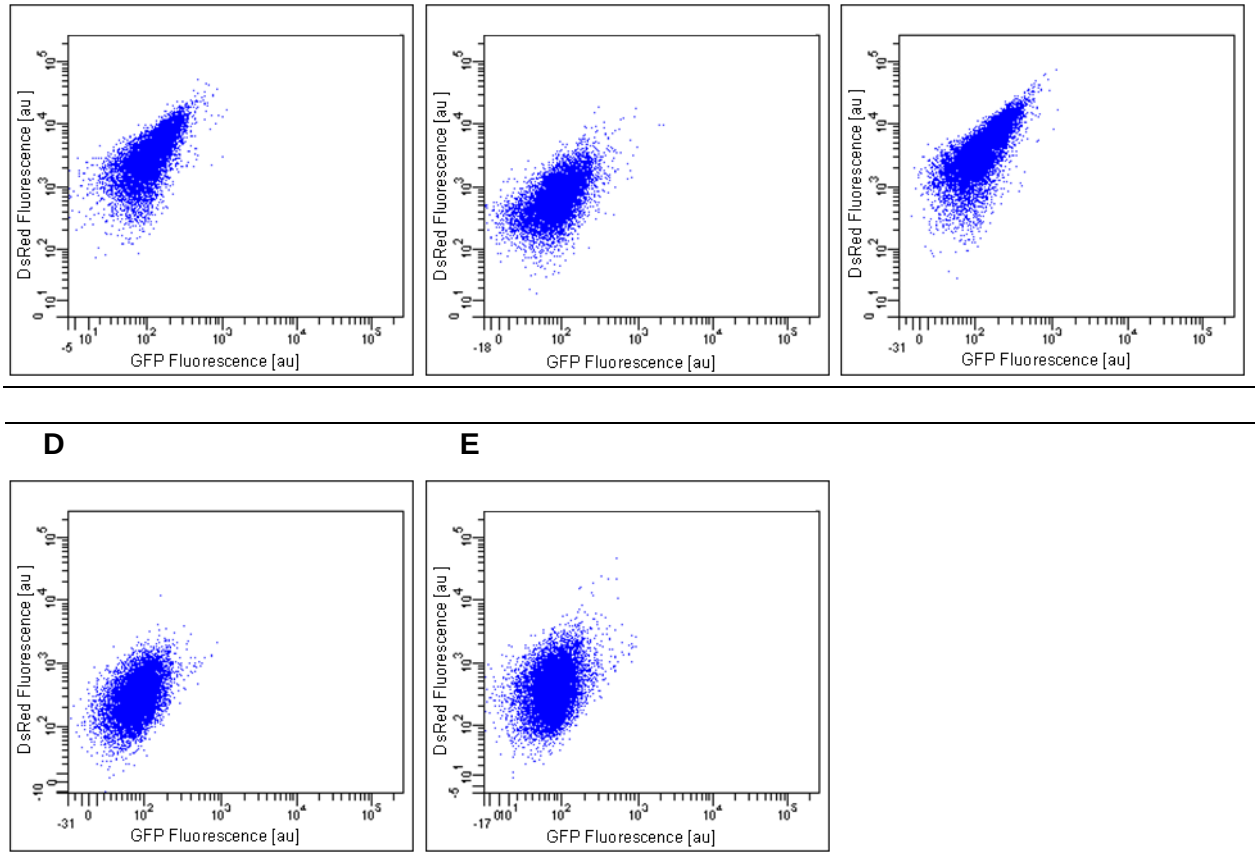

Fig. 41: FACS analysis of Master 1 cell clones containing a DsRed RMCE acceptor construct

Following transfection of CHO DG44 cells with a DsRed RMCE acceptor construct (vector 957), DsRed positive clones were isolated by FACS sorting. All grown clones were expanded and analyzed with regard to DsRed fluorescence by flow cytometry. Five clones showing the highest fluorescence are depicted: (A) clone 32, (B) clone 41, (C) clone 42, (D) clone 43 and (E) clone 46.

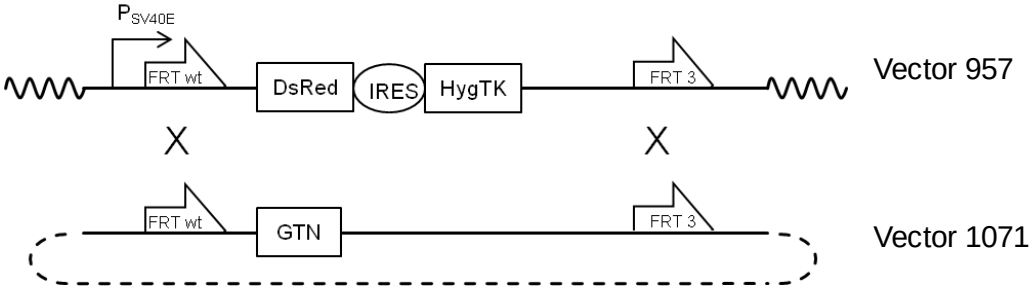

Fig. 42: Schematic representation of RMCE procedure

During the RMCE procedure clones were transfected with 6 µg of vector 1071, and 1 µg of the Flpo vector 721. Three days after transfection, the used Medium D2 was replaced by Medium D2 containing 500 mg/L G418. Only three clones grew up under these conditions and were analyzed by FACS on day 27.

	A1 before RMCE	**A2** after RMCE
FACS analysis of Clone 41	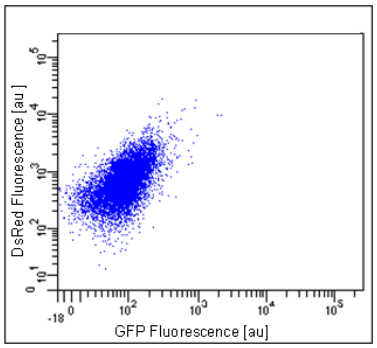	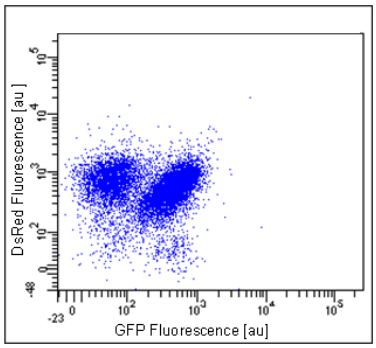
DsRed fluorescence [au]	833	662
GFP fluorescence [au]	95	321

	B1 before RMCE	**B2** after RMCE
FACS analysis of Clone 43	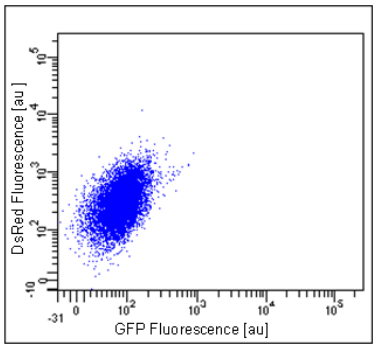	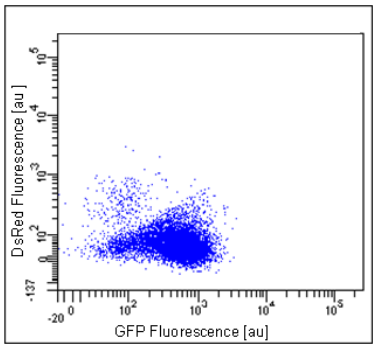
DsRed fluorescence [au]	370	71
GFP fluorescence [au]	85	536

	C1 before RMCE	**C2** after RMCE
FACS analysis of Clone 46	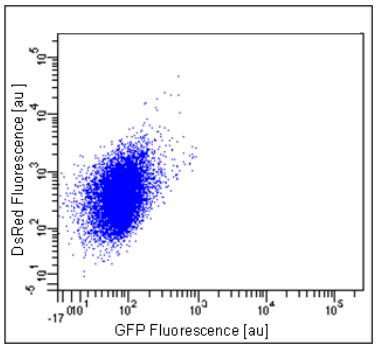	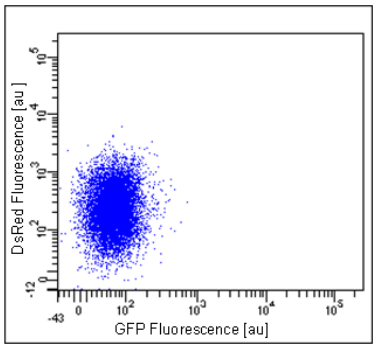
DsRed fluorescence [au]	562	313
GFP fluorescence [au]	82	66

Fig. 43: FACS analysis of Master 1 cell clones before and after RMCE

5 Master 1 cell clones stably transfected with a DsRed RMCE acceptor construct (vector 957) were co-transfected with a GTN RMCE donor and a FLPO construct and cultivated for 24 days in Medium D2 containing 500 mg/L G418. All growing clones were analyzed with regard to GFP and DsRed fluorescence by flow cytometry and their mean fluorescence intensities (after RMCE) were determined: clone 41 (A2), clone 43 (B2), clone 46 (C2). For comparison reasons, corresponding FACS data generated before transfection are shown for each clone (A1, B1 and C1).

As seen in Fig. 43 (A2), clone 41 showed two populations, the one being positive for DsRed and GFP fluorescence and the other for DsRed only. This implies that several DsRed RMCE acceptor cassettes are present in the genome of clone 41 and that this clone was only partially exchanged. For clone 46, a reduction in DsRed but no relevant increase in GFP fluorescence was observed after the RMCE procedure (Fig. 43 C1, C2), indicating that the DsRed RMCE acceptor construct was not authentically exchanged for the GTN donor construct. Possibly, clone 46 contains multiple copies of the DsRed RMCE acceptor construct at the same integration site, some of which have been excised by the flippase. In conclusion it can be stated that both clones (Clone 41 and 46) are not suitable for further experiments.

Finally, after transfection with the GTN RMCE donor construct, clone 43 showed a reduction of DsRed and an increase of GFP fluorescence Fig. 43 (B1, B2). Based on these results it was concluded, that the DsRed RMCE acceptor construct of clone 43 can be authentically exchanged. Consequently, clone 43 was renamed as Master 1 cell line and used for further experiments.

6.5. Generation and analysis of Mock and Master 2 cell lines

To provide an adequate test system for the evaluation of the ER stress reporter constructs, additional cell lines had to be created based on the Master 1 cell line. So called Master 2 cell lines stably expressing a recombinant model antibody were generated by means of a dhfr selection procedure. As control a corresponding mock cell line expressing only dhfr was developed (see schematic presentation in Fig. 36). For the Mock cell line development, 1 x 10^6 cells of the Master 1 cell line were transfected with 10 µg of vector 1096 (linearized with BspHI, see Fig. 44) and mini-pools were generated according to the standard procedure and cultivated in Medium D3 containing 200 mg/L Hygromycin B and 10 nM MTX.

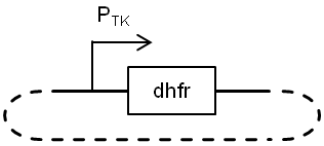

Fig. 44: Schematic representation of vector 1096

On day 32, the best growing mini-pools were selected and transferred to Medium D3 containing 200 mg/L Hygromycin B and 25 nM MTX. On day 54, the best growing mini-pools were used to isolate single clones by FACS. Cells were cultivated in Medium D3 containing 200 mg/L Hygromycin B and 25 nM MTX, 8 grown clones were randomly selected and expanded up to shake flask scale. Since all clones were growing very well, anyone was chosen, defined as Mock cell line and this clone was used for further experiments.

For the development of Master 2 cell lines, 1 x 10^6 cells of the Master 1 cell line were transfected with 10 µg of vector 726 (linearized with BspHI, see Fig. 45) and mini-pools were generated according to the standard procedure and cultivated in Medium D3 containing 200 mg/L Hygromycin B and 10 nM MTX.

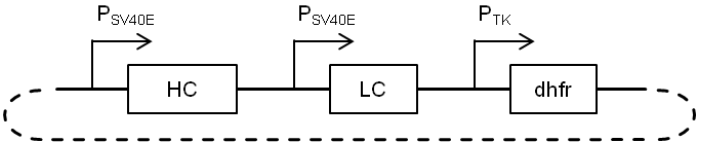

Fig. 45: Schematic representation of vector 726

Based on the results of a non-quantitative ELISA, the 48 best-producing mini-pools were selected and transferred to Medium D3 containing 200 mg/L Hygromycin B and 25 nM MTX. Following the amplification procedure, the 10 best-producing mini-pools were selected by qELISA and used to isolate single clones by FACS. All growing clones were transferred to

24 well plates and cultivated in Medium D3 containing 200 mg/L Hygromycin B, and 25 nM MTX. The 48 best-producing clones were identified by nqELISA and expanded up to the 6 well scale.

Tab. 39: Overview of growth and productivity data for the selected clones on 6 well scale

Clone	1	9	19	21	26	30	31	32	33	36	37	39
Viable cell conc. [10^5 c/mL]	13.4	26.8	30.7	20.0	27.6	13.8	25.5	26.2	23.3	28.7	22.8	21.1
Viability [%]	91	95	93	95	95	96	95	95	96	95	96	96
Product conc. [mg/L]	38	19	20	23	21	21	31	30	24	25	40	26
Cell sp. productivity [pg/cell/day]	23	8	9	12	9	14	16	15	12	12	21	16

The 12 best-producing clones were determined by qELISA (see Tab. 39) and analyzed in a fed-batch process. Fig. 46 shows the fed-batch performance of the 3 best-producing clones regarding growth, viability and product formation.

A

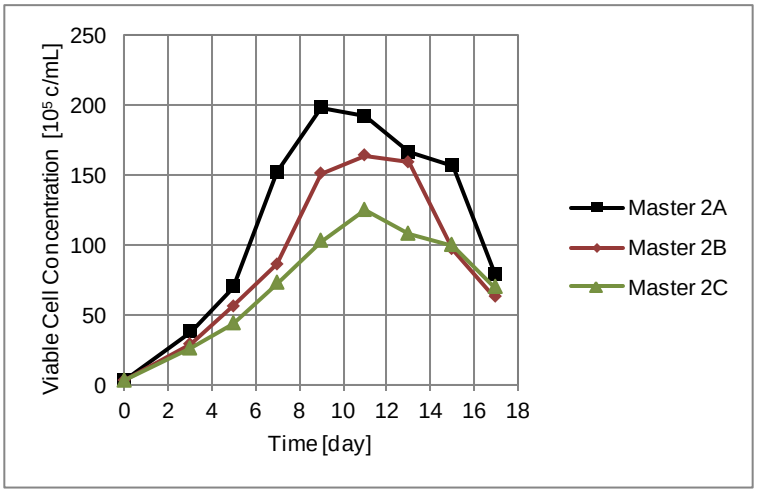

B

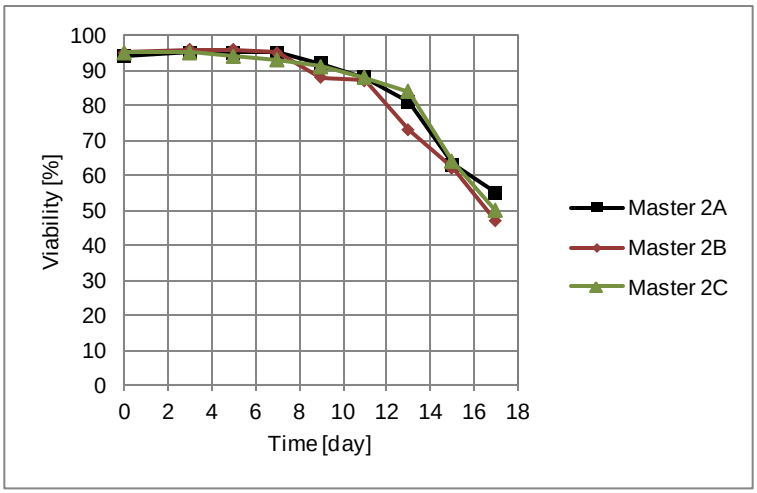

C

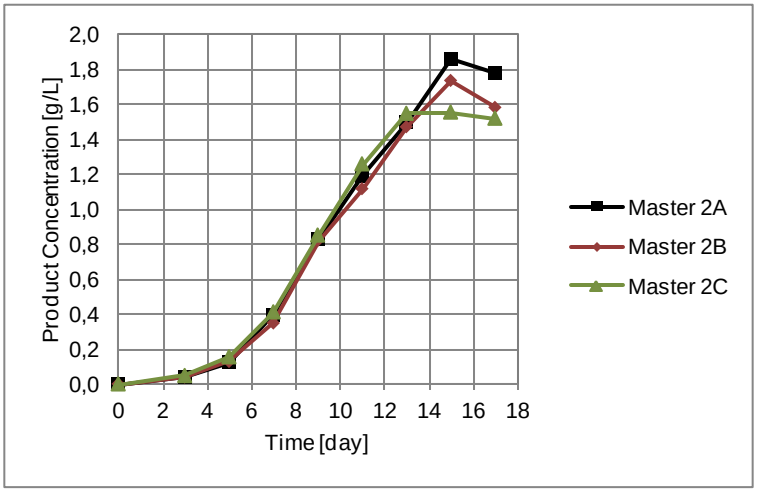

Fig. 46: Fed-batch experiment with selected Master 2 cell lines

All clones listed in Tab. 39 were subjected to a fed-batch experiment. During the process all cultures were daily analyzed with regard to viable cell concentration (A), viability (B) and product concentration (C). On the end of the experiment cell clone 9, 39 and 31 were selected and respectively termed Master 2A, 2B and 2C cell line.

Tab. 40: Overview of fed-batch results for the selected Master 2 cell lines

	Master 2A	Master 2B	Master 2C
Peak viable cell density [10^7 c/mL]	198	164	125
Product concentration on day 15 [g/L]	1.9	1.7	1.6
Cell specific productivity on day 3 [pg/cell/day]	9	11	15

During the fed-batch process Clone 9, clone 39 and clone 31 produced the highest amount of antibody and were defined as Master 2 cell lines, termed Master 2A, 2B and 2C, respectively. Fig. 46 shows the fed-batch performance of the selected Master cell lines regarding growth, viability and product formation. The most important results are listed in Tab. 40. From the combined data, it was concluded, that all three clones showed production characteristics and could be used for further experiments.

6.6. Generation of ER stress reporter cell lines

6.6.1. Generation of ER stress reporter constructs (RMCE donors)

According to the results obtained in chapter 6.3, several ER stress promoters and regulatory elements were used to create a number of reporter constructs, which were intended to indicate antibody expression levels based on GFP fluorescence. A first set of ER stress reporter constructs contained an SV40 basal promoter followed by eGFP and three copies of the transcription factor binding sites ERSE I, ERSE II, UPRE and AARE in front of the promoter. Moreover, a control construct was generated only comprising the SV40 basal promoter and eGFP (Fig. 47). The chosen binding sites are present in many promoters involved in ER stress pathways and have been reported to play a prominent role during ER stress responses (Yoshida 1998; Roy 1999; Kokame 2001; Wang 2000; Ma 2004; Lee 2002).

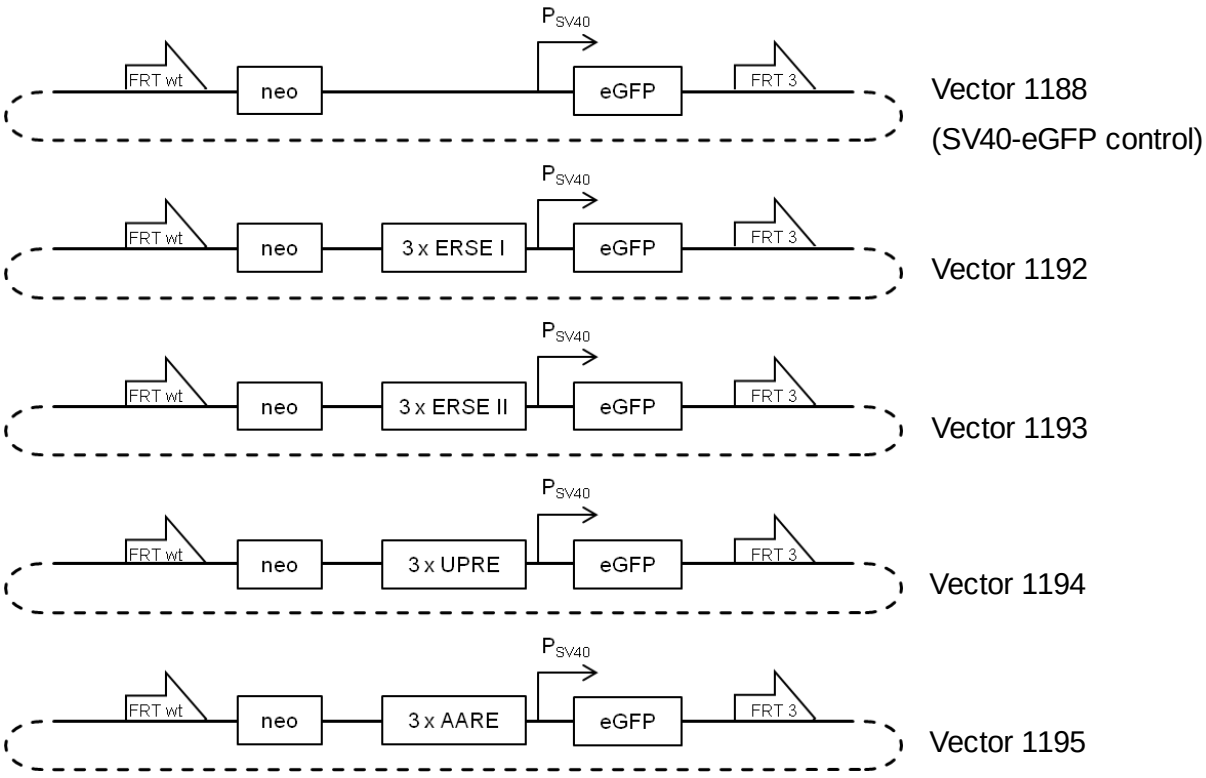

Fig. 47: Overview of used ER stress reporter and control constructs (containing eGFP)

All ER stress reporter constructs contain a promoterless neomycin resistance gene, three ER stress response elements (transcription factor binding sites 3 x ERSE I, 3 x ERSE II, 3 x UPRE or 3 x AARE), and a SV40 basal promoter followed by eGFP. The whole cassette is flanked by heterospecific FRT-sites (FRTwt and FRT3) enabling their use as RMCE donors. Vector 1188 is used as a control vector and did not contain any transcription factor binding site

It has previously been demonstrated, that the promoters of CALR, GRP78, and GRP94 as well as the unusual cytosolic splicing process of an XBP1 intron were affected by the unfolded protein response (Llewellyn 1996; Yoshida 1998; Renna 2007; Back 2006; Yoshida 1998; Llewellyn 1996, Lee 2002). Therefore, in a second set of vectors, the mentioned promoters as well as the SV40 basal promoter were placed in front of the d2eGFP reporter gene (Fig. 48).

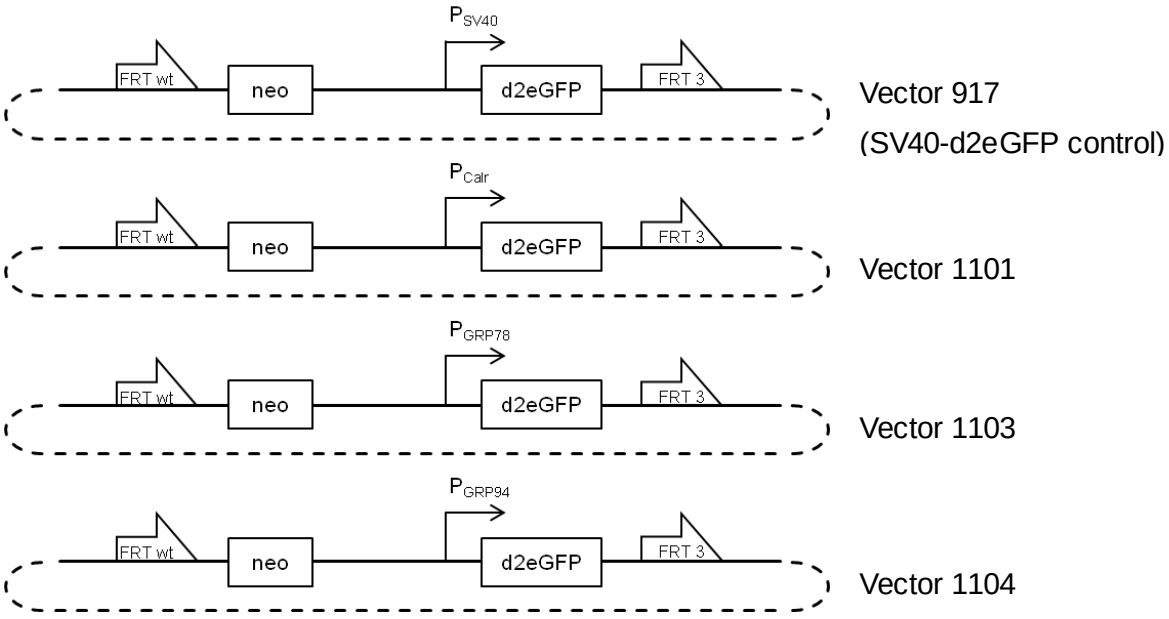

Fig. 48: Overview of used ER stress reporter and control constructs (containing d2eGFP)

As depicted in Fig. 47 also the ER stress reporter constructs contain a promoterless neomycin resistance gene, a natural promoter including their 5' UTR (with the exception of the Kozak sequence) followed by d2eGFP. The whole cassette is flanked by heterospecific FRT-sites (FRTwt and FRT3) enabling their use as RMCE donors. Vector 917 is used as a control vector and contains just a SV40 basal promoter followed by d2eGFP.

Finally, an artificial d2eGFP construct was generated, comprising the XPB1 intron (Back 2006; Iwawaki 2004) placed between the GFP coding region and the adjacent destabilizing PEST element (see chapter 5.2.3 and Li and Coffino 1993). The rationale of this construct was as follows: upon ER stress, the XBP1 intron is spliced out, thereby causing a shift in the coding sequence, which brings an artificial stop codon in frame with the eGFP sequence. By this mechanism, the addition of the PEST signal to eGFP is prevented, resulting in a more stable version of GFP. In contrast, without any ER stress splicing is not stimulated and the ribosome reads though the artificial stop codon (is not in frame). By this mechanism the PEST sequence is fused to the GFP and the protein degradation is accelerated resulting in lower GFP fluorescence.

Fig. 49: Overview of used ER stress reporter construct (containing an artificial variant of d2eGFP)

The ER stress reporter construct contain a promoterless neomycin resistance gene, SV40 basal promoter followed by eGFP fused on a XBP1 fragment and a PEST sequence (construct as described in chapter 5.2.3). The whole cassette is flanked by heterospecific FRT-sites (FRTwt and FRT3) enabling their use as RMCE donors.

In accord with the promoter-outside concept (Qiao 2009) all above mentioned ER stress reporter and control constructs (Fig. 47, Fig. 48 and Fig. 49) were additionally equipped with a promoterless neomycin resistance gene and flanked by two heterospecific FRT-sites enabling their use as RMCE donors. Thus, by RMCE the constructs could be specifically integrated into pre-defined genomic loci of cell lines tagged with a DsRed acceptor construct. Cells undergoing RMCE could then be selected for their persistence in the presence of G418.

6.6.2. Generation and analysis of ER stress reporter cell lines by RMCE

In order to identify and establish the best possible ER stress reporter system for antibody expression, all constructs described in chapter 6.6.1 were evaluated. For this purpose, each vector was introduced into the Master 2A, 2B and 2C as well as into the Mock cell line by RMCE, as illustrated in Fig. 37 and Fig. 50. All used cell lines were previously tagged with the same DsRed RMCE acceptor construct at the same genomic locus. Therefore, a good comparability of the obtained results was ensured, because disturbing influences due to different genomic integration sites and varying copy numbers could be excluded.

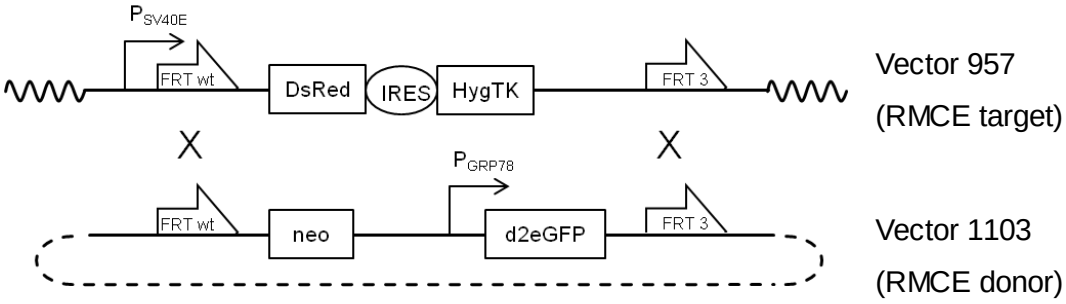

Fig. 50: Schematic representation of the cassette exchange procedure

During the cassette exchange procedure, the bicistronic DsRed-IRES-HygTK construct was exchanged by a promoterless reporter construct coding for a neomycin resistance gene and a GRP78 promoter followed by d2eGFP. After the exchange procedure, the neomycin resistance gene was localized behind the SV40E promoter and the gain clones were resistant to G418.

1 x 10^6 cells of each cell line were co-transfected with 6 µg of every ER stress reporter or control construct and 1 µg vector 673, coding for the Flpo flippase. Two days after transfection, all pools were transferred to Medium D3 supplemented with 25 nM MTX and 500 mg/L G418. A ganciclovir negative selection as described by Qiao (2009) was not performed. In contrast on day 7, all cells were analyzed by FACS and GFP positive clones were isolated by single cell sorting as depicted in Fig. 51 and cultivated in Medium C1.

SV40-eGFP control

Mock Rep	Master 2A Rep	Master 2B Rep	Master 2C Rep
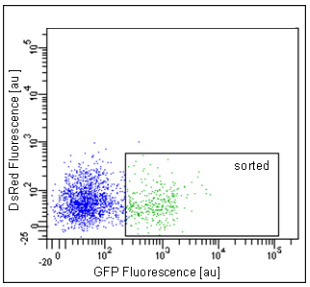	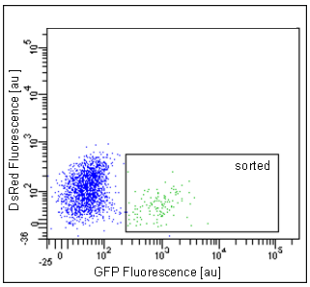	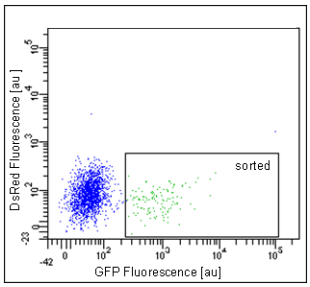	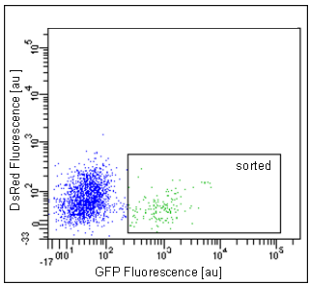
991	1033	1143	1171

3 x ERSE I

Mock Rep	Master 2A Rep	Master 2B Rep	Master 2C Rep
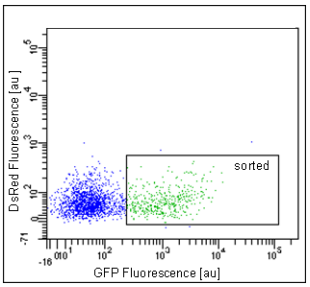	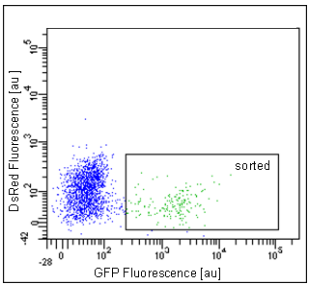	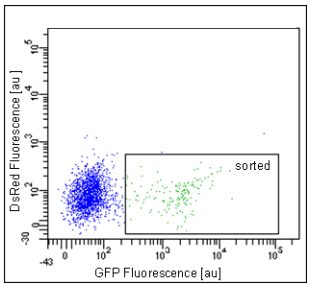	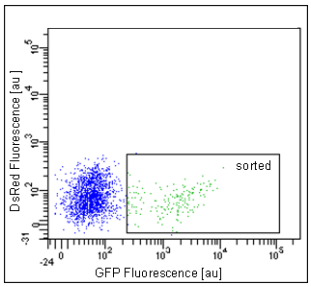
1604	2113	2605	2070

3 x ERSE II

Mock Rep	Master 2A Rep	Master 2B Rep	Master 2C Rep
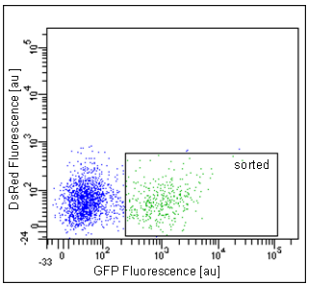	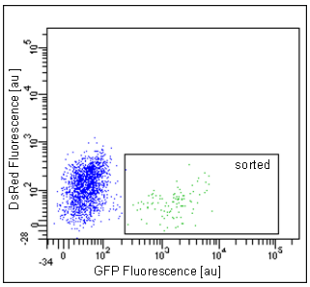	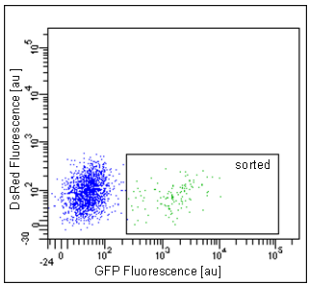	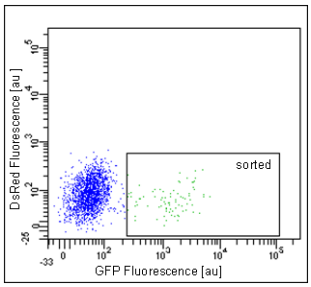
1426	1935	2029	1668

3 x UPRE

Mock Rep	Master 2A Rep	Master 2B Rep	Master 2C Rep
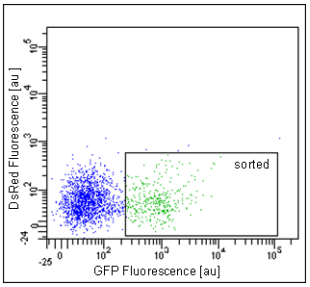	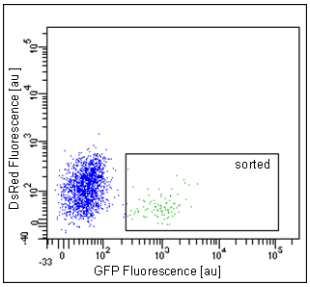	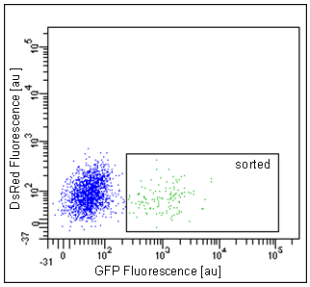	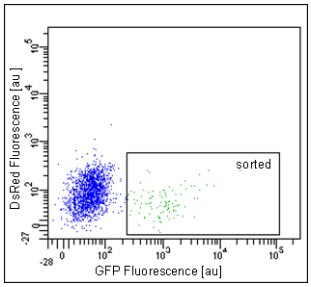
1099	1048	1362	1501

3 x AARE

Mock Rep	Master 2A Rep	Master 2B Rep	Master 2C Rep
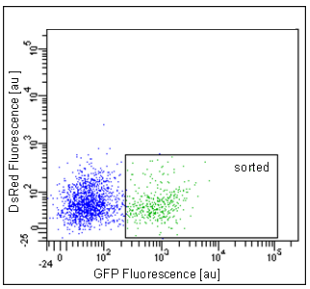	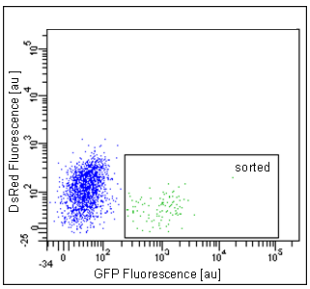	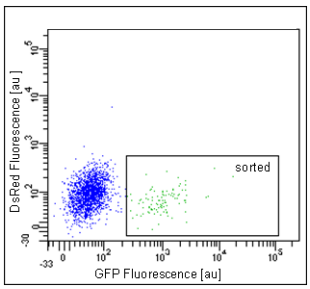	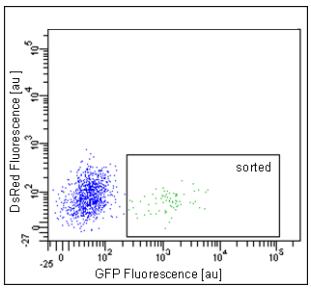
1083	1244	1357	1527

SV40-d2eGFP control

Mock Rep	Master 2A Rep	Master 2B Rep	Master 2C Rep
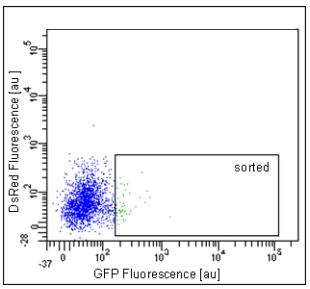	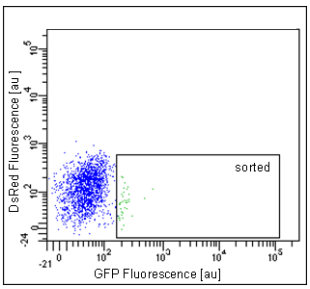	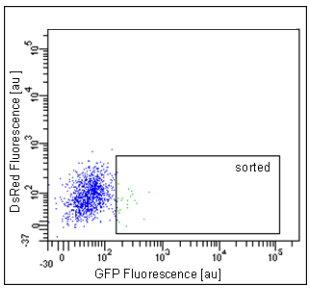	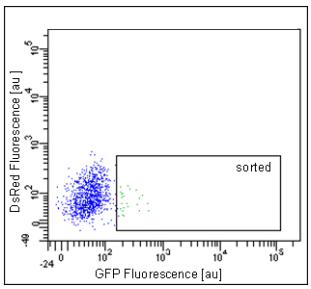
265	224	254	263

Intron

Mock Rep	Master 2A Rep	Master 2B Rep	Master 2C Rep
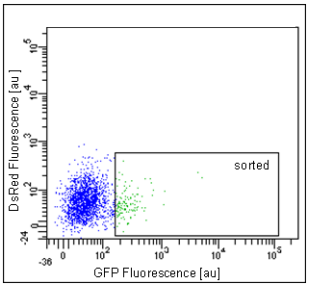	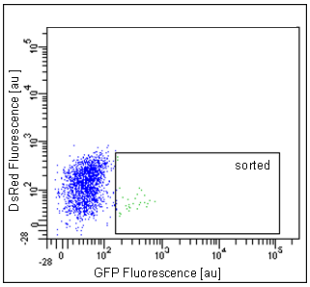	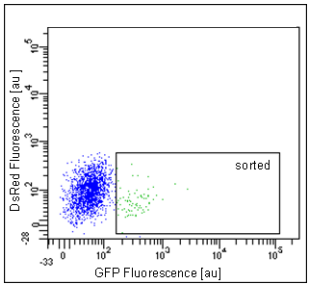	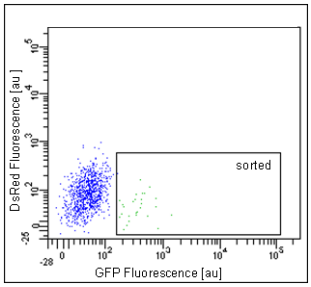
347	338	395	401

CALR

Mock Rep	Master 2A Rep	Master 2B Rep	Master 2C Rep
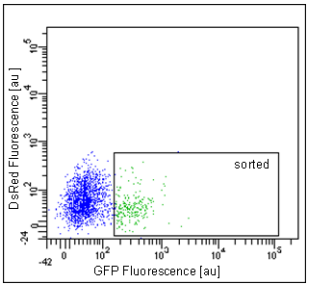	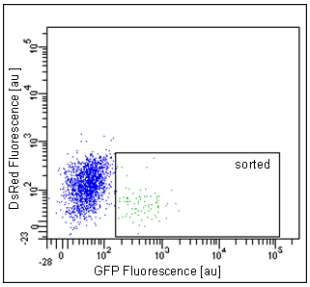	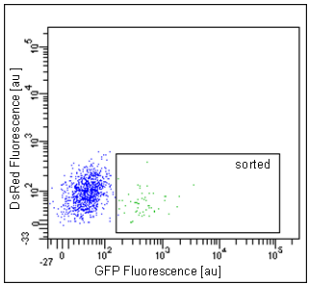	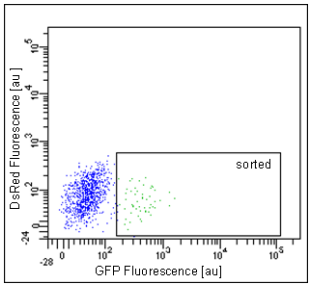
364	513	568	459

GRP78

Mock Rep	Master 2A Rep	Master 2B Rep	Master 2C Rep
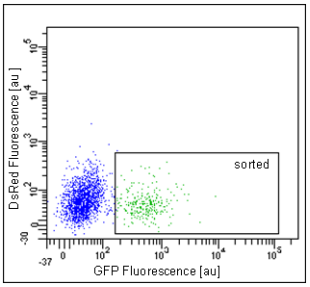	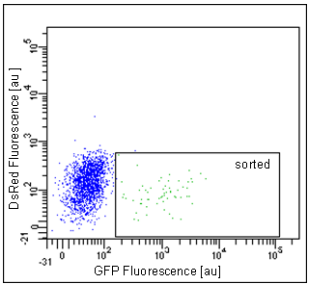	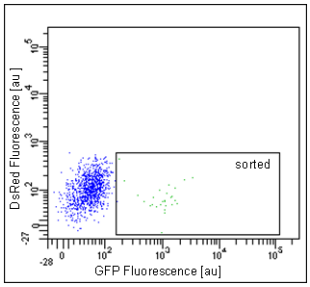	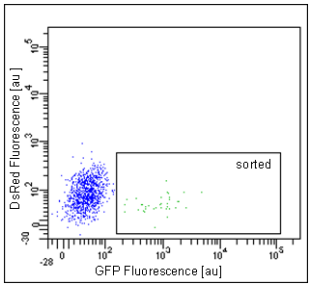
662	1315	1098	1029

GRP94

Mock Rep	Master 2A Rep	Master 2B Rep	Master 2C Rep
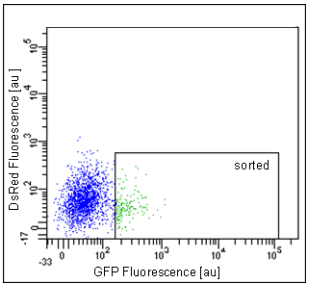	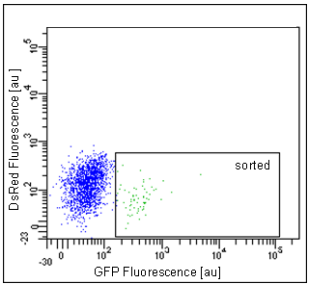	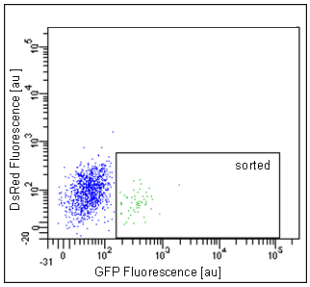	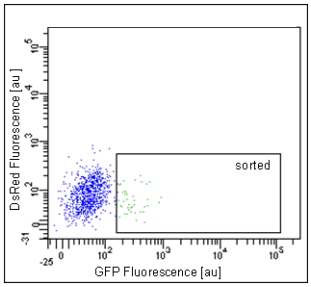
282	476	391	322

Fig. 51: FACS analysis and single cell sorting of Master 2 and Mock cell lines after RMCE with ER stress reporter or control constructs

The Mock, Master 2A, Master 2B and Master 2C cell lines were co-transfected with a Flpo vector and the indicated ER stress reporter or control constructs and cultivated in Medium D3 supplemented with 25 nM MTX and 500 mg/L G418. On day 7, all cell pools were analyzed regarding DsRed and GFP fluorescence by flow cytometry and GFP positive single clones were isolated by sorting as indicated (gate "sorted"). The mean GFP fluorescence [au] of the gated population of each cell pools is depicted below each image.

Tab. 41: Overview of analysed pools

The Mock, Master 2A, Master 2B and Master 2C cell lines were analysed as described in Fig. 51 and the ratio between the whole population and the gated population (likely exchanged clones) was calculated.

	Exchanged clones [%] **Mock Rep**	Exchanged clones [%] **Master 2A Rep**	Exchanged clones [%] **Master 2B Rep**	Exchanged clones [%] **Master 2C Rep**
SV40-eGFP control	17	6	6	7
3 x ERSE I	20	9	8	9
3 x ERSE II	18	5	6	4
3 x UPRE	18	5	6	5
3 x AARE	19	5	5	7
SV40-d2eGFP control	3	2	2	2
Intron	6	2	4	3
CALR	12	4	5	6
GRP78	13	3	3	4
GRP94	8	3	5	4

After single cell sorting all 431 grown clones were expanded in Medium D3 containing 25 nM MTX and 500 mg/L G418 and analyzed for correct cassette exchange. Correct cassette exchange means that the DsRed RMCE acceptor construct is removed and authentically replaced by the donor construct and that no random integration events occurred. In order to verify this, genomic DNA of all clones was prepared and subjected to PCR analysis (see

chapter 5.2.5). Authentic exchange events, unexchanged clones and random integrations of the donor construct could be detected by using appropriate primer pairs as schematically depicted in Fig. 52. The obtained results are exemplified in Fig. 52 based on a small number of clones.

A

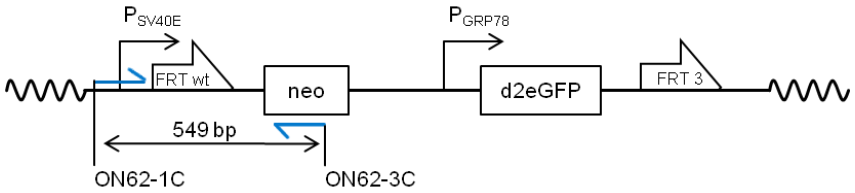

B

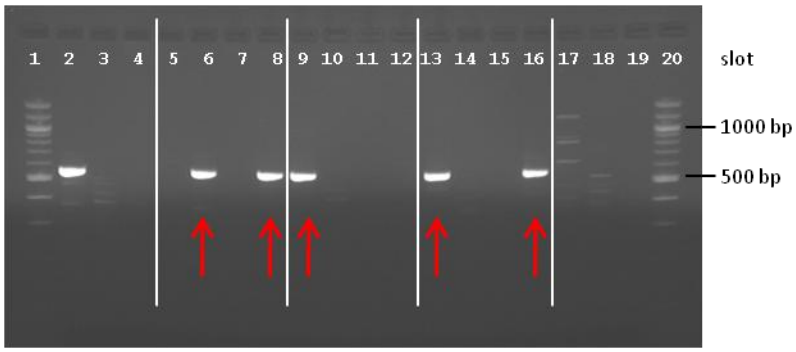

C

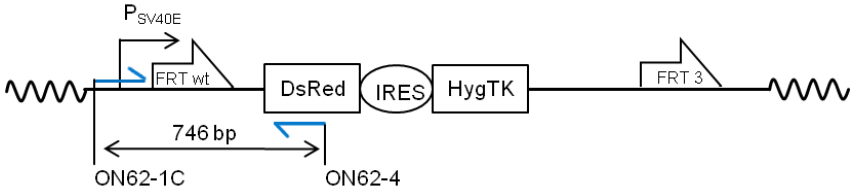

D

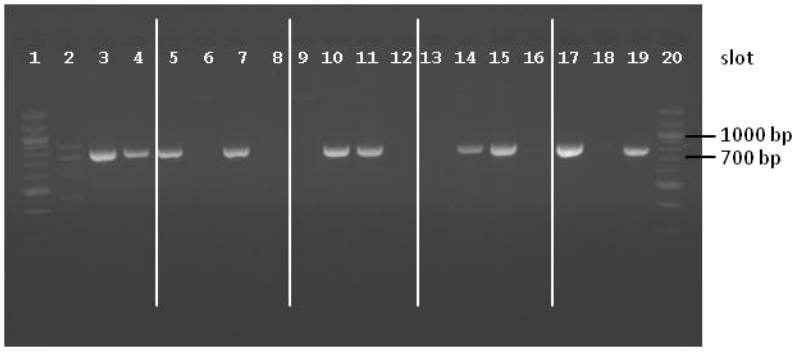

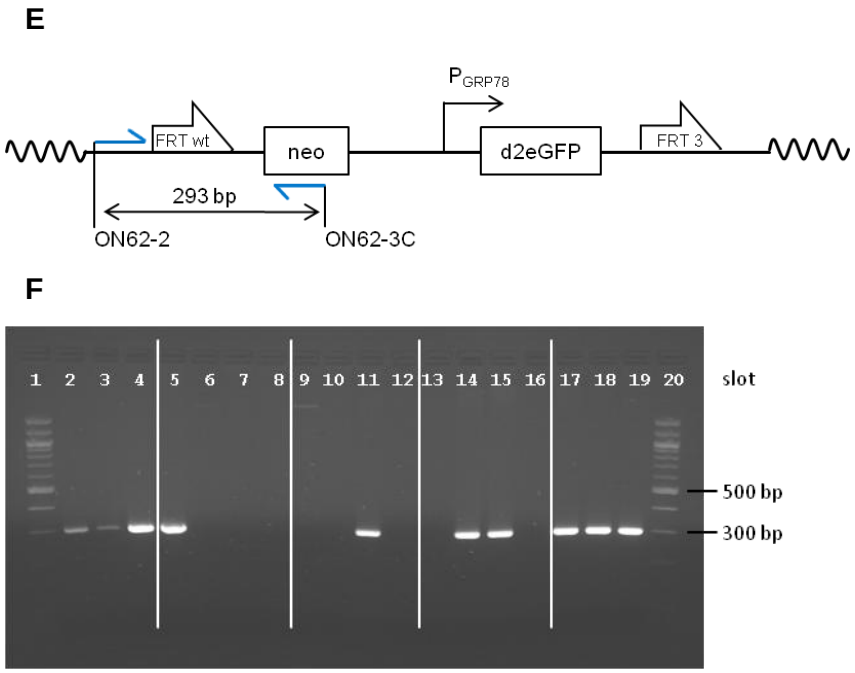

Fig. 52: PCR analysis of Mock and Master 2 cell clones exchanged with ER stress reporter or control constructs

The Mock, Master 2A, Master 2B and Master 2C cell lines were subjected to RMCE using different ER stress reporter or control constructs followed by the isolation of GFP positive clones by cell sorting. As described in chapter 5.2.5, genomic DNA was prepared from all grown clones and analyzed by PCR using specific primer pairs to identify authentic exchange events (A), unexchanged clones (C) and random integrations of the donor construct (E). The obtained results are exemplified based on a small number of clones (B, D and F). Authentically exchanged clones, which showed no additional random integrations are highlighted by red arrows.

Upon analysis of all samples, 174 clones were identified, that showed authentic exchange and no additional random integrations (see Tab. 42). They were referred to as Mock Reporter, Master 2A Reporter, Master 2B Reporter, and Master 2C Reporter and used for further experiments.

Tab. 42: Overview of clones with authentic exchanged reporter or control constructs (174 clones)

Detailed information about these clones is shown in Fig. 64

	Number of clones **Mock Rep**	Number of clones **Master 2A Rep**	Number of clones **Master 2B Rep**	Number of clones **Master 2C Rep**
SV40-eGFP control	4	8	5	10
3 x ERSE I	1	6	5	3
3 x ERSE II	1	3	0	3
3 x UPRE	3	5	7	4
3 x AARE	3	6	4	0
SV40-d2eGFP control	1	10	4	5
Intron	4	11	4	0
CALR	3	5	6	1
GRP78	7	4	1	7
GRP94	3	9	5	3

All other clones were not exchanged or contained randomly integrated ER stress reporter or control cassettes. Actually, 14% of these clones were correctly exchanged, but showed additional random integrations, whereas 68% were not exchanged and had only random integrations. 18% of all clones did not grow in Medium D3 containing 25 nM MTX and 500 mg/L G418, these clones were neither exchanged or showed random integrations.

6.7. Evaluating the influence of antibody expression on ER stress reporter constructs

Different ER stress reporter constructs were evaluated by analyzing the influence of antibody expression on the reporter protein level based on the cell lines generated in chapter 6.6.2. For this reason, GFP fluorescence of all generated Mock Reporter, Master 2A Reporter, Master 2B Reporter, and Master 2C Reporter cell lines was measured by FACS and normalized to the corresponding control constructs. This was done on pool level, 7 days after transfection, as well as for all isolated and correctly exchanged clones.

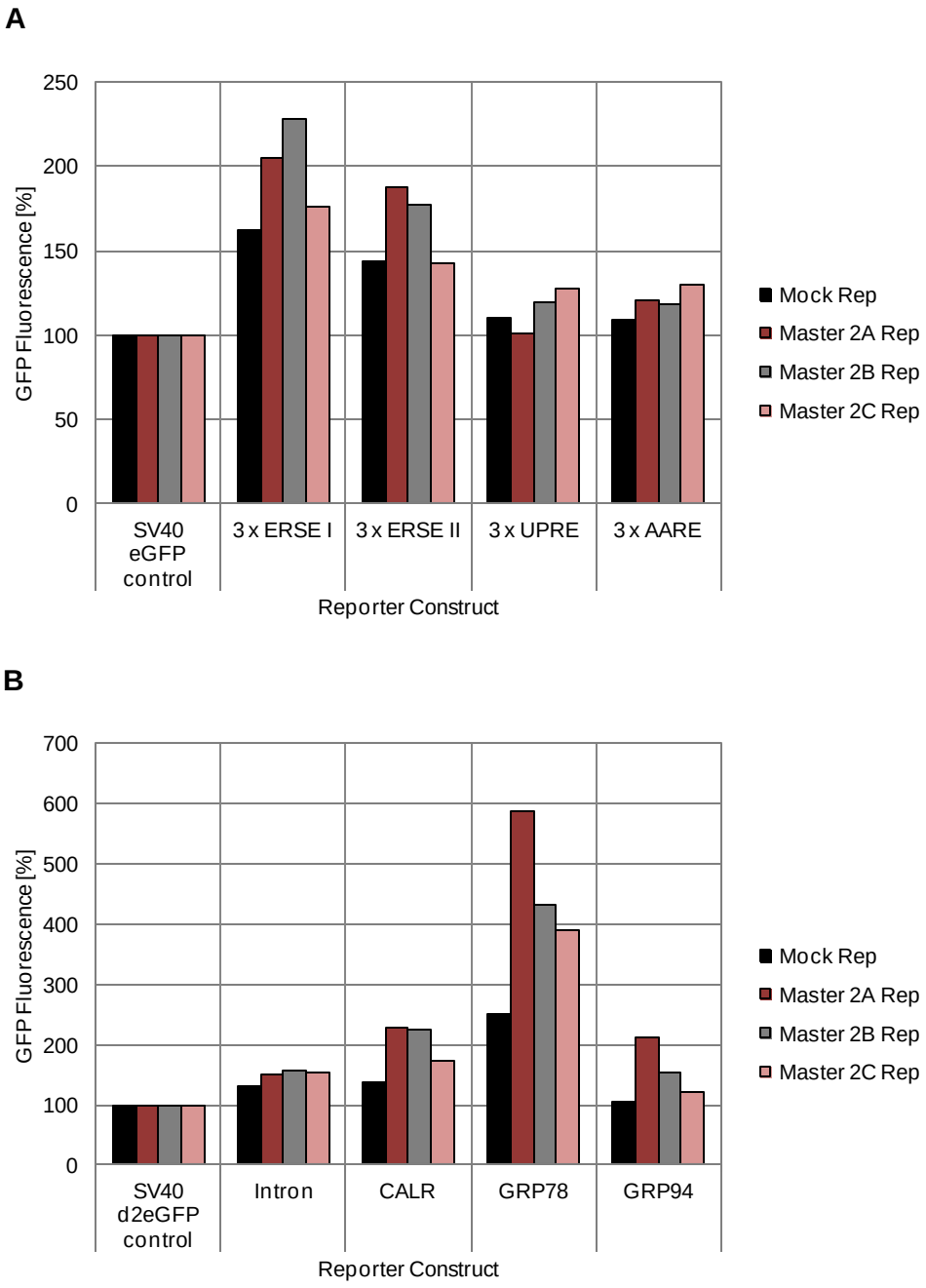

Fig. 53: FACS analysis of exchanged cell pools derived from Mock and Master 2 cell lines

The Mock, Master 2A, Master 2B and Master 2C cell lines were co-transfected with a Flpo vector and the indicated ER stress reporter or control constructs and cultivated in Medium D3 supplemented with 25 nM MTX and 500 mg/L G418. On day 7, all cell pools were analyzed regarding GFP fluorescence by flow cytometry and the mean fluorescence intensities of the GFP positive populations were determined (cf. Fig. 51 gate "sorted"). The obtained values were normalized to the fluorescence of the corresponding SV40-eGFP control (A) or SV40-d2eGFP control (B) construct, which was set to 100%.

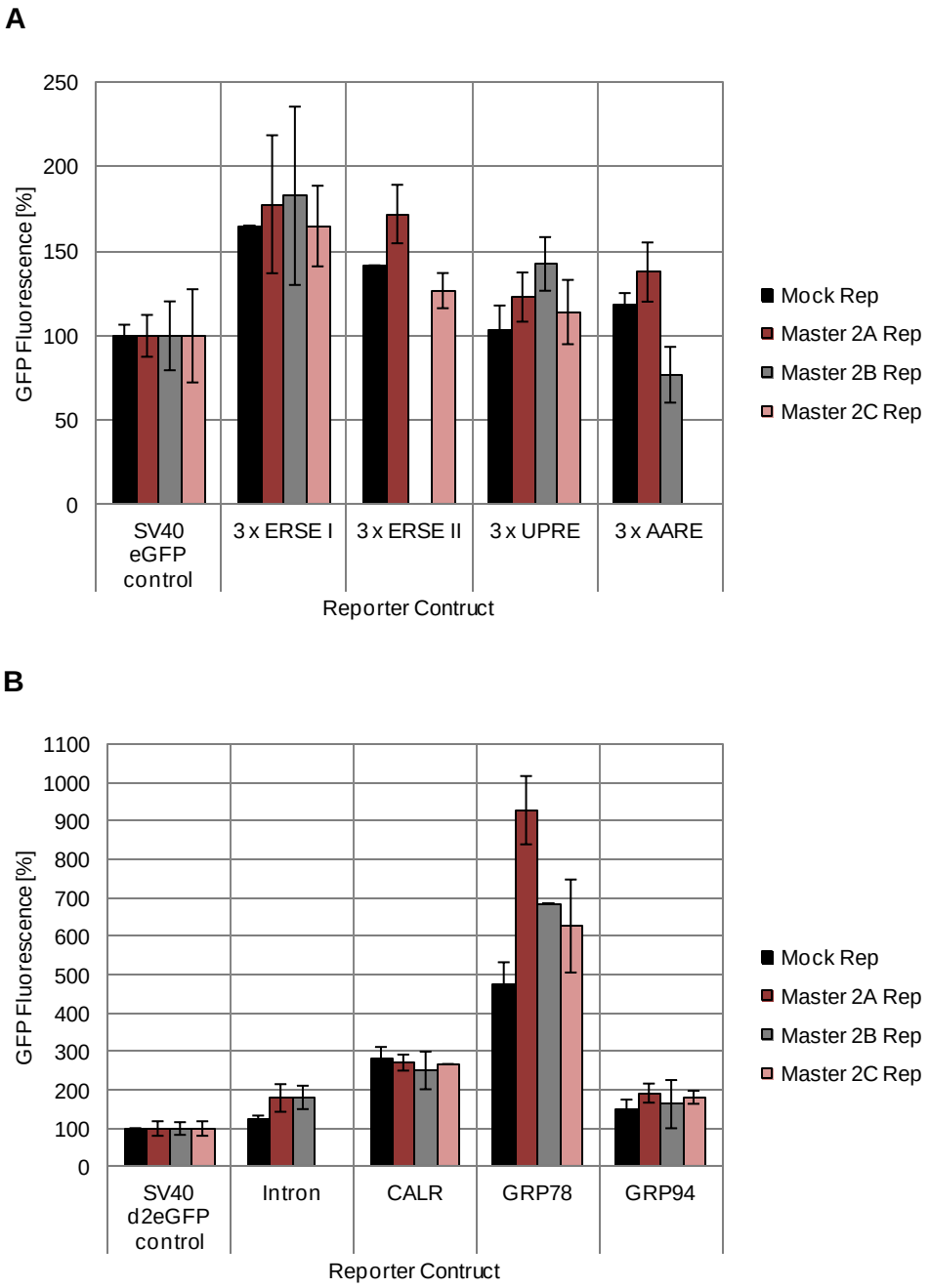

Fig. 54: FACS analysis of Mock and Master 2 cell clones authentically exchanged with ER stress reporter or control constructs

The Mock, Master 2A, Master 2B and Master 2C cell lines were subjected to RMCE using the indicated ER stress reporter or control constructs followed by the isolation of GFP positive clones by cell sorting. As described in chapter 5.2.5, all grown clones were evaluated for authentic exchange by PCR on genomic DNA (cf. Fig. 52). Correct clones were analyzed regarding GFP fluorescence by flow cytometry and the mean GFP fluorescence intensities of the whole populations were determined. The obtained values were normalized to the mean fluorescence of the corresponding SV40-eGFP control (A) or SV40-d2eGFP control (B) clones, which were set to 100%. The values represent the average of several independent experiments, as summarized in Tab. 42 (detailed information is shown in Fig. 64).

Basically, similar results were obtained both on pool and clone level (compare Fig. 53 and Fig. 54), indicating the robustness of the used test system. Moreover, all clones derived from the same reporter construct showed similar GFP levels (small standard deviations in Fig. 54), which confirms the generation of isogenic subclones by using the RMCE approach.

As seen in Fig. 53 and Fig. 54, when introduced into the Mock cell line, most ER stress reporter constructs mediated increased GFP levels compared to the SV40-eGFP or SV40-d2eGFP control constructs just equipped with a basal SV40 promoter. This implies that most tested transcription factor binding sites were able to stimulate the activity of the SV40 basal promoter and that the natural promoters of CALR, GRP78 and GRP94 showed generally higher transcription rates than the SV40 promoter. However, significant differences between Mock and Master 2A, 2B and 2C Reporter cell lines could not be observed for any construct with exception of the vector containing the GRP78 promoter. In this case, the GFP fluorescence of the Master 2A, 2B and 2C Reporter cells was markedly increased when compared to the respective Mock cell line and in addition a correlation between GFP fluorescence and antibody concentration was observed (cf. Tab. 40).

From these data it was concluded, that only the GRP78 promoter is stimulated by antibody expression and that all other constructs did not show any significant effect and therefore cannot be used as reporters for antibody productivity. By way of contrast, the GRP78 ER stress reporter construct might represent an adequate detection system to identify clones producing high amounts of antibody.

6.8. Impact of BFA or CSN treatment on ER stress reporter constructs

So far, the response of the ER stress reporter constructs to antibody expression was only tested at moderate productivities (1.6–1.9 g/L in a fed-batch process). Consequently, the extent of the stimulation that could possibly be reached by the individual reporter constructs was unclear. In order to analyze, whether the used constructs have the potential to indicate also clones with higher productivities, increased ER stress was artificially triggered by the ER stress inducing reagents Brefeldin A (BFA) and Castanospermine (CSN) (Pollard 2007; Wang 2000; Saul 1985; Ahmed 1995). For this purpose, randomly selected Master 2A and Mock Reporter cell lines (generated in chapter 6.6.2) were treated with 10 µg/mL BFA or 100 µg/mL CSN for one day and the GFP fluorescence was analyzed by FACS.

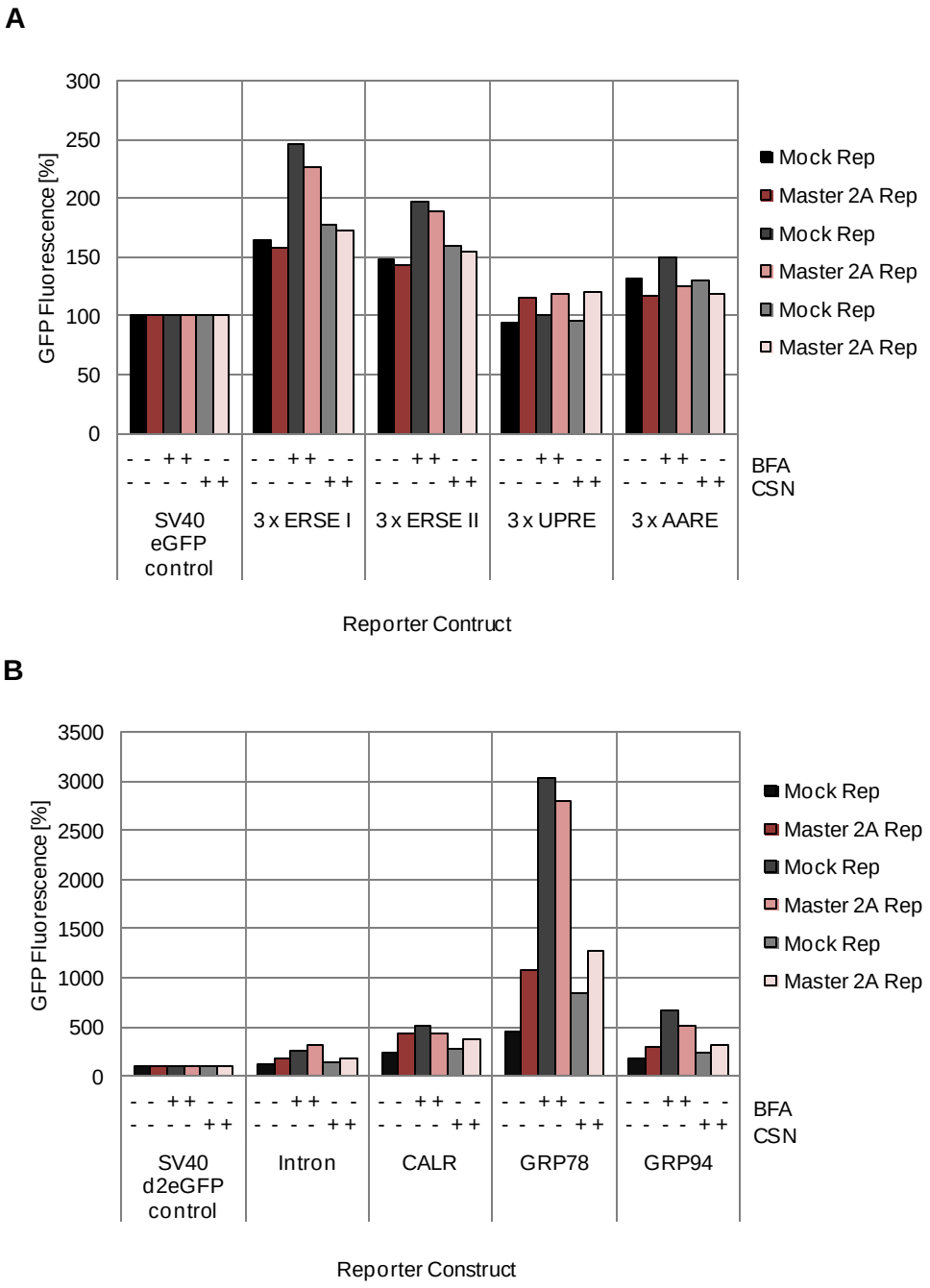

Fig. 55: FACS analysis of Mock and Master 2 Reporter cell lines treated with BFA or CSN

One Mock and Master 2A Reporter cell clone containing the indicated ER stress reporter or control constructs, respectively, were cultivated for one day in Medium D3 under three different conditions: without BFA and CSN, supplemented with 10 µg/mL BFA or supplemented with 100 µg/mL CSN. Subsequently, cells were analyzed regarding GFP fluorescence by flow cytometry and the mean fluorescence intensities of the GFP positive populations were determined. The obtained values were normalized to the mean fluorescence of the corresponding SV40-eGFP control (A) or SV40-d2eGFP control (B) clones, which were set to 100%.

The CSN treatment did not result in increased GFP fluorescence for any ER stress reporter construct with exception of the one comprising the GRP78 promoter. (Fig. 55 A and B). By BFA treatment, it was possible to stimulate the Mock and the Master 2A Reporter cells containing the 3 x ERSE I, 3 x ERSE II and GRP78 constructs (Fig. 55 A and B). Interestingly, in case of the Mock GRP78 and Master 2A GRP78 Reporter cells GFP fluorescence was increased up to 6-fold, when compared to untreated cells. From these results it was concluded, that especially the GRP78 reporter system was not maximally stimulated by the present antibody levels and that there should be a high potential to detect also clones with clearly enhanced productivities.

6.9. Establishment of a novel ER stress based selection system for the isolation of high-producing clones

In the preceding chapters, the GRP78 promoter was identified as most promising response element to establish a novel selection system for high-expressing clones based on ER stress. In the last part of the present thesis, this system was evaluated regarding its suitability to identify and isolate high producers. For this purpose, in a first step, a stable reporter cell line was created by the integration of a construct comprising GFP, driven by the trunc GRP78 promoter. In contrast to the previously applied reporter construct, this time a truncated promoter region and the more stable eGFP were used, resulting in an improved performance (data not shown). Furthermore, no FRT-sites were included in order to keep the possibility of RMCE for potential future applications. In a second step, the created reporter cell line was subjected to a standard cell line development procedure employing an expression construct for a model antibody (both steps are depicted in Fig. 56). Finally, the obtained clones were analyzed with regard to a potential correlation between productivity and GFP fluorescence.

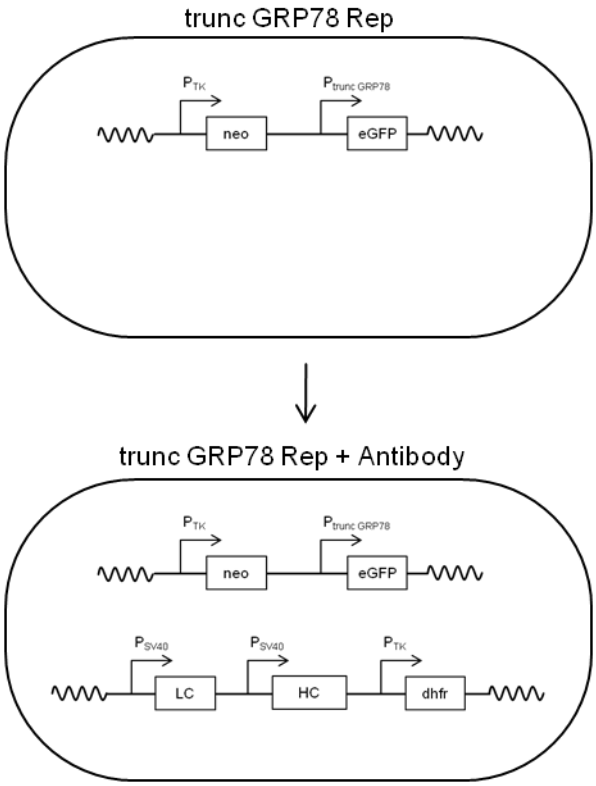

Fig. 56: Schematic representation of the generation of the trunc GRP78 Reporter cell line stably expressing a recombinant antibody

For the generation of the reporter cell line, 1 x 10^6 CHO DG44 cells were transfected with 10 µg of circular vector 527 (see Fig. 57).

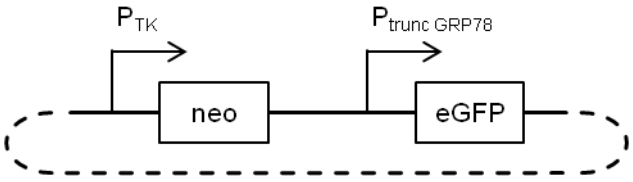

Fig. 57: Schematic representation of vector 527

One day after transfection, cells were transferred into Medium D2 containing 250 mg/mL G418 and subcultivated every 3 to 4 days, in the same medium. After 26 days, the G418 concentration was reduced to 100 mg/mL and GFP positive single clones were isolated by FACS. The 13 best-growing clones were expanded in Medium D2 containing 100 mg/mL G418 and analyzed by flow cytometry regarding their GFP fluorescence. One clone showing a suitable GFP fluorescence, a very high viability and good growth behaviour was chosen and referred to as trunc GRP78 Reporter cell line (Fig. 58).

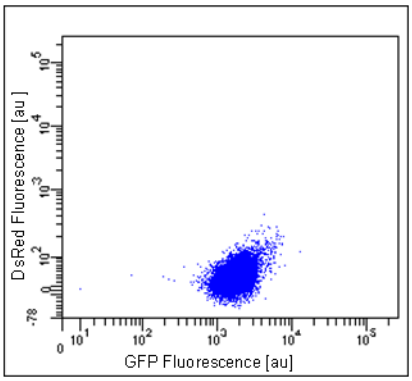

Fig. 58: FACS analysis of trunc GRP78 Reporter cell line

In order to generate a trunc GRP78 Reporter cell line stably expressing a recombinant antibody, the cells were transfected with 7.5 µg of linearized vector 314, coding for a model antibody (see Fig. 59).

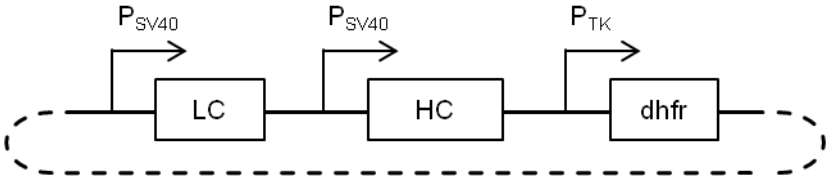

Fig. 59: Schematic representation of vector 314

Two days after transfection, cells were transferred to Medium D3 containing 100 mg/mL G418 and 25 nM MTX and subcultivated every 3 to 4 days in the same medium. After 18 d, these cells were subjected to a copy number amplification by increasing the MTX concentration to 300 nM. After about 14 day, cells had recovered from the treatment and randomly selected single cells were isolated by FACS. All grown clones were expanded up to the 6 well scale and antibody concentrations were determined by qELISA. Seven clones showing high viabilities, good growth behaviour and high cell specific productivities (see Tab. 43) were selected for further evaluation in a fed-batch process.

Tab. 43: Overview of growth and productivity data for selected production clones derived from the trunc GRP78 Reporter cell line cultivated under standard conditions

Clone	**42**	**71**	**76**	**94**	**97**	**104**	**115**
Viable cell concentration [10^5 c/mL]	20.5	15.7	20.7	15.0	30.6	17.2	10.4
Viability [%]	96	93	96	90	97	96	91
Product concentration [mg/L]	46	42	54	42	222	45	30
Cell specific productivity [pg/cell/day]	17	18	20	19	62	18	17

As shown in Fig. 60, all clones showed similar viabilities over the whole process, but clearly different growth behaviour and product concentrations ranging from 0.5 to 2.1 g/L at day 11. The most important results are summarized in Tab. 44.

A

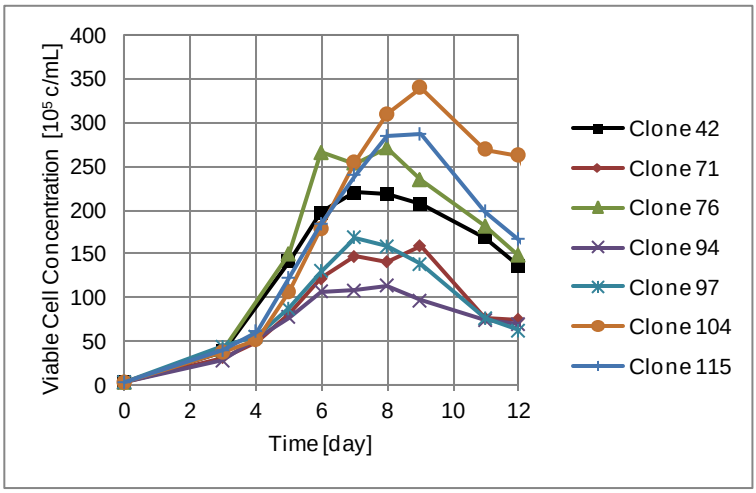

B

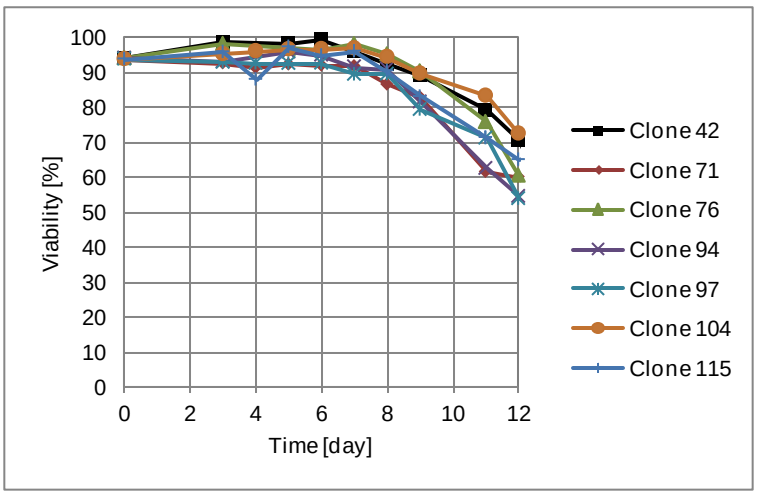

C

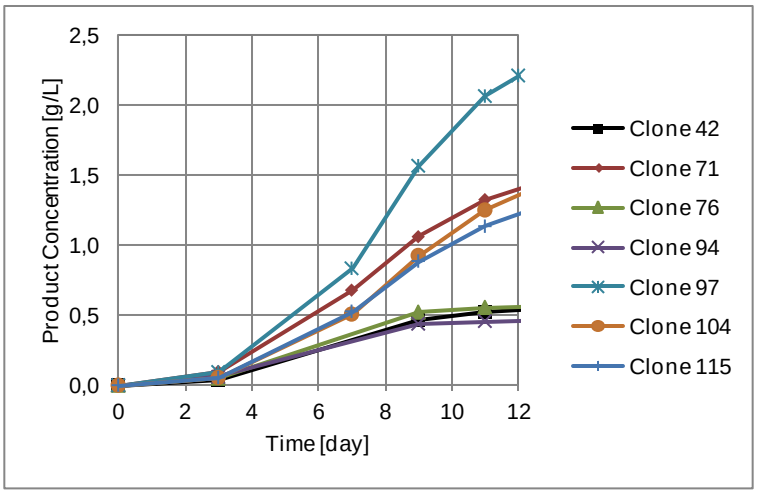

Fig. 60: Fed-batch Experiments with selected production clones derived from the trunc GRP78 Reporter cell line

The indicated production clones, generated based on the trunc GRP78 Reporter cell line were subjected to fed-batch experiments. During the process all cultures were daily analyzed with regard to viable cell concentration (A), viability (B) and product concentration (C).

Tab. 44: Overview of fed-batch results for selected clones derived from the trunc GRP78 Reporter cell line

Clone	42	71	76	94	97	104	115
Viable cell concentration on day 8 [10^5 c/mL]	219	141	271	114	158	310	285
Product concentration on day 11 [g/L]	0.52	1.33	0.56	0.46	2.07	1.25	1.14
Cell specific productivity on day 3 [pg/cell/day]	8	27	12	18	21	13	13

In order to analyze whether there is a correlation between GFP fluorescence and antibody productivity all clones selected in Tab. 43 were analysed by FACS and the GFP fluorescence was plotted against viable cell concentration, final product concentration and the cell specific productivity observed during the fed-batch process.

A

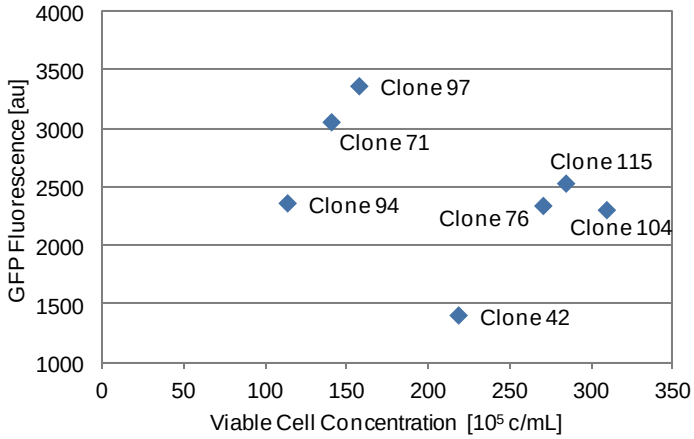

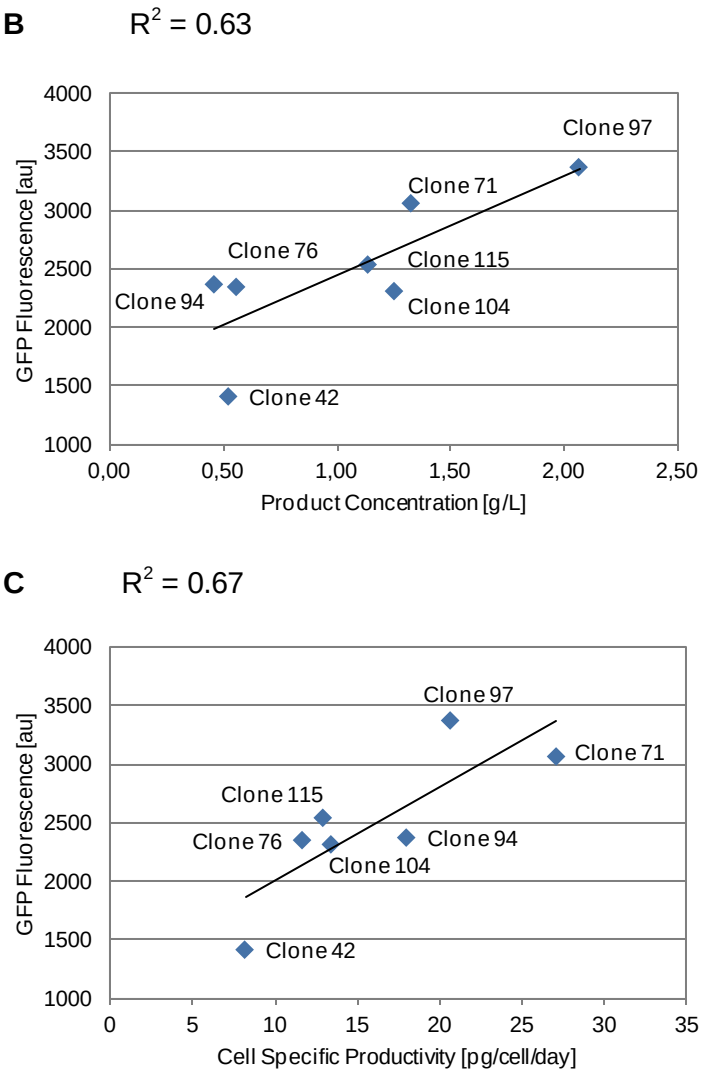

Fig. 61: Correlation between fed-batch performance (including antibody productivity) and GFP fluorescence in production clones derived from the trunc GRP78 Reporter cell line

7 production clones derived from the tunc GRP78 Reporter cell line were analyzed regarding GFP fluorescence by flow cytometry and mean fluorescence intensities were determined. In parallel, viabilities were measured with a CASY cell counter. All clones were cultivated in fed-batch experiments and viable cell concentration, product concentrations as well as specific productivities were determined. For each clone, GFP fluorescences were plotted against viable cell concentration on day 8 (A), product concentrations measured on day 11 (B) and cell specific productivities calculated on day 3 (C).

As expected, no correlation was observed between GFP fluorescence and viable cell concentration (Fig. 61 A), whereas both specific productivity (Fig. 61 C) and final product concentration (Fig. 61 B) correlated well with the GFP level. These results indicate, that the here introduced ER stress reporter system introduced here can be applied to identify and isolate high producing clones in a rapid and simple manner, just by measuring their GFP fluorescence.

Generally, all analyzed clones showed only moderate antibody expression levels. It can be assumed that clones with higher productivities could not be isolated because the truncated GRP78 reporter system was maximal stimulated by the present antibody levels. In order to investigate, whether also clones with higher productivities could be detected by the ER stress reporter system, it was evaluated whether a further stimulation of the system was possible. For this purpose, clone 42, clone 71 and clone 97 were either cultivated in Medium D6 containing 50 mg/L G418 and 300 nM MTX or in the same medium additional supplemented with 10 µg/mL BFA and 100 µg/mL CSN, respectively, for one day. Subsequently, the mean GFP fluorescence was determined by FACS and plotted against the final product concentration obtained in a fed-batch process as described in Fig. 60. Moreover, the relative mRNA levels of endogenous GRP78 were measured by real time RT-PCR for all clones.

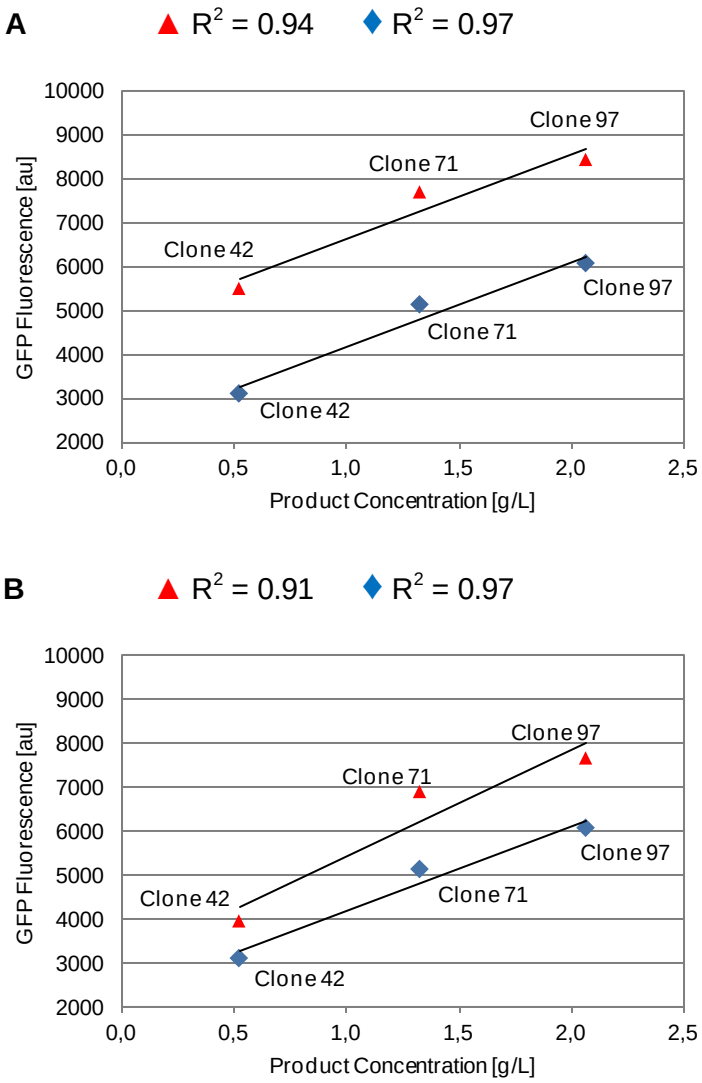

Fig. 62: FACS analysis of selected production clones derived from the tunc GRP78 Reporter cell line after treatment with BFA or CSN

Selected production clones derived from the trunc GRP78 Reporter cell line were cultivated for one day in Medium D6 containing 50 mg/L G418 and 300 nM MTX under three different conditions: without BFA and CSN, supplemented with 10 µg/mL BFA or supplemented with 100 µg/mL CSN. Subsequently, cells were analyzed regarding GFP fluorescence by flow cytometry and mean fluorescence intensities were determined (see Fig. 65). For each clone, the obtained values were plotted against product concentrations determined in fed-batch experiments on day 11. (A) Blue rhombi: untreated, red triangles: treated with BFA. (B) Blue rhombi: untreated, red triangles: treated with CSN.

As shown in Fig. 62, GFP fluorescence was clearly increased for all clones upon treatment with CSN and BFA. Interestingly, the fluorescence level was raised by a similar factor for all clones, independently of the respective basal fluorescence. Consistently, the transcription of GFP78 was also induced upon treatment with BFA (Fig. 63). The relative GRP78 mRNA level was analysed for BFA treated clone 42, clone 71, and clone 97. These levels were compared with untreated clones and the results are shown in the following figure.

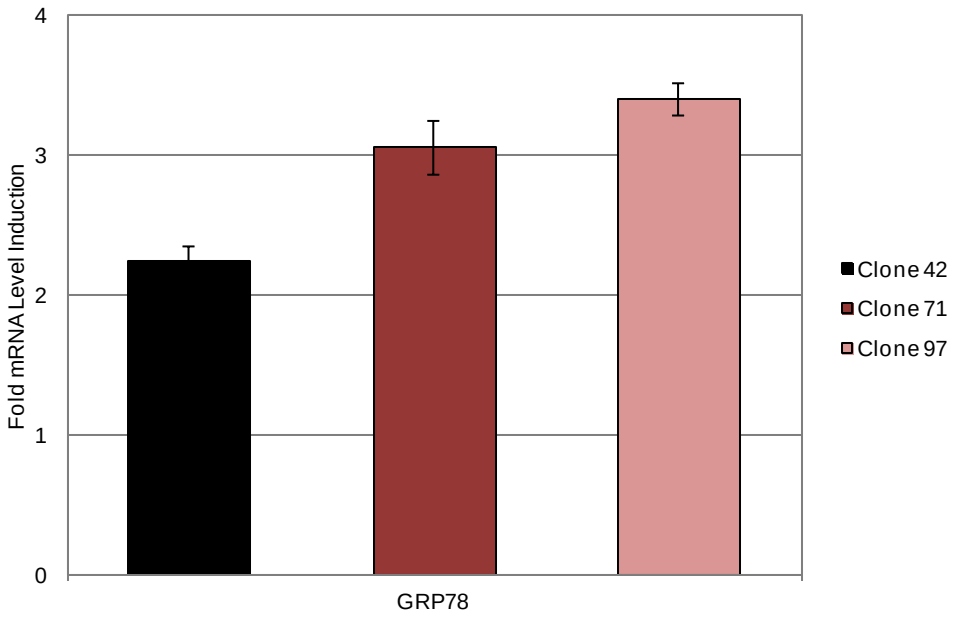

Fig. 63: Real time RT-PCR analysis of selected production clones derived from the trunc GRP78 Reporter cell line after treatment with BFA

Selected production clones derived from the tunc GRP78 Reporter cell line were cultivated for one day in Medium D6 containing 50 mg/L G418 and 300 nM MTX and in Medium D6 medium supplemented 10 µg/mL BFA. Subsequently, RNA was isolated from cells and relative mRNA levels of endogenous GRP78 were measured by real time RT-PCR and normalized using the neomycin resistance gene expression as described in chapter 5.4.6. Fold mRNA level induction represents the ratio of treated to untreated cells. The values represent the average of three independent experiments.

Based on the obtained results it was concluded, that a further stimulation of the reporter system can be achieved, which implies that also clones with higher productivities should be detectable.

7. Discussion

7.1. Increase of antibody secretion by signal peptide optimization

Platform technologies suitable for the development of stable cell lines for the high level production of recombinant proteins depend on an efficient expression system. Therefore, many efforts have been made to improve existing expression systems, mostly by trying to optimize transcription or translation efficiencies or to prevent gene silencing (Bode 2003; Hancock 2000; Williams 2005; Kwaks 2005; Zahn-Zabal 2001). However, some approaches also focus on downstream processes like protein secretion or folding. In this context, the translocation of secretory proteins into the lumen of the endoplasmic reticulum (ER) has been postulated to be a limiting step within the classical secretory pathway. Consistently, Knappskog (2007), Rance (2010) and Zhang (2005) have demonstrated that protein secretion can be improved by alternative signal peptides (signal sequences). Based on these observations, potent signal peptides, which result in an enhanced secretion of recombinant antibodies from CHO cells, should be identified during the first part of the present study.

In order to find potent signal peptides, an extensive literature research was preformed and 16 promising natural signal peptides from different species as well as 3 artificial signal peptides (as seen in Tab. 34) were selected and fused to the heavy and the light chain of a recombinant model antibody. CHO K1 cells were transiently transfected with corresponding expression constructs and the antibody concentration in the culture medium was determined 4 days after transfection. Compared to the control signal peptide A2, the cell specific productivity was increased by 50-60% using signal peptide B and by 75-100% using signal peptide E in two independent experiments. All other analyzed signal peptides resulted in productivities similar to or even lower than the control. By co-expressing renilla luciferase as an internal control, it could be excluded that the observed effects were due to different transfection efficiencies (Fig. 27 and Fig. 28).

Several obtained results were not in line with the expectations. For example, the used wild-type immunoglobulin signal peptides as well as the cystatin-S signal peptide mediated only relatively weak secretion, although the latter one was predicted to be the strongest one of 168 signal peptides analyzed by the hidden Markov model (Barash 2002). In the same report, the azurocidin signal peptide was ranked at position 12, but it clearly outperformed both the cystatin-S and the control signal peptide in this study. On the other hand, this observation is in good agreement with another study, where the azurocidin signal peptide has been used to express various proteins in insect cells and was characterized as very potent (Olczak 2006). Surprisingly, all artificial signal peptides, which were designed in order to meet all published

requirements for optimal protein secretion, resulted in low or very low antibody expression levels. On the other hand, the signal peptide derived from human albumin, which has been previously described as very weak when tested in CHO cells (Knappskop 2007; Hesketh 2005 (WO 2005/001099 A2)), showed the best performance of all analyzed signal peptides. These partially inconsistent observations might be explained by the following factors: (i) the mechanistic complexity of the translocation process into the ER (comprising signal peptide recognition, targeting and translocation as well as signal peptide cleavage), that makes it very difficult to predict the efficiency of a signal peptide in silico. (ii) The application of a huge variety of test systems and reporter proteins in the literature, which can have a strong influence on the performance of a signal peptide. Especially the usage of a dimeric and complex molecule, such as a recombinant antibody, during this study complicates the comparison with data from the literature, which are often generated with monomeric reporter molecules. Otherwise this fact illustrates the importance of the selected secretory protein during this study.

As shown in chapter 6.1.1, signal peptides B and E fused to the N-terminus of the heavy and the light chain of a model antibody mediated a clear increase in secretion efficiency compared to the control signal peptide A2. Based on these results it was evaluated whether a further improvement of these signal peptides could be achieved through the optimization of their design by specific mutations. All introduced mutations were chosen based on literature data and are depicted in Tab. 35. For example, in signal peptide E1, an unusual arginine was replaced by leucine and in a reverse approach a tyrosine at the same position was replaced by an arginine in signal peptide B1, based on the observations of von Heijne 1983. Signal peptide E2 and E3 were generated in order to create an optimal Kozak sequence (ACC-AUG-G) Kozak (1986 Jan, 1987). For this purpose, threonine was substituted by alanine or alanine was additionally inserted directly downstream of the methionine start codon. In mutant E4, an alanine and in mutant E5 a threonine was substituted by leucine within the h-region, because Belin (1996) has reported, that the translocation efficiency could be increased by a higher hydrophobicity of the h-region. Additionally, the length of the signal peptide was reduced by the deletion (mutant E6) or extended by the insertion (mutant E7) of a leucine within the hydrophobic core in order to test the influence on the signal peptide cleavage efficiency as described by Nilsson 2002. Finally, in mutant E8 the AGG codon of arginine was exchanged by a synonymous CGC codon in order to reduce the stability of a secondary mRNA structure, which was predicted by the “AUG_hairpin” program (Kochetov 2007). In this way, the efficiency of translation initiation should be improved, resulting in enhanced protein synthesis (Baim 1985; Kozak 1986 May; Kozak 1990).

All mutated signal peptides were fused to the heavy and the light chain of a model antibody and inserted into second generation expression vectors. The constructs were transiently transfected into CHO K1 cells and the antibody concentration was measured 3 days after transfection. With exception of signal peptide E3, which mediated a similar or slightly lower protein secretion than signal peptide E and B, all mutations resulted in clearly decreased productivities compared to the corresponding wild-type signal peptides (Fig. 30 and Fig 31). An impact of differing transfection efficiencies on the results was excluded by the co-expression of renilla luciferase as transfection control. The most likely explanation for the discrepancy between these observations and data from the literature are differences in the experimental design. Whereas signal peptides were fused to the light and the heavy chain of a recombinant antibody in the present thesis, monomeric reporter molecules such as gaussia luciferase, vargula luciferase or secreted alkaline phosphatase (SEAP) are used for the majority of all other studies. However, it has been reported that the amino acid sequence downstream of a signal peptide can affect its efficiency (Folz 1986; Andrews 1988; Wiren 1988). Additionally, literature data were generated with different cell lines from various organisms, which might be often not comparable to CHO suspension cells.

In transient transfection experiments, signal peptide B, E and E3 were the most potent ones and it was observed that transient antibody expression levels and the productivity of the corresponding stable cell line often do not correlate (Rance 2010; Kalwy 2006). Hence, it was necessary to analyze the performance of the signal peptides in stably expressing cells, in order to find out whether they can be applied to increase the productivity of cell lines. For this purpose, signal peptide B, E, E3 and A2 (control) were fused to a recombinant model antibody and inserted into third generation expression vectors. The generated constructs were employed for a standard cell line development based on DG44 cells and the dhfr selection system by using the mini-pool method. At the 6 well level, the cell specific productivities of all obtained mini-pools were determined and the top 20 were selected for each signal peptide. These were transferred to Production°Medium, expanded to shake flask level and analyzed again regarding their productivity. As shown in Tab. 37 and Fig. 33, for all mini-pools good growth behaviour and similar viabilities were observed at the 6 well and shake flask level, independent of the signal peptide used. Finally, all mini-pools were subjected to a fed-batch production process of 13 days. The fed-batch experiment was of great importance, because the commercial suitability of an expression cell line is determined by its performance in a production process, especially by the achieved final product concentration. Furthermore, it has been reported, that the cell specific productivity of a cell line is not always consistent with the product concentration obtained during a fed-batch process (Birch 2006).

Fig. 33 and Fig. 34 shows, that all tested signal peptides clearly outperformed the control (A2) regarding the measured product concentration. As expected, generally higher cell specific productivities were determined at the 6 well level in Medium D3 than at shake flask level in Production°Medium (Fig. 32). This can be explained by increased evaporation and inferior growth conditions in 6 well plates and Medium D3, respectively. The best results were obtained for signal peptide B, which mediated an average cell specific productivity of 40 pg/cell/day with some mini-pools reaching up to 90 pg/cell/day (Fig. 32). Signal peptide E and E3 showed average values of 20-30 pg/cell/day, whereas about 10 pg/cell/day were measured on average for signal peptide A2 (Fig. 32). On the last day of the fed-batch experiment, an average final concentration of 1.6 g/L was obtained for signal peptide B, whereas 1.2 g/L was reached with signal peptide E and E3 and only 0.7 g/L with signal peptide A2. Moreover, top productivities of 3.3 and 4 g/L were observed for mini-pools derived from signal peptide B (see Fig. 34). Interestingly, there was quite a good overall correlation between the fed-batch results, the cell specific productivities determined at shake flask and 6 well level and even the transient expression results.

In conclusion, the combined data indicate that particularly signal peptide B, but also signal peptide E and E3 can be used to generate cell lines with clearly improved production rates suitable for commercial purposes. According to the literature, such cell lines should reach cell specific productivities of at least 20 pg/cell/day (Chusainow 2009; Wurm 2004; Borth 2000; Fann 2000; Huang 2007; Jiang 2006; Lattenmayer 2007; Birch 2005) and during a typical production process based on a clonal CHO cell line 1-5 g/L antibody should accumulate within 14 days (Schlatter 2010 Sep; Birch 2005; Kelley 2009 Sep-Oct; Trexler-Schmidt 2009; Gagnon 2010 Lindgren 2009; Kennard 2006). The fact, that both requirements could be met with mini-pools instead of clonal cell lines and in a non-optimized fed-batch process makes the potency of the investigated signal peptides even more obvious.

7.2. Development of an alternative selection system for high producing clones

It has been reported, that the selection of a high-expressing clone is a particularly labor-intensive and time-consuming step during the development of cell lines for the manufacturing of recombinant proteins (Borth et al. 2000; Carroll 2004; Birch 2006). One of the main challenges is the identification and isolation of rare high producer clones out of the vast majority of low- and medium-expressing clones. Therefore, efficient platform technologies have to allow the selection of high-producing cell lines in a fast and simple way. Interestingly, the overexpression and accumulation of unfolded proteins in the ER triggers different pathways like the unfolded protein response (UPR) or the ER overload response (EOR). During this process, the protein load of the ER is measured and genes related to protein modification, folding or degradation as

well as genes for the amino acid transport and many other genes are activated (Rao 2004; Kaufman 1999; Kozutsumi 1988; El-Hadi 2005). In this context, it was one aim of the present study to develop a novel selection method which uses ER stress pathways for rapid identification and isolation of high-expressing production clones.

It has been reported, that the promoters of CALR, GRP78 and GRP94 as well as the cytosolic splicing of the XBP1 intron are stimulated by the unfolded protein response (Llewellyn 1996; Yoshida 1998; Renna 2007; Back 2006; Yoshida 1998; Lee 2002). During the first set of the experiments, it was investigated whether these ER stress elements could be activated by the overexpression of a recombinant model antibody and particularly whether there is a correlation between the extent of stimulation and the antibody expression rate. Hence, the levels of CALR, GRP78, GRP94 and spliced XBP1 mRNA of CHO DG44 wild-type cells and 8 clones with different antibody productivities were determined by real time RT-PCR. As depicted in Fig. 38, transcription of GRP78 and GRP94 as well as the cytosolic splicing of XBP1 were stimulated in an antibody-dependent manner, whereas no correlation was observed for CALR. These results suggested, that the promoters of GRP78 and GRP94 as well as an intron-containing XBP1 fragment could be used as response elements for the detection of clones producing high amounts of antibody. Moreover, it has been reported, that especially the transcription factor binding sites ERSE I, ERSE II, UPRE and AARE, which are also present in the tested promoters, are important for the ER stress response (Yoshida 1998; Roy 1999; Kokame 2001; Wang 2000; Ma 2004). Consequently, these binding sites could be also employed for the identification of high producers.

Therefore, the transcription factor binding sites ERSE I, ERSE II, UPRE, AARE as well as the promoter regions of CALR, GRP78, GRP94 and an intron-containing XBP1 fragment were used to create 8 different ER stress reporter constructs as shown in Fig. 47, Fig. 48 and Fig. 49. The rationale for these constructs was to develop a reporter system that allows the rapid and simple identification and isolation of high-producing clones only based on GFP fluorescence (exemplified shown in Fig. 35). In order to establish a detection system for high-expressing clones, the most suitable ER stress reporter construct had to be determined. Therefore, all generated constructs were compared regarding their response to antibody expression. For these experiments, several antibody producing cell lines (Master 2A, 2B, 2C) and one mock cell line, all containing a genomically anchored DsRed RMCE construct, were generated as depicted in Fig. 36. Subsequently, the ER stress reporter constructs (see Tab. 45) were introduced into each cell line by targeted integration (RMCE), clones were isolated and authentically exchanged clones were evaluated with regard to GFP fluorescence.

Tab. 45: Overview about all ER stress reporter and control constructs

ER stress reporter constructs	ER stress reporter constructs
SV40-eGFP control	SV40-d2eGFP control
3 x ERSE I	XBP1 Intron
3 x ERSE II	CALR
3 x UPRE	GRP78
3 x AARE	GRP94

By using RMCE, reliable and comparable results were obtained because all reporter and control constructs were integrated at the same genomic locus (confirmed by small standard deviations in Fig. 54). In this way, misinterpretations due to different gene copy numbers and genomic integration sites or disturbing effects, which are sometimes observed during transient transfection, could be excluded. Well exchanged clones were isolated by FACS, and the correctness of the exchange procedures was proved by an analytical PCR on genomic DNA (chapter 6.6.2). The clones were termed Master 2A Reporter, Master 2B Reporter, Master 2C Reporter and Mock Reporter cell line. Most ER stress reporter constructs showed an increased GFP fluorescence compared to the control constructs (SV40-eGFP and SV40-d2eGFP control). Based on these results, it can be concluded that the tested transcription factor binding sites are able to stimulate the SV40 basal promoter and the natural promoters of CALR, GRP78 and GRP94 are more active than the SV40 basal promoter. However, neither the ER stress response elements (ERSE I, ERSE II, UPRE, AARE) nor the CALR and the GRP94 promoter or the XBP1 fragment were significantly stimulated by antibody expression (compare Mock and Master 2A, 2B, 2C Reporter cell lines in Fig. 53 and Fig. 54). In contrast, the activity of the GRP78 promoter was strongly enhanced in antibody producing cells: whereas the Mock Reporter clones exhibited an averaged increase in GFP fluorescence of 3.7 fold. In comparison the Master 2A, 2B and 2C Reporter clones exhibited an increase between 5.3 and 8.3 fold compared to the control cell lines (Fig. 53 and Fig. 54).

It has been reported, that the accumulation of incompletely assembled immunoglobulin heavy chains in the ER (e.g. after transfection of heavy chains in absence of light chains) can activate the ER stress pathway (Pahl 1995 Jun; Kaufman 1999) by binding of the luminal ER stress sensor GRP78 (BIP) to the heavy chains (Pahl 1999; Hendershot 1987; Kaloff 1995; Haas 1983; Bole 1986). However, during the present study, ER stress was triggered by the expression of both heavy and light chain of an immunoglobulin, which forms a completely assembled antibody. Because it has been shown, that GRP78 binds to immunoglobulin light chains shortly after their translation (Gardner 1993; Nakaki 1989; Knittler 1992; Lenny 1991), this interaction might explain how even the expression of intact antibodies can activate ER

stress pathways. Surprisingly, only the GRP78 ER stress reporter construct showed a significant stimulation upon antibody expression, whereas all other tested constructs were not affected. Mammalian ER stress responses are generally mediated by different cis-acting elements such as ERSE I, ERSE II, UPRE and AARE (see Tab. 46 for consensus sequences), which are placed within the regulatory regions of several promoters.

Tab. 46: Cis-acting elements and their consensus sequences

Cis-acting elements are shown with their consensus sequences according to Yoshida 1998; Kokame 2001; Wang 2000; Fafournoux 2000 and Ma 2004. Notations: R = A or G, K = G or T, N = A or C or G or T

Cis-acting element	Consensus sequence
ERSE I	CCAAT-NNNNNNNNN-CCACG
ERSE II	ATTGGNCCACG
UPRE	TGACGTGR
AARE	RTTKCATCA

Obviously, none of these elements by itself is sufficient to stimulate the transcription of the GFP reporter upon antibody expression (cf. 3 x ERSE I, 3 x ERSE II, 3 x UPRE, 3 x AARE reporter constructs). The obtained results rather indicate, that a specific combination of response elements might be necessary to detect ER stress triggered by antibody production. Such a combination could be present in the natural GRP78 promoter, whereas the composition contained in the GRP94 and the CALR promoter seem to be inappropriate. Promoter analyses show that ERSE I sites are present in the promoters of GRP78, GRP94 and CALR, whereas a GGC triplet within the N9 ERSE I spacer (CCAAT-NNNNGGCNN-CCACG) is only found in the GRP78 promoter. This GGC triplet has been reported to play an important role in the stimulation of ESRE I (Roy 1999). As mentioned above, it can be excluded that the CCAAT-NNNNGGCNN-CCACG element alone is responsible the stimulation of the GRP78 promoter, because the 3 x ERSE I construct consists of the same element and was not activated. Furthermore, the GRP78 promoter contains 2 UPRE (TGACGGGA and TGACGTAA), one AARE (ATAGCATCA) and one ERSE II (ATTGGTCCATG) sites all differing as indicated from the corresponding consensus sequences used in the 3 x UPRE, 3 x AARE and 3 x ERSE II constructs. A further explanation for the observed results might be that the ER stress triggered by antibody expression was only sufficient to stimulate the GRP78 reporter construct but not all other constructs. Alternatively, the activation of the GRP78 reporter by antibody production could be due to a so far unknown ER stress-independent mechanism, which does not involve the mentioned ER stress response elements.

For the GRP78 ER stress reporter construct, a significant stimulation upon antibody expression was observed. Since the analyzed Master 2A, 2B and 2C cell lines showed only moderate productivities between 9 and 15 pg/cell/day (resulting in 1.6 to 1.9 g/L in a 15 day fed-batch experiment), additional experiments were necessary to evaluate if the system is applicable to the identification of high-producers. For that purpose, it should be analyzed whether at higher ER stress levels a further stimulation of the reporter constructs was observed. It has been shown, that ER stress can be triggered by different drugs such as Brefeldin A (BFA) and Castanospermine (CSN). Whereas BFA blocks the exit of secretory proteins from the ER, resulting in the activation of UPR and ERO, CSN disturbs the formation of complex N-glycosylated proteins, thereby activating the UPR pathway (Pahl 1995 Jun; Wang 2000; Saul 1985; Ahmed 1995). Hence, Mock and Master 2A Reporter cell lines were treated with BFA and CSN and the GFP fluorescence was measured (see Fig. 55). With exception of GRP78, none of the reporter cell lines was stimulated by CSN, whereas a significant activation was observed for the Master 2A 3 x ERSE I, 3 x ERSE II, GRP78 and GRP94 Reporter cell lines. The GRP78 reporter construct showed the strongest effect, resulting in a 2-3 fold GFP fluorescence upon BFA treatment. Compared to data from the literature, this is an unusually strong stimulation of GRP78. A possible explanation is, that a very large GRP78 promoter fragment of 1500 bp containing almost the whole 5' UTR was used, whereas others employed shorter fragments for their studies (Renna 2007; Li 1993; Yang 1997). Moreover, the GRP78 promoter fragment of the present thesis was derived from the chinese hamster (Cricetulus griseus), whereas the fragments in other reports were usually isolated from mouse (Mus musculus). Based on the obtained results, it was concluded, that especially in case of the GRP78 reporter construct, the detection of clones with specific productivities far beyond 15 pg/cell/day should be possible.

In the last part of this thesis, the suitability of the novel ER stress detection system to identify and isolate high-producing clones was evaluated. For this purpose, a cell line was generated by stably introducing a reporter construct comprising GFP driven by a truncated GRP78 promoter region. Subsequently, the obtained reporter cell line was stably transfected with an expression vector encoding a model antibody and MTX amplification was performed. Several clones, characterized by different productivities were isolated and analyzed regarding GFP fluorescence. As illustrated in Fig. 61, the overexpression of the recombinant antibody resulted in an increased activity of the GRP78 reporter construct. Additionally, a strong correlation was found between the amount of secreted antibody and GFP fluorescence as well as between cell specific productivity and GFP fluorescence. These results indicate, that the used reporter system is able to display the level of antibody expression (IgG) in recombinant CHO cells. However, the system was only tested with clones with moderate productivities. Therefore, further experiments should elucidate, if the system possesses the potential to detect also high-

producers. For this reason a selection of clones was treated with the ER stress inducers BFA and CSN and the GFP fluorescence was determined. Additionally, the mRNA levels of endogenous GFP78 were measured by real time RT-PCR. For all clones, a strong stimulation both of the reporter system and endogenous GRP78 was observed. Based on these results, it was concluded, that the novel ER stress based selection system, developed during this thesis, should also be suitable to identify and isolate clones expressing high amounts of antibody.

8. Outlook

In the first part of the present thesis, two natural signal peptides (derived from human azurocidin and human albumin) have been found, that mediate highly efficient secretion of a recombinant antibody. However, it has been reported, that the efficiency of a signal peptide can be affected by the sequence immediately downstream of the peptide. For this reason, further studies are required to analyze whether the identified signal peptides can be universally used to improve the secretion of any recombinant protein or whether the observed effects are limited to certain products. To clarify this issue, the performance of the selected signal peptides will be evaluated for a variety of antibodies and non-antibody proteins (e.g. Fc-fusion proteins). Furthermore, various propeptides could be tested to enhance the product concentration or to improve the quality of the expressed gene of interested. Such propeptides could be also very advantageous to ensure a proper signal peptide processing independently of the expressed protein.

In the second part of this thesis, a novel ER stress based technology for the identification and isolation of clones expressing high amounts of antibodies, out of a pool mainly consisting of low- and medium-producing cells has been established. The basic principle of the developed method is, that a Master GRP78 cell line (harbouring a GRP78 reporter construct) can be transfected with a gene of interest for example a recombinant antibody. This leads to the upregulation of the GRP78 reporter construct and an increased amount of the reporter gene (GFP) can be detected by FACS. Hence, sorting for clones with a very high GFP fluorescence should enable the isolation of high productive clones. Further studies are necessary to evaluate the performance of this system especially compared to other selection methods such as cell surface staining with fluorescently labelled antibodies or co-expression of GFP (analogous to Brezinsky 2003 and Enenkel 2008 (US 7384744 G)). Moreover, the applicability of the technology to other recombinant antibodies as well as non-antibody products has to be investigated. In order to smoothly integrate the system into the existing platform technology, a suitable Master GRP78 Reporter cell line needs to be identified, which should be characterized by the following features: ability to produce high amounts of adequately glycosylated recombinant proteins, good growth behaviour in all applied media and low production of toxic metabolic by-products such as lactate and ammonium. Finally, the selection procedure has to be optimized by the determination of appropriate sorting parameters like the fraction of GFP positive cells, which should be isolated, and the ideal time after transfection to perform the sorting procedure

9. Appendix

9.1. FACS analysis of Mock Reporter and Master 2 Reporter cell lines

SV40-eGFP control			
Mock Rep	Master 2A Rep	Master 2B Rep	Master 2C Rep
Clone 29-1	Clone 30-2	Clone 31-2	Clone 32-2
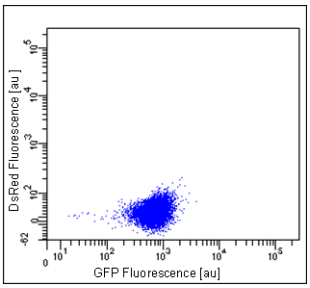	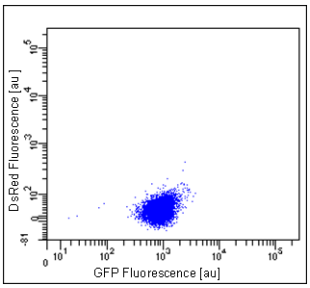	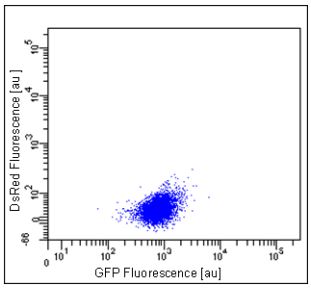	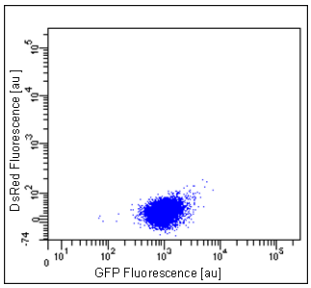
708	871	795	998
Clone 29-2	Clone 30-3	Clone 35-1	Clone 32-4
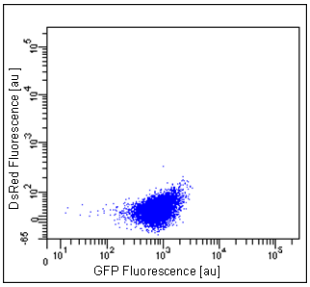	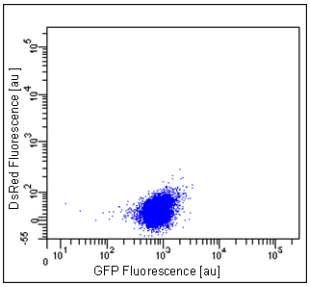	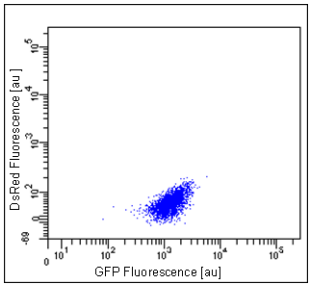	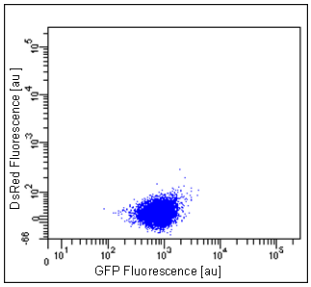
797	801	1353	795
Clone 29-3	Clone30-5	Clone 35-2	Clone 36-1
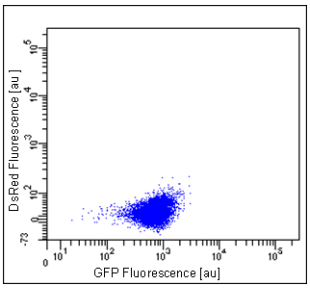	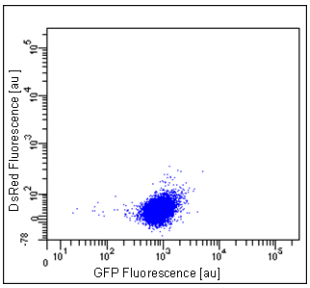	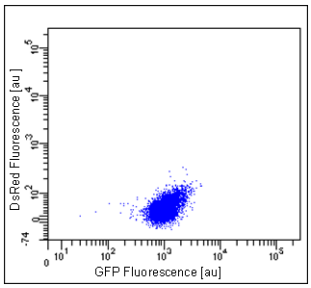	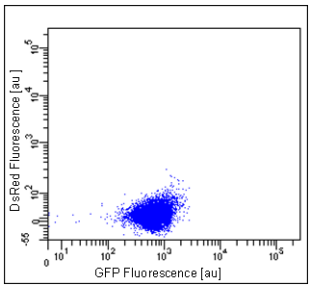
719	852	1077	674
Clone 33-4	Clone 30-8	Clone 35-3	Clone 36-2
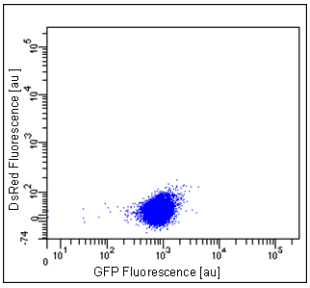	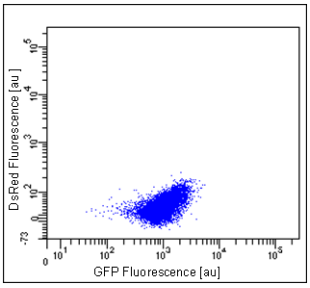	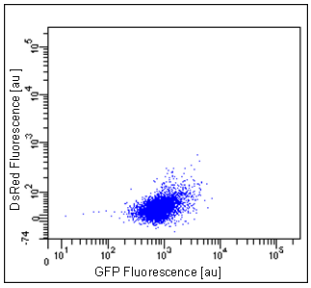	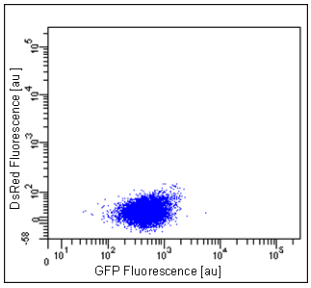
826	1055	889	510

Clone 30-11

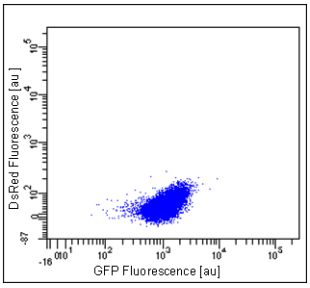

1128

Clone 35-4

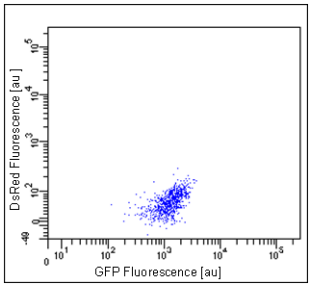

1308

Clone 36-3

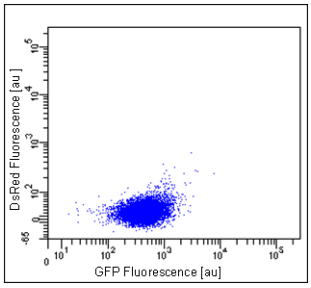

471

Clone 30-12

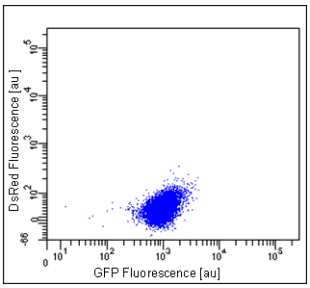

969

Clone 36-4

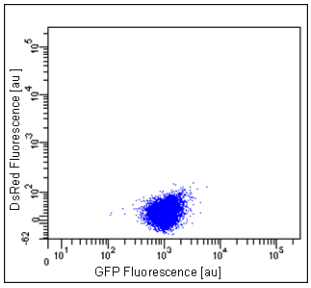

1013

Clone 30-13

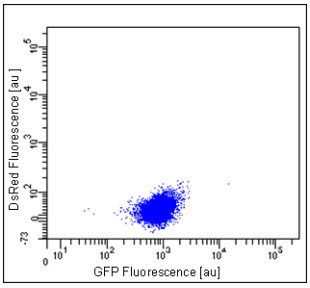

822

Clone 36-5

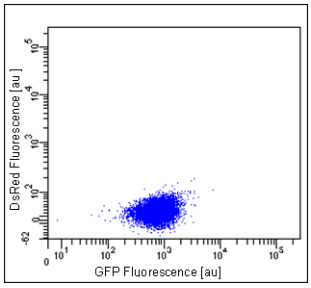

773

Clone 30-15

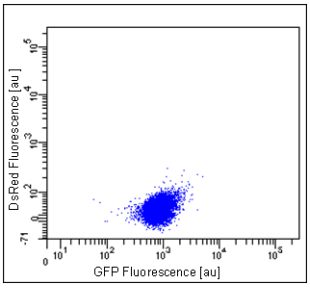

829

Clone 36-7

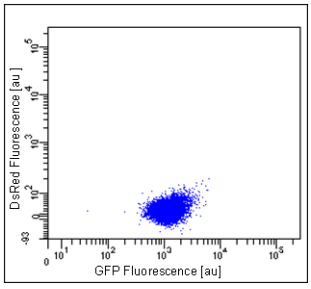

1230

Clone 36-8

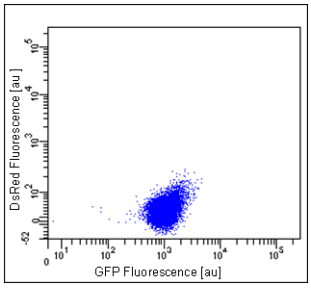

1066

Clone 36-9

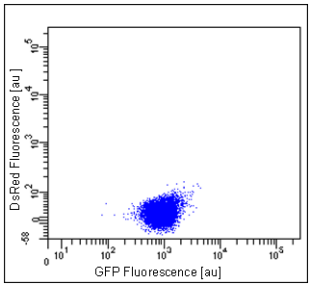

898

3 x ERSE I

Mock Rep	Master 2A Rep	Master 2B Rep	Master 2C Rep
Clone 33-8	Clone 30-16	Clone 31-6	Clone 32-7
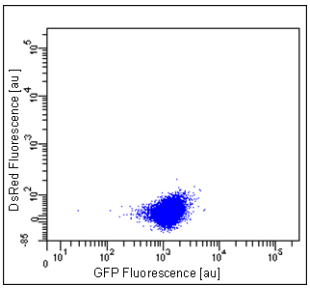	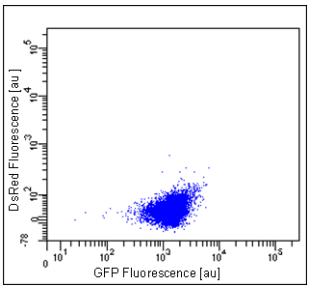	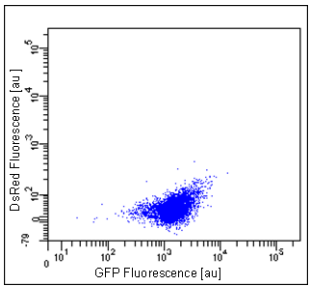	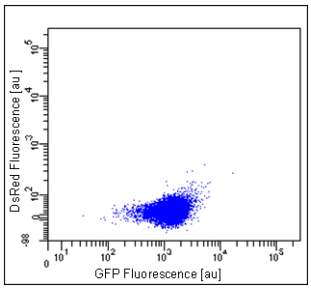
1260	1424	1612	1300
	Clone 30-17	Clone 31-7	Clone 36-10
	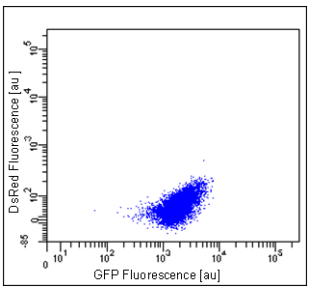	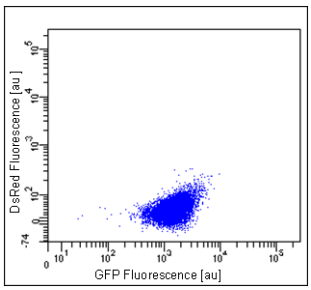	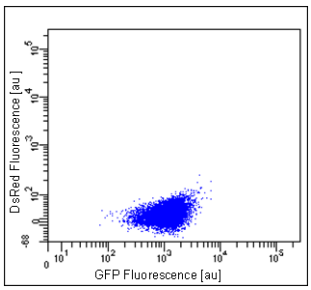
	1868	1602	1202

Clone 30-21

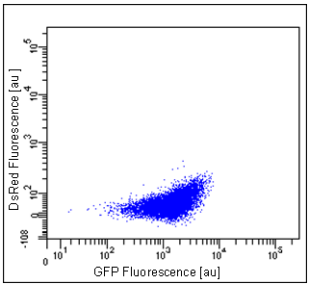

1593

Clone 35-5

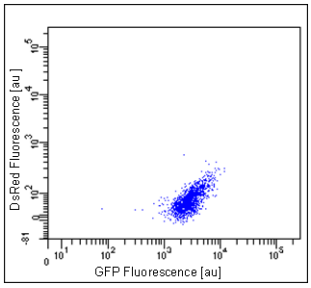

3005

Clone 36-11

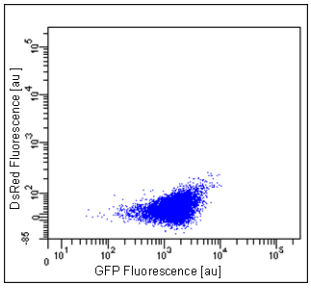

1669

Clone 30-24

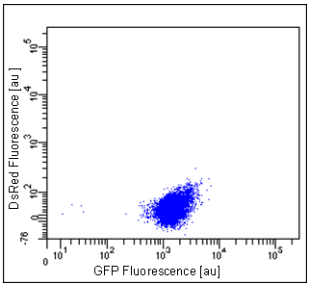

1474

Clone 35-6

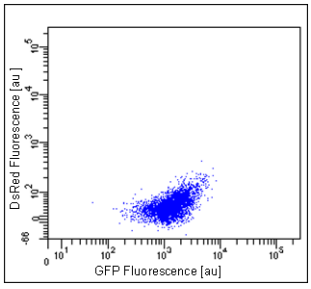

1479

Clone 34-5

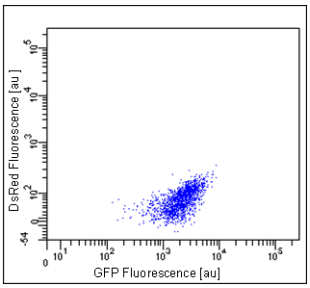

2300

Clone 35-7

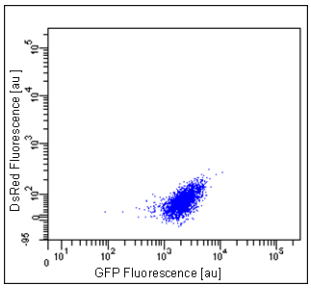

2217

Clone 34-8

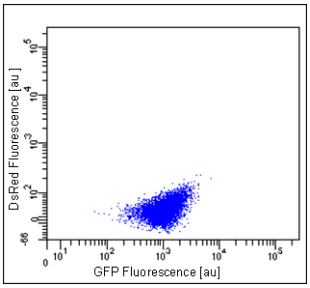

1115

3 x ERSE II

Mock Rep	Master 2A Rep	Master 2B Rep	Master 2C Rep
Clone 33-18	Clone 30-28		Clone 32-8
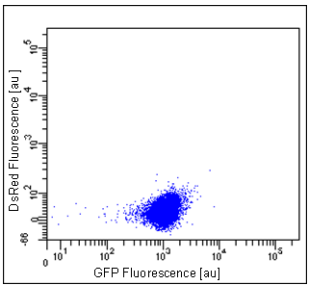	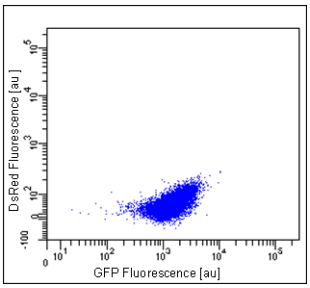		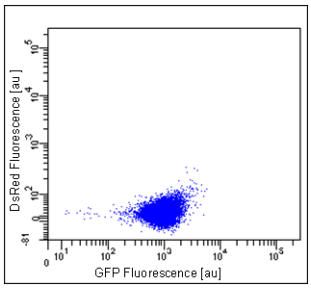
1080	1584		998
	Clone 30-37		Clone 36-13
	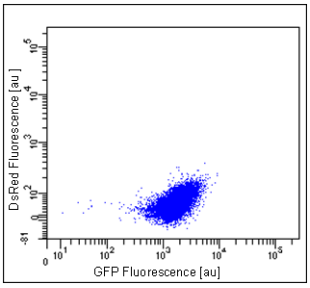		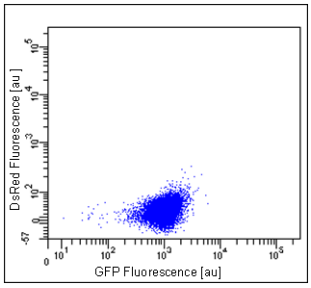
	1766		1015
	Clone 34-15		Clone 36-15
	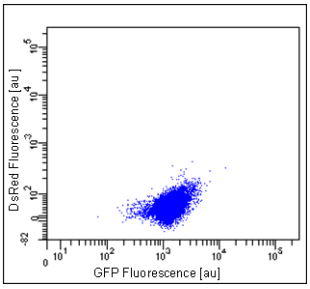		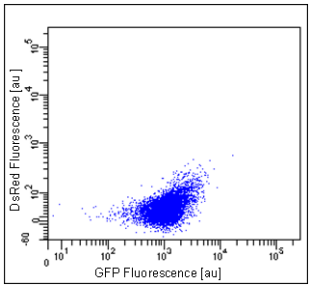
	1378		1192

3 x UPRE

Mock Rep	Master 2A Rep	Master 2B Rep	Master 2C Rep
Clone 29-8	Clone 30-39	Clone 31-12	Clone 32-9
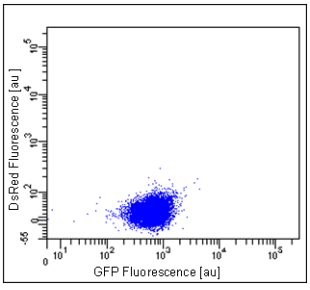	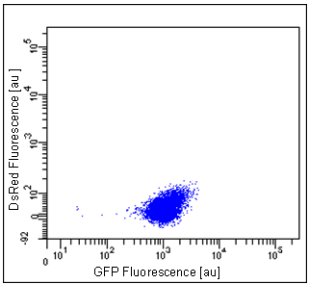	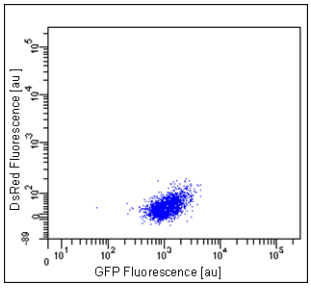	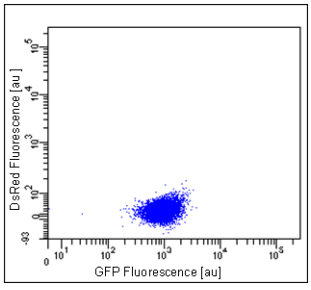
658	1086	1166	960

Clone 33-22	Clone 30-42	Clone 35-14	Clone 36-16
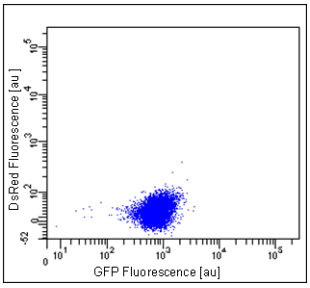	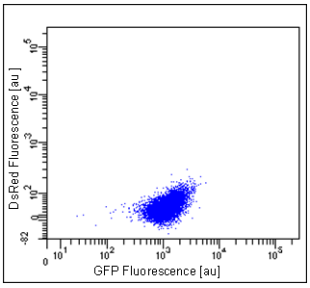	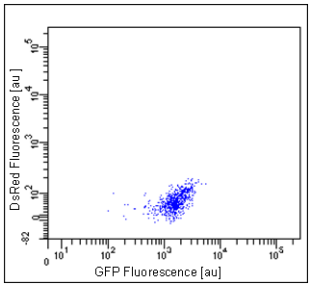	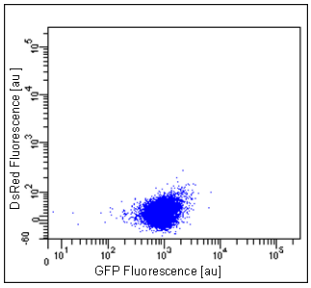
792	1126	1654	925

Clone 33-24	Clone 34-19	Clone 35-15	Clone 36-17
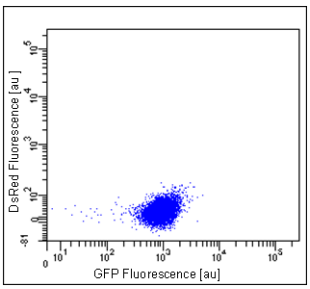	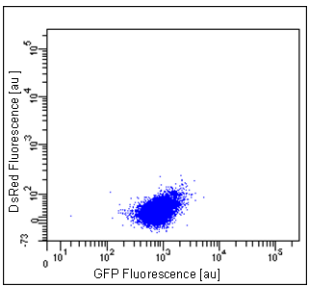	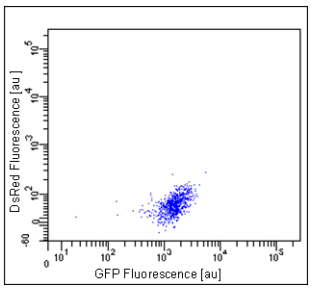	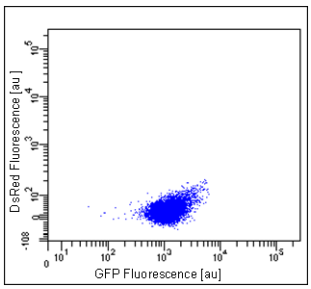
923	855	1590	1205

	Clone 34-20	Clone 35-16	Clone 36-19
	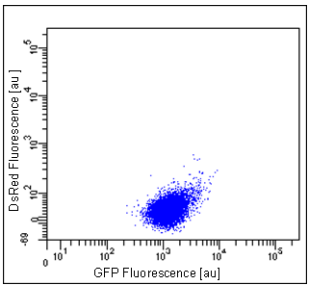	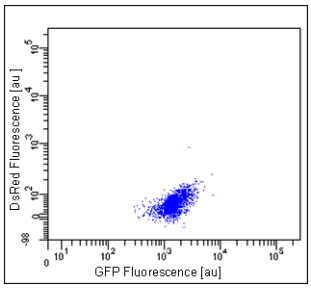	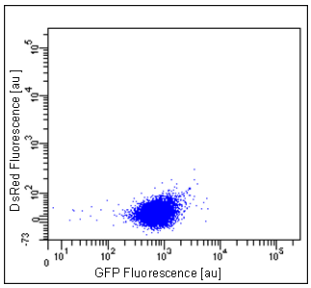
	1296	1582	756

	Clone 34-23	Clone 35-17
	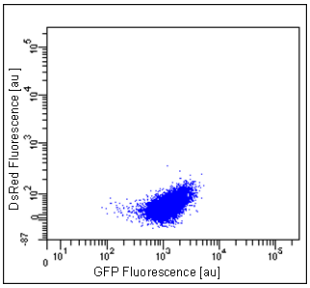	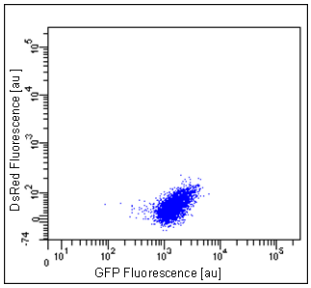
	1267	1507

Clone 35-18

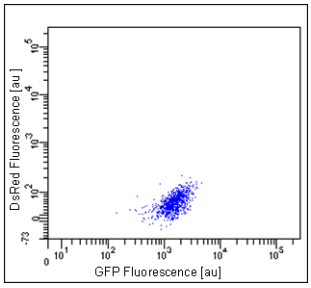

1561

Clone 35-19

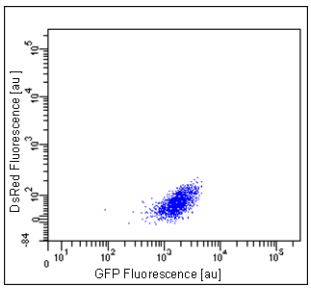

1761

3 x AARE

Mock Rep	Master 2A Rep	Master 2B Rep	Master 2C Rep
Clone 29-9	Clone 30-45	Clone 31-17	
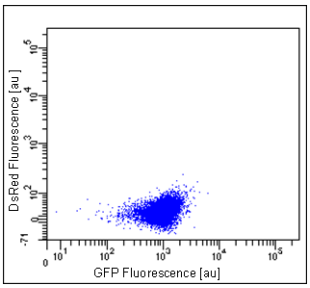	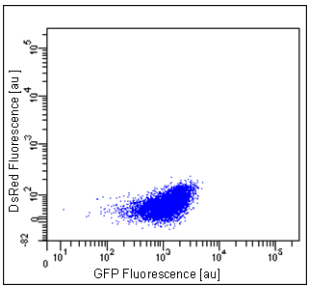	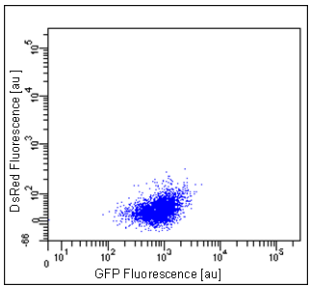	
976	1277	864	
Clone 33-28	Clone 30-46	Clone 31-19	
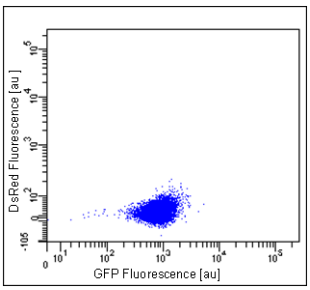	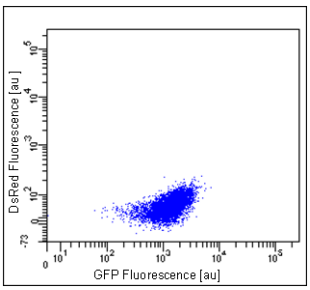	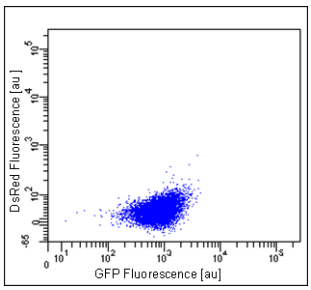	
851	1375	856	

Clone 33-33

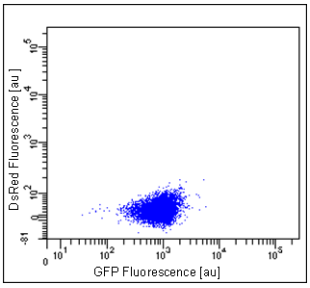

879

Clone 30-49

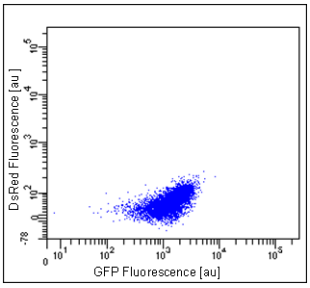

1374

Clone 35-22

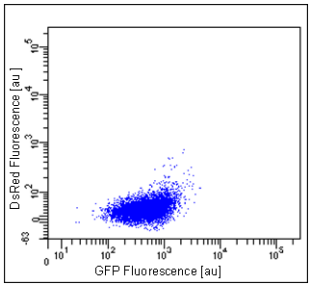

559

Clone 30-50

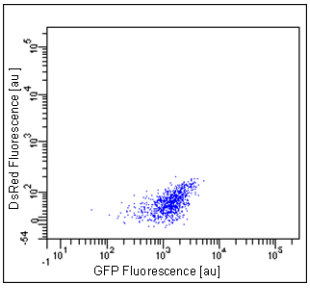

1451

Clone 35-25

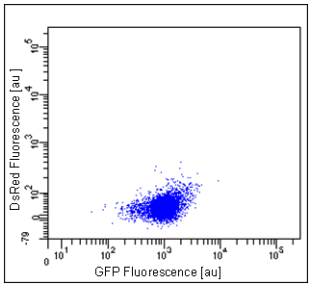

1060

Clone 30-51

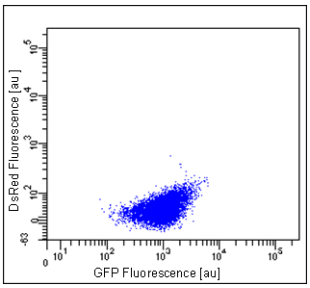

1040

Clone 34-25

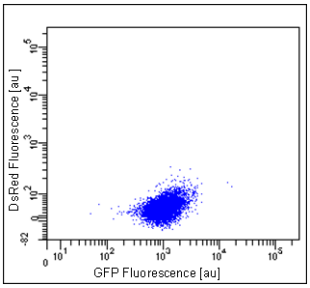

1052

SV40-d2eGFP control

Mock Rep	Master 2A Rep	Master 2B Rep	Master 2C Rep
Clone 33-39	Clone 30-53	Clone 31-35	Clone 32-14
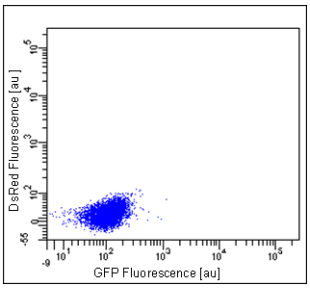	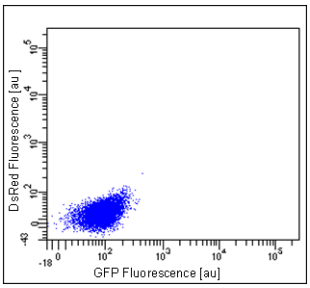	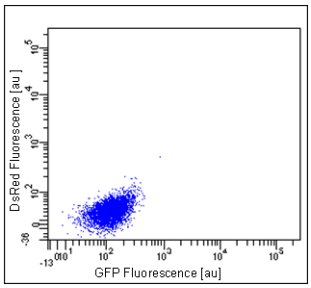	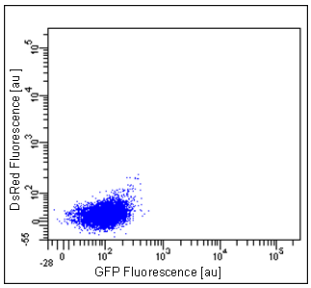
108	92	122	103
	Clone 30-56	Clone 31-36	Clone 32-15
	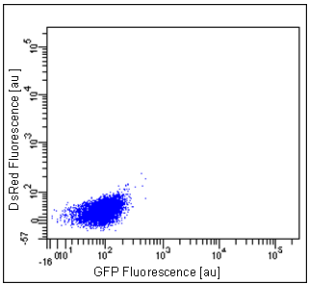	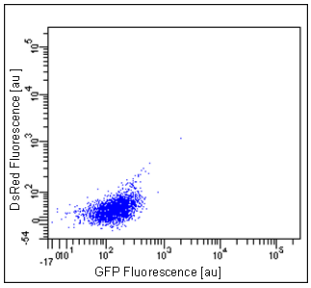	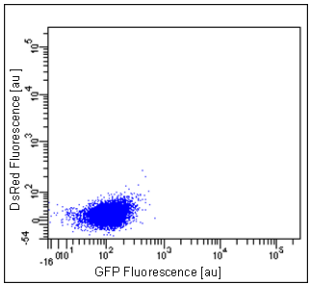
	88	150	117
	Clone 30-57	Clone 31-37	Clone 36-24
	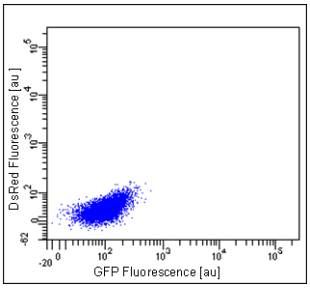	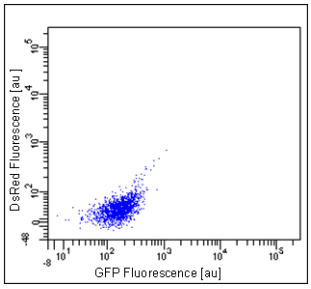	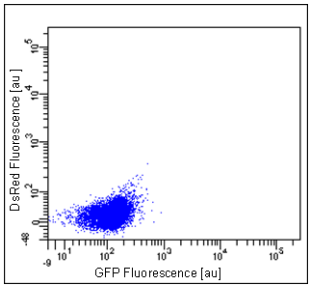
	104	174	118
	Clone 30-59	Clone 35-27	Clone 36-25
	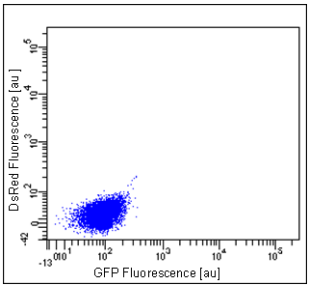	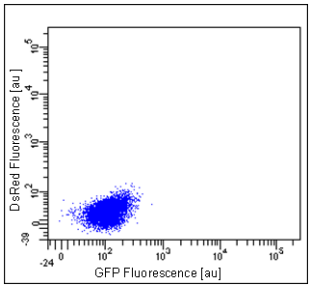	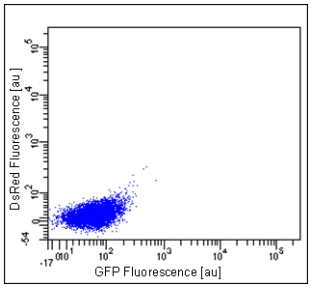
	91	116	66

Clone 30-60

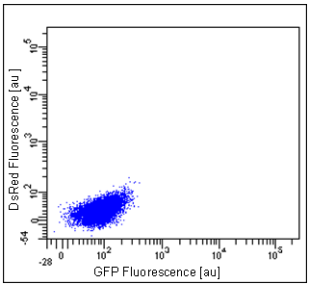

89

Clone 36-26

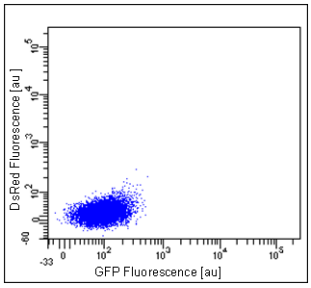

97

Clone 30-63

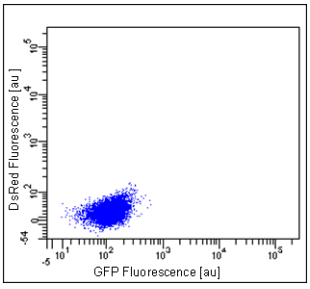

117

Clone 34-28

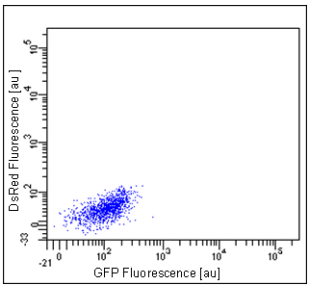

116

Clone 34-29

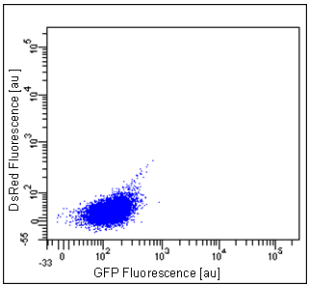

136

Clone 34-35

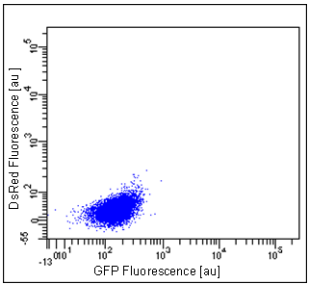

154

Clone 34-38

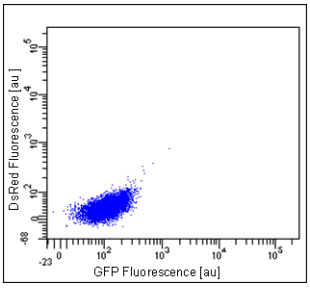

114

Intron

Mock Rep	Master 2A Rep	Master 2B Rep	Master 2C Rep
Clone 29-14	Clone 30-69	Clone 31-20	
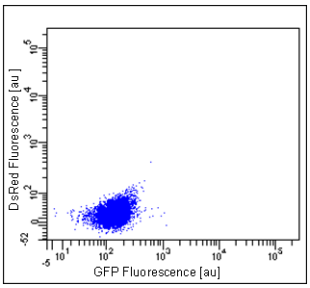	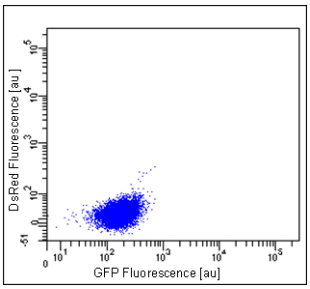	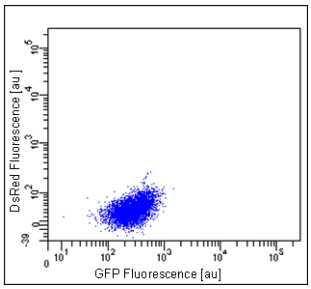	
140	168	285	
Clone 29-17	Clone 30-72	Clone 31-23	
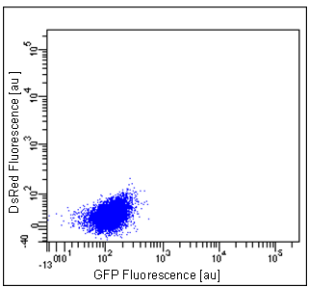	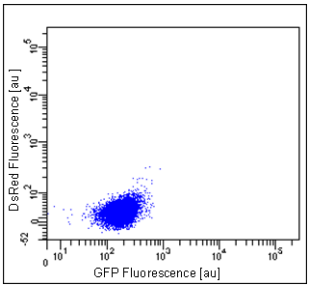	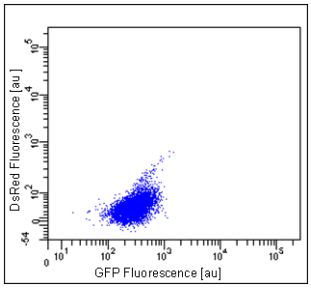	
123	175	307	

Clone 33-44

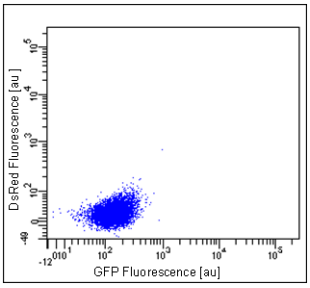

145

Clone 30-73

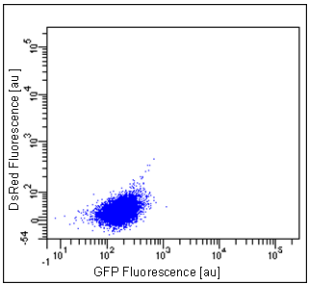

174

Clone 35-39

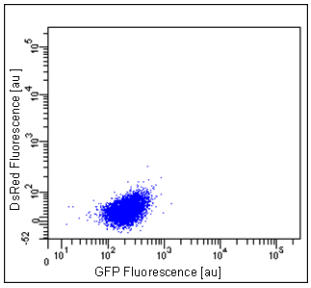

205

Clone 33-46

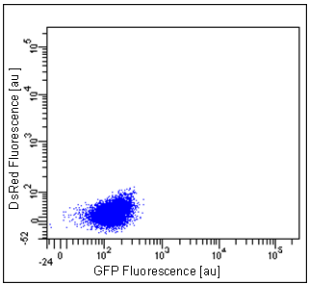

137

Clone 30-74

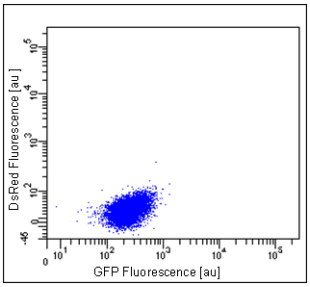

241

Clone 35-43

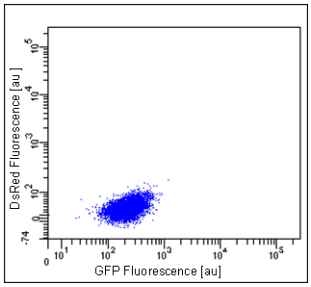

220

Clone 30-75

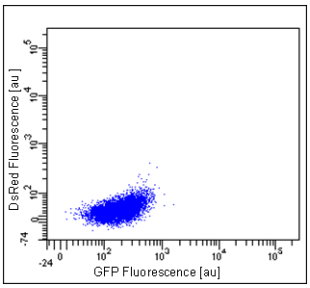

186

Clone 30-77

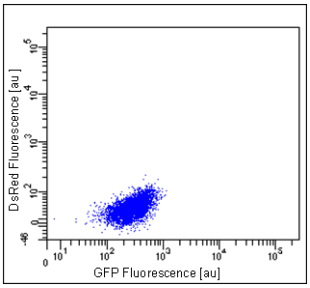

292

Clone 30-78

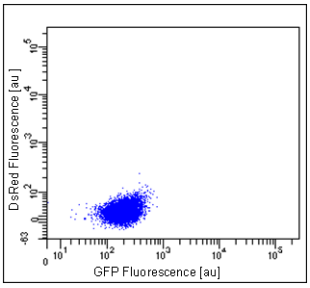

200

Clone 34-40

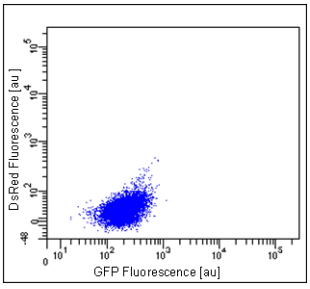

207

Clone 34-41

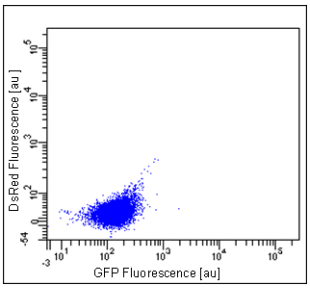

144

Clone 34-42

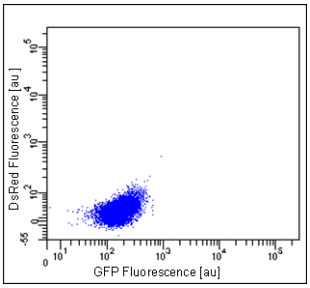

167

Clone 34-44

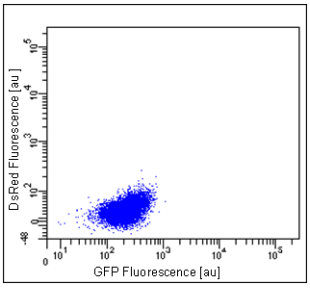

220

CALR

Mock Rep	Master 2A Rep	Master 2B Rep	Master 2C Rep
Clone 29-21	Clone 30-79	Clone 31-26	Clone 36-27
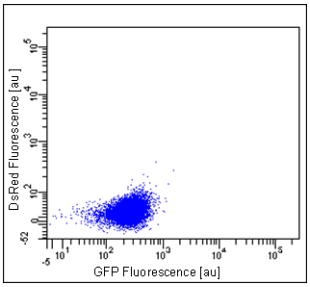	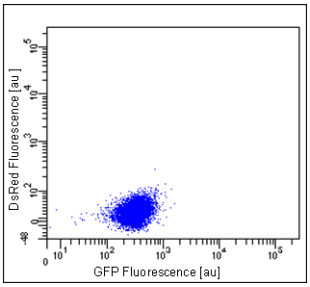	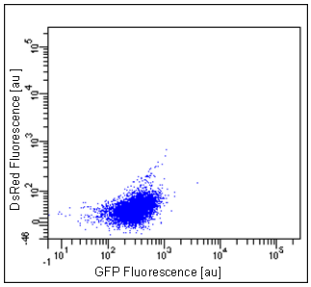	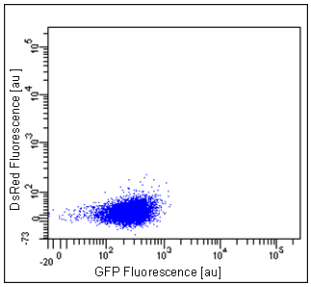
261	314	306	268
Clone 29-23	Clone 30-80	Clone 31-27	
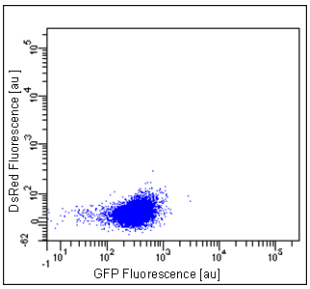	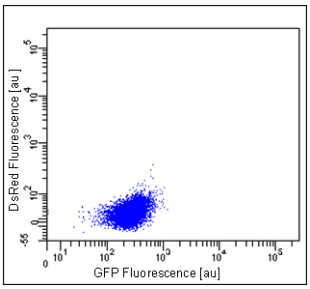	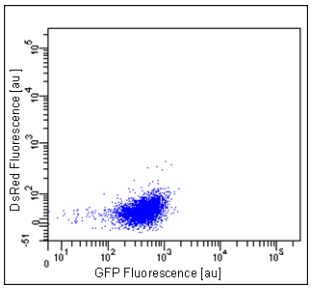	
329	267	441	
Clone 33-49	Clone 30-81	Clone 31-28	
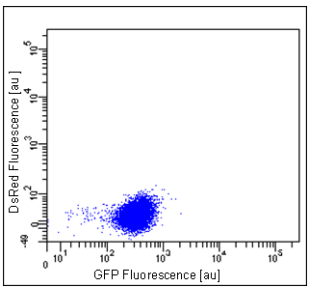	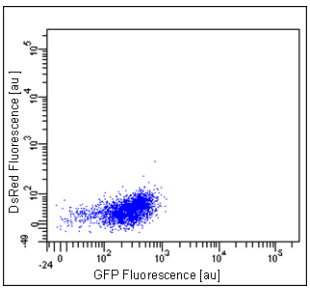	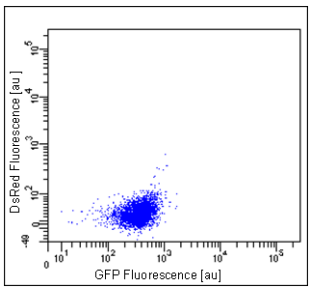	
327	284	363	

Clone 30-84	Clone 31-29
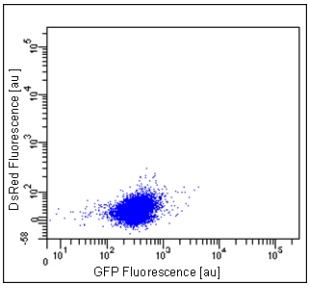	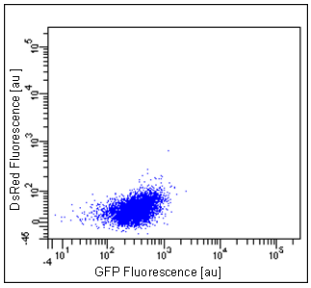
333	334

Clone 30-86	Clone 35-45
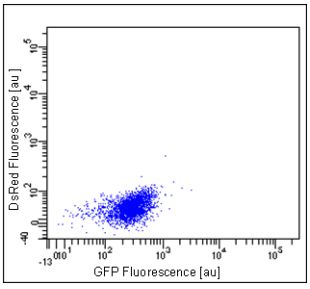	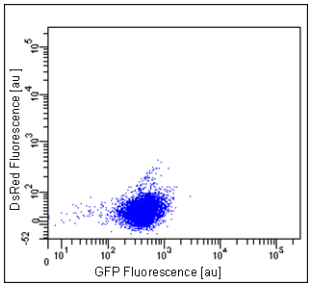
297	430

Clone 35-48
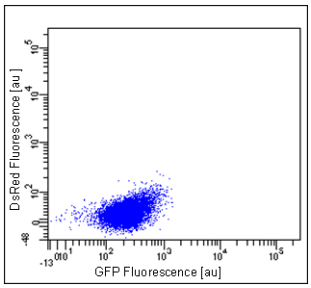
243

GRP78

Mock Rep	Master 2A Rep	Master 2B Rep	Master 2C Rep
Clone 29-25	Clone 34-53	Clone 31-31	Clone 32-21
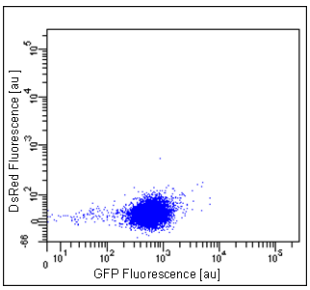	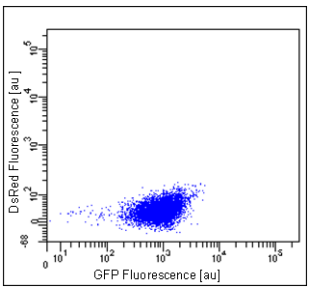	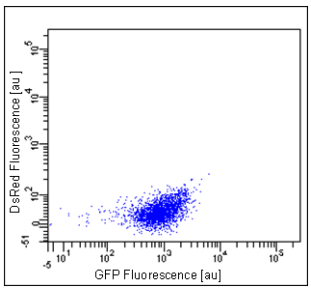	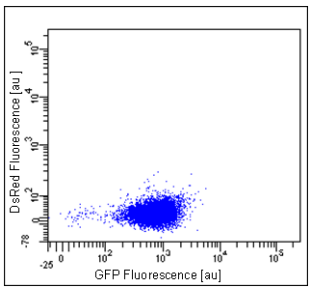
602	970	964	752

Clone 29-28

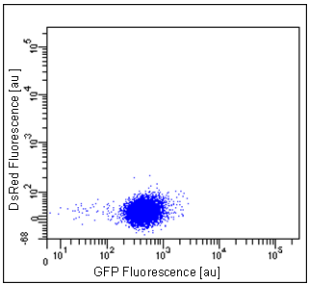

448

Clone 34-55

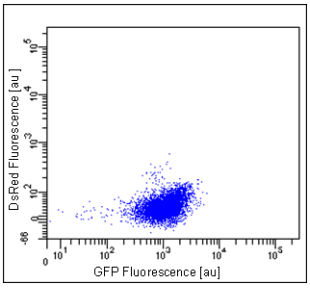

1147

Clone 32-22

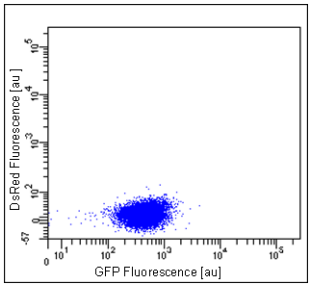

453

Clone 29-30

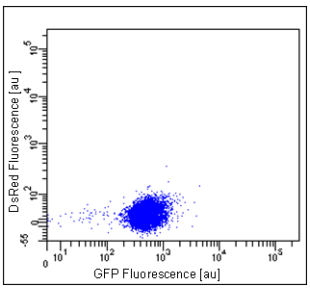

506

Clone 34-58

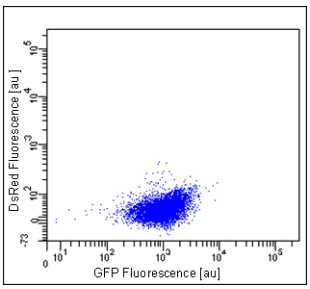

1080

Clone 32-23

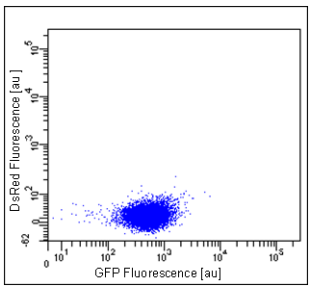

541

Clone 29-31

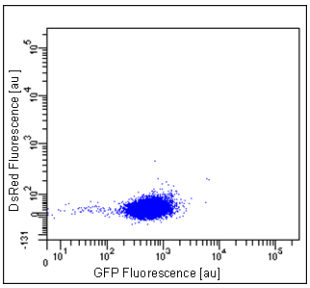

585

Clone 34-60

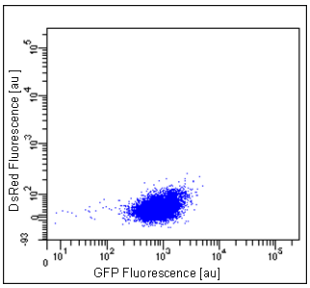

893

Clone 32-25

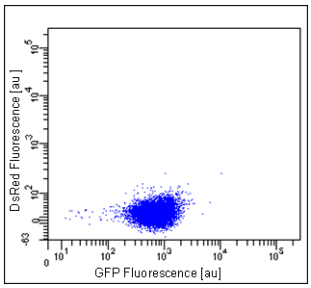

739

Clone 29-32

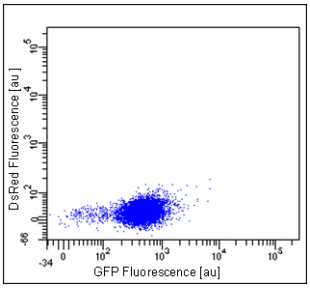

458

Clone 36-29

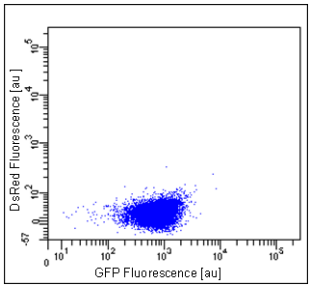

781

Clone 33-54		Clone 36-30	
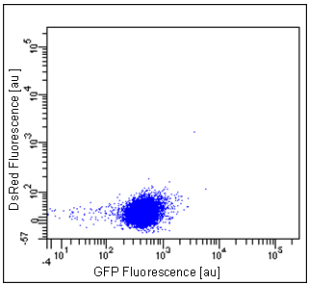		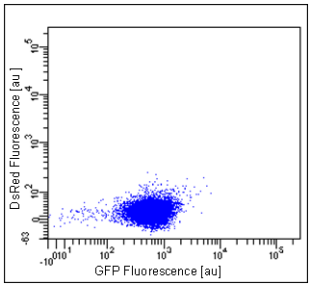	
448		622	
Clone 33-55		Clone 36-31	
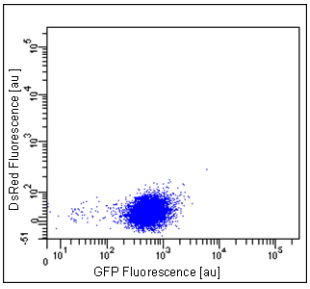		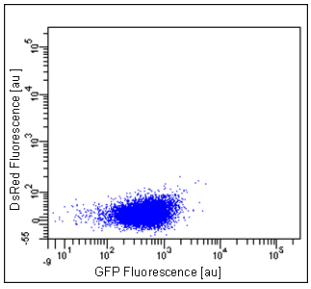	
553		511	

GRP94

Mock Rep	Master 2A Rep	Master 2B Rep	Master 2C Rep
Clone 29-33	Clone 30-92	Clone 31-33	Clone 32-26
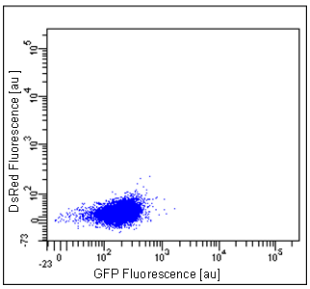	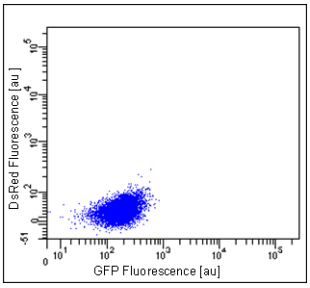	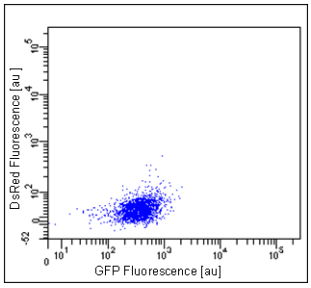	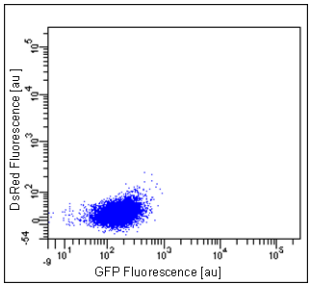
186	177	384	165
Clone 29-34	Clone 30-93	Clone 35-64	Clone 32-27
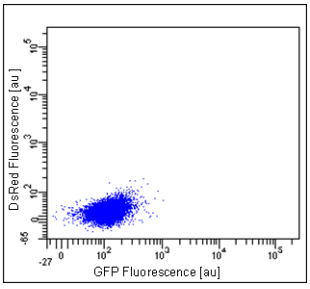	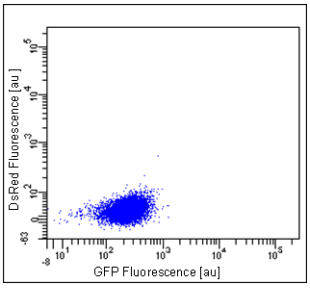	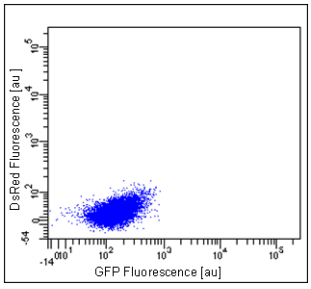	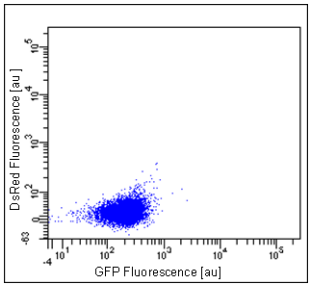
119	240	158	205

Clone 33-58

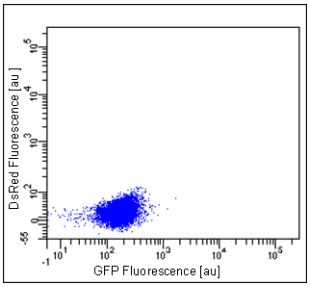

175

Clone 30-95

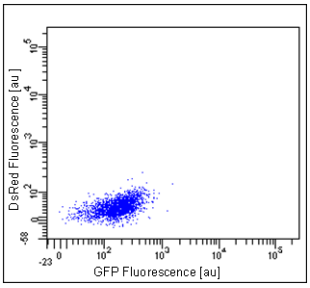

186

Clone 35-65

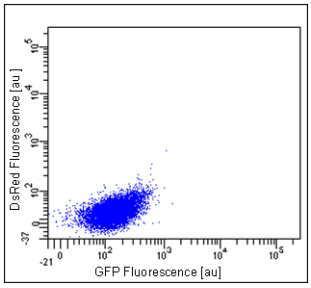

147

Clone 32-29

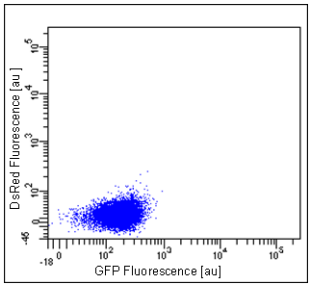

175

Clone 30-96

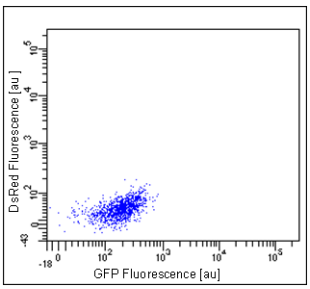

203

Clone 35-66

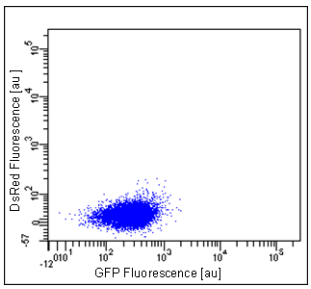

269

Clone 34-66

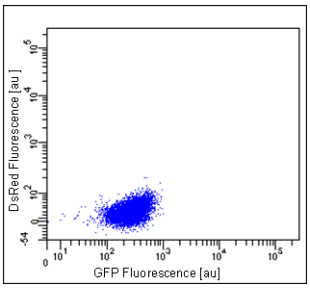

269

Clone 35-67

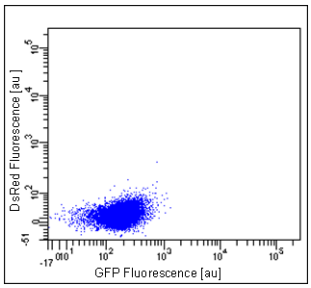

190

Clone 34-67

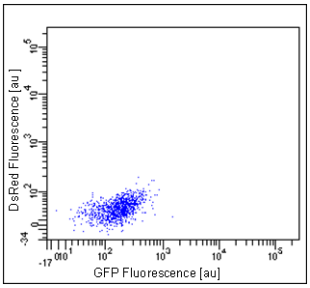

187

Clone 34-69

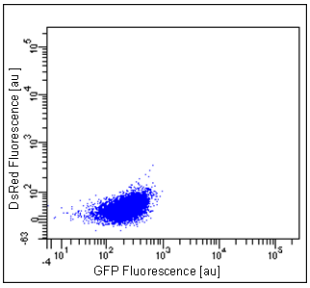

221

Clone 34-70

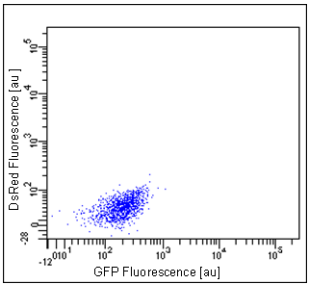

211

Clone 34-72

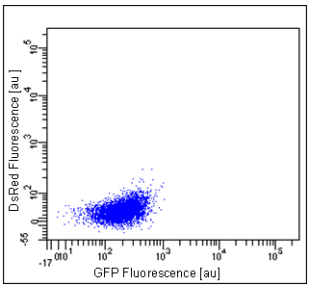

210

Fig. 64: FACS analysis of Mock Reporter and Master 2 Reporter cell lines

The Mock Reporter and Master 2 Reporter cell lines were generated and analysed regarding GFP fluorescence by flow cytometry as described in chapter 6.6.2 (Fig. 54). All results (mean GFP fluorescence [au]) are depicted below each image.

Untreated

Clone 42

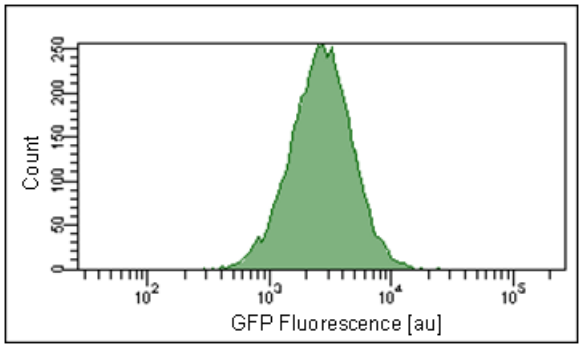

3100

Clone 71

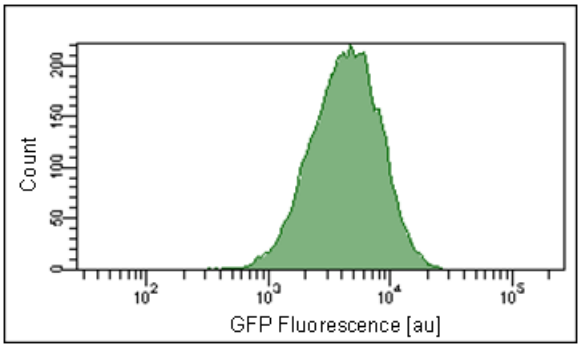

5130

Clone 97

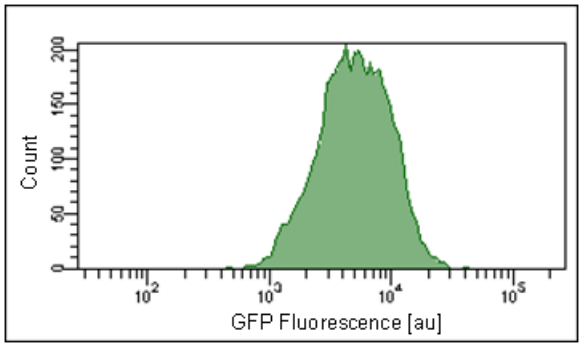

6071

BFA treated

Clone 42

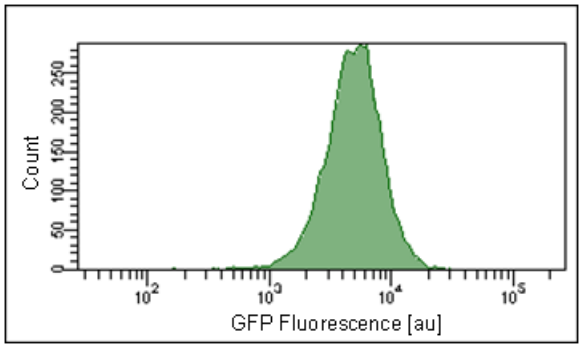

5494

Clone 71

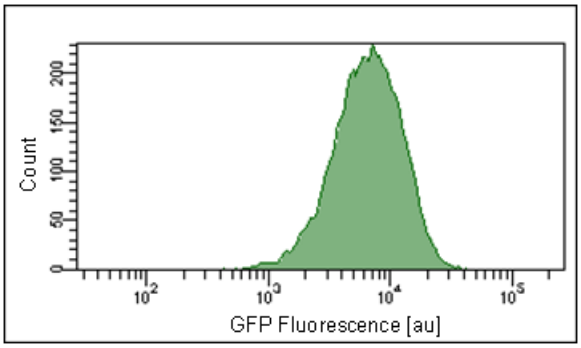

7693

Clone 97

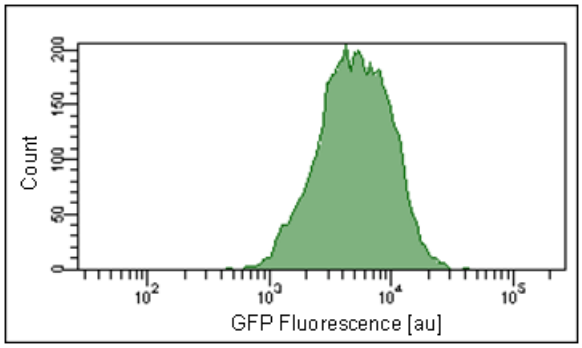

8437

CSN treated

Clone 42

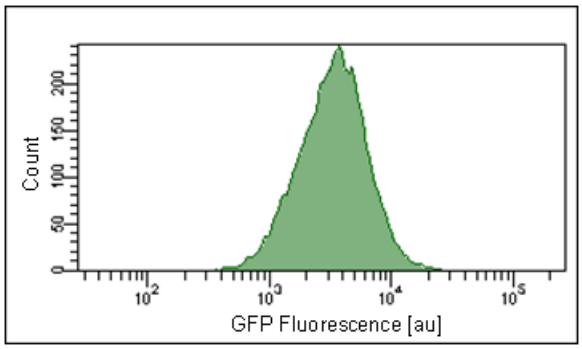

3948

Clone 71

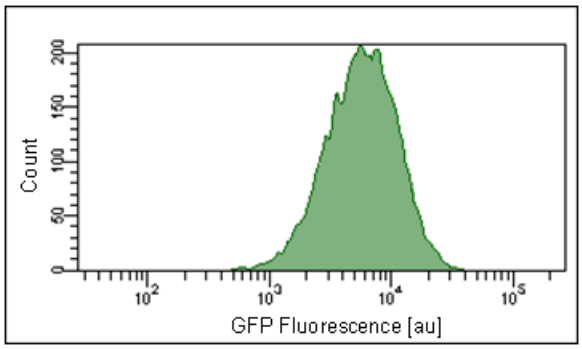

6896

Clone 97

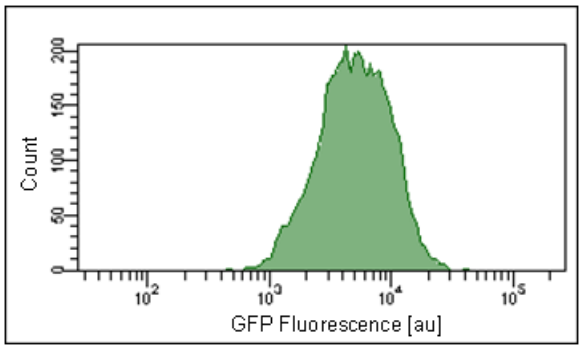

7662

Fig. 65: FACS analysis of selected production clones derived from the tunc GRP78 Reporter cell line after treatment with BFA or CSN

The tunc GRP78 Reporter cell line stably expressing a recombinant antibody were generated and analysed regarding GFP fluorescence by flow cytometry as described in chapter 6.9 (Fig. 62). All results (mean GFP fluorescence [au]) are depicted below each image.

9.2. Abbreviations

5,6,7,8-THF	5,6,7,8-tetrahydrofolate
7,8-DHF	7,8-dihydrofolate
AARE	amino acid response element
ARE	Adenine uridine rich element
ATCC	American type culture collection
ATF4	activating transcription factor 4
ATF6	activating transcription factor 6
au	arbitrary units
Becton	Becton Dickinson
Bethyl	Bethyl Laboratories
BFA	Brefeldin A
Bio-Rad	Bio-Rad Laboratories
BIP	binding immunoglobulin protein
bp	base pairs
BSA	bovine serum albumin
CALR	calreticulin
CANX	calnexin
CD	Chemical Defined
cell strainer tube	Polystyrene Round-Bottom Tube with Cell Strainer Cap 5 mL
CERT	ceramide transfer protein
Cf.	compare
CHO	chinese hamster ovary
CHOP	transcription factor C/EBP homologous protein
CMV	cytomegalo virus
c-region	C-terminal region
CSN	Castanospermine
d2eGFP	enhanced green fluorescent protein, MODC PEST fusion protein
dhfr	dihydrofolate reductase gene
DNA	Deoxyribonucleic acid
dsDNA	Double stranded DNA
DSMZ	German Collection of Microorganisms and Cell Cultures
DsRed	Discosoma sp. red fluorescent protein
E. coli	*Escherichia coli*
E.Bühler	Edmund Bühler
e.g.	for example

eGFP	enhanced green fluorescent protein
eIF2	eukaryotic translation initiation factor 2
ELISA	enzyme linked immunosorbent assay
EOR	ER overload response
ER	endoplasmic reticulum
ERAD	ER associated degradation
ERSE	ER stress element
FA	folic acid
FACS	fluorescence activated cell sorting
FB Serum	Fetal Bovine Serum
Fig.	figure
FRT 3	flip recombinase target mutant 3
FRT wt	flip recombinase target wild-type
G418	G-418 Sulphate
GC content	guanine cytosine content
gDNA	genomic DNA
GFP	green fluorescent protein
Gln	L-Glutamine
Gly	Glycine
GOI	gene of interest
Greiner	Greiner bio-one
GRP78	glucose regulated protein 78 kDa
GRP94	glucose regulated protein 94 kDa
GTN	GFP, thymidine kinase, neomycin phosphotransferase fusion protein
h	hour
HC	Heavy Chain
Herolab	Herolab Laborgeräte
HPLC	High Pressure Liquid Chromatography
h-region	hydrophobic core
hRluc	Renilla luciferase gene
HRP	horse radish peroxidase
HT supplement	hypoxanthine, thymidine supplement
HygTK	hygromycin, thymidine kinase fusion gene
IgG	immunoglobulin G
IRE1	inositol requiring enzyme 1
IRES	internal ribosome entry site
JNK	c-Jun N-terminal kinase

κ	kappa
kb	kilo base
LB	Luria Bertani
LC	light Chain
MARs	matrix attachment regions
min	minute
MODC	murine ornithine decarboxylase
mRNA	messenger RNA
MTX	methotrexate
NEB	New England Biolabs
Neo	neomycin phosphotransferase gene
NF	nuclear factor
nqELISA	non-qualitative ELISA
n-Region	N-terminal region
OD	Optical density
Omega	Omega Bio-Tek
ON	Oligonucleotide
PAA	PAA Laboratories
PAC	puromycin N-acetyl transferase
PBS	Dulbecco's phosphate buffered saline
P_{CMV}	cytomegalo virus promoter
PCR	polymerase chain reaction
PDI	disulfide isomerase
PERK	PKR-like ER kinase
PEST	proline, glutamic acid, serine, threonine rich sequence
PID	protein disulfide isomerase
PKR	Pancreatic eIF2a kinase
PRL	renilla specific product concentration
P_{SV40}	Simian virus 40 promoter
P_{SV40E}	Simian virus 40 promoter with enhancer
P_{TK}	thymidine kinase promoter
qELISA,	qualitative ELISA
Q_P	cell specific product concentration
R^2	Coefficient of determination
Rep	Reporter
RLU	Relative Light Units
RMCE	recombinase mediated cassette exchange

RNA	ribonucleic acid
Roth	Carl Roth
rpm	rounds per minute
RT-PCR	real time PCR
s	second
SP	Signal peptide
SR	Spacer region (unique nucleotide sequence)
SRP	signal recognition particle
STAR	stabilizing and antirepressor element
SV40	Simian virus 40
SV40E	Simian virus 40 with enhancer
Tab.	table
TB	Terrific Broth
TBE	Tris-borat-EDTA
TC Plate	tissue culture plate
TF	Transcription factor
Thermo	Thermo Scientific
TK	thymidine kinase
T_M	Hybridization Temperature
TRAM protein	translocating chain-associated membrane protein
Tris	Tris[hydroxymethyl]aminoethane
U	unit (enzyme activity)
UCOEs	ubiquitous chromatin opening elements
UPR	unfolded protein response
UPRE	unfolded protein response element
UTR	untranslated region
VCD	viable cell density (viable cell concentration)
WFI	water for injection
Wt	wild-type
XBP1	X-box binding protein 1
XBP1(sp.)	spliced X-box binding protein 1

10. References

10.1. Literature

Addison, C.L. et al. (1997). Comparison of the human versus murine cytomegalovirus immediate early gene promoters for transgene expression by adenoviral vectors. J. Gen. Virol. 78(Pt 7): 1653-1661.

Ahmed, S.P. et al. (1995). Antiviral activity and metabolism of the castanospermine derivative MDL 28,574, in cells infected with herpes simplex virus type 2. Biochem. Biophys. Res. Commun. 208(1): 267-273.

Andrews, D.W. et al. (1988). Sequences beyond the cleavage site influence signal peptide function. J. Biol. Chem. 263(30): 15791-15798.

Antoniou, M. et al. (2003). Transgenes encompassing dual-promoter CpG islands from the human TBP and HNRPA2B1 loci are resistant to heterochromatin-mediated silencing. Genomics. 82(3): 269-279.

Back, S.H. et al. (2006). Cytoplasmic IRE1alpha-mediated XBP1 mRNA splicing in the absence of nuclear processing and endoplasmic reticulum stress. J. Biol. Chem. 281(27): 18691-18706.

Baer, A. Et al. (2001). Coping with kinetic and thermodynamic barriers: RMCE, an efficient strategy for the targeted integration of transgenes. Curr. Opin. Biotechnol. 12(5): 473-480.

Baer, A.E.M. (2002). Funktioneller Vergleich von S/MARs ('scaffold/matrix attachment regions') und Insulatoren im chromosomalen Kontext. Technischen Universität Carolo-Wilhelmina zu Braunschweig.

Bailey, W. et al. (2009). The extremely slow and variable activity of dihydrofolate reductase in human liver and its implications for high folic acid intake. PNAS 106(36): 15424-15429.

Baim, S.B. et al. (1985). A Mutation allowing an mRNA Secundary Structure Diminshes Translation of S. cerevisiae Iso-1-Cytochrome c. Mol Cell Biol. 5(8): 1839-1846.

Barash, S. et al. (2002). Human secretory signal peptide description by hidden markov model and generation of a strong artificial signal peptide for secreted protein expression. Biochemical and Biophysical Research Communications 294(4): 835-842.

Barnes, L.M. et al. (2003 Mar). Stability of protein production from recombinant mammalian cells. Biotechnol. Bioeng. 81(6): 631–639.

Barnes, L.M. et al. (2004). Molecular definition of predictive indicators of stable protein expression in recombinant NS0 myeloma cells. Biotechnol. Bioeng. 85(2): 115-121.

Barnes, L.M. et al. (2006). Mammalian cell factories for efficient and stable protein expression. Curr. Opin. Biotechnol. 17(4): 381-386.

Belin, D. et al.(1996). A two-step recognition of signal sequences determines the translocation efficiency of proteins. The EMBO Journal 15(3): 468-478.

Benton, T. et al. (2002). The use of UCOE vectors in combination with a preadapted serum free, suspension cell line allows for rapid production of large quantities of protein. Cytotechnology. 38(1-3): 43-46.

Brezinsky, S.C. et al. (2003). A simple method for enriching populations of transfected CHO cells for cells of higher specific productivity. J. Immunol Methods. 277(1-2): 141-155.

Birch, J. Lonza. (2005). The Importance of Developing a High Yield of Product. European Antibody Congress. Lyon. France.

Birch, J.R. et al. (2006). Antibody production. Adv. Drug. Deli. Rev. 58(5-6): 671-685.

Blobel, G. el at. (1975). Transfer of proteins across membranes. II. Reconstitution of functional rough microsomes from heterologous components. J. Cell Biol. 67(3): 852-862.

Bode, J. et al. (1992). Biological significance of unwinding capability of nuclear matrix-associating DNAs. Sience. 255(5041): 195-197.

Bode, J. et al. (2000). The Transgeneticist´s Toolbox: Novel Methods for the Targeted Modification of Eukaryotic Genomes. Biol. Chem. 381(9-10): 801-813

Bode, J. et al. (2003). Architecture and utilization of highly expressed genomic sites. New Comprehensive Biochemistry. 38: 551-572.

Bole, D.G. et al. (1986). Posttranslational association of immunoglobulin heavy chain binding protein with nascent heavy chains in nonsecreting and secreting hybridomas. J. Cell Biol. 102(5): 1558-1566.

Borth, N. et al. (2000). Efficient selection of high-producing subclones during gene amplification of recombinant Chinese hamster ovary cells by flow cytometry and cell sorting. Biotechnol. Bioeng. 71(4): 266-273.

Borth, N. et al. (2005). Effect of increased expression of protein disulfide isomerase and heavy chain binding protein on antibody secretion in a recombinant CHO cell line. Biotechnol. Prog. 21(1): 106-111.

Boulikas, T. (1993). Nature of DNA sequences at the attachment regions of genes to the nuclear matrix. J. Cell Biochem. 52(1): 14-22.

Bruch, M.D. et al. (1989). Helix formation and stability in a signal sequence. Biochemistry 28(21): 8554-8561.

Calfon, M. et al. (2002). IRE1 couples endoplasmic reticulum load to secretory capacity by processing the XBP-1 mRNA. Nature 415(6867): 92–96.

Carroll, S. et al. (2004). The selection of high-producing cell lines using flow cytometry and cell sorting. Expert. Opin. Biol. Ther. 4(11): 1821–1829.

Chen, X. et al. (2002). The luminal domain of ATF6 senses endoplasmic reticulum (ER) stress and causes translocation of ATF6 from the ER to the Golgi. J. Biol. Chem. 277(15): 13045-13052.

Cho, D.Y. et al. (2003). Molecular Chaperone GRP78/BiP Interacts with the Large Surface Protein of Hepatitis B Virus In Vitro and In Vivo. J. Virol. 77(4): 2784–2788.

Chou, P.Y. et al. (1978). Empirical predictions of protein conformation. Annu. Rev. Biochem. 47: 251-276.

Chusainow, J. et al. (2009 Mar). A study of monoclonal antibody-producing CHO cell lines: what makes a stable high producer? Biotechnol. Bioeng. 102(4): 1182-1196.

den Dunnen, J. et al. (2001). Nomenclature for the description of human sequence variations. Hum. Genet. 109(1): 121-124.

Dübel, S. (2007 Mar). Recombinat therapeutic antibodies. Appl. Mircobiol. Biotechnol. 74(4): 723-729

Earl, P.L. et al. (1991). Folding, interaction with GRP78-BiP, assembly, and transport of the human immunodeficiency virus type 1 envelope protein. J. Virol. 65(4): 2047–2055.

El-Hadi, M. (2005). Mdg1 und die UPR: Stellung und Funktion des Hsp40-Chaperones in der Unfolded Protein Response. Albert-Ludwigs-Universität Freiburg i. Br. Freiburg.

Fafournoux, P. et al. (2000). Amino acid regulation of gene expression. Biochem. J. 351(Pt 1): 1-12.

Fann, C.H. et al. (2000). Limitations to the amplification and stability of human tissue-type plasminogen activator expression by Chinese hamster ovary cells. Biotechnol. Bioeng. 69(2): 204-212.

Florin, L. et al. (2009). Heterologous expression of the lipid transfer protein CERT increases therapeutic protein productivity of mammalian cells. J. Biotechnol. 141(1-2): 84-90.

Folz, R.J. et al. (1986). Deletion of the propeptide from human preproapolipoprotein A-II redirects cotranslational processing by signal peptidase. J. Biol. Chem. 261(31): 14752-14759.

Folz, R.J. et al. (1988). Substrate specificity of eukaryotic signal peptidase. Site-saturation mutagenesis at position -1 regulates cleavage between multiple sites in human pre (delta pro) apolipoprotein A-II. J. Biol. Chem. 263(4): 2070-2078.

Gagnon, M. Pfizer. (2010). Optimizing Media – Achieving Super Soup. CHO Cell Culture Improvements Using a Controlled Nutrient Limiting Feed Strategy. Bioprocessing Short Courses. Boston. USA.

Gardner, A.M. et al. (1993). Rapid degradation of an unassembled immunoglobulin light chain is mediated by a serine protease and occurs in a pre-Golgi compartment. J. Biol. Chem. 268(34): 25940-25947.

Garrick, D. et al. (1998). Repeat-induced gene silencing in mammals. Nat. Genet. 18(1): 56-59

Gierasch, L.M. (1989). Signal sequences. Biochemistry 28(3): 923-930.

Gorlich, D. et al. (1992). A mammalian homolog of SEC61p and SECYp is associated with ribosomes and nascent polypeptides during translocation. Cell. 71(3): 489-503.

Haas, I.G. et al. (1983). Immunoglobulin heavy chain binding protein. Natur 306(5941): 387-389.

Hancock, R.A. (2000) New look at the nuclear matrix. Chromosoma. 109(4): 219-225.

Harding, H.P. et al. (1999). Protein translation and folding are coupled by an endoplasmic-reticulum-resident kinase. Nature 397(6716): 271-274.

Harding, H.P. et al. (2000). Regulated translation initiation controls stress-induced gene expression in mammalian cells. Mol. Cell. 6(5): 1099-1108.

Harland, L. et al. (2002). Transcriptional regulation of the human TATA binding protein gene. Genomics. 79(4): 479-482.

Haze, K. et al. (1999). Mammalian transcription factor ATF6 is synthesized as a transmembrane protein and activated by proteolysis in response to endoplasmic reticulum stress. Mol. Biol. Cell. 10(11): 3787-3799.

Hendershot, L. et al. (1987 Mar). Assembly and secretion of heavy chains that do not associate posttranslationally with immunoglobulin heavy chain-binding protein. J. Cell Biol. 104(3): 761-767.

Heng, H.H.Q. et al. (2004). Chromatin loops are selectively anchored using scafford/matrix-attachment regions. J. Cell. Sci. 117(Pt 7): 999-1008.

Hesse, F. et al. (2000). Developments and improvements in the manufacturing of human therapeutics with mammalian cell cultures. Trends Biotechnol. 18(4): 173-180.

Hofmann, K.J. et al. (1991). Mutations of the alpha-galactosidase signal peptide which greatly enhance secretion of heterologous proteins by yeast. Gene 101(2): 105-111.

Huang, Y. et al. (2007). An efficient and targeted gene integration system for high-level antibody expression. Immunol. Methods 322(1-2): 28-39.

Iwawaki, T. et al. (2004). A transgenic mouse model for monitoring endoplasmic reticulum stress. Nature Medicine 10(1): 98-102.

Jiang, Z. et al. (2006). Regulation of recombinant monoclonal antibody production in chinese hamster ovary cells: a comparative study of gene copy number, mRNA level, and protein expression. Biotechnol. Prog. 22(1): 313-318.

Johnson, A.E. et al. (1999). The translocon: a dynamic gateway at the ER membrane. Annu. Rev. Cell Dev. Biol. 15: 799-842

Jungnickel, B. et al. (1995). A posttargeting signal sequence recognition event in the endoplasmic reticulum membrane. Cell. 82(2): 261-270.

Kalies, K.U. et al. (1994). Binding of ribosomes to the rough endoplasmic reticulum mediated by the Sec61p-complex. J. Cell Biol. 126(4): 925-934.

Kaloff, C.R. et al. (1995). Coordination of Immunoglobulin Chain Folding and Immunoglobulin Chain Assembly Is Essential fort he Formation of Functional IgG. Immunity 2(6): 629-637.

Kalwy, S. et al. (2006). Toward more efficient protein expression. Keep the message simple. Molecular Biotechnology 34(2): 151-156.

Kaufman, R.J. et al. (1982). Amplification and expression of sequences cotransfected with a modular dihydrofolate reductase cDNA gene. J. Mol. Biol. 159(4): 601-621.

Kaufman, R.J. (1999). Stress signaling from the lumen of the endoplasmic reticulum: coordination of gene transcriptional and translational controls. Genes Dev. 13(10): 1211-1233.

Keenan, R.J. et al. (1998). Crystal structure of the signal sequence binding subunit of the signal recognition particle. Cell. 94(2): 181-191.

Kelley, B. Genentec. (2009). Industrialization of mAb production technology: the bioprocessing industry at a crossroads. MAbs. 1(5): 443-452.

Kennard, M. et al. (2006). Generation of stable, high MAb expressing CHO cell lines using the ACE System. Chromos Burnaby.

Kim, J.M. et al. (2004). Improved recombinant gene expression in CHO cells using matrix attachment regions. J. Biotechnol. 107(2): 95-105.

Knappskog, S. et al. (2007 Mar). The level of synthesis and secretion of Gaussia princeps luciferase in transfected CHO cells is heavily dependent on the choice of signal peptide. Journal of Biotechnology. 128(4): 705–715.

Knittler, M.R. et al. (1992). Interaction of BiP with newly synthesized immunoglobulin light chain molecules: cycles of sequential binding and release. EMBO J. 11(4): 1573-1581.

Kochetov, A.V. et al. (2007). AUG_hairpin: prediction of a downstream secondary structure influencing the recognition of a translation start site. BMC Bioinformatics 8: 318.

Kokame, K. et al. (2001 Mar). Identification of ERSE-II, a new cis-acting element responsible for the ATF6-dependent mammalian unfolded protein response. J. Biol. Chem. 276(12): 9199-9205.

Kozak, M. (1986 Jan). Point mutations define a sequence flanking the AUG initiator codon that modulates translation by eukaryotic ribosomes. Cell 44(2): 283-292.

Kozak, M. (1986 May). Influences of mRNA secondary structure on initiation by eukaryotic ribosomes. Proc. Natl. Acad. Sci. USA 83(9): 2850-2854.

Kozak, M. (1987). An analysis of 5'-noncoding sequences from 699 vertebrate messenger RNAs. Nucleic Acid Res.15(20): 8125-8148.

Kozak, M. (1990). Downstream secondary structure facilitates recognition of initiator codons by eukaryotic ribosomes. Proc. Natl. Acad. Sci. USA 87(21): 8301-8305.

Kozutsumi, Y. et al. (1988 Mar). The presence of malfolded proteins in the endoplasmic reticulum signals the induction of glucose-regulated proteins. Nature 332(6163): 462–464.

Kwaks, T.H. et al. (2003). Identification of antirepressor elements that confer high and stable protein production in mammalian cells. Nat. Biotechnol. 21(5): 553-558.

Kwaks, T.H. et al. (2005). Targeting of a histone acetyltransferase domain to a promoter enhances protein expression levels in mammalian cells. J. Biotechnol. 115(1): 35-46.

Kwaks, T.H. et al. (2006). Employing epigenetics to augment the expression of therapeutic proteins in mammalian cells. Trends Biotechnol. 24(3): 137-42.

Lai, E. et al. (2007). Endoplasmic reticulum stress: signaling the unfolded protein response. Physiology (Bethesda) 22: 193-201.

Lattenmayer, C. et al. (2007 Mar). Characterisation of recombinant CHO cell lines by investigation of protein productivities and genetic parameters. J. Biotechnol. 128(4): 716-725.

Lee, A.H. et al. (2003). XBP-1 regulates a subset of endoplasmic reticulum resident chaperone genes in the unfolded protein response. Mol. Cell Biol. (21): 7448-7459.

Lee, K. (2002). IRE1-mediated unconventional mRNA splicing and S2P-mediated ATF6 cleavage merge to regulate XBP1 in signaling the unfolded protein response. Genes Dev. 16(4): 452-466.

Lemberg, M.K. et al. (2002). Requirements for signal peptide peptidase-catalyzed intramembrane proteolysis. Mol. Cell. 10(4): 735-744.

Lenny, N. et al. (1991). Regulation of endoplasmic reticulum stress proteins in COS cells transfected with immunoglobulin mu heavy chain cDNA. J. Biol. Chem. 266(30): 20532-20537.

Li, M. et al (2000). ATF6 as a transcription activator of the endoplasmic reticulum stress element: Thapsigargin stress-induced changes and synergistic interactions with NF-Y and YY1. Molecular and cellular Biology 20(14): 5096–5106.

Li, W.W. et al. (1993). Transactivation of the grp78 promoter by Ca2+ depletion. A comparative analysis with A23187 and the endoplasmic reticulum Ca(2+)-ATPase inhibitor thapsigargin. J. Biol. Chem. 268(16): 12003-12009.

Li, X. Coffino, P. (1993). Degradation of ornithine decarboxylase: exposure of the C-terminal target by a polyamine-inducible inhibitory protein. Mol. Cell. Biol. 13(4): 2377-2383.

Lindgren, K. et al. (2009). Automation of cell line development. Cytotechnology 59(1): 1-10.

Liu, W.M. et al. (1995). Cell stress and translational inhibitors transiently increase the abundance of mammalian SINE transcripts. Nucleic Acids Res. 23(10): 1758–1765.

Llewellyn, D.H. et al. (1996). Induction of calreticulin expression in HeLa cells by depletion of the endoplasmic reticulum Ca2+ store and inhibition of N-linked glycosylation. Biochem. J. 318(2): 555-560.

Ludwig, D.L. (2006). Mammalian expression cassette engineering for high-level protein production. BioProcess International: 14-23.

Lyko, F. et al. (1995). Signal sequence processing in rough microsomes. J. Biol. Chem. 270(34): 19873-19878.

Ma, Y. et al. (2004). Herp is dually regulated by both the endoplasmic reticulum stress-specific branch of the unfolded protein response and a branch that is shared with other cellular stress pathways. J. Biol. Chem. 279(14): 13792-13799.

Martin-Noya, A. et al. (1999). Multiple myeloma with numerous intranuclear Russell bodies. Haematologica 84(2): 179-180.

Martoglio, B. et al. (1995). The protein-conducting channel in the membrane of the endoplasmic reticulum is open laterally toward the lipid bilayer. Cell. 81(2): 207-214.

Martoglio, B. et al. (1997). Signal peptide fragments of preprolactin and HIV-1 p-gp160 interact with calmodulin. EMBO J. 16(22): 6636-6645.

Martoglio, B. et al. (1998). Signal sequences: more than just greasy peptides. 8(10): 410-415

Martoglio, B. (2003). Intramembrane proteolysis and post-targeting functions of signal peptides. Biochem. Sic. Trans. 31(Pt 6): 1243-1247.

Meusser, B. et al. (2005). ERAD: the long road to destruction. Nat. Cell Biol. 7(8): 766-772.

Meyer, M. et al. (1992). Hepatitis B virus transactivator MHBst: activation of NF-κB, selective inhibition by antioxidants and integral membrane localization. EMBO J. 11(8): 2991–3001.

Mothes, W et al. (1997). Molecular mechanism of membrane protein integration into the endoplasmic reticulum. Cell. 89(4): 523-533.

Mothes, W. et al. (1998). Signal sequence recognition in cotranslational translocation by protein components of the endoplasmic reticulum membrane. J. Cell Biol. 142(2): 355-364.

Nakaki, T. et al. (1989). Enhanced transcription of the 78,000-dalton glucose-regulated protein (GRP78) gene and association of GRP78 with immunoglobulin light chains in a nonsecreting B-cell myeloma line (NS-1). Mol. Cell Biol. 9(5): 2233-2238.

Nielsen, H. et al. (1997). Identification of prokaryotic and eukaryotic signal peptides and prediction of their cleavage sites. Protein Eng. 10(1): 1-6.

Nilsson, I. et al. (2002). Cleavage of a tail-anchored protein by signal peptidase. FEBS Lett. 516(1-3): 106-108.

Nothwehr, S.F. et al. (1989). Eukaryotic signal peptide structure/function relationships. Identification of conformational features which influence the site and efficiency of co-translational proteolytic processing by site-directed mutagenesis of human pre(delta pro)apolipoprotein A-II. J. Biol. Chem. 264(7): 3979-3987.

Olczak, M. et al. (2006). Comparison of different signal peptides for protein secretion in nonlytic insect cell system. Analytical Biochemistry 359(1): 45-53.

Qiao, J. et al. (2009). Novel tag-and-exchange (RMCE) strategies generate master cell clones with predictable and stable transgene expression properties. J Mol Bio. 390(4): 579-594.

Pahl, H.L. et al. (1995 Mar). Expression of influenza virus hemagglutinin activates transcription factor NF-κB. J. Virol. 69(3): 1480–1484.

Pahl, H.L. et al. (1995 Jun). A novel signal transduction pathway from the endoplasmic reticulum to the nucleus is mediated by transcription factor NF-κB. EMBO J. 14(11): 2580–2588.

Pahl, H.L. et al. (1996). Activation of transcription factor NF-κB by adenovirus E3/19K requires its ER-retention. J. Cell Biol. 132(4): 511–522.

Pahl, H.L. et al. (1997). The ER-overload response: activation of NF- κB. Trends Biochem. Sci. 22(2): 63-67.

Pahl, H.L. (1999). Signal transduction from the endoplasmic reticulum to the cell nucleus. Physiol. Rev. 79(3): 683-701.

Perlman, D. et al. (1983). A putative signal peptidase recognition site and sequence in eukaryotic and prokaryotic signal peptides. J. Mol. Biol. 167(2): 391-409.

Pikaart, M.J. et al. (1998). Loss of transcriptional activity of a transgene is accompanied by DNA methylation and histone deacetylation and is prevented by insulators. Genes. Dev. 12(18): 2852-2862.

Ping, J. et al. (1993). Effect of heavy chain signal peptide mutations and NH2-terminal chain length on binding of anti-digoxin antibodies. J. Biol. Chem. 268(31): 23000-23007.

Pollard, T.D. et al. (2007 1. Edition). Cell Biology. Springer-Verlag. Berlin. 2. Edition

Rance, J. et al. (2010). Evaluation of Alternative Signal Sequences. Cells and Culture. ESACT Proceedings 4(3): 271-274.

Rao, R.V. et al. (2004). Coupling endoplasmic reticulum stress to the cell death program. Cell Death and Differentiation 11(4): 372-380.

Rapoport, T.A. (1986). Protein translocation across and integration into membranes. CRC Crit. Rev. Biochem. 20(1): 73-137.

Raymond, C.S. et . (2007). High-efficiency FLP and PhiC31 site-specific recombination in mammalian cells. PLoS One 2(1): e162.

Recillas-Targa, F. et al. (2002). Position-effect protection and enhancer blocking by the chicken beta-globin insulator are separable activities. PNAS 99(10): 6883–6888.

Renna, M. et al. (2007). Regulation of ERGIC-53 gene transcription in response to endoplasmic reticulum stress. J. Biol. Chem. 282(31): 22499-22512.

Roy, B. et al. (1999). The mammalian endoplasmic reticulum stress response element consists of an evolutionarily conserved tripartite structure and interacts with a novel stress-inducible complex. Nucleic Acids Res. 27(6): 1437-1443.

Russell, W. (1890). An address on a characteristic organism of cancer. British Medical Journal 2(1563): 1356-1360.

Saul, R. et al. (1985). Castanospermine inhibits alpha-glucosidase activities and alters glycogen distribution in animals. Proc. Nati. Acad. Sci. USA 82(1): 93-97.

Schlake, T. et al. (1994). Use of mutated FLP recognition target (FRT) sites for the exchange of expression cassettes at defined chromosomal loci. Biochemistry 33(43): 12746-12751.

Schlatter, S. Boehringer Ingelheim. (2010 Oct). BI-HEX – Von der DNA zum kommerziellen Prozess – Optimierung der Prozessentwicklung zur Herstellung von therapeiutischen Antikörpern. 1. Laupheimer Zelltage. Laupheim. Germany.

Schlatter, S. Boehringer Ingelheim. (2010 Sep). From DNA to Commercial Process Optimising Process Development to Generate Antibodies for Therapeutic Use. Antibody Development and Manufacturing. Berlin. Germany.

Schmidt, F.R. (2004). Recombinant expression systems in the pharmaceutical industry. Appl. Microbiol. Biotechnol. 65(4): 363-372.

Shaffer, A.L. et al. (2004). XBP1, downstream of Blimp-1, expands the secretory apparatus and other organelles, and increases protein synthesis in plasma cell differentiation. Immunity. 21(1): 81-93.

Shen, J. et al. (2005). ER stress signaling by regulated proteolysis of ATF6. Methods 35(4): 382-389.

Shuster, J.R. (1991). Gene expression in yeast: protein secretion. Curr. Opin. Biotechnol. 2(5): 685-690.

Sidrauski, C. et al. (1997). The transmembrane kinase Ire1p is a site-specific endonuclease that initiates mRNA splicing in the unfolded protein response. Cell 90(6): 1031–1039.

Stemmer, W.R. et al. (1993). Increased antibody expression from *Escherichia coli* through wobble-base library mutagenesis by enzymatic inverse PCR. Gene 123(1): 1-7.

Stern, B. et al. (2007). Improving mammalian cell factories: The selection of signal peptide has a major impact on recombinant protein synthesis and secretion in mammalian cells. Trends in Cell & Molecular Biology 2: 1-17.

Szegezdi, E. et al. (2006). Mediators of endoplasmic reticulum stress-induced apoptosis. EMBO Rep. 7(9): 880-885.

Tan, N.S. et al. (2002). Engineering a novel secretion signal for cross-host recombinant protein expression. Protein Eng. 15(4): 337-345.

Trexler-Schmidt, M. et al. (2009). Purification strategies to process 5 g/L titers of monoclonal antibodies. BioPharm. Intl. Supplement. 8-15.

Tsai, B. et al. (2002). Retro-translocation of proteins from the endoplasmic reticulum into the cytosol. Nat. Rev. Mol. Cell Biol. 3(4): 246-255.

Tsuchiya, Y. et al. (2003). Gene design of signal sequence for effective secretion of protein. Nucleic Acids Res. Suppl. (3): 261-262.

Tsuchiya, Y. et al. (2004). Structural requirements of signal peptide in insect cell. Nucleic Acids Symposium (48): 181-182.

Urlaub, G. et al. (1983). Deletion of the diploid dihydrofolate reductase locus from cultured mammalian cells. Cell 33(2): 405-412.

Varki, A. et al. (1999). Essentials of Glycobiology. Cold Spring Harbor Laboratory Press. Cold Spring Harbor. New York. 2. Edition.

Vattem, K.M. et al. (2004). Reinitiation involving upstream ORFs regulates ATF4 mRNA transation in mammalian cells. Proc. Natl. Acad. Sci. USA. 101(31): 11269–11274.

Voigt, S. et al. (1996). Signal sequence-dependent function of the TRAM protein during early phases of protein transport across the endoplasmic reticulum membrane. J. Cell Biol. 134(1): 25-35.

von Heijne, G. (1983). Patterns of amino acids near signal-sequence cleavage sites. Eur. J. Biochem. 133(1): 17-21.

von Heijne, G. (1985). Signal sequences: The limits of variation. J. Mol. Biol. 184(1): 99-105.

von Heijne, G. (1986). Towards a comparative anatomy of N-Terminal Topogenic Protein Sequences. J. Mol. Biol. 189(1): 239-42.

von Heijne, G. (1998). Life and death of a signal peptide. Nature 396(6707): 111 and 113.

Wagner, R. (2009). Rentschler. The CMO Sense: Stadium-specific Flexible Solutions for Therapeutic Protein Manufacturingin Fed-batch and Continuous Cell Culture Processes. European Compliance Academy. Prague. Czech Republic.

Walsh, G. et al. (2006). Post-translational modifications in the context of therapeutic proteins. Nat. Biotechnol. 24(10): 1241-1252.

Walter, P. et al. (1981). Translocation of proteins across the endoplasmic reticulum III. Signal recognition protein (SRP) causes signal sequence-dependent and site-specific arrest of chain elongation that is released by microsomal membranes. J. Cell Biol. 91(2 Pt 1): 557-561.

Walter, P. at al. (1994). Signal sequence recognition and protein targeting to the endoplasmic reticulum membrane. Annu. Rev. Cell Biol. 10: 87-119.

Wang, Y. et al. (2000). Activation of ATF6 and an ATF6 DNA binding site by the endoplasmic reticulum stress response. J. Biol. Chem. 275(35): 27013-27020.

West, A.G. et al. (2005). Remote control of gene transcription. Hum. Mol. Genet. 14(Spec No1): R101-R111

Williams, S. et al. (2005). CpG-island fragments from the HNRPA2B1/CBX3 genomic locus reduce silencing and enhance transgene expression from the hCMV promoter/enhancer in mammalian cells. BMC Biotechnol. 5: 17.

Winder, R. (2005). Cell culture grows capacity; capacity expansions address the 'crunch' for biopharmaceutical manufacturing. Chemistry and Industry: 21-22.

Wiren, K.M. et al. (1988). Importance of the propeptide sequence of human preproparathyroid hormone for signal sequence function. J. Biol. Chem. 263(36): 19771-19777.

Wurm, F.M. (2004). Production of recombinant protein therapeutics in cultivated mammalian cells. Nat. Biotechnol. 22(11): 1393-1398.

Yamamoto, Y. et al. (1989). Important role of the proline residue in the signal sequence that directs the secretion of human lysozyme in Saccharomyces cerevisiae. Biochemistry. 28(6): 2728-2732.

Yang, Q. et al. (1997). Location of the internal ribosome entry site in the 5' non-coding region of the immunoglobulin heavy-chain binding protein (BiP) mRNA: evidence for specific RNA-protein interactions. Nucleic Acid Res. 25(14): 2800-2807.

Ye, J. et al. (2000). ER stress induces cleavage of membrane-bound ATF6 by the same proteases that process SREBPs. Mol. Cell. 6(6): 1355-1364.

Yoshida, H. et al. (1998). Identification of the cis-acting endoplasmic reticulum stress response element responsible for transcriptional induction of mammalian glucose-regulated proteins. Involvement of basic leucine zipper transcription factors. J. Biol. Chem. 273(50): 33741-33749.

Yoshida, H. et al. (2001). XBP1 mRNA is induced by ATF6 and spliced by IRE1 in response to ER stress to produce a highly active transcription factor. Cell 107(7): 881–891.

Young, R. (2008). Important topics in the expression of recombinant antibodies from CHO cells. Cell line Development and Engineering Workshop. Prague.

Zahn-Zabal, M. et al. (2001). Development of stable cell lines for production or regulated expression using matrix attachment regions. J. Biotechnol. 87(1): 29-42.

Zhang, L. et al. (2005). Alteration in the IL-2 signal peptide affects secretion of proteins in vitro and in vivo. The Journal of Gene Medicine 7(3): 354-365.

Zheng, N. et al. (1996). Signal sequences: the same yet different. Cell. 86(6): 849-852.

10.2. Patents

AU 2002/338947 B2. Schweickhardt, R.L. et al. Applied Research Systems ARS Holding N.V. Methods of increasing protein expression levels

WO 2004/009819 A2. Sleep, D. Delta Biotechnology limited. Gene and polypeptide sequences.

WO 2005/001099 A2. Hesketh, J. et al. Unitargeting research AS. Protein expression system.

WO 2008/148519 A2. Young, R. et al. Lonza Biologics PLC. Mammalian expression vector with a highly effient secretory signal sequence.

US 7384744 G. Enenkel, B. et al. Boehringer Ingelheim Pharma GmbH & Co., KG. Expression vector, methods for the production of heterologous gene products and for the selection of recombinant cells producing high levels of such products

11. Acknowledgements

I would like to express my deepest gratitude and my sincere appreciation to those who made this thesis possible such as my doctoral advisor Professor Dr. Jürgen Bode (Hans Borst-Center, Hannover Medical School) for all of the support, scientific advises and very productive discussions about RMCE and many other techniques.

My gratefulness and special thanks to Professor Dr. Stefan Dübel for giving me the opportunity of being a Ph.D. student at the Institute of Biochemistry and Biotechnology, Technical University of Braunschweig and his scientific recommendations and suggestions which helped me to develop the experimental approach.

Special thanks to Professor Dr. Sigmund Lang (apl. Professor Technical University of Braunschweig) for being the chairperson of the doctoral committee.

Special thanks to Dr. Christoph Zehe (Head of Cell Line Development, Cellca GmbH) for all of the helpful discussions and suggestions about the used experiments and methods during the last years. I am also grateful for his generous support and the corrections of this thesis.

I am also obliged to Dr. Aziz Cayli (CEO of Cellca GmbH) who gave me the opportunity to do most of the experiments in the laboratories of the Cellca GmbH. Thanks also for trust, all of the advices and helpful discussions.

Great thanks also to Professor Dr. Peter Dürre and Iris Steiner (Institute for Microbiology and Biotechnology, Ulm, Germany) for their helpful support and the opportunity to used several laboratories, as well as, the equipment of the University of Ulm. Also special thanks to Birgit Rose and Andreas Hiergeist for here help with different analytical assays.

Thinking back on my Ph.D. period at the Cellca GmbH it was a very intensive and fruitful period of my life. I will never forget the moments of hard work but also the pleasure during collective excursions and the nice friendly working atmosphere during this time. I would like to express my gratitude to all former and current employees of the Cellca GmbH for their support during my whole doctor thesis.

Finally, I want to thank all members of my family for their continuous love and generous support during the whole thesis. Especially I would like to express my deepest gratitude to my wife and to my daughter. None of the achievements would have been possible without their help and deep comprehension.